Comparative Evaluation of Power Plants with CO_2 Capture: Thermodynamic, Economic and Environmental Performance

Dissertation

Dipl.-Ing. Fontina Petrakopoulou

Berlin

Comparative Evaluation of Power Plants with CO_2 Capture: Thermodynamic, Economic and Environmental Performance

vorgelegt von
Diplom-Ingenieurin
Fontina Petrakopoulou
aus Griechenland

von der Fakultät III – Prozesswissenschaften
der Technischen Universität Berlin
zur Erlangung des akademischen Grades
Doktor der Ingenieurwissenschaften
– Dr.-Ing. –

genehmigte Dissertation

Promotionsausschuss

Vorsitzender: Prof. Dr.-Ing. Felix Ziegler
Berichter: Prof. Dr.-Ing. Georgios Tsatsaronis
Berichter: Prof. Dr.-Ing. Günter Wozny

Tag der wissenschaftlichen Aussprache: 6.12.2010

Berlin, 2011
D 83

Foreword

This work has been conducted during my stay as a research assistant at the Institute for Energy Engineering and Protection of the Environmental of the Technische Universität Berlin. During the period of September 2006 – September 2009, this research was supported by the European Commission's Marie Curie 6th Framework Programme of the CT-2005-019296-INSPIRE training network.

With this opportunity, I would like to express my gratitude to the people that facilitated the completion of this work.

I am most especially grateful to Professor George Tsatsaronis, who supervised this work and was always willing, helpful, creative and patient. His support was the most important motivator to complete this work.

Professor Tatiana Morosuk was always present and willing to assist. Her energy and excitement brightened some cloudy days!

I would like to thank Professor Günter Wozny for the review of this thesis. I am also thankful to Professor Felix Ziegler for his willingness to chair my thesis defence.

I am indebted to the students that contributed to this work: Anna Carrasai, Christopher Paitazoglou, Costanza Piancastelli, Foteini Kokkali, Ivan Gallio and Marlene Cabrera.

Special thanks to my colleagues from the INSPIRE network and the Institute for Energy Engineering and Protection of the Environmental for the fruitful collaboration, eventful meetings and nice experiences gathered. My close and fulfilling collaboration with Dr. Alicia Boyano Larriba deserves a special reference.

For the comfort of a personal licence for the software EbsilonProfessional by Evonik Energy Services GmbH, I am very grateful.

I truly appreciate the help from my companion, Alex Robinson. Without his presence and support, the completion of this work would have been more difficult and definitely not as fun!

Finally, I would like to thank my family for their understanding and eternal encouragement.

Berlin, October 2010

Fontina Petrakopoulou

In memory of Matteo Milanesi

Synopsis

CCS (*Carbon Capture and Sequestration)* in the energy sector is seen as a bridge technology for CO_2 mitigation, due to the ever-growing environmental impact of anthropogenic-emitted greenhouse gases. In this work, eight power plant concepts using CO_2 capture technologies are assessed based on their efficiency, economic feasibility and environmental footprint.

Exergy-based analyses are used for evaluating the considered power plants through comparison with a reference plant without CO_2 capture. While conventional exergy-based analyses provide important information that can lead to improvements in plant performance, additional insight about individual components and the interactions among equipment can aid further assessment. This led to the development of advanced exergy-based analyses, in which the exergy destruction, as well as the associated costs and environmental impacts are split into avoidable/unavoidable and endogenous/exogenous parts. Based on the avoidable parts, the potential for improvement is revealed, while based on the endogenous/exogenous parts, the component interactions are obtained.

Among the examined plants with CO_2 capture, the most efficient are those working with oxy-fuel technology. An exergoeconomic analysis shows a minimum increase in the relative investment cost (in €/kW) of 80% for the conventional approach (chemical absorption) and an increase of 86% for the oxy-fuel plant with chemical looping combustion. The latter shows a somewhat decreased environmental impact when compared to that of the reference plant. On the contrary, the plant with chemical absorption results in a higher environmental penalty due to its high efficiency penalty. Therefore, accepting that all assumptions and data related to the calculations of the environmental impacts are reliable, efficiency improvement seems to be a more significant factor in potentially decreasing a plant's environmental impact. With advanced exergy-based analyses, interdependencies among components are identified, and the real potential for cost- and environmental-related improvement is revealed. A common trend for all plants examined is that most thermodynamic inefficiencies are caused by the internal operation of the components. Additionally, avoidable quantities are generally found to be low for components with high costs and environmental impacts, leaving a relatively narrow window of improvement potential.

Table of Contents

Appendices

List of Figures

List of Tables

Nomenclature

Symbols

a	Size exponent
A	Surface area (m^2)
b	Environmental impact per unit of exergy (Pts/GJ)
$\dot{B}$	Environmental impact rate associated with exergy (Pts/h)
c	Cost per unit of exergy (€/GJ)
$\dot{C}$	Cost rate associated with an exergy stream (€/h)
d_i, d_o	Inside and outside tube diameter (in)
$\dot{E}$	Exergy rate (MW)
f	Exergoeconomic factor (%)
f_b	Exergoenvironmental factor (%)
G	Total inlet flue gas flow rate (kmol/h); gas mass velocity (lb/ft^2h)
h_i, h_o	Tube-side and gas-side coefficients (W/m^2K)
h_c, h_N	Convective and non-luminous heat transfer coefficients(W/m^2K)
K	Constant
L	Total sorbent flow rate (kmol/h); beam length (m)
$\dot{m}$	Mass flow rate (kg/s)
mw_{lean}	Average molecular weight of the lean sorbent (kg/kmol)
p	Pressure (bar)
r	Relative cost difference (%)
r_b	Relative environmental impact difference (%)
S_T, S_L	Longitudinal and transverse pitch (in)
T	Temperature (°C)
U_o	Overall heat transfer coefficient (W/m^2K)
$\dot{V}$	Volumetric flow rate (m^3/s)
y	Exergy destruction ratio (%)
$\dot{Y}$	Component-related environmental impact (Pts/h)
y_{CO_2}	CO_2 concentration (w/w, %)
$\dot{Z}$	Cost rate associated with capital investment (€/h)

Subscripts

CH	Chemical (exergy)

D	Destruction (exergy)
F	Fuel (exergy)
i, j	Entering and exiting exergy stream indices
in	Incoming
is	Isentropic (efficiency)
k, r, Y, W	Component indices
L	Loss (exergy)
l, m, n	Counting indices
out	Outgoing
P	Product (exergy)
PH	Physical (exergy)
pol	Polytropic (efficiency)
tot	Overall system
mech	Mechanical (efficiency)

Superscripts

AV	Avoidable
UN	Unavoidable
UN,EN	Unavoidable endogenous
UN,EX	Unavoidable exogenous
AV,EN	Avoidable endogenous
AV,EX	Avoidable exogenous
MX	Mexogenous
PF	Pollutant formation

Abbreviations

AR	Air reactor
ASU	Air separation unit
ATR	Autothermal reformer
AZEP	Advanced zero emission plant
CAU	Chemical absorption unit
CC	Combustion chamber
CCS	Carbon capture and storage
CEPCI	Chemical engineering plant cost index
CLC	Chemical looping combustion
COA-CO_2	Cost of avoided CO_2
COE	Cost of electricity
COND	Condenser
COOL	Cooler
CPO	Catalytic partial oxidation
CT	Cooling tower

DB	Duct burner
EC	Economizer
ECBMR	Enhanced coal bed methane recovery
EGR	Enhanced gas recovery
EIE	Environmental impact of electricity
EOR	Enhanced oil recovery
EV	Evaporator
FC	Fuel cost
FCI	Fixed capital investment
FG	Flue gas
FR	Fuel reactor
GEN	Generator
GT	Gas turbine
HP / IP / LP	High pressure / intermediate pressure / low pressure
HT / LP	High temperature / low temperature
HTT	High-temperature turbine
HRSG	Heat-recovery steam generator
HX	Heat exchanger
IC	Investment cost
ID	Inside diameter
IGCC	Integrated gasification combined cycle
LCA	Life cycle assessment
LCIA	Life cycle impact assessment
LHV	Lower heating value
LNG	Liquefied natural gas
LPG	Liquefied petroleum gases
LPT	Low-pressure gas turbine
MEA	Monoethanolamine
MCM	Mixed conducting membrane
MMV	Measurement, monitoring and verification
MSR	Hydrogen separating membrane
NG	Natural gas
NG PH	Natural gas preheater
O&M	Operating and maintenance costs
OC	Oxygen carrier
OD	Outside diameter
PEC	Purchased equipment Cost
RH	Reheater
SH	Superheater
ST	Steam turbine
TCI	Total capital investment
TRR	Total revenue requirement

Greek symbols

ε	Exergetic efficiency (%)
$\in_g$	Gas emissivity
η	Energetic efficiency (%)
λ	Excess air fraction
ρ	Density (lb/ft^3)
τ	Annual operating hours
φ_{lean}	Lean sorbent CO_2 loading

1. Introduction

Greenhouse gases absorb and trap heat in the lower atmosphere. A continuous, rapid increase in anthropogenic atmospheric greenhouse gas concentrations since the industrial revolution has led to pronounced temperature increases and climate change. Accounting for about 80% of the enhanced global warming effect, CO_2 is thought to be the main contributor among the greenhouse gases (VGB PowerTech, 2004). Electric-power generation remains the single largest source of CO_2 emissions, equal to those of the rest of the industrial sectors combined (IPCC, 2005). Additionally, most of the energy demand across the globe is covered by fossil fuels that generate large amounts of pollutants like CO_2, CH_4 and NO_X. An ever-increasing demand for energy prolongs environmental aggravation, but it simultaneously acts as a strong motivator for the development of new technologies to mitigate climate change. As mentioned in the IPCC report (2005), measures to reduce the increasing man-made CO_2 concentration in the atmosphere include: (1) reducing energy demand; (2) increasing the efficiency of energy conversion and/or fuel utilization; (3) switching to less carbon intensive fuels; (4) increasing the use of renewable energy sources or nuclear energy; (5) sequestering CO_2 by enhancing biological absorption capacity in forests and soils and (6) *carbon capturing and storing* (CCS).

Carbon capture and storage is a three step process: (1) CO_2 capture and compression to a high pressure, (2) CO_2 transport to a selected storage site and (3) CO_2 storage. CCS from power plants is a topic that started attracting attention from a large group of scientists only a little more than three decades ago, as a powerful tool for limiting the impact of fossil-fuel use on the climate (Herzog, 2001). This field is, therefore, still in its infancy, but expertise is growing.

When evaluating options for CO_2 capture from power stations, engineers are faced with a large variety of alternative approaches. However, dissimilar assumptions and hypotheses in evaluations make the comparison and assessment of different concepts difficult, if not infeasible. Moreover, although several alternative approaches for capturing CO_2 have been proposed in such a short time, few appear promising with respect to efficiency and cost, while the environmental impact of the technologies is still unknown. Although energy-based comparative studies of selected CO_2 capture technologies have been sporadically performed in the last decade (e.g., Kvamsdal et al., 2007; Bolland, 1991; Bolland and Mathieu, 1998), a complete presentation and comparison of a fair number of alternative methods is still missing. Any emission reduction (up to practically 100%) can be achieved with a sufficiently high level of expenditure. The question, however, is whether a CO_2 capture technology is a reasonable measure when balancing the benefit to the environment against a greatly increased cost and risk (VGB PowerTech, 2004).

This thesis aims to evaluate a variety of CO_2 capture technologies, taking into account both the economic and the environmental perspectives (risk assessment is not included). Eight low- or zero-emission power plants with different CO_2 capture technologies are presented and compared under equivalent conditions, based on their efficiency, economic feasibility and environmental footprint. The focus is the evaluation of CO_2 capture technologies integrated in combined cycle power plants operating with natural gas and used for electricity production. Advantages and disadvantages of each technology and ways to reduce the cost and environmental impact associated with electricity production, while keeping the CO_2 emissions at a minimum level, are discussed.

The methods used for the evaluation of the plants are based on exergy principles. An *exergetic analysis* is the first step in evaluating an energy conversion system, identifying the source and cause of incurred thermodynamic inefficiencies (Bejan et al., 1996; Tsatsaronis and Cziesla, 2002; Moran and Shapiro, 2008; Tsatsaronis and Cziesla, 2009). The combination of an exergetic analysis with an *economic analysis* and a *life cycle assessment* constitutes the *exergoeconomic analysis* (Bejan et al. 1996; Tsatsaronis and Cziesla 2002; Lazzaretto and Tsatsaronis, 2006) and the *exergoenvironmental analysis* (Meyer et al., 2009; Tsatsaronis and Morosuk, 2008a and 2008b), respectively.

With *conventional exergy-based analyses*, information about improvements of an energy conversion system is revealed. Monetary costs and environmental impacts are assigned to all exergy streams of the plants, as well as to the exergy destruction incurred within each plant component, exposing appropriate compromises among thermodynamic, economic and environmental considerations. However, although conventional exergy-based analyses uncover a path towards plant improvement, they suffer from some limitations, which are addressed by *advanced exergy-based analyses*.

Advanced exergy-based methods identify mutual interdependencies among plant components, and reveal the real improvement potential both at the component and plant level (Tsatsaronis, 1999a; Tsatsaronis and Park, 2002; Cziesla et al., 2006; Morosuk and Tsatsaronis, 2006a, 2006b, 2007a, 2007b, 2008a, 2008b, 2009a and 2009b; Tsatsaronis et al., 2006; Tsatsaronis and Morosuk, 2007, 2010; Kelly 2008; Boyano et al., 2009; Kelly et al, 2009; Tsatsaronis et al., 2009). Data obtained from advanced exergy-based methods are crucial for pinpointing strengths and weaknesses of complex plants with a large number of interrelated components.

This thesis is the first evaluation of CO_2 capture technologies using exergoeconomic and exergoenvironmental analyses, and it is the first complete and thorough application of the advanced methods to complex energy conversion systems in general. Chapter 2 provides a short description of the different steps involved in CCS technology, as well as an overview of the state of the art. Global CCS projects are also presented and categorized based on their size, application sector and state of realization (Section 2.2). A detailed description of the eight CO_2 capture technologies considered in this thesis, and their incorporation into power plants, is provided in Section 2.3. Chapter 3 presents the exergy-based methods used for the evaluation of the plants. Both conventional and advanced exergy-based methods are described, and all the required

mathematical equations and variables of the methodologies are included. Chapter 4 presents the application of the exergy-based methods to the simulated systems and the results obtained. Lastly, conclusions and future plans are included in Chapter 5. The appendices and the supplemental data provide additional detailed information for the analytical study of the results.

2. CO_2 capture from power plants

2.1 Carbon capture and storage (CCS)

The three steps comprising CCS are CO_2 capture, transport and storage. Transport and storage of carbon dioxide are not the focus of this thesis. However, here, in order to present the complete chain of the CCS process, information about all three steps is provided.

2.1.1 CO_2 capture

CO_2 capture methods can be classified into two main categories[1], depending on whether the CO_2 is captured before or after the combustion process (Figure 2.1). However, the main distinction among capture methods stems from the treatment of the fuel used: when no treatment of the fuel occurs, the method is classified as *post-combustion capture*, while when the fuel undergoes a de-carbonization process, the method is classified as *pre-combustion capture*.

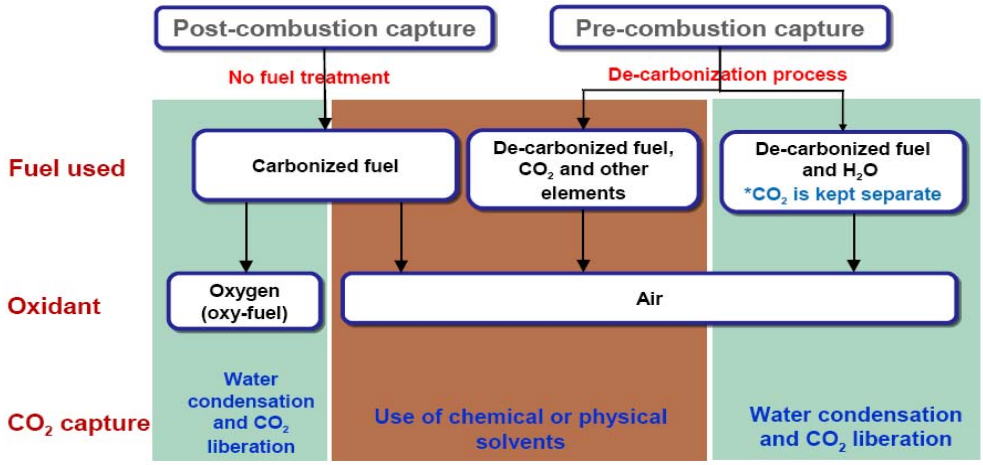

Figure 2.1: CO_2 capture groups and their characteristics

When air is used as the oxidant in post-combustion capture, CO_2 is captured with chemical or physical solvents. The most conventional representative of this type of CO_2 capture is *chemical absorption*, a process developed about 70 years ago to remove acid gases

[1] In literature, CO_2 capture technologies are generally separated into three groups: post-, pre- and oxy-combustion concepts. Although post- and pre-combustion refer to when the carbon capture takes place, oxy-combustion refers to the oxidant type used in the combustion process. Here the distinction is based exclusively on when the carbon capture takes place. Thus, oxy-combustion is considered part of the post-combustion methods (since the produced CO_2 is separated after the combustion process).

from natural gas streams (Herzog, 2001). The advantages of post-combustion capture are that existing plants can be retrofitted with a capture unit without further rearrangements, and that the technology is well established. However, the prominent disadvantage of the method is the very significant amount of thermal energy required for the regeneration of the chemicals used, resulting in a significant efficiency penalty. In recent years, many studies have reviewed different post-combustion technologies and compared the effectiveness of different types of absorbents for chemical absorption (e.g., Rubin and Rao, 2002; Kothandaraman et al., 2009). Analyses have yet to reveal any significant breakthrough, so chemical absorption remains one of the most energy intensive methodologies.

When oxygen is used as the oxidant in post-combustion capture (*oxy-fuel combustion*), the energy demand is reduced, when compared to chemical absorption, and the CO_2 separation process is simplified. Because oxygen is used, the combustion products consist mainly of water vapour and carbon dioxide; the carbon dioxide is freed after the water is condensed without requiring further treatment, keeping the energy demand of CO_2 separation at relatively low levels. In addition, with oxy-fuel combustion, NO_X emissions are reduced to less than 1 ppm for natural gas use (Sundkvist et al., 2005). The most common method to produce oxygen for large-scale oxy-fuel plants is a cryogenic *air separation unit* (ASU). However, compression and the energy requirement of the distillation column included in the process result in a relatively high cost that makes the method less attractive. Oxy-fuel concepts also have implementation challenges associated with technological limitations of the components (Wilkinson et al., 2003; Anderson et al. 2008). Nevertheless, there has recently been a large increase in projects associated with newly introduced oxy-fuel approaches. These technologies include oxygen-separating membranes and new types of reactors that seem promising with respect to their efficiency and their relatively low CO_2 capture cost (e.g., (Kvamsdal et al., 2007).

In pre-combustion methods, suitable de-carbonization methods are applied to the available fuel to separate the carbon contained in it before the combustion process. The goal is to produce a hydrogen-based fuel that will result in clean combustion gases. If the de-carbonization method results in a mixture of CO_2 and gases that do not allow the required purity of CO_2 for separation (e.g., CO_2 mixed with N_2), chemical absorption is used. Otherwise, if the produced CO_2 is kept separate by the de-carbonization process, no additional treatment is needed and the CO_2 is captured after water condensation. The de-carbonization of the fuel is highly energy demanding, relatively expensive and its implementation requires large structural changes to any pre-existing plant. One of the most well-known technologies that can be easily adopted for pre-combustion capture is the gasification of coal. From this process syngas is produced, which can be used in gas turbines, increasing the overall efficiency of the plant. However, *integrated gasification combined cycles* (IGCCs), present challenges that delay the broader acceptance of this technology.

2.1.2 CO_2 transport

Once CO_2 has been captured, it must be transported to a storage facility as gas, liquid or solid. Transportation can be performed via pipeline, ship, rail, truck or a combination of these means.

Transport of CO_2 by pipeline in the liquid phase (above 7.58 MPa, ambient temperature) is, at present, the most economical means of moving large quantities of CO_2 long distances. Transportation infrastructure would be needed for large quantities of CO_2 to make a significant contribution to climate change mitigation, and would imply a large network of pipelines. As growth continues, it may become more difficult to secure rights-of-way for the pipelines, particularly in highly populated zones that produce large amounts of carbon dioxide. Existing experience has only been in zones with low population densities, and safety issues will most probably become more complicated in populated areas. Although some experience has been gained by *enhanced oil recovery* (EOR) operations, the standards required for CCS are not necessarily the same and, therefore, new minimum standards for pipeline quality for CCS are required (IPCC, 2005).

In some cases, transport of CO_2 by ship may be economically more attractive, particularly when the CO_2 must be moved over large distances or overseas (IPCC, 2005). The properties of liquefied CO_2 are similar to those of *liquefied petroleum gases* (LPG). LPG technology could be scaled-up to large CO_2 carriers, transporting CO_2 by ship in a similar way (typically at a pressure of 0.7 MPa).

Road and rail tankers are also technically feasible options when there is no access to pipeline facilities or when the captured gas must be transferred over large distances. Here the CO_2 is transported at a temperature of -20°C and at a pressure of 2 MPa. These systems are more expensive compared to pipelines and ships, except on a very small-scale.

2.1.3 CO_2 storage

Available alternative choices for CO_2 storage are shown in Table 2.1. Carbon dioxide capture with storage in deep geological formations is currently the most advanced and the most likely approach to be deployed on a large scale in the future. Possible geological storage formations include oil and gas fields, saline formations, and coal beds (see Figure 2.2).

Table 2.1: Storage options (WorleyParsons, 2009)[a]

Geological	Ocean	Beneficial reuse	Terrestrial
Saline formations	CO_2 lakes	Enhanced oil recovery (EOR)	Forest lands
Depleted oil and gas reservoirs	Solid hydrate	Enhanced gas recovery (EGR)	Agricultural lands including biochar
Unmineable coal seams	Dissolution	Enhanced coal bed methane recovery (ECBMR)	Grassland and grazing land management
Salt caverns		Algae farming for recycling	Deserts and degraded lands
Basalt formations		Other industrial manufacturing	Wetlands or peat lands
Shale formations			

[a] CO_2 can also be stored in other materials, i.e., through mineral carbonation (IPCC, 2005)

Everywhere under a thin overlay of soils or sediments, the earth's surface is made up primarily of two types of rocks: those formed by cooling magma and those formed as thick accumulations of sand, clay, salts, and carbonates over millions of years. Sedimentary basins consist of many layers of sand, silt, clay, carbonate, and evaporite (rock formations composed of salt deposited from evaporating water). The sand layers provide storage space for oil, water, and natural gas. The silt, clay and evaporite layers provide the seal that can trap these fluids underground for periods of millions of years and longer (Benson and Franklin, 2008).

Sedimentary basins often contain many thousands of meters of sediments, where the tiny pore spaces in the rocks are filled with salt water (saline formations). Oil and gas reservoirs are found under such fine-textured rocks and the mere presence of the oil and gas demonstrates the presence of a suitable reservoir seal. In saline formations, where the pore space is initially filled with water, after the CO_2 has been underground for hundreds to thousands of years, chemical reactions will dissolve some or all of the CO_2 in the salt water, and eventually some fraction of the CO_2 will be converted into carbonate minerals, thus becoming part of the rock itself.

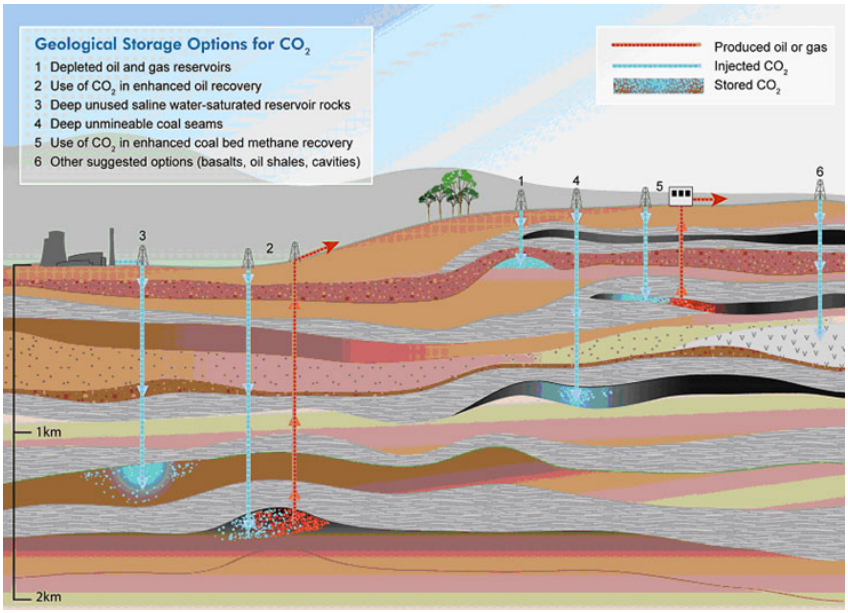

Figure 2.2: Options for geological storage of CO_2 (CO2CRC) [2]

2.2 State of the art of CCS

The first commercial plants with post-combustion CO_2 capture were constructed in the late 1970s and early 1980s in the United States. These projects did not treat CO_2 as a pollutant, but as a new economic resource (Herzog, 2001), separating and injecting CO_2 into oil reservoirs to increase their productivity (EOR). This also led to the first long-distance CO_2 pipelines. However, with the decline of the oil price in the mid-1980s, the separation of CO_2 was too expensive, forcing the closure of these capture facilities. An exception is the North

[2] http://www.co2crc.com.au/

Table 2.2: Operating CCS projects in the power generation industry (Source: WorleyParsons, 2009)

Project name	Capture type	Country	Feedstock	Size	CO_2 use (current or planned)
Sua Pan	Post-combustion	Botswana	Coal	109,500 tpa CO_2, 20MW	Carbonation of brine
Loy Yang Power (LYP)/CSIRO PCC Project	Post-combustion	Australia	Coal	1,000 tpa CO_2	Vent
Munmorah PCC Pilot Plant Project	Post-combustion	Australia	Coal	3,000 tpa CO_2	Vent
Hazelwood Carbon Capture Project	Post-combustion	Australia	Coal	10,000 tpa	Chemically sequestered
Huaneng Co-Generation Power Plant CO_2 Capture Project	Post-combustion	China	Coal	3,000 tpa CO_2	Industrial (food, medical)
Esbjerg Pilot Plant	Post-combustion	Denmark	Coal	8,760 tpa CO_2	Vent
OxPP – Vattenfall Oxyfuel Pilot	Oxyfiring	Germany	Coal	100,000 tpa CO_2, 30MWth	Storage and industrial
Sumitomo Chemicals Plant CO_2 Project	Post-combustion	Japan	Gas, Coal, Oil	54,750 – 60,225 tpa CO_2, 8MWe	Food industry
Nanko Pilot Plant	Post-combustion	Japan	Natural Gas	730 tpa CO_2, Power 0.1 MWe	Vent
Warrior Run Power Plant	Post-combustion	USA	Coal	54,750 tpa CO_2	Food processing and related purposes
Bellingham Cogeneration Facility	Post-combustion	USA	Natural Gas	116,800 tpa CO_2	Food-grade
IMC Global Inc. Soda Ash plant, Trona	Post-combustion	USA	Coal	292,000 tpa CO_2	Carbonation of brine
We Energies Pleasant Prairie Chilled Ammonia Pilot Project	Post-combustion	USA	Coal	15,000 tpa CO_2 at full capacity	Vent
AES Shady Point LLC power plant	Post-combustion	USA	Coal	65,700 tpa CO_2	Food processing

Table 2.3: Operating commercial-scale, integrated CCS projects (Source: WorleyParsons, 2009)

Project name	State/District, Country	Estimated operation date	Capture facility	Capture type	Transport type	Storage type	Appr. CO_2 storage rates
Rangely EOR Project	Colorado, USA	1986	Shute Creek gas processing facility	NG processing	285 km Pipeline	Beneficial reuse (EOR)	1.0 Mtpa
Sleipner	North Sea, Norway	1996	CO_2 separated from produced gas – gas processing platform	NG processing	Pipeline (capture and storage at same location)	Geological (saline aquifer) (16.3 Mt stored at the end of 2008)	1.0 Mtpa
Val Verde CO_2 Pipeline	Texas, USA	1998	Five natural gas processing plants	NG processing	132km Pipeline	Beneficial reuse (EOR)	1.0 Mtpa
Weyburn Operations	Saskatchewan, Canada	2000 (using CO_2 as flooding agent)	Great Plains Synfuels plant, Dakota Gasification	Pre-combustion	330 km Pipeline	Beneficial reuse (EOR)	2.4 Mtpa
In Salah	Ouargla, Algeria	2004	Natural gas processing plant	NG processing	14 km Pipeline	Geological (3.0 Mt stored to date)	1.2 Mtpa
Salt Creek EOR	Wyoming, USA	2006	Shute Creek gas processing facility	NG processing	201 km Pipeline	Beneficial reuse (EOR)	2.4 Mtpa
Snøhvit CO_2 Injection	Barents Sea, Norway	2007	Snøhvit LNG Plant	NG processing	160 km Pipeline	Geological	0.7 Mtpa

American Chemical Plant in Trona, CA, which produces CO_2 for the carbonation of brine. This plant started operation in 1978 and still operates today as the largest CCS-related project in the power generation industry (VGB PowerTech, 2004).

In the last 20 years, there has been a significant outbreak of theoretical and commercial CCS projects. Fortunately, there are available sources keeping track of the progress, providing data for all completed and planned projects around the globe. An overview of large-scale CCS projects in the power generation industry is provided by the Carbon Dioxide Capture and Storage Power Plant Project Database of Massachusetts Institute of Technology (MIT)[3], while a complete list of CCS projects in all different industrial sectors can be found on the website of National Energy Technology Laboratory (NETL)[4]. Additionally, a survey of all available projects is provided in the recent report of the Global CCS Institute (WorleyParsons, 2009). The latter survey is used here to present a short overview of the currently active and planned CCS projects.

In the power generation industry, there are currently 14 operating CO_2 capture projects in the world (Table 2.2), 13 of which use post-combustion technology and 1 that uses oxy-combustion. All of these projects are small-scale, capturing less than 290 ktpa of CO_2, with the majority of them capturing less than 100 ktpa. None include geological storage or EOR. It should be noted that the two largest plants (with 292 and 117 ktpa of CO_2) are located in the USA (projects Trona and Bellingham). Outside the power generation industry, there are 7 commercial-scale[5], integrated[6] projects operating to date, 6 of which perform NG processing (Table 2.3).

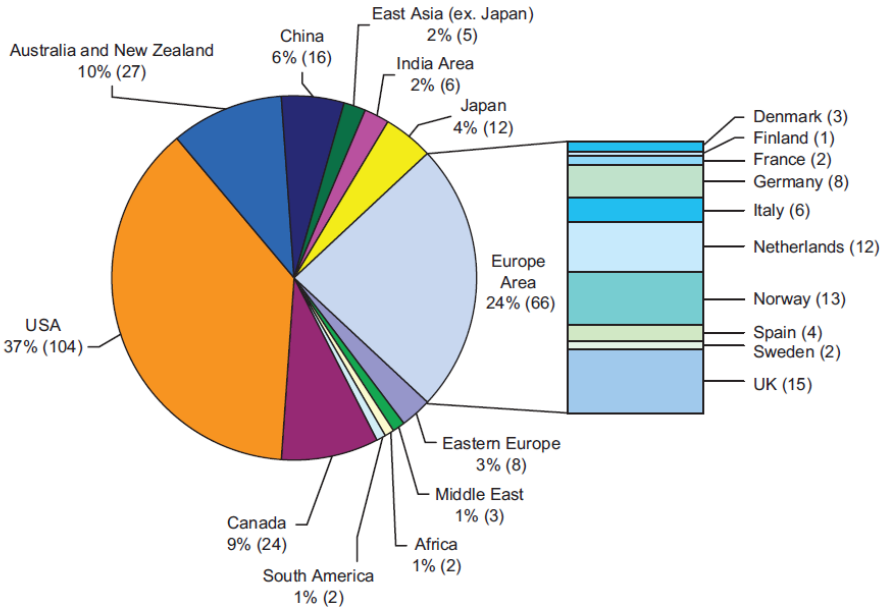

Figure 2.3: 275 CCS projects of all industrial sectors and scales, categorized by country (Source: WorleyParsons, 2009)

[3] http://sequestration.mit.edu/tools/projects
[4] http://www.netl.doe.gov/technologies/carbon_seq/database/index.html
[5] Commercial scale is considered the scale with a storage rate higher than 1Mtpa of CO_2.
[6] Integrated projects are projects that include all three steps of the CCS chain: CO_2 capture, transport and storage.

In total, 499 activities are listed as CCS projects (WorleyParsons, 2009). From these 499 activities, 275 CCS projects[7] are recognized as projects that "produce advancement in components, systems and processes and *support* the commercialization of integrated CCS solutions with emissions greater than 25,000 tpa of CO_2". The breakdown of the projects by countries is shown in Figure 2.3. From the 275 CCS projects, 213 are active or planned, 34 have already been completed, 26 have been cancelled or delayed and from 2 projects, the status was withheld. No integrated projects have been completed at any scale. The breakdown, both by scale and type, of the completed 34, small-scale projects is shown in Table 2.4.

Table 2.4: Completed CCS projects of all industrial sectors (WorleyParsons, 2009)

Bench	Pilot	Demonstration	Commercial	N/C	Capture	Storage	Transport & storage
3	15	10	1	5	18	15	1

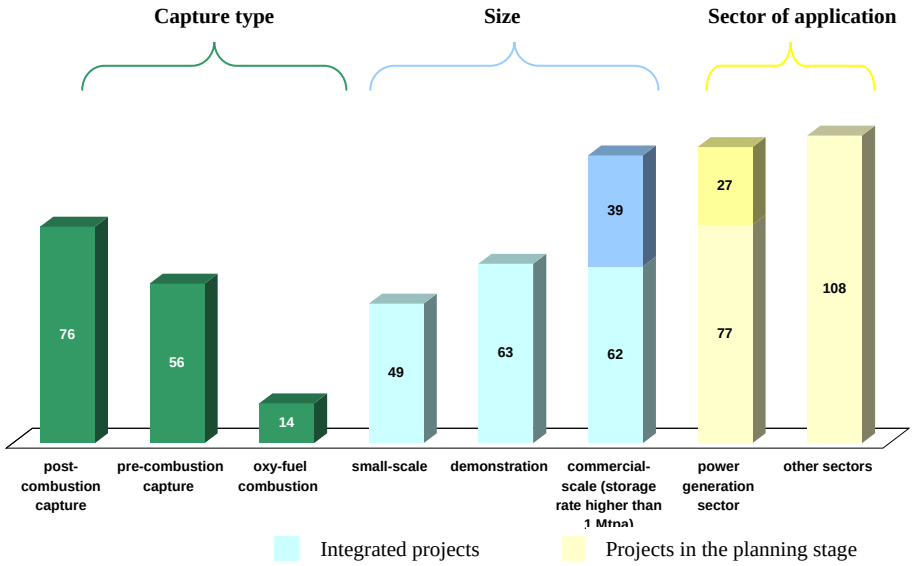

Figure 2.4: Breakdown of the 213[8] active/planned projects classified by capture type (green), size (blue) and sector (yellow) (WorleyParsons, 2009)

Three different breakdowns of the 213 active or planned projects are shown in Figure 2.4 in different colors: the CO_2 capture technology used is shown in green (oxy-fuel is shown separately for clarity), the scale of the plants in blue and the applied sector in yellow. Some additional information is presented in different color shades. It is clear that post-combustion technology is the dominant capture method. 49% of the active or planned projects (105 projects) are in the power generation sector, 77 of which are in the planning stage and 27 (shown in dark yellow) in the stages of construction or operation. In total, 101 are commercial-scale projects, 62 of which are integrated. From the 62 integrated projects, 27 are

[7] Academic studies are not included.
[8] 159 of the 213 active or planned projects employ a form of CO_2 capture.

in Europe, 15 in the United States of America, 7 in Australia, 6 in Canada, 4 in China and 1 in each of the following: Algeria, Malaysia and United Arab Emirates. 41 of the integrated projects are commercial-scale integrated CCS projects in the power generation sector, 38 of them use coal as fuel and most of them integrate geological storage or perform beneficial reuse (EOR; *enhanced gas recovery*, EGR or *enhanced coal bed methane recovery*, ECBMR).

EOR projects are common practice in Canada, USA and the UAE. Due to limited experience in geological storage, on one hand, and the mature technology related to EOR projects on the other, when possible, beneficial use of CO_2 is preferred. Although EOR could incorporate robust *measurement, monitoring and verification* (MMV) systems to evaluate the capacity and quality of a CO_2 storage reservoir, only a limited number of operations include MMV. There are 22 active or planned, commercial-scale, integrated projects with geological storage in Europe. In constrast, only one CCS project has already started performing geological storage in Algeria (In Salah, NG processing in operation since 2004) and one is planned (to operate in 2018) in the United States (Illinois, FutureGen). The storage sites of two facilities in the United States have not been determined yet.

Currently there are three integrated operating projects with CO_2 geological storage (outside the power generation industry): Sleipner operating since 1996, In Salah operating since 2004 (commercial-scale projects) and Snøhvit operating since 2007. In all three of these projects, gas processing is performed. In Sleipner and Snøhvit, offshore storage is being realized to examine the potential for further use of storage sites below the sea floor. There are also another four integrated commercial-scale CCS projects, all of which perform EOR: three in the United States: Rangely in Colorado, Val Verde in Texas and Salt Creek in Wyoming, in operation since 1986, 1998 and 2006, respectively, and one in Saskatchewan, Canada: Weyburn operations, in operation since 2000. The two largest projects are the Salt Creek and the Weyburn, storing 2.4 Mtpa each.

2.3 The plants considered in this study

This thesis compares eight technologies for CO_2 capture in power plants producing electricity. The structure and operation of the systems with CO_2 capture have been based on a base plant without CO_2 capture, the *reference plant*. Basic parameter values were determined for this plant and have been kept constant in the simulations of the plants with CO_2 capture.

To consider comparable power systems, either the fuel input or the power output of the facilities should be kept constant. The choice of a specified power output would lead to different sizes of similar plant components, since, for example, a respective increase in the power output of the *gas turbine* (GT) system would be required to compensate for the power consumed by the CO_2 compression unit. With completely different GT systems, a comparison would not have been meaningful. Thus, the fuel supply has been kept constant for all plants. The resulting output has then been calculated according to structural and operating requirements of each CO_2 capture method. The goal is to reveal to which extent the construction and

Table 2.5*: Main operating parameters (see also Appendix B)

Ambient air
15°C, 1.013 bar, 60% relative humidity
Composition (mol%): N_2 (77.3), O_2 (20.73), CO_2 (0.03), H_2O (1.01), Ar (0.93)

Fuel
14 kg/sec, 15°C, 50 bar, LHV = 50,015 kJ/kg
Natural gas composition (mol%): CH_4 (100.0)

Gas turbine system & CO_2/H_2O gas turbine (GT1 and GT2)
Compressor (C1): polytropic efficiency 94%, mechanical efficiency: 99%, pressure ratio: 16.8
Air turbine (GT1): polytropic efficiency: 91%, mechanical efficiency: 99%, cooling air: 11% of incoming air
CO_2/H_2O turbine (GT2): polytropic efficiency: 91%
Generators: electrical efficiency: 98.5%
Combustion chamber: pressure drop: 3%, losses: 1%, λ=2.05

Steam cycle
HRSG: 1 reheat stage, 3-pressure-levels (except the S-Graz cycle): HP (124 bar), IP (22 bar), LP (4.1 bar)
HRSG pressure drop: hot side: 30 mbar (20 mbar in the S-Graz cycle), cold side: 10% in each pressure-level
SHs, ECONs (HP, IP, LP): ΔT_{min}: 20°C
EVAPs (HP, IP, LP): Approach temperature: 6°C, pinch point: 10°C
Live steam temperature: (ref.plant) 560°C, (plant with CLC) 497°C
Steam turbine polytropic efficiency: HP (90%), IP (92%), LP (87%)
Condenser operating pressure: 0.05 bar, ΔT_{min}: 10°C

MCM reactor:
Pressure drop: 0.07 bar
Oxygen separation: 38%
MCM HTHX outlet temperature: 1250°C

CLC unit (Reactors)
Adiabatic reactors, oxygen carrier: NiO/Ni (no losses)
Inlet pressure: 17 bar
Reactors pressure drop: 3%
Fuel conversion: 98%

Shifters
Pressure drop: 3%

CO_2 compression unit (4 intercooled stages)
Compressors polytropic efficiency (4 stages): see Appendix B
CO_2 end pressure: 103 bar

Cooling water: inlet/outlet temperature: 21°C/31°C
CO_2 condenser exit temperature: 30°C
Coolers exit temperature: 40°C
Coolers pressure drop (4 stages): see Appendix B

Pumps total eff. (including motor) 61 – 90% (see Appendix B)

Chimnie: pressure drop: 0.015 bar

If not otherwise stated, the common components of the plants operate under the same conditions

operation of zero or near-zero emission plants are effective and feasible, from economic, environmental and thermodynamic viewpoints.

The plants with CO_2 capture are: a plant with *chemical absorption using monoethanolamine*, five oxy-fuel plants (a *simple oxy-fuel plant*, the *S-Graz cycle*, two variations of an *advanced zero emission plant* with both 100% and 85% CO_2 capture and a *plant with chemical looping combustion*) and two pre-combustion CO_2 capture plants (a plant with a *hydrogen separating membrane* and a plant with an *autothermal reformer*). These plants have been chosen as representatives of promising technologies for CO_2 capture from power plants, as presented in various references (e.g., Kvamsdal et al., 2007; Bolland and Mathieu, 1998).

In all of the oxy-fuel concepts, the oxygen reacts with the provided fuel in nearly stoichiometric conditions (excess air fraction: λ=1.05) (Kvamsdal et al., 2007). In the remaining plants, the excess air fraction is set by limiting the outlet temperature of the reactors. The fuel used in every simulation is methane. This assumption has been made to simplify the analysis, since the composition of natural gas can differ depending on its source. The ambient conditions, as well as the composition of the input streams, are shown in Table 2.5, where selected operating parameters of the simulated plants are provided. Detailed flow diagrams of the plants and all thermodynamic data (mass flows, temperatures, pressures, compositions) at the stream level are provided in Appendix A. If not otherwise stated, common components of the plants operate under the same conditions as the reference plant. The efficiencies of compressors and expanders considered in each plant are shown in Appendix B. As volumetric components, their isentropic efficiencies are directly related to the volume of the gas used.

The GT system of the plants is simulated with three separate components: a compressor, a *reactor/combustion chamber* (CC) and an expander. This allows the adjustment and examination of the operation of each component separately. To use realistic variables for the simulation of the gas turbine system, the software GateCycle has been used. From the available GT library, the Siemens gas turbine; model V94.3, 50 Hz, with net power of 263 MW was chosen for the reference plant. An increase of 2.5% in the isentropic efficiencies of the system is assumed, in an attempt to account for technological advancement achieved by the time the examined power plants might be realized. The inlet temperature and pressure of the expander of the GT system have been kept constant in all plants, except in the simple oxy-fuel plant and the S-Graz cycle, where the inlet temperature was set to 1400°C and the inlet pressure to 40 bar, according to available literature (see section 2.3.4).

The steam cycle of the plants includes three-pressure-level *heat recovery steam generators* (HRSGs, 124/22/4.1 bar) with one reheat stage, except for the S-Graz cycle, where a single-level HRSG has been used, in order to satisfy the structural requirements of the concept. The overall pressure loss assumed along the hot side (flue gas) of the HRSGs depends on the number of pressure levels in each plant (Appendix B). The distribution of the overall pressure loss to the individual *heat exchangers* (HXs) of the HRSGs depends both on the number of components constituting the HRSGs and on the temperature reduction of the gas in each component (Appendix B).

Each pump and compressor smaller than 3 MW is supplied by a motor. When the power requirement is higher, the component is supplied by integrated *steam turbines* (STs). For

example, *intermediate-pressure* (IP) steam is expanded down to 0.1 bar to produce the necessary power to feed the CO_2 compression units, as well as the recycling compressors (where used). For larger energy demand (due to larger compressor sizes, e.g. the simple oxy-fuel plant and S-Graz cycle), small expanders are used. It is assumed that components on the same shaft operate at the same speed and no gears are required.

Lastly, in all of the plants with CO_2 capture, the CO_2 stream is sent to a *flue gas condenser* (FG COND), where most of the included water vapor is extracted. The almost pure CO_2 is then compressed in a four-stage, intercooled, compression unit to a final pressure of 103 bar. An exception is the ATR plant, where only two CO_2 compressors are used, due to the higher exit pressure of the extracted CO_2 stream. Carbon dioxide at over 100 bar and 30°C is in liquid phase and is ready for transport and sequestration. A more detailed description of specific characteristics of each plant and each CO_2 capture technology is provided in the following.

2.3.1 The reference plant

The *reference plant* is a combined cycle power plant without CO_2 capture, and it is used as the base case for the simulation of plants that incorporate CO_2 capture. A simplified flow diagram is shown in Figure 2.5, while its detailed diagram can be found in Appendix A (Figure A.1.1).

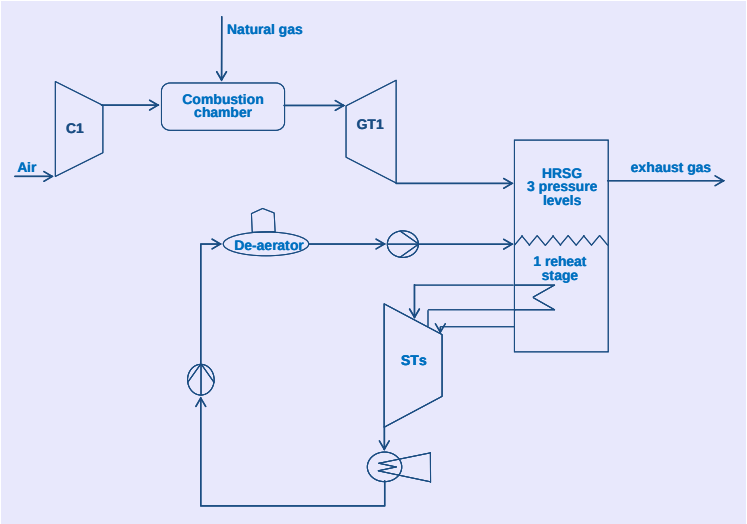

Figure 2.5: Simplified diagram of the reference plant

Flue gas exiting the CC at 628 kg/sec is led to the expander (GT1) of the plant and from there to the HRSG. The combustion products enter the HRSG with a pressure of 1.058 bar at 580°C. In the HRSG, the gas provides thermal energy to produce steam at three pressure levels, 124/22/4.1 bar, and it is then exhausted to the atmosphere at 95°C. High-pressure steam produced at 560°C is expanded to 23 bar in the *high-pressure steam turbine* (HPST) and returns to the HRSG, where it is reheated to 560°C. The reheated steam is sent to the *intermediate-pressure steam turbine* (IPST), where it is expanded to 4.1 bar. The low-pressure steam is then mixed with low-pressure superheated steam from the low-pressure-level HRSG and it is led to the *low-pressure steam turbine* (LPST), where it is expanded to 0.05 bar. The

steam is condensed in the condenser, preheated, led to the de-aerator of the plant and further conveyed to the feed water pumps to continue the cycle. Operating parameters of the plant are provided in Table 2.5.

2.3.2 The plant with chemical absorption using monoethanolamine (MEA plant)

The plant with post-combustion capture bears minimal structural changes when compared to the reference plant. The modifications needed to incorporate CO_2 capture here are: (1) the addition of a *chemical absorption unit* (CAU) at the outlet of the exhaust gases, (2) the extraction of low-pressure steam to produce adequate thermal energy for the regeneration of the chemical solvent used and (3) the addition of STs to drive the flue gas and the CO_2 compressors (C2 & C3-C6 in Figure A.6.1). The last two points result in a significant decrease in the power output and, consequently, in the efficiency of the overall system. A simple diagram of the plant with chemical absorption capture is shown in Figure 2.6. The grey box highlights the additional parts of this plant, when this is compared to the reference plant. The detailed flow diagram of the plant is shown in Figure A.6.1 of Appendix A. The flue gas entering the CAU of the plant consists of 3.9% (v/v) CO_2, resulting in 38 kg/sec of CO_2, 85% of which is captured. The solution used consists of 40% MEA.

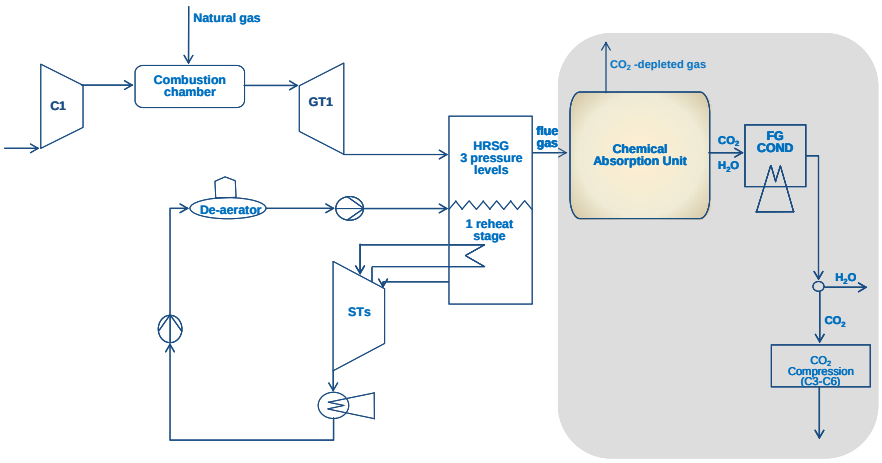

Figure 2.6: Simplified diagram of the MEA plant (grey box highlights differences from the reference plant)

In the CAU, the CO_2-rich gas enters the absorber flowing upwards, counter-current to the lean MEA solution (Figure 2.7). After the CO_2 is absorbed, the clean gas is exhausted to the atmosphere and the CO_2–rich solution is heated in a HX and sent to a regenerator. In the regenerator, low-pressure steam extracted from the ST of the plant provides the necessary thermal energy to regenerate the absorption medium. In this thesis, all of the components included in the CAU have been simulated as a black box with the embedded Equations (2.1)-(2.4) derived from (Rubin and Rao, 2002). Two input streams (the steam that provides the regeneration heat and the exhaust gas of the power plant) and three output streams (the

exiting liquid water, the CO_2 stream and the stream containing the remaining elements of the flue gas) have been considered.

$$\left(L/G\right) = \exp\left(-1.4352 + 0.1239 \times y_{CO_2} + 3.4863 \times \varphi_{lean} + 0.0174 \times \eta_{CO_2} - 0.0397 \times C + 0.0027 \times T_{fg,in}\right) \quad (2.1)$$

$$\left(Q/L\right) = \exp\left(-2.4452 - 0.0037 \times y_{CO_2} - 6.2743 \times \varphi_{lean} + 0.0254 \times C\right) \times 100 \quad (2.2)$$

$$\left(T_{fg,out}\right) = 41.15 + 0.062 \times T_{fg,in} + 1.307 \times y_{CO_2} - 18.872 \times \varphi_{lean} + 0.270 \times C) \quad (2.3)$$

$$\left(mw_{lean}\right) = 16.907 + 2.333 \times \varphi_{lean} + 0.204 \times C \quad (2.4)$$

Here, L is the total sorbent flow rate (kmol/h), G is the total inlet flue gas flow rate (kmol/h), y_{CO_2} is the CO_2 concentration in the inlet flue gas (v/v %), φ_{lean} is the lean sorbent CO_2 loading that represents the part of the leftover CO_2 within the regenerated solvent (mol CO_2/mol MEA), $\dot{Q}$ is the total sorbent regeneration heat requirement (GJ/hr), C is the MEA concentration in the sorbent (w/w %), $T_{fg,in}$ is the temperature of the flue gas entering the CO_2 absorber (°C), $T_{fg,out}$ is the temperature of the flue gas leaving the CO_2 absorber (°C) and mw_{lean} is the average molecular weight of the lean sorbent (kg/kmol).

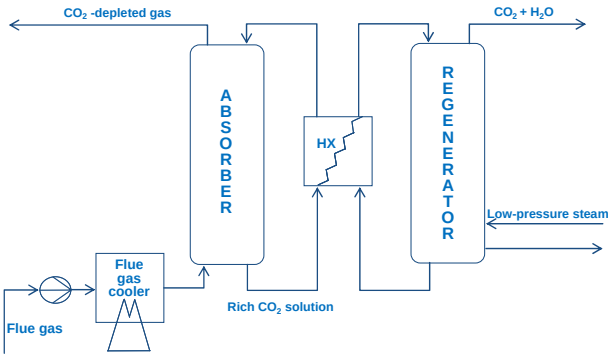

Figure 2.7: Simplified diagram of a CAU

MEA is not included as a chemical compound in the simulation software (EbsilonProfessional, 2010), rendering the calculation of its thermodynamic variables impossible. This leaves us with two choices: either no consideration of solvent losses (φ_{lean}=0) or consideration of losses that cause a minor violation of mass conservation because no MEA input stream is considered. Without lean solvent CO_2 loading, the MEA is assumed to be fully regenerated. This results in a relatively large amount of regeneration energy (6 MW/kg of CO_2 captured). Therefore, the lean solvent CO_2 loading has been varied from 0.0-0.3 mol CO_2/mol MEA. The influence of this variation on the energetic efficiency and on the energy requirement of the plant is shown in Figure 2.8. As can be seen, with mean value of the lean solvent CO_2 loading (0.2 mol CO_2/mol MEA), the energy requirement is reduced from 6 MW/kg of CO_2, calculated without losses, to 3.7 MW/kg of CO_2. In Chapter 4, the MEA plant is evaluated with both 0.0 and 0.2 mol CO_2/mol MEA (MEA-0 and MEA-0.2), to further assess the effect of this variable.

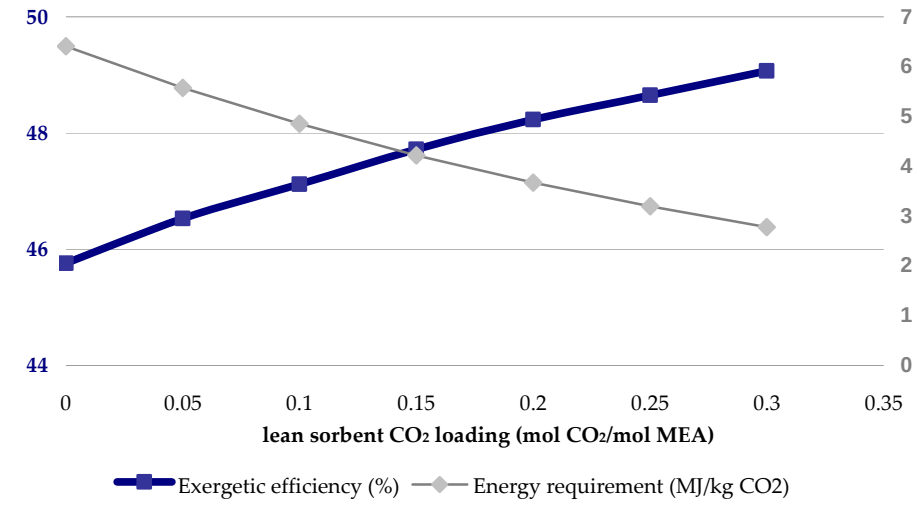

Figure 2.8: Exergetic efficiency (blue line) and energy requirement (grey line) relative to the lean sorbent CO_2 loading

2.3.3 The simple oxy-fuel concept

A simplified diagram of the oxy-fuel plant is shown in Figure 2.9. The detailed flow diagram can be found in Appendix A (Figure A.10.1). The main differences relative to the reference plant are: (1) the incorporation of an ASU and (2) an additional recirculation loop of the flue gas to keep the combustion temperature within acceptable limits.

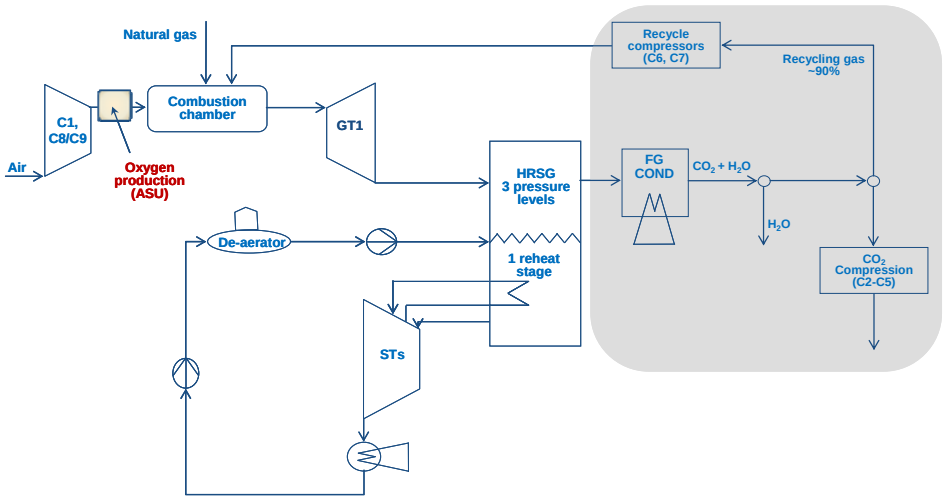

Figure 2.9: Simplified diagram of the simple oxy-fuel plant (grey box highlights differences with the reference plant)

The oxygen stream generated in the ASU contains 95% O_2 and 5% (w/w) Ar. This composition was chosen to avoid the presence of nitrogen in the gas (Anderson et al, 2003; Anderson and Johnsson, 2005). The penalty for O_2 compression is calculated to be ca. 1.5 MJ/kg of O_2 (including compressors C1, C8 & C9 of Figure A.10.1). The CC operates at 40 bar.

After the oxy-fuel combustion, the flue gas passes through the HRSG of the plant and it is led to the FG COND of the plant. Part of the gas is then led to the CO_2 compressor unit, while the rest of the gas is compressed in the recycle compressors (C6 & C7 of Figure A.10.1) and it is sent back to the CC to control the outlet temperature of the combustion products.

2.3.4 The S-Graz cycle

The Graz cycle, developed in 1985 by Jericha (Jericha, 1985), was presented as a combined cycle power plant with a high-temperature steam cycle, using hydrogen as fuel. According to the initial idea, hydrogen and oxygen should be derived from the splitting of water using solar energy. However, the lack of technology related to solar energy in the 1990s made the realization of the initial *Graz Cycle* infeasible. This led to the introduction of fossil fuels to the layout of the concept in 1995 (Jericha and Fesharaki, 1995). The working fluid of the plant consisted of approximately 75% water vapor and 25% CO_2, while changes were also made in 2000 to include the use of syngas instead of methane (Jericha et al., 2000). A reduction in the steam content in favor of a higher concentration of CO_2, with the intent to reduce the compression work was considered, which led to a subsequent reduction of the inlet temperature of the CC. In 2004, the steam content was increased back to its initial values and the name of the cycle was changed to *S-Graz Cycle* (Sanz et al., 2005). This concept considered a relevant increase in the inlet temperature of the CC and a decrease in the amount of thermal energy transferred there by the recycling stream, while the mass flow rate of the cooling steam used for the *high-temperature turbine* (HTT, GT1 & GT2 of Figure A.7.1) of the plant was increased.

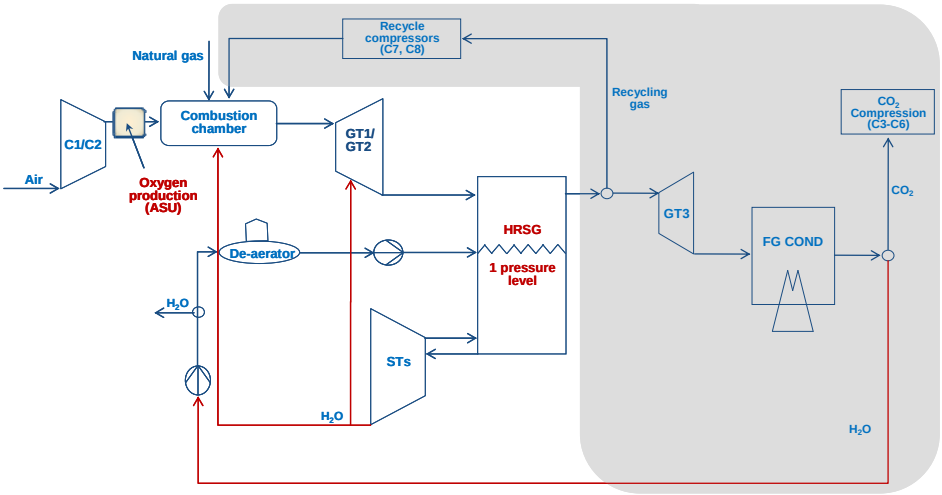

Figure 2.10: Simplified diagram of the S-Graz cycle (grey box highlights differences with the reference plant and red lines show new connections)

A simplified diagram of the S-Graz cycle is shown in Figure 2.10. As in the simple oxy-fuel plant, the penalty for the O_2 (95% O_2 and 5% Ar) compression is 1.5 MJ/kg of O_2 (including compressors C1, C9 & C10 of Figure A.7.1) and the CC operates at 40 bar. After the HRSG, the gas is separated into two parts: one part is led to a *low-pressure gas turbine*

(LPT/GT3) followed by the FG COND of the plant, while the remaining gas is sent back to the CC, after it is compressed in the recycle compressors (C7 & C8, compression with intermediate cooling). The recycling compressors require large amounts of power due to the large mass flow of the recycled flue gas. Thus, they are assumed to be driven by the main expander of the plant, the HTT.

2.3.5 The advanced zero emission plant with 100% CO_2 capture (AZEP 100)

The AZEP with approximately 100% CO_2 capture is referred to here as the *AZEP 100*. The configuration of the AZEP 100 is shown in Figure 2.11, while a detailed diagram of the concept can be found in Appendix A (Figure A.3.1). In the AZEP, the conventional CC of the GT system is replaced by the *mixed conducting membrane* (MCM) reactor, in which the necessary oxygen for the oxy-fuel combustion is produced (Sundkvist et al., 2001 and 2005; Griffin et al., 2005; Möller et al., 2006). The MCM reactor, shown in Figures 2.12 and A.4.1, consists of a mixed conducting membrane, a high- and a low-temperature heat exchanger (HTHX MCM and LTHX MCM in Figure A.4.1), a bleed gas heat exchanger (Air HX) and a CC (Sundkvist et. al., 2007).

The MCM consists of complex crystalline structures, which incorporate oxygen ion vacancies. The operation of the membrane is based on oxygen adsorption. Oxygen atoms of the incoming air are adsorbed onto the surface of the membrane. The atoms are then decomposed into ions and the oxygen ions occupy the oxygen vacancies of the membrane. The transfer of the oxygen ions is counterbalanced by an opposite electron flow. The selectivity of the membranes is infinite as long as the membrane surface is perfect, i.e., no cracks or pores are present. For the purpose of this thesis, the MCM is simulated as a black box using data provided in (Jordal et al., 2004).

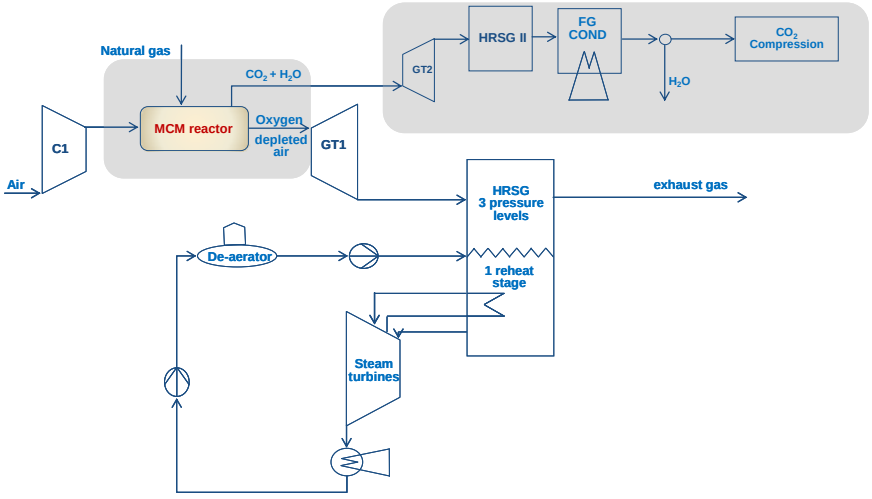

Figure 2.11: Simplified diagram of the AZEP 100 (grey box highlights differences with the reference plant)

In the AZEP, air is compressed in the compressor (C1) of the plant to 17 bar. 90% of the air enters the MCM reactor and it is heated to 900°C in the LTHX of the reactor. Close to 38% of the oxygen included in the air is separated in the MCM and it is transferred at a temperature of 490°C to the reactor's CC with the help of a recycling sweep gas. The circulated sweep gas entering the CC (60% v/v H_2O, 30% v/v CO_2, 10% v/v O_2) is also used to control the temperature of the combustion process. By specifying the mass flow of this gas, and setting the excess air ratio (λ) of the CC, the mass flow of the methane is determined. The methane is preheated to 250°C in a gas-gas heat exchanger (NG PH) before it is sent to the CC of the reactor. The combustion products that consist of 33.5% v/v CO_2, 66% v/v H_2O and 0.5% v/v O_2, expand in a CO_2/H_2O expander (GT2) to 1.051 bar and are then driven to the secondary, single-pressure-level HRSG of the plant. The oxygen-depleted air (14% v/v O_2) exits the MCM at 1000°C and it is heated to 1200°C (restricted due to material and reactor design constraints) in the HTHX of the reactor. It is mixed with 10% of the incoming air, exits the reactor and it is expanded in the main GT of the plant to 1.058 bar and 497°C. The mixture is then sent to the main, three-pressure-level HRSG of the plant. There, the heat provided by the gas is used to produce steam at three pressure levels, as in the reference plant. In the *high-pressure superheater* (HPSH) and the *reheater* (RH) of the plant the steam is heated to a temperature not higher than 477°C, due to the relatively low outlet temperature of the GT system and the predetermined minimum temperature difference in the heat exchangers. Additionally, steam is generated in the secondary HRSG of the plant (HRSG II).

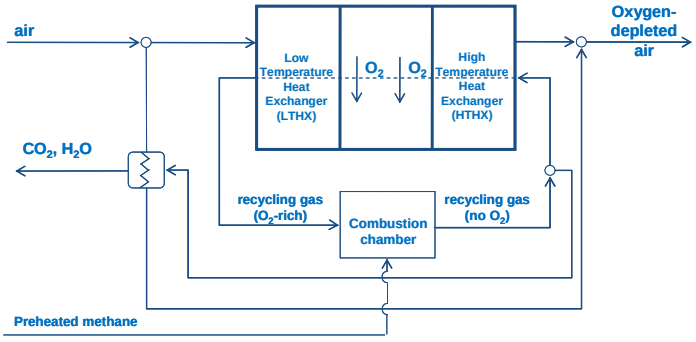

Figure 2.12: Structure of the MCM reactor

2.3.6 The advanced zero emission plant with 85% CO_2 capture (AZEP 85)

The AZEP 85 operates in a similar way to the AZEP 100, but it incorporates a supplementary firing (*duct burner*, DB) at the exit of the MCM reactor (Sundkvist et al., 2005). The DB is used to increase the, otherwise materially-limited, exit temperature of the MCM reactor. The outlet gas temperature of this secondary combustion is near 1300°C, a temperature that enhances the overall efficiency of the plant. Cooling of the turbine blades has not been taken into account in the simulation of this plant. In the supplementary firing, part of the provided fuel is burned with the oxygen left in the oxygen-depleted air. The gas emissions from this supplementary burning process are not treated, thus the CO_2 capture of the plant is decreased by approximately 15%. Since the mass flow of the separated CO_2 in the AZEP 85 is smaller than that of the AZEP 100, the power needed for its compression is lower.

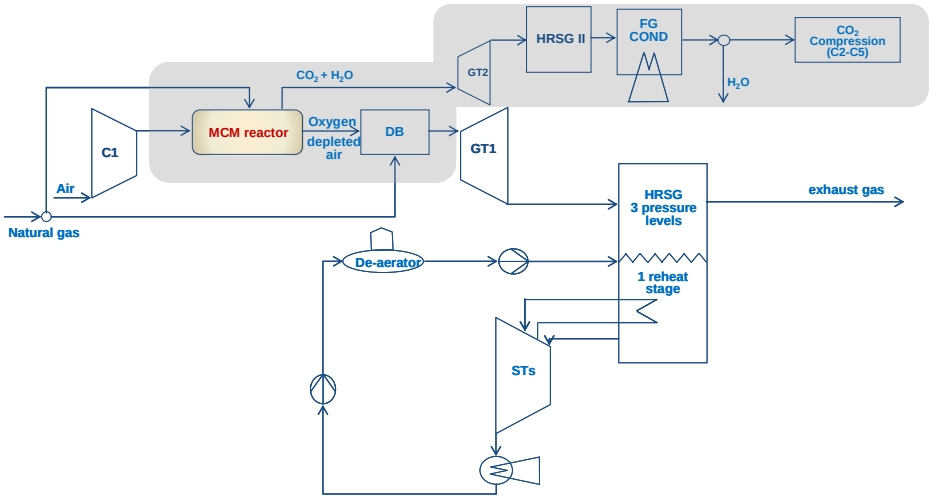

Figure 2.13: Simplified diagram of the AZEP 85 (grey box highlights differences with the reference plant)

Although the structure of the AZEP 85 (Figures 2.13 and A.2.1) is similar to that of the AZEP 100, the temperature profiles of the HXs differ, due to the increased inlet temperature of the expander of the GT system in the case of the AZEP 85. This causes an increase in the inlet flue gas temperature of the main HRSG to 580°C, which is used to heat the steam to 560°C. In this way, the steam cycle works more efficiently in this plant than in the AZEP 100.

2.3.7 The plant with chemical looping combustion (CLC plant)

Previous studies (Richter and Knoche, 1983; Hossain and de Lasa, 2008) show that CLC has the potential to become a relatively efficient and low cost technology. The process was first introduced by Lewis and Gilliland in 1954. In 1968 it was proposed by Knoche and Richter as an option for decreasing irreversibilities in combustion processes, but later it was identified as having important advantages due to its nitrogen-free CO_2 production. This allows minimal contribution to NO_x emissions and also CO_2 separation with minimal thermodynamic losses (Brandvoll and Bolland, 2004; Hossain and de Lasa, 2008). CLC has been examined using natural gas (Brandvoll and Bolland, 2004; Lyngfelt and Thunman, 2005; Abad et al., 2006, 2007; Naqvi and Bolland, 2007; Bolhàr-Nordenkampf et al., 2008; Kolbitsch et al., 2008), synthetic gas (Jin and Ishida, 2004; Abad et al., 2006, 2007; Klara, 2007) and hydrogen (Brandvoll et al., 2003).

In this plant, the conventional CC is replaced by two reactors, an *oxidizing* or *air reactor* (AR) and a *fuel reactor* (FR), as shown in Figure 2.14. A metal oxide is used as a solid oxygen carrier (OC) between these two reactors, thus no direct contact between the air and the fuel takes place. Atmospheric air is introduced into the AR, where the metal (or metal oxide) is oxidized. The metal oxide then exits the AR and it is fed to the FR, where the fuel combusts with the transported oxygen to produce CO_2 and H_2O. At the same time, the metal oxide is reduced and led back to the AR continuing its loop between the two reactors. The resulting carbon dioxide can be easily separated after water condensation, without further costly

energy requirements. The design of the reactors is based on two interconnected fluidized beds and should have advantages over alternative designs, since good contact between the gas and the solid material is required. In recent years, various arrangements of alternative designs of the fluidized beds (Lyngfelt et al., 2001; Mattison and Lyngfelt, 2001; Abad et al., 2006), as well as alternative GT configurations (Brandvoll and Bolland, 2004; Naqvi et al., 2005; Naqvi and Bolland, 2007) for integrating CLC in power plants, have been proposed and examined.

The net reaction of CLC (Figure 2.14) and its heat generation is equal to that of the fuel combustion. The oxidation is an exothermic reaction, whereas the reduction can be either exothermic or endothermic, depending on the fuel and the metal oxide. The OC reduction with CH_4 is endothermic for all oxides examined, with the exception of CuO. Conversely, when syngas is used, the metal reduction is always exothermic. This can be considered as an advantage of coal-gas use when compared to CH_4, since the coal-gas reaction is driven with stronger intensity due to its exothermic character. Part of the produced thermal energy during the oxidation is used in the reduction, if the latter is endothermic.

Many different metals have been suggested as oxygen carriers, mainly based on nickel, Ni (Brandvoll and et., 2003; Jin and Ishida, 2004; Lyngfelt and Thunman, 2005; Johansson et al., 2006; Bolhàr-Nordenkampf et al., 2008; Kolbitsch et al., 2008), iron, Fe (Johansson et al., 2006; Abad et al., 2007; Klara, 2007) and manganese, Mn (Abad et al., 2006; Johansson et al., 2006). Important factors are the reduction and oxidation rates, the chemical and mechanical stabilities, as well as the price and the environmental characteristics of the oxidizer. Generally Ni and its corresponding oxides show higher oxidation and reduction rates compared to Fe and Mn, as well as greater durability after many repeated cycles. A detailed status of the development with respect to oxygen carrier alternatives is presented in Lyngfelt et al. (2008).

The compressed air and the preheated methane are sent to the CLC reactors that are simulated here as a black box. In the FR, 98% of the methane provided is assumed to react with oxygen transferred from the AR. The remaining unreacted 2% of the fuel is not recycled back to the fuel reactor, but is regarded as a loss. The air ratio – the ratio between the oxygen included in the air and the oxygen needed for stoichiometric combustion – required to achieve outlet temperatures of the air and the fuel reactors of 1200°C and 930°C, respectively, is set to 2.9. These temperatures are also the inlet temperatures of the expanders of the plant, for which no cooling has been taken into account. It has been suggested that the inlet temperature of the CO_2/H_2O expander (GT2) should be as low as 900°C, to increase the conversion of the fuel in the FR and the energy available for oxidation of the metal in the AR (Lewis and Gilliland, 1954; Brandvoll and Bolland, 2004; Bolhàr-Nordenkampf et al., 2008, Abad et al., 2007; Naqvi and Bolland, 2007). With this lower temperature, a lower cost for the expander is also achieved. A higher temperature in the FR, equal to that at the outlet of the AR could bring an increase in the energetic efficiency of about 1 percentage point (to 54.2%), if the CH_4 conversion is assumed to remain constant. A Ni-based OC is considered, and the CH_4 reacting is fully converted to CO_2. A simplified diagram of the energy conversion plant is shown in Figure 2.15, while the detailed can be found in Appendix A (Figure A.5.1).

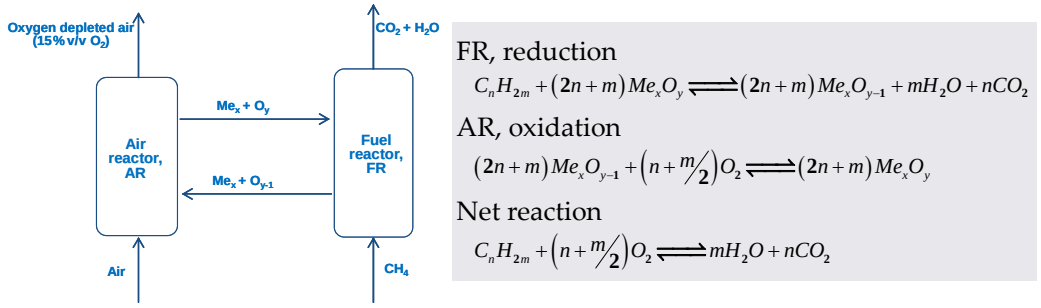

Figure 2.14: Configuration of the CLC unit and the chemical reactions

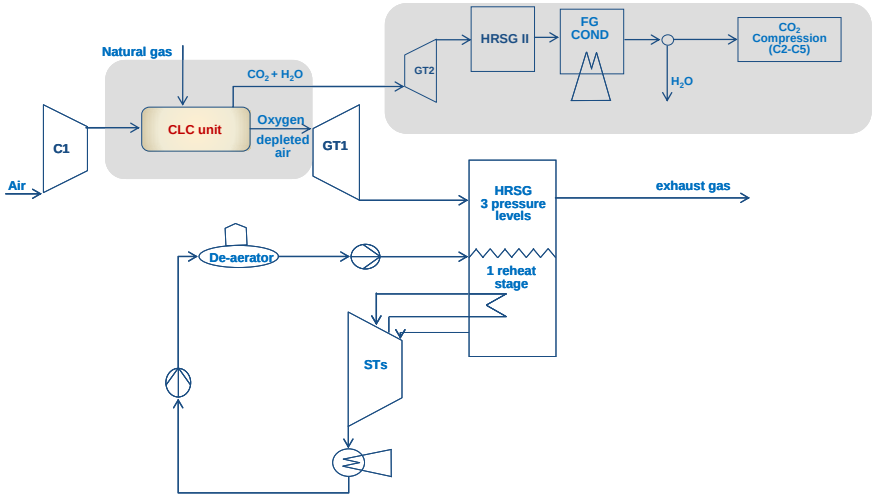

Figure 2.15: Simplified diagram of the CLC plant (grey box highlights differences with the reference plant)

The two streams exiting the CLC unit are the combustion products, consisting of CO_2 and water vapor, and the oxygen depleted air, consisting of 15% v/v O_2. The oxygen depleted air exits the main GT system at 659 kg/sec and it is led to the main HRSG of the plant. The high-pressure steam produced has a temperature of 500°C, which is lower than that of the reference case due to the lower temperature at the exit of GT1 and the minimum temperature difference defined in the HXs (ΔT_{min}=20°C). The combustion products (CO_2 stream) are expanded in a CO_2/H_2O expander (GT2) and are then sent to a secondary HRSG (HRSG II), where additional steam is produced. The CO_2-rich gas is finally cooled in a FG COND and compressed.

2.3.8 The plant using a methane steam reforming membrane with hydrogen separation (MSR plant)

This plant incorporates a hydrogen-separating membrane reactor (Figures 2.16 and A.9.1). The included membrane uses thermal energy from the flue gas to reform the fuel entering the plant into CO_2, H_2 and H_2O. 99.7% of the generated hydrogen is automatically

separated in the membrane, swept by intermediate-pressure steam at 17 bar and led to the CC of the plant. The remaining produced gases (CO_2 and H_2O) exit the membrane and the CO_2 is captured after water condensation (Jordal et al., 2004; Johannessen and Jordal, 2005).

The provided methane is mixed with steam (mass ratio 1:4) extracted from a HPST (50 bar). The mixture is preheated and led to the feed side of the reactor at a temperature of 600°C (Figure 2.17). The reforming process is a strongly endothermic reaction, for which thermal energy is provided by the combustion products of the plant. After the reforming process, the exothermic shifting reaction follows. 99.8% of the incoming methane is reformed and 99% of the produced CO is shifted (Bottino et al., 2006). The membrane separates the feed and permeate sides of the reactor. The hydrogen formed is continuously transported through the membrane and swept by IP steam provided to the permeate side of the reactor. To have sufficient energy for the reforming process of the reactor and for the HRSG of the plant, a supplementary firing is added after the CC, increasing the temperature of the combustion gases to 960°C (Jordal et al., 2004).

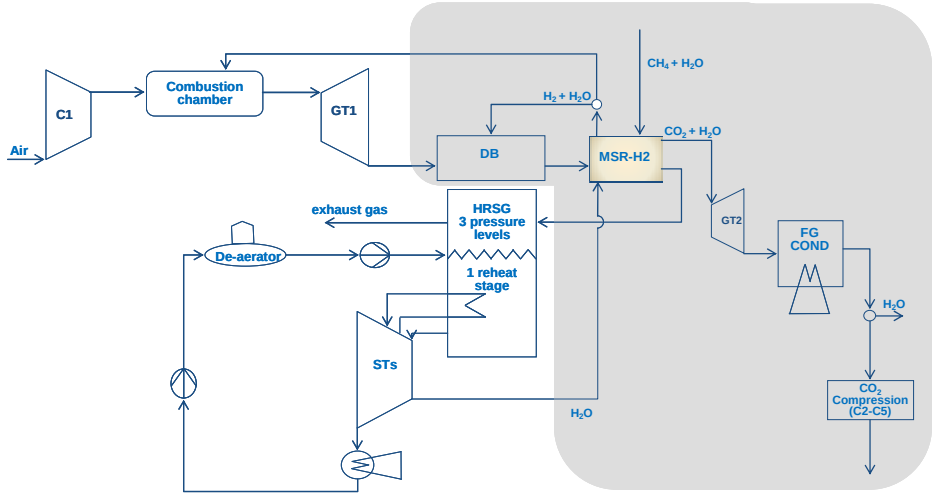

Figure 2.16: Simplified diagram of the MSR plant (grey box highlights differences with the reference plant)

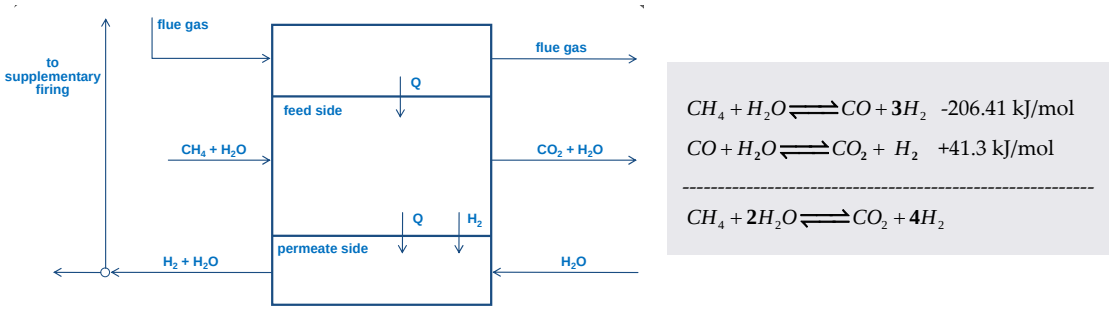

Figure 2.17: Configuration of the MSR reactor and the chemical reactions

2.3.9 The plant using an autothermal reformer (ATR plant)

In the ATR, both partial and complete combustion give the necessary heat for reforming the methane. In more detail, an ATR consists of an adiabatic vessel where the catalyst is placed and the three main reactions shown on the right side of Figure 2.18 can be considered (Horn et al., 2007). While the first and second reactions are the *steam reforming* and *water shift* reactions, respectively, the third reaction is a combination of the total combustion that usually takes place in an oxygen-rich environment and *catalytic partial oxidation* (CPO). CPO has received considerable attention in recent years because of its close to 100% CH_4 conversion and its high H_2 yields. The amount of methane converted in the reaction depends on the steam to carbon (S/C) and the carbon to oxygen (C/O) ratios. As a result of the work of Luwei Chen et al. (2007), an optimal C/O inlet ratio of 2 was set for an ATR operating at 15 bar and 850°C, allowing x and y of the CPO to be set to 1.2 and 0.9, respectively, as shown in Equation 2.5. The S/C ratio was also set to 2.

$$CH_4 + 0.95O_2 \rightleftharpoons 1.2H_2 + 0.9CO + 0.8H_2O + 0.1CO_2 \tag{2.5}$$

The necessary air is supplied by compressor extraction (Figures 2.18 and A.8.1). The equilibrium temperature of the mixed stream is approximately 380°C, a temperature too low for the ATR working at 850°C. For this reason, a HX is used for the preheating of the gas stream. The ATR outlet stream, a mixture of the combustion and the reforming products, exits the unit at 850°C and is used to preheat the ATR inlet stream to 640°C. After the ATR, the gas is sent to the two shift reactors of the plant, where the produced CO is converted to CO_2 and H_2O. The simulation of the shift reactors has been realized with the calculation of the equilibrium

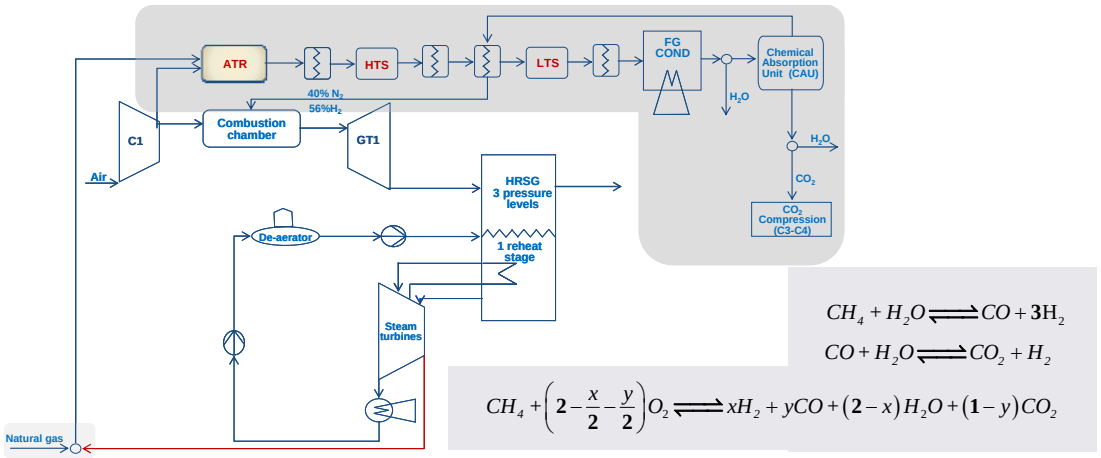

Figure 2.18: Simplified diagram of the plant with an ATR (grey box highlights differences with the reference plant)

constants of the reaction, which is controlled by the equilibrium temperature. Because of the high percentage of nitrogen in the gas, chemical absorption is needed to capture the produced CO_2. Therefore, the gas is sent to a CAU (CAU, Figure A.8.1) after it is cooled to 60°C (otherwise the volume of the stream would require a larger CO_2 capture unit). The necessary thermal energy for the regeneration of the chemical solvent (MEA) is provided from low-pressure steam extraction. After the CAU, the captured CO_2 is led to the compression unit, while the rest of the hydrogen-rich gas (fuel) is sent to the CC.

2.4 Simulation software

All simulations have been performed with versions *6.0* and *7.0* of the software *EbsilonProfessional* (EbsilonProfessional, 2010). *GateCycle* (GE Enter Software LLC, 2000), *AspenPlus* (Aspen Plus, 2009) and *EES* (EES, 2009) have been used redundantly, for operational and programming confirmation. The software *EbsilonProfessional* has been chosen as the main simulation software because of its easily accessible modelling options. User-programmable components were necessary in this study, because many of the required components in CO_2 capture technology have not yet been included in commercially available simulation software.

2.5 Preliminary comparison

2.5.1 Simulation results

All plants with CO_2 capture, except the AZEP 85, the MEA and ATR plants, perform with approximately 100% CO_2 capture. As shown in Table 2.6, the best performance was achieved by the two AZEPs (with the AZEP 85 first) and the CLC plant. Comparing the simple oxy-fuel plant and the S-Graz cycle, some differences should be noted. Relative to the simple oxy-fuel plant, GT1 in the S-Graz cycle results in a higher power output, although the expander drives much larger recycle compressors. This power difference stems mainly from the large amount of water vapor, reaching the 87% v/v, in the expanded gas in the case of the S-Graz.

A large efficiency decrease was also found for the MSR plant. In this plant, less power is produced in the GT and ST systems, while more power is required by the CO_2 compressors than, for example, in the other pre-combustion technology, the ATR plant. Thus, the overall net power of the MSR plant is found to be lower than that of the ATR plant.

The operation of the MEA plant differs depending on the lean sorbent CO_2 loading (i.e., the prescribed solvent losses). When a higher value is assumed, the regeneration requirement of the plant decreases, resulting in an increased net power output (i.e., increased plant efficiency).

A more detailed comparison and evaluation of the plants is provided in Chapter 4, where the results of the exergy-based analyses are presented.

Table 2.6: Efficiency, generated power, and internal power consumption of the plants (shown in order of descending efficiency)

	Ref. plant	**AZEP 85**	**AZEP 100**	**CLC**	**S-Graz**	**MEA[a]**	**ATR**	**MSR**	**Simple oxy-fuel**
Energetic efficiency (%LHV)	58.9	55.7	53.9	53.7	50.3	50.5 (47.8)	48.5	47.8	44.8
GT1 – $\dot{W}_{net}$, after generator (MW)	288.0	239.6	232.0	239.6	285.1 [b]	288.0	268.7	257.0	243.0 [d]
STs – $\dot{W}$ after generator (MW)	125.7	97.9	83.6	86.2	30.4	67.0 (47.8)	72.5	44.1	104.6
GT2 - after generator (MW) [c]	-	53.7	63.1	51.4	69.5	-	-	50.8	-
Additional ST(s) (MW)	-	21.1	24.8	15.7	-	33.3	9.9	-	19.1
CO_2 compressors, (MW)	-	-13.8	-16.3	-15.7	-18.8	-14.7 (13.9)	-5.6	-16.0	-19.1
Recycle/ fuel compressors (MW)	-	-7.3	-8.6	-	-225.2	-	-4.3	-	-118.5
Flue gas compressor (MW)	-	-	-	-	-12.5 (C2)	-18.5	-	-	-
ASU compressors (MW)		-	-	-	-34.2	-	-	-	-34.1
Remaining components (MW)	-1.2	-1.3	-1.2	-1.1	-1.5	-1.2	-1.3	-1.3	-1.2
Net Power output (MW)	412.5	389.9	377.5	376.0	352.0	353.8 (334.6)	339.8	334.5	312.3

[c] Results for 0.0 and 0.2 mol CO_2/mol MEA lean sorbent CO_2 loading

[b] The GT of the S-Graz cycle (GT1 & GT2) drives the air, the recycle and the ASU compressors (C1, C7-C10)

[c] In the S-Graz cycle this turbine refers to the low-pressure gas turbine (GT3)

[d] In the simple oxy-fuel plant the GT1 drives the recycle compressors (C6 and C7)

2.5.2 Additional considerations

When different plants are compared, several parameters must be taken into consideration. These parameters differ among the plants and depend on, among other things, structure, technology and operation.

An important criterion is that some of the plants presented in this thesis employ already commercialized technology (e.g., the MEA and the ATR plants), whereas others include components not yet available on the market. These are, therefore, components of uncertain effectiveness, cost and operation.

The plant that could be applied with the least possible implementation challenges is the MEA plant, since its structure is approximately the same as that of the reference plant. Furthermore, its operation mainly depends on the chemical chosen. In contrast, the operation of the other power plants depends on a combination of factors, such as material and technology development (like membrane, ASU and turbine development). These factors, that determine the plant availability, cannot be estimated easily.

Furthermore, some of the plants are more complex than others, since they include structural subsystems, like recirculation gas routes (e.g., the simple oxy-fuel plant and the S-Graz cycle). The higher the number of these subsystems, the more challenging and involved the operation of a plant becomes.

Although not considered here, another criterion for the evaluation of a plant could be the quantity of resources (e.g., water) required. In some plants, like in the ATR and MSR plants, the need for a constant additional water supply is dominant. This would demand specific conditions and extra environmental consideration.

Safety and maintainability are also very important issues to consider when CCS technologies are considered. Components under development should satisfy safety constraints and must be examined under realistic conditions. More safety issues are

associated with the sequestration of the CO_2, where all possible options must be thoroughly examined and their viability must be guaranteed before large-scale facilities for CO_2 capture are established.

Uncertainties related to the above-mentioned points have not been considered in this thesis because they lie outside its scope, but they should be considered in the future.

3. Methodology – exergy-based analyses

3.1 State of the art

Exergy as an idea was conceived in the 19th century by Carnot, but the concept was applied to industrial processes in the 20th century. The theoretical foundations of the exergetic analysis (formulated well before 1970) have been further expanded and supported by a large number of published work over the last 40 years. Thus, the use of exergetic analysis has developed rapidly and its connection to economic (*exergoeconomic analysis*) and environmental (e*xergoenvironmental analysis*) principles was only a matter of time, practice and expertise.

The idea of combining exergy with costs was first introduced in the beginning of the 1930s by J. H. Keenan (1932), while the first application to an air separation plant was presented in an unpublished lecture in 1949 by M. Benedict and E. Gyftopoulos (1980). In the 1960s, an application of the methodology to the optimal selection of steam piping by Obert and Gaggioli (1963) was realized. During that period numerous activities and publications by a large group of scientists set the foundations of the methodology (e.g., Evans and Tribus, 1962, 1965; El-Sayed and Evans, 1970; El-Sayed and Aplenc, 1970). Further applications are those of Bergmann and Schmidt (1965), Szargut (1967, 1971, 1974), Gaggioli (1977), Fehring and Gaggioli (1977), Gaggioli et al. (1978), Wepfer (1979, 1980), Beyer (1972, 1978, 1979), Knoche and Funk (1977) and Eisermann (1979). In 1984, the term *exergoeconomics* was introduced, by Tsatsaronis (1984) as an accurate and unambiguous characterization of a combination of economics with the exergy concept. Later contributions to the field include those by Valero (1986, 1989, 1994), Lozano and co-workers (1986, 1994, 1989), Frangopoulos (1983, 1987, 1988, 1992, 1994), von Spakovsky (1986, 1994), Knoche and Hesselmann (1985, 1986), Lazzaretto and Andreatta (1995), Toffolo and Lazzaretto (2003), Verda and Borchiellini (2002) and the research groups of Tsatsaronis (Tsatsaronis and Winhold, 1984, 1985a, 1985b, 1986; Lin and Tsatsaronis 1993; Tsatsaronis, 1987, 1993, 1995, 1999a, 2008, 2009; Tsatsaronis and Pisa, 1994; Tsatsaronis and Krane, 1994; Tsatsaronis and Moran, 1997; Lazzaretto and Tsatsaronis, 1997, 2006; Morosuk and Tsatsaronis, 2008a, 2009a, 2009b, Petrakopoulou et al., 2010a-f; Tsatsaronis et al., 1989, 1990, 1991, 1992a, 1992b, 1993, 1994a, 1994b, 2006, 2008, 2009, Tsatsaronis and Cziesla, 2002, 2009).

The common thread behind all exergoeconomic methodologies is the use of exergy instead of energy as the commodity of value, and the application of the *exergy costing principle*, i.e., the assignment of costs to exergy. Exergoeconomic methods can be divided into two main groups: (1) exergoeconomic accounting methods (e.g., Obert and Gaggioli, 1963;

Gaggioli, 1977; Tsatsaronis, 1984; Valero et al., 1986) and (2) Lagrangian-based approaches (e.g., Evans and Tribus, 1965; Frangopoulos, 1983; Tribus and El-Sayed, 1980, 1981, Evans et al., 1983).

In exergoeconomic accounting methods, cost balances are explicitly formulated and resources used in the production process are valued at the costs at which they were purchased or generated. The aim is to (a) provide product stream costs, (b) evaluate components and systems, and (c) iteratively improve energy systems. The Lagrangian-based approaches use mathematical techniques to calculate costs. These methods aim to allow optimization of a system as a whole and the calculation of marginal costs.

Accounting and Lagrangian-based methods are interrelated, since their development took place in the same time period, under similar considerations and on similar theoretical bases. When the fuel and product definitions are the same, the costs calculated by both methods are the same. It can also be proven that the cost balances and auxiliary equations used in accounting methods can be obtained through derivatives in the Lagrangian-based approaches. As a result, the use of one methodology or another differs only in practical implementation. Accounting methodologies have no limitations with respect to the complexity of the system being considered. Lagrangian-based methods are limited when complex systems are considered. Therefore, there have been no new developments or interesting applications of these methods in recent years. In addition, the books that deal with some aspects of exergoeconomics (e.g., Moran, 1982; Kenney, 1984; Kotas, 1985; Szargut et al., 1988; Bejan et al., 1996; El-Sayed, 2003) are outdated. In this thesis, accounting methods have been used.

Although exergoeconomics have been applied over the last few decades, the exergoenvironmental analysis appeared only very recently (Tsatsaronis and Morosuk, 2008a, 2008b; Meyer, 2009). This analysis basically aims to modify the exergoeconomic analysis to convert the problem from involving an economic assessment to involving an ecological evaluation.

The main objective of the implementation of an exergy-based approach is to find appropriate trade-offs between fuel cost and investment cost or environmental impact, in order to improve a process. Nonetheless, the *conventional* exergy-based analyses, mentioned above, have some significant limitations: they do not provide information about (1) component interactions or (2) real potential for improvement (Tsatsaronis, 1999b). To address the shortcomings of the conventional methods, *advanced exergetic, exergoeconomic and exergoenvironmental analyses* were developed. In advanced exergy-based analyses, the thermodynamic inefficiencies, costs and environmental impacts associated with each plant component are split into endogenous/exogenous, avoidable/unavoidable parts, as well as into their combined parts: avoidable endogenous/exogenous and unavoidable endogenous/exogenous parts (Tsatsaronis and Park, 2002; Tsatsaronis and Morosuk, 2007a, 2007b, 2010; Cziesla et al., 2006; Morosuk et al., 2008a; Morosuk and Tsatsaronis, 2006, 2007, 2008b; Kelly et al., 2009).

The advanced exergy-based analyses have been developed in the last 10 years (Tsatsaronis, 2008). These analyses provide valuable information about how, and to what extent, changes in a plant component affect the operation, costs and environmental impact of

the remaining plant components and the overall plant. In addition, with these approaches the real potential for improvement is revealed through the distinction between avoidable and unavoidable parts. Such results save engineering time and shed light onto the necessary steps needed for the optimization of a system. Until today, advanced exergetic and exergoeconomic analyses have only been applied to relatively simple systems (Morosuk and Tsatsaronis, 2006, 2008a, 2009a; 2009b, 2010; Tsatsaronis et al., 2007a, 2007b, 2009, 2010), while applications of the advanced exergoenvironmental analysis have not yet been completed. This thesis is the first complete application of advanced exergetic, exergoeconomic and exergoenvironmental methods to complex power plants.

3.2 Conventional exergy-based analyses

Conventional exergetic, exergoeconomic and exergoenvironmental analyses constitute a rigorous evaluation of energy conversion systems. In exergoeconomic and exergoenvironmental analyses, investment costs and environmental impacts, calculated through an economic analysis and an *life cycle assessment* (LCA), respectively, are linked to irreversibilities (Meyer, 2009; Tsatsaronis and Morosuk, 2008a, 2008b; Petrakopoulou et al., 2010a, 2010b). A detailed description of the results of each analysis is provided below, while the application of the methods is described in Appendix B.

3.2.1 Exergetic analysis

An exergetic analysis reveals the locations and causes of inefficiency and loss in an energy conversion system and provides insight into factors that cannot be found with an energetic analysis. For a considered process, the exergetic analysis consists of a system of balance equations, stated at the component level, and a general equation for the overall system. The *rate of product exergy* of component *k*, $\dot{E}_{P,k}$, is the exergy of the desired output resulting from the operation of the component, while the *rate of fuel exergy* of the same component, $\dot{E}_{F,k}$, is the expense in exergetic resources for the generation of the desired output. The *rate of exergy destruction* within component *k*, $\dot{E}_{D,k}$, is calculated as the difference between its rate of fuel and product exergy ($\dot{E}_{D,k} = \dot{E}_{F,k} - \dot{E}_{P,k}$). For the analysis at the component level, streams exiting a component are considered either as part of the product, or they are used in the definition of the component's fuel. Thereafter, *exergy loss* is only defined for the overall system (tot): $\dot{E}_{L,tot} = \dot{E}_{F,tot} - \dot{E}_{P,tot} - \dot{E}_{D,tot}$.

The exergetic efficiencies of component *k* and the overall system consisting of n-components are defined by Equations (3.1) and (3.2), respectively:

$$\varepsilon_k = \frac{\dot{E}_{P,k}}{\dot{E}_{F,k}} = 1 - \frac{\dot{E}_{D,k}}{\dot{E}_{F,k}} \tag{3.1}$$

$$\varepsilon_{tot} = \frac{\dot{E}_{P,tot}}{\dot{E}_{F,tot}} = 1 - \frac{\sum_{k=1}^{n} \dot{E}_{D,k} + \dot{E}_{L,tot}}{\dot{E}_{F,tot}} \tag{3.2}$$

General guidelines for the definition of exergetic efficiencies have been proposed in Lazzaretto and Tsatsaronis (2006). In dissipative components, like condensers, intercoolers and throttling valves, exergy is destroyed without any useful product in the component itself; thus, no exergetic purpose can be defined (Bejan et al., 1996; Lazzaretto and Tsatsaronis, 2006). The essential role of these components is to serve other plant components, leading to a more efficient operation of the overall system.

Variables of the exergetic analysis, related to exergy destruction and exergy loss are the exergy destruction ratio (defined both at the component level and the overall system, Equations (3.3) and (3.4) and the exergy loss ratio (defined only for the overall plant, Equation 3.5).

$$y_{D,k} = \frac{\dot{E}_{D,k}}{\dot{E}_{F,tot}} \tag{3.3}$$

$$y_{D,tot} = \frac{\dot{E}_{D,tot}}{\dot{E}_{F,tot}} \tag{3.4}$$

$$y_{L,tot} = \frac{\dot{E}_{L,tot}}{\dot{E}_{F,tot}} \tag{3.5}$$

The exergy destruction ratio is a measure of the contribution of the exergy destruction within each component to the reduction of the overall exergetic efficiency. It can be used to compare dissimilar components of the same system, while the total exergy destruction and exergy loss ratios can be used to compare different thermodynamic systems.

With the exergetic analysis the main sources of thermodynamic irreversibilities within a plant are identified. If necessary, modifications to the plant can then be applied, in order to reduce these inefficiencies. Since the adoption and/or the development of systems are mainly driven by economics, the thermodynamically optimal design can be used as the starting point for cost reduction and eventually for cost minimization. Nowadays, the concept of *cost* could also be substituted with *environmental impact*, since a rapid increase in energy demand is foreseen that will impact the environment significantly.

The methodology of an economic analysis and an LCA (as they apply to thermodynamic systems), as well as their combination with an exergetic analysis, are described below.

3.2.2 Exergy and economics

3.2.2.1 Economic analysis

Through an economic analysis, the economic feasibility of the construction and operation, as well as the cost of the generated product of a facility can be estimated. To conduct an economic analysis, different approaches can be used. In this thesis the *total revenue requirement* (TRR) method is used (Bejan et al., 1996).

The most troublesome part of cost estimates for large power stations is the calculation of the *purchased equipment cost* (PEC). A wide variety of data relating size and cost of different types of components can be found in literature. However, most of these data consider facilities much smaller than large-scale power stations. To calculate costs of large-scale components using available data that consider reference equipment of different capacity, a scaling exponent must be determined and used. This exponent, α, is assumed to stay constant within a given size range and it is usually lower than unity, expressing that a percentage increase in the equipment cost is smaller than the percentage increase in capacity (Bejan et al., 1996):

$$C_Y = C_W \left(\frac{X_Y}{X_W} \right)^{\alpha} \tag{3.6}$$

Equation 3.6 is used to calculate the cost of purchased equipment (C_Y) of a new capacity (X_Y), when a given cost (C_W) at a certain capacity (X_W) is known. In absence of specific cost information an exponent value of 0.6 may be used.

When a base cost, C_B, representing the cheapest possible design with basic materials at low temperature and pressure is known, different factors depending on material, temperature, pressure and design, (f_m, f_T, f_p, f_d) should be determined to estimate the *fixed capital investment* (FCI). The cost of the module (i.e, the FCI) is then calculated as: $C_M = C_B f_m f_T f_p f_d f_{BM}$. The bare module factor f_{BM} considers any supporting equipment and connections required, and it also includes all indirect costs related to the equipment. The PEC is then calculated as a percentage of the FCI using specified modular factors (e.g., Guthrie, 1974).

When all costs have been calculated, they must be brought to the same reference year that is used as the base year for all cost calculations (*ref.*). This is realized using cost indices that are basically inflation indicators for both the reference year and the year of the calculated, known costs (*calc.*):

$$C_{ref.Y} = C_{calc.,Y} \frac{Index_{ref.}}{Index_{calc.}} \tag{3.7}$$

From the PEC, the cost rate $\dot{Z}_k$ of each component *k* is estimated using Equation (3.8).

$$\dot{Z}_k = \frac{(carrying\_charges + O\&M)}{(PEC_{tot} \times \tau)} \times PEC_k \tag{3.8}$$

Here, τ represents the annual operating hours and O&M the operating and maintenance costs of the plant. The carrying charges are calculated subtracting the fuel and O&M costs of the plant from its TRR (Bejan et al., 1996). $\dot{Z}_k$ is associated with both the *investment cost* (IC) and the O&M costs of component k ($\dot{Z}_k = \dot{Z}_k^{IC} + \dot{Z}_k^{O\&M}$), but it is mainly determined by the investment cost. The calculated cost rates are used as input for the exergoeconomic analysis.

3.2.2.2 Exergoeconomic analysis

An exergoeconomic analysis is an appropriate combination of an exergetic analysis with economic principles. This is achieved through exergy costing, by which a specific cost c is assigned to each exergy stream of the plant. The specific cost of stream i, c_i, multiplied by the exergy of the same stream, $\dot{E}_i$, provides the cost rate $\dot{C}_i$, associated with stream i:

$$\dot{C}_i = c_i \dot{E}_i \tag{3.9}$$

To perform an exergoeconomic analysis on a plant, cost balances are stated at the component level resulting in a system of balance equations. For example, the cost balance of component k is stated as follows:

$$\sum_{i=1}^{l} \dot{C}_{i,k} - \sum_{j=1}^{m} \dot{C}_{j,k} + \dot{Z}_k = 0 \tag{3.10}$$

Here, $\sum_{i=1}^{l} \dot{C}_{i,k}$ is the sum of the cost rates associated with the l steams entering component k and $\sum_{j=1}^{m} \dot{C}_{j,k}$ is the sum of the cost rates associated with the m streams leaving component k.

In the system of balance equations, when the number of unknown stream costs is larger than the number of equations stated, auxiliary statements are required. For each component, streams entering are assumed to be known, while streams leaving the component are unknown. When the number of the outgoing exergy streams of a component is higher than one (m > 1), m-1 auxiliary equations are needed. The P-principle (on the product side) and the F-principle (on the fuel side) are used to determine the auxiliary equations (Lazzaretto and Tsatsaronis, 2006). The P-principle states that the cost per unit of exergy is supplied to all streams that belong to the definition of the product of the component at the same cost. The F-principle states that the cost, associated with the exergy removed from a considered component, has the same specific cost as the exergy supplied to the upstream components.

When the necessary balance equations are stated and solved, the exergoeconomic evaluation follows. Through the evaluation, iterative steps to improve and finally optimize

the considered system are revealed. An important outcome of the exergoeconomic analysis is the relation of exergy destruction with costs:

$$\dot{C}_{D,k} = c_{F,k}\dot{E}_{D,k} \tag{3.11}$$

where, $c_{F,k}$ is the specific cost of fuel of component *k.*

The calculation of the cost of exergy destruction facilitates the evaluation of plant components and allows comparison between cost of exergy destruction and investment cost. The components are first ranked and evaluated based on their total costs $\dot{C}_{D,k} + \dot{Z}_k$. The higher the costs are, the more significant the effect of the component to the overall plant. The contribution of the capital cost, $\dot{Z}_k$, to the sum of costs is expressed by the exergoeconomic factor f_k, defined by Equation (3.12).

$$f_k = \frac{\dot{Z}_k}{\dot{Z}_k + \dot{C}_{D,k}} \tag{3.12}$$

The exergoeconomic factor depends on the operation of each component. However, for each component type, there are some common value ranges that usually apply (lower than 55% for HXs; 35-75% for compressors/turbines; higher than 90% for pumps). High values of the factor f suggest a reduction in the investment costs, while low values of f suggest a reduction in the incurred irreversibilities. Depending on the calculated values, trade-offs between exergy destruction and investment costs are suggested. The goal is to improve the overall plant from both thermodynamic and economic viewpoints.

Another important variable of the exergoeconomic evaluation is the relative cost difference, r_k. For a given component *k*, the difference between the specific cost of product, $c_{P,k}$, and the specific cost of fuel, $c_{F,k}$, depends on the cost of exergy destruction, $\dot{C}_{D,k}$, and the related $\dot{Z}_k$.

$$r_k = \left(\frac{c_{P,k} - c_{F,k}}{c_{F,k}} \right) = \frac{\dot{C}_{D,k} + \dot{Z}_k}{c_{F,k}\dot{E}_{P,k}} \tag{3.13}$$

Information about compromises between the cost of exergy destruction and the investment cost of components, resulting from the exergoeconomic evaluation, can be used for the iterative design improvement of the plant. The objective is to reduce the cost associated with the product of the overall plant.

3.2.3 Exergy and environmental impacts

3.2.3.1 Life cycle assessment

In analogy to the economic analysis used to calculate costs, an LCA is used to assess the environmental impact associated with a product over its lifetime (Meyer et al., 2009). It is carried out following the guidelines of international standard approaches (ISO 14004).

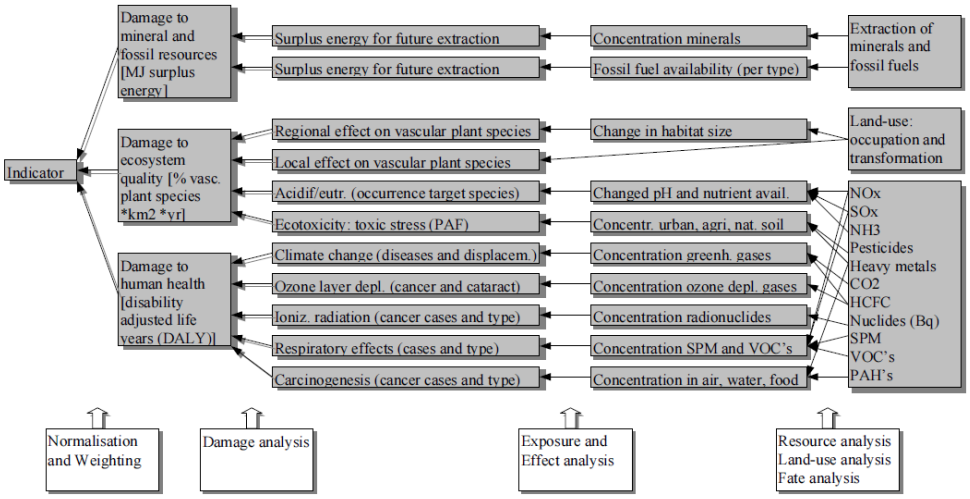

Figure 3.1: General structure of the Eco-indicator 99 LCIA method (Source: Goedkoop and Spriensma, 2000)

The quantification of environmental impacts caused by depletion and emissions of a natural resource can be carried out using different *life cycle impact assessment* (LCIA) methods. The damage-oriented impact analysis method Eco-indicator 99 is considered here (Goedkoop and Spriensma, 2000). Eco-indicator 99 defines three categories of damage: (1) damage to human health, (2) damage to the ecosystem and (3) depletion of resources. After calculating the environmental effects of the different categories, the values are optionally normalized, weighted and the result is expressed in *Eco-indicator points* (Pts). Higher values of the Eco-indicator are associated with higher damage. Depending on the attitude and perspective of different societies, there is a *weighting per perspective* represented by three *Archetypes*:

- *Hierarchists* keep a balance between short and long-term perspectives and take environmental damages into account based on consensus.
- *Egalitarians* weigh the effect on future generations and take all possible effects into account, even with minimal scientific proof.
- *Individualists* focus on the present, neglecting long-term effects and take only proven effects into account.

The archetype of the hierarchists has been adopted in this thesis.

The standard Eco-indicator 99 inventory values are available for the production and processing of a large number of materials, for transport processes, for disposal scenarios, etc. The impact is calculated with reference to the annual environmental impact of a European inhabitant. The scale is chosen in such a way that the value of 1 Point is representative for one

thousandth of the yearly environmental load of one average European inhabitant (this value is calculated by dividing the total environmental load in Europe by the number of inhabitants and multiplying it by 1000).

The application of an LCA assists in understanding the formation of environmental impacts in energy conversion systems at the component level and provides information about the influence of thermodynamic inefficiencies in the arrangement of environmental impacts. However, an LCA on its own is not capable of allocating the environmental impact of fuel consumption to the specific components of a system. This is performed with an exergoenvironmental analysis (Meyer, 2009).

3.2.3.2 Exergoenvironmental analysis

In an exergoenvironmental analysis, the concepts of exergy and environmental impact are combined. The component-related environmental impact of component *k*, $\dot{Y}_k$, is obtained in an LCA considering the entire life cycle of the component. It is the sum of the environmental impact of: (a) construction, $\dot{Y}_k^{CO}$, (including manufacturing, transport and installation), (b) operation and maintenance, $\dot{Y}_k^{OM}$ and (c) the disposal, $\dot{Y}_k^{DI}$, of component *k*:

$$\dot{Y}_k = \dot{Y}_k^{CO} + \dot{Y}_k^{OM} + \dot{Y}_k^{DI} \tag{3.14}$$

Similar to the exergoeconomic analysis, the exergoenvironmental analysis is performed with a system of equations stated at the component level. The environmental impact balance for component *k* states that the sum of the environmental impact associated with all input streams of the component equals the sum of the environmental impact associated with all output streams of the same component:

$$\sum_{i=1}^{l} \dot{B}_{i,k} - \sum_{j=1}^{m} \dot{B}_{j,k} + \dot{Y}_k + \dot{B}_k^{PF} = \mathbf{0} \tag{3.15}$$

Here, $\dot{B}_{i/j} = b_{i/j}\dot{E}_{i/j}$ (*b*: specific environmental impact of stream *i*/*j*), $\sum_{i=1}^{l} \dot{B}_{i,k}$ is the sum of the environmental impacts associated with the *l* steams entering component *k*, $\sum_{j=1}^{m} \dot{B}_{j,k}$ is the sum of the environmental impacts associated with the *m* streams leaving component *k* and $\dot{B}_k^{PF}$ is the impact of pollutant formation. The latter is related to the production of pollutants within a component is charged to the specific component, representing the potential impact that could be caused by the generated pollutants. Pollutant formation is defined only when a chemical reaction take place; in any other case, it is zero. It is calculated as:

$$\dot{B}_k^{PF} = \sum_i b_i^{PF} \left(\dot{m}_{i,out} - \dot{m}_{i,in} \right) \tag{3.16}$$

where, $\dot{m}_{in}$ and $\dot{m}_{out}$ are the mass flow rates of pollutants entering and exiting component *k*, respectively. The pollutant streams that are taken into account here include: CO, CO_2, CH_4 and NO_X.

When auxiliary equations need to be formulated, to make the number of the unknowns equal to the number of equations, the same principles are valid as for the exergoeconomic analysis.

The environmental impact of the exergy destruction is calculated as:

$$\dot{B}_{D,k} = b_{F,k}\dot{E}_{D,k} \tag{3.17}$$

Here, $b_{F,k}$ is the specific environmental impact of the fuel provided to component *k*. $\dot{B}_{D,k}$ can then be compared to the component-related impact of component *k*, $\dot{Y}_k$. This is the first step in evaluating the plant components, by revealing those with the highest effect on the overall plant.

The exergoenvironmental analysis not only identifies the components with the highest environmental impact, but it also reveals the possibilities for improvement, in order to decrease the environmental impact of the overall plant. These improvement possibilities can be identified through the sum of the component-related environmental impact and the impact of exergy destruction, $\dot{Y}_k + \dot{B}_{D,k}$, the exergoenvironmental factor, $f_{b,k}$, and the relative environmental impact difference, $r_{b,k}$.

$$f_{b,k} = \frac{\dot{Y}_k}{\dot{Y}_k + \dot{B}_{D,k}} \tag{3.18}$$

$$r_{b,k} = \frac{\left(b_{F,k} - b_{P,k}\right)}{b_{F,k}} = \frac{\dot{B}_{D,k} + \dot{Y}_k}{b_{F,k}\dot{E}_{P,k}} \tag{3.19}$$

With the exergoenvironmental factor, the contribution of the component-related impact, $\dot{Y}_k$, to the total environmental impact, $\dot{Y}_k + \dot{B}_{D,k}$ is expressed at the component level. In theory, when the value of $f_{b,k}$ is relatively high, $\dot{Y}_k$ is dominant, whereas when the value of $f_{b,k}$ is low, exergy destruction is dominant. Thus, the higher the exergoenvironmental factor, the higher the influence of the component-related impact on the overall performance of the plant. In practice, the results of the exergoenvironmental factor differ from those of the exergoeconomic factor significantly: the component-related impact is very low when compared to the impact associated with the operation of the plant (exergy destruction). Therefore, the values of $f_{b,k}$ are lower than 1% for the majority of the components. This is discussed in more detail in Chapter 4, where the results of the analyses are presented.

The environmental impact difference of component *k*, $r_{b,k}$, depends on the impact of its exergy destruction and its component-related impact. Thus, it is an indicator of the reduction potential of the component. After the calculation and evaluation of the mentioned variables,

design changes are suggested, in order to reduce the environmental impact associated with the product of the overall process.

3.3 Advanced exergy-based analyses

With conventional exergy-based analyses, the locations, magnitudes and causes of irreversibilities, costs and environmental impacts are identified, and a general direction for improvement is indicated. However, none of the conventional analyses are able to reveal interactions among plant components or to estimate the real potential for improvement. Without consideration of component interactions, optimization strategies can be misguided, especially when complex systems with a large number of mutually-affected components are considered. *Advanced exergy-based analyses* attempt to address this shortcoming.

Part of the exergy destruction, cost and environmental impact of a system can be avoided with structural modifications, reduction of the investment costs/environmental impacts or efficiency improvements of individual components. Exergy destruction, costs and environmental impacts that can be avoided through technically feasible design and/or operational improvement are considered *avoidable,* (AV). AV quantities play the main role in the determination of improvement steps, as well as the estimation of the improvement potential of a system. The remaining exergy destruction, costs and environmental impacts, associated with physical, technological and economic constraints, that cannot be avoided, are considered *unavoidable,* (UN). Additionally, exergy destruction, costs and environmental impacts can be separated depending on their source: if they are incurred by component interactions, they are *exogenous* (EX), while if they stem from the operation of the component itself, they are *endogenous* (EN). Using the endogenous and exogenous quantities, interactions among components and improvement alternatives are identified. Furthermore, the avoidable and unavoidable estimates are further split into their endogenous and exogenous parts. A schematic example of the paths to split irreversibilities is shown in Figure 3.2. The same process is applied to costs and environmental impacts.

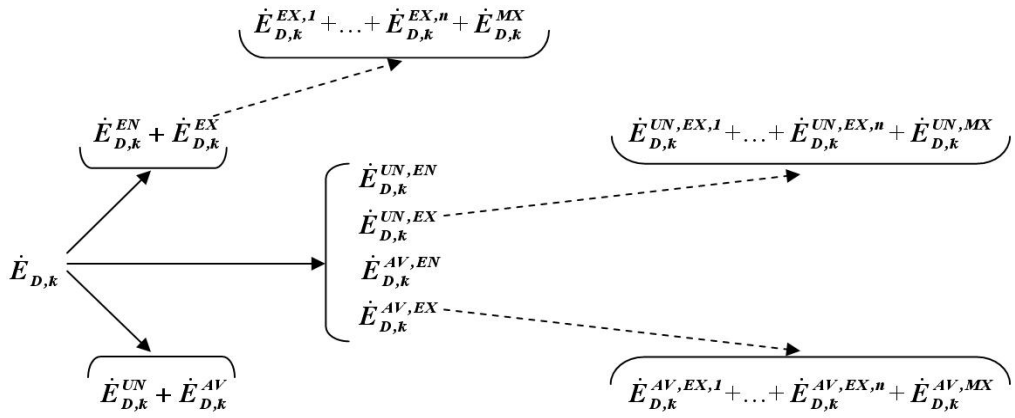

Figure 3.2: Options for splitting the exergy destruction in an advanced exergetic analysis (Source: Morosuk and Tsatsaronis, 2008b)

3.3.1 Advanced exergetic analysis

3.3.1.1 Splitting the rate of exergy destruction

To distinguish whether exergy destruction within a component is caused by the component itself (endogenous, $\dot{E}_{D,k}^{EN}$) or by the operation of other plant components (exogenous, $\dot{E}_{D,k}^{EX}$), the operating conditions of the system must be modified. To calculate the endogenous exergy destruction of component *k*, the considered component must operate under real conditions, while all other components of the process operate without irreversibilities (theoretically). In all cases, the power output of the overall plant is kept constant and equal to the initial simulation (real case). When chemical reactions take place, theoretical conditions cannot easily be defined. To overcome this problem, different methods have been proposed (Kelly et al., 2009). The exergy balance method is more appropriate for complex systems and it has been applied here.

The exogenous part ($\dot{E}_{D,k}^{EX}$) is calculated by subtracting the endogenous exergy destruction from the real exergy destruction, $\dot{E}_{D,k}^{real}$:

$$\dot{E}_{D,k}^{EX} = \dot{E}_{D,k}^{real} - \dot{E}_{D,k}^{EN} \tag{3.20}$$

The exogenous exergy destruction is, thus, the exergy destruction imposed on component *k* through the operation of the remaining *n-1* plant components that constitute the overall process. The $\dot{E}_{D,k}^{EX}$ of component *k* can also be traced to the specific components that cause it. The sum of the individual exogenous exergy destruction terms differs from the exogenous exergy destruction of component *k*. This difference is the *mexogenous exergy destruction* (MX, $\dot{E}_{D,k}^{MX}$) and it originates from the simultaneous interactions of the components of the process (Morosuk and Tsatsaronis, 2008b):

$$\dot{E}_{D,k}^{MX} = \dot{E}_{D,k}^{EX} - \sum_{\substack{r=1 \\ r\neq k}}^{n} \dot{E}_{D,k}^{EX,r} \tag{3.21}$$

with $\sum_{\substack{r=1 \\ r\neq k}}^{n} \dot{E}_{D,k}^{EX,r} = \sum_{\substack{r=1 \\ r\neq k}}^{n} \left(\dot{E}_{D,k}^{EN,r+k} - \dot{E}_{D,k}^{EN} \right)$.

As mentioned earlier, technological and economic limitations determine a minimum value of exergy destruction. This unavoidable part of exergy destruction, $\dot{E}_{D}^{UN}$, is calculated considering each component in isolation, separated from the system. The ratio of exergy destruction per unit of product exergy $\left(\dot{E}_{D}^{*}/\dot{E}_{P}\right)_{k}^{UN}$ is calculated assuming operation with high efficiency and low losses. For component *k*, with rate of product exergy in the real case $\dot{E}_{P,k}^{real}$, the unavoidable exergy destruction is calculated as:

$$\dot{E}_{D,k}^{UN} = \dot{E}_{P,k}^{real}\left(\frac{\dot{E}_D^*}{\dot{E}_P}\right)_k^{UN} \tag{3.22}$$

When the unavoidable part of the exergy destruction within component *k* is known, the avoidable part is obtained with Equation (3.23):

$$\dot{E}_{D,k}^{AV} = \dot{E}_{D,k}^{real} - \dot{E}_{D,k}^{UN} \tag{3.23}$$

For dissipative components no rate of product exergy can be defined, thus no distinction between avoidable and unavoidable exergy destruction has been made.

3.3.1.2 Splitting the avoidable and unavoidable rates of exergy destruction into endogenous and exogenous parts

The unavoidable endogenous and exogenous exergy destruction $\left(\dot{E}_{D,k}^{UN,EN}\right.$ and $\left.\dot{E}_{D,k}^{UN,EX}\right)$ within component *k* is calculated with Equations (3.24) and (3.25):

$$\dot{E}_{D,k}^{UN,EN} = \dot{E}_{P,k}^{EN}\left(\frac{\dot{E}_D^*}{\dot{E}_P}\right)_k^{UN} \tag{3.24}$$

$$\dot{E}_{D,k}^{UN,EX} = \dot{E}_{D,k}^{UN} - \dot{E}_{D,k}^{UN,EN} \tag{3.25}$$

The avoidable endogenous and exogenous exergy destruction $\left(\dot{E}_{D,k}^{AV,EN}\right.$ and $\left.\dot{E}_{D,k}^{AV,EX}\right)$ is then calculated by subtracting the corresponding unavoidable part from the total endogenous and exogenous exergy destruction, respectively:

$$\dot{E}_{D,k}^{AV,EN} = \dot{E}_{D,k}^{EN} - \dot{E}_{D,k}^{UN,EN} \tag{3.26}$$

$$\dot{E}_{D,k}^{AV,EX} = \dot{E}_{D,k}^{EX} - \dot{E}_{D,k}^{UN,EX} \tag{3.27}$$

3.3.1.3 Calculating the total avoidable exergy destruction

In general, high avoidable exergy destruction reveals high improvement potential for a component. However, it is possible that a component has relatively low avoidable exergy destruction, but relatively high total avoidable exogenous exergy destruction (exergy destruction caused by the component both within itself and to the other components of the system). Thus, an evaluation should take into account all data available and the conclusions should be adjusted accordingly. To facilitate the identification of the real improvement potential of plant components, the total amount of avoidable exergy destruction caused by each component *k* is defined (Morosuk and Tsatsaronis, 2008b):

$$\dot{E}_{D,k}^{AV,\Sigma} = \dot{E}_{D,k}^{AV,EN} + \sum_{\substack{r=1 \\ r\neq k}}^{n} \dot{E}_{D,r}^{AV,EX,k} \tag{3.28}$$

Here, $\sum_{\substack{r=1 \\ r\neq k}}^{n} \dot{E}_{D,r}^{AV,EX,k}$ is the sum of the avoidable exergy destruction caused by component *k* within the remaining *n*-1 plant components. Each part of this sum is calculated for each component *r* separately, via the unavoidable exogenous exergy destruction. The unavoidable exogenous exergy destruction is calculated through the unavoidable endogenous exergy destruction of each component *r*, when *r* and *k* operate under real conditions (Morosuk and Tsatsaronis, 2008b),:

$$\dot{E}_{D,r}^{UN,EN,r+k} = \dot{E}_{P,r}^{EN,r+k} \left(\frac{\dot{E}_D^*}{\dot{E}_P} \right)_r^{UN} \tag{3.29}$$

$\dot{E}_{P,r}^{EN,r+k}$ is the $\dot{E}_P$ of component *r*, when components *r* and *k* operate under real conditions and all remaining components operate under theoretical conditions. The unavoidable exogenous exergy destruction in component *r* due to component *k*, $\dot{E}_{D,r}^{UN,EX,k}$, is calculated as:

$$\dot{E}_{D,r}^{UN,EX,k} = \dot{E}_{D,r}^{UN,EN,r+k} - \dot{E}_{D,r}^{UN,EN} \tag{3.30}$$

Finally, the avoidable exogenous exergy destruction of component *r* caused by component *k*, is found by subtracting the unavoidable exogenous exergy destruction from the total exogenous exergy destruction caused to *r* by component *k*:

$$\dot{E}_{D,r}^{AV,EX,k} = \dot{E}_{D,r}^{EX,k} - \dot{E}_{D,r}^{UN,EX,k} \tag{3.31}$$

3.3.2 Advanced exergoeconomic analysis

3.3.2.1 Splitting the cost rates of investment and exergy destruction

Similar to exergy destruction, the endogenous and exogenous parts of investment cost and cost of exergy destruction are the parts related to internal operating conditions and to component interactions, respectively. Moreover, depending on whether the costs can be avoided or not, they can be split into avoidable and unavoidable parts, respectively. All equations used for these calculations are shown in Table 3.1.

3.3.2.2 Calculating the total rates of avoidable costs

To identify the real potential for improving plant components, the sum of both avoidable costs associated with exergy destruction and avoidable investment costs are calculated at the component level:

$$\dot{C}_{D,k}^{AV,\Sigma} = \dot{C}_{D,k}^{AV,EN} + \sum_{\substack{r=1 \\ r\neq k}}^{n} \dot{C}_{D,r}^{AV,EX,k} \tag{3.32}$$

$$\dot{Z}_{k}^{AV,\Sigma} = \dot{Z}_{k}^{AV,EN} + \sum_{\substack{r=1 \\ r\neq k}}^{n} \dot{Z}_{r}^{AV,EX,k} \tag{3.33}$$

$\sum_{\substack{r=1 \\ r\neq k}}^{n} \dot{C}_{D,r}^{AV,EX,k}$ and $\sum_{\substack{r=1 \\ r\neq k}}^{n} \dot{Z}_{r}^{AV,EX,k}$ are the total avoidable cost rates associated with the exogenous exergy destruction and investment cost of component *r*, respectively, caused by component *k*. The term related to the avoidable exogenous investment cost is calculated for each component *r* separately, via the unavoidable exogenous investment cost of the component caused by component *k*, $\dot{Z}_{r}^{UN,EX,k}$:

$$\dot{Z}_{r}^{AV,EX,k} = \dot{Z}_{r}^{EX,k} - \dot{Z}_{r}^{UN,EX,k} \tag{3.34}$$

The unavoidable exogenous part of the cost is calculated through the unavoidable endogenous cost, $\dot{Z}_{r}^{UN,EN}$:

$$\dot{Z}_{r}^{UN,EX,k} = \dot{Z}_{r}^{UN,EN,r+k} - \dot{Z}_{r}^{UN,EN} \tag{3.35}$$

where, $\dot{Z}_{D,r}^{UN,EN,r+k} = \dot{E}_{P,r}^{EN,r+k}\left(\frac{\dot{Z}}{\dot{E}_P}\right)_r^{UN}$, with $\dot{E}_{P,r}^{EN,r+k}$ equivalent to $\dot{E}_{P,r}$, when components *r* and *k* operate under real conditions and all remaining components operate theoretically.

To compare the avoidable cost of exergy destruction with the avoidable investment cost, the cost of exergy destruction must be split into its sources, as well. The avoidable exogenous cost of exergy destruction is calculated with Equation (3.36):

$$\dot{C}_{D,r}^{AV,EX,k} = c_{F,r}^{real} \dot{E}_{D,r}^{AV,EX,k} \tag{3.36}$$

where, $\dot{E}_{D,r}^{AV,EX,k}$ has been calculated using Equation (3.31).

The total cost, upon which the performance of a component is evaluated, is the sum of the avoidable cost rates of exergy destruction and investment.

Table 3.1: Splitting the costs

TERM	Definition of cost rate	Cost rate of investment, $\dot{Z}_k$, and exergy destruction, $\dot{C}_{D,k}$, *(of component k)*	Comments
Endogenous ($\dot{Z}^{EN}$, $\dot{C}_D^{EN}$)	Cost rate within component *k* associated with the operation of the component itself	$\dot{Z}_k^{EN} = \dot{E}_{P,k}^{EN}\left(\frac{\dot{Z}}{\dot{E}_P}\right)_k^{real}$ $\dot{C}_{D,k}^{EN} = c_{F,k}^{real}\dot{E}_{D,k}^{EN}$	$\dot{E}_{P,k}^{EN}$ *: Rate of product exergy of component k when the remaining components operate theoretically* $\dot{E}_P^{real}$ *and* $\dot{Z}^{real}$ *: Rate of product exergy and investment cost in the real case* $c_{F,k}^{real}$ *: Average cost per unit of fuel exergy provided to component k in the real case*
Exogenous ($\dot{Z}^{EX}$, $\dot{C}_D^{EX}$)	Cost rate within component *k* caused by the remaining components	$\dot{Z}_k^{EX} = \dot{Z}_k^{real} - \dot{Z}_k^{EN}$ $\dot{C}_{D,k}^{EX} = \dot{C}_{D,k}^{real} - \dot{C}_{D,k}^{EN}$	
Mexogenous ($\dot{Z}^{MX}$, $\dot{C}_D^{MX}$)	Difference between exogenous and sum of split exogenous cost rates for component *k*, caused by simultaneous interactions between the component and the remaining components of the plant	$\dot{Z}_k^{MX} = \dot{Z}_k^{EX} - \sum_{\substack{r=1 \\ r\neq k}}^{n}\dot{Z}_k^{EX,r}$ $\dot{C}_{D,k}^{MX} = \dot{C}_{D,k}^{EX} - \sum_{\substack{r=1 \\ r\neq k}}^{n}\dot{C}_{D,k}^{EX,r}$	$\sum_{\substack{r=1 \\ r\neq k}}^{n}\dot{Z}_k^{EX,r} = \sum_{\substack{r=1 \\ r\neq k}}^{n}\left(\dot{Z}_k^{EN,r+k} - \dot{Z}_k^{EN}\right)$, *with* $\dot{Z}_k^{EN,r+k} = E_P^{EN,r+k}\left(\frac{\dot{Z}_k}{\dot{E}_{P,k}}\right)^{real}$ $\sum_{\substack{r=1 \\ r\neq k}}^{n}\dot{C}_{D,k}^{EX,r} = \sum_{\substack{r=1 \\ r\neq k}}^{n}\left(\dot{C}_{D,k}^{EN,r+k} - \dot{C}_{D,k}^{EN}\right)$, *with* $\dot{C}_{D,k}^{EN,r+k} = c_{F,k}^{real}\dot{E}_{D,k}^{EN,r+k}$
Unavoidable ($\dot{Z}^{UN}$, $\dot{C}_D^{UN}$)	Cost rate that cannot be avoided	$\dot{Z}_k^{UN} = \left(\frac{PEC^{UN}}{PEC^{real}}\right)_k \times \dot{Z}_k^{real}$ for HXs % of $\dot{Z}_k^{real}$ for other components $\dot{C}_{D,k}^{UN} = c_{F,k}^{real}\dot{E}_{D,k}^{UN}$	$\dot{Z}_k^{UN}$ *: Unavoidable investment cost rate, i.e., minimum cost associated with component k. For each heat exchanger a new simulation of the component in isolation, operating with low effectiveness and high irreversibilities, is required. For other components, part of their* $\dot{Z}^{real}$ *is chosen as unavoidable.* PEC_k^{UN} *: Purchased equipment cost of component k, calculated at the unavoidable conditions* $\dot{E}_D^{UN}$ *: Unavoidable part of exergy destruction rate (calculated in an advanced exergetic analysis with most favorable operating conditions that result in the lowest possible exergy destruction).*
Avoidable ($\dot{Z}^{AV}$, $\dot{C}_D^{AV}$)	Cost rate that can be avoided	$\dot{Z}_k^{AV} = \dot{Z}_k^{real} - \dot{Z}_k^{UN}$ $\dot{C}_{D,k}^{AV} = \dot{C}_{D,k}^{real} - \dot{C}_{D,k}^{UN}$	
Unavoidable Endogenous ($\dot{Z}^{UN,EN}$, $\dot{C}_D^{UN,EN}$)	Unavoidable cost rate within component *k* associated with the operation of the component itself	$\dot{Z}_k^{UN,EN} = \dot{E}_{P,k}^{EN}\left(\frac{\dot{Z}^*}{\dot{E}_P}\right)_k^{UN}$ $\dot{C}_{D,k}^{UN,EN} = c_{F,k}^{real}\dot{E}_{D,k}^{UN,EN}$	$\left(\frac{\dot{Z}^*}{\dot{E}_P}\right)_k^{UN} = \left(\frac{\dot{Z}^{UN}}{\dot{E}_P^{real}}\right)_k$ $\dot{E}_D^{UN,EN}$ *: Unavoidable endogenous part of exergy destruction rate (calculated in an advanced exergetic analysis)*
Unavoidable Exogenous ($\dot{Z}^{UN,EX}$, $\dot{C}_D^{UN,EX}$)	Unavoidable cost rate within component *k* caused by the remaining components	$\dot{Z}_k^{UN,EX} = \dot{Z}_k^{UN} - \dot{Z}_k^{UN,EN}$ $\dot{C}_{D,k}^{UN,EX} = \dot{C}_{D,k}^{UN} - \dot{C}_{D,k}^{UN,EN}$	
Avoidable Endogenous ($\dot{Z}^{AV,EN}$, $\dot{C}_D^{AV,EN}$)	Avoidable cost rate within component *k* associated with the operation of the component itself	$\dot{Z}_k^{AV,EN} = \dot{Z}_k^{EN} - \dot{Z}_k^{UN,EN}$ $\dot{C}_{D,k}^{AV,EN} = \dot{C}_{D,k}^{EN} - \dot{C}_{D,k}^{UN,EN}$	
Avoidable Exogenous ($\dot{Z}^{AV,EX}$, $\dot{C}_D^{AV,EX}$)	Avoidable cost rate within component *k* caused by the remaining components	$\dot{Z}_k^{AV,EX} = \dot{Z}_k^{EX} - \dot{Z}_k^{UN,EX}$ $\dot{C}_{D,k}^{AV,EX} = \dot{C}_{D,k}^{EX} - \dot{C}_{D,k}^{UN,EX}$	

3.3.3 Advanced exergoenvironmental analysis

As briefly discussed in the description of the conventional exergoenvironmental analysis, the component-related environmental impact, $\dot{Y}_k$, is significantly lower than the impact associated with the operation of the plant (represented by the exergy destruction). Therefore, $\dot{Y}_k$ has not been split here. The focus is rather on the impacts related to the exergy destruction and pollutant formation (Boyano et al., 2010). Like the exergy destruction, the environmental impacts associated with exergy destruction and pollutant formation are separated into avoidable/unavoidable, endogenous/exogenous and the respective combined parts. The equations used to perform this analysis are shown in Table 3.2.

3.3.3.1 Calculating the total avoidable environmental impact of pollutant formation and exergy destruction

As mentioned in the description of the advanced exergoenvironmental analysis, to identify the real improvement potential of plant components, the total avoidable environmental impact associated with exergy destruction must be calculated at the component level:

$$\dot{B}_k^{PF,AV,\Sigma} = \dot{B}_k^{PF,AV,EN} + \sum_{\substack{r=1 \\ r\neq k}}^{n} \dot{B}_r^{PF,AV,EX,k} \tag{3.37}$$

$$\dot{B}_{D,k}^{AV,\Sigma} = \dot{B}_{D,k}^{AV,EN} + \sum_{\substack{r=1 \\ r\neq k}}^{n} \dot{B}_{D,r}^{AV,EX,k} \tag{3.38}$$

Here, $\sum_{\substack{r=1 \\ r\neq k}}^{n} \dot{B}_r^{PF,AV,EX,k}$ and $\sum_{\substack{r=1 \\ r\neq k}}^{n} \dot{B}_{D,r}^{AV,EX,k}$ are the total avoidable environmental impacts of pollutant formation and exergy destruction of component *r*, respectively, caused by component *k*. The avoidable exogenous impact of exergy destruction is calculated with Equation (3.39):

$$\dot{B}_{D,r}^{AV,EX,k} = b_{F,r}^{real} \dot{E}_{D,r}^{AV,EX,k} \tag{3.39}$$

where $\dot{E}_{D,r}^{AV,EX,k}$ has been calculated for all components in a preceding advanced exergetic analysis.

The term related to the avoidable exogenous environmental impact of pollutant formation is calculated for each component *r* separately, via the unavoidable exogenous impact of pollutant formation caused by component *k*, $\dot{B}_r^{PF,UN,EX,k}$:

$$\dot{B}_r^{PF,AV,EX,k} = \dot{B}_r^{PF,EX,k} - \dot{B}_r^{PF,UN,EX,k} \tag{3.40}$$

The unavoidable exogenous environmental impact of pollutant formation is calculated through its unavoidable endogenous impact, $\dot{B}_r^{PF,UN,EN}$:

$$\dot{B}_r^{PF,UN,EX,k} = \dot{B}_r^{PF,UN,EN,r+k} - \dot{B}_r^{UN,EN} \tag{3.41}$$

$\dot{B}_{D,r}^{PF,UN,EN,r+k} = \dot{E}_{P,r}^{EN,r+k} \left(\frac{\dot{B}^{PF}}{\dot{E}_P} \right)_r^{UN}$, with $\dot{E}_{P,r}^{EN,r+k}$ equivalent to the $\dot{E}_{P,r}$, when components r and k operate under real conditions and all remaining components operate theoretically.

The total avoidable environmental impacts (Equations 3.37 and 3.38) reveal the components with the largest influence on the overall plant. Actions to improve their operation should lead to an improvement of the impact of the plant as a whole.

Table 3.2: Splitting the environmental impacts

TERM	Definition of environmental impact	Environmental impact of pollutant formation, $\dot{B}_k^{PF}$ and exergy destruction, $\dot{B}_{D,k}$ *(for component k)*	Comments
Endogenous ($\dot{B}_k^{PF,EN}$, $\dot{B}_{D,k}^{EN}$)	Impact within component *k* associated with the operation of the component itself	$\dot{B}_k^{PF,EN} = \sum_i b_i^{PF} \left(\dot{m}_{i,out} - \dot{m}_{i,in}\right)^{EN}$ $\dot{B}_{D,k}^{EN} = b_{F,k}^{real} \dot{E}_{D,k}^{EN}$	b_i^{PF} *: Specific pollutant formation (varies depending on the pollutant)* $\left(\dot{m}_{i,out} - \dot{m}_{i,in}\right)^{EN}$ *: mass flow difference of pollutant i, between outlet and inlet in the endogenous case* $b_{F,k}^{real}$ *: Average specific environmental impact per unit of fuel exergy of component k in the real case*
Exogenous ($\dot{B}_k^{PF,EX}$, $\dot{B}_{D,k}^{EX}$)	Impact associated with component *k* caused by the remaining components	$\dot{B}_k^{PF,EX} = \dot{B}_k^{PF,real} - \dot{B}_k^{PF,EN}$ $\dot{B}_{D,k}^{EX} = \dot{B}_{D,k}^{real} - \dot{B}_{D,k}^{EN}$	
Mexogenous ($\dot{B}_k^{PF,MX}$, $\dot{B}_{D,k}^{MX}$)	Difference between exogenous and sum of split exogenous impacts for component *k*, caused by simultaneous interactions between the component and the remaining components of the plant	$\dot{B}_{D,k}^{MX} = \dot{B}_{D,k}^{EX} - \sum_{\substack{r=1 \\ r\neq k}}^{n} \dot{B}_{D,k}^{EX,r}$	$\sum_{\substack{r=1 \\ r\neq k}}^{n} \dot{B}_{D,k}^{EX,r} = \sum_{\substack{r=1 \\ r\neq k}}^{n} \left(\dot{B}_{D,k}^{EN,r+k} - \dot{B}_{D,k}^{EN}\right)$ *, with* $\dot{B}_{D,k}^{EN,r+k} = b_{F,k}^{real} \dot{B}_{D,k}^{EN,r+k}$
Unavoidable ($\dot{B}_k^{PF,UN}$, $\dot{B}_{D,k}^{UN}$)	Impact that cannot be avoided	$\dot{B}_k^{PF,UN} = \sum_i b_i^{PF} \left(\dot{m}_{i,out} - \dot{m}_{i,in}\right)$ $\dot{B}_{D,k}^{UN} = b_{F,k}^{real} \dot{E}_{D,k}^{UN}$	$\dot{B}_k^{PF,UN}$ *: The unavoidable environmental impact of pollutant formation rate includes all emissions of* CO_2 *when complete combustion takes place (i:* CO_2 *)* $\dot{E}_D^{UN}$ *: Unavoidable part of exergy destruction rate (calculated in an advanced exergetic analysis with most favorable operating conditions that result in the lowest possible exergy destruction).*
Avoidable ($\dot{B}_k^{PF,AV}$, $\dot{B}_{D,k}^{AV}$)	Impact that can be avoided	$\dot{B}_k^{PF,AV} = b_{NO_X}^{PF} \dot{m}_{NO_X,out}$ $\dot{B}_{D,k}^{AV} = \dot{B}_{D,k}^{real} - \dot{B}_{D,k}^{UN}$	$\dot{B}_k^{PF,AV}$ *: NOx emissions that can be avoided assuming, for example, different excess air fraction (* λ *)*
Unavoidable Endogenous ($\dot{B}_k^{PF,UN,EN}$, $\dot{B}_{D,k}^{UN,EN}$)	Unavoidable impact associated with component *k* caused by the operation of the component itself	$\dot{B}_k^{PF,UN,EN} = \dot{E}_{P,k}^{EN} \left(\frac{\dot{B}_k^{PF^*}}{\dot{E}_{P,k}}\right)^{UN}$ $\dot{B}_{D,k}^{UN,EN} = b_{F,k}^{real} \dot{E}_{D,k}^{UN,EN}$	$\left(\frac{\dot{B}^{PF^*}}{\dot{E}_P}\right)_k^{UN} = \left(\frac{\dot{B}^{PF,UN}}{E_P^{real}}\right)_k$
Unavoidable Exogenous ($\dot{B}_k^{PF,UN,EX}$, $\dot{B}_{D,k}^{UN,EX}$)	Unavoidable impact within component *k* caused by the remaining components	$\dot{B}_k^{PF,UN,EX} = \dot{B}_k^{PF,UN} - \dot{B}_k^{PF,UN,EN}$ $\dot{B}_{D,k}^{UN,EX} = \dot{B}_{D,k}^{UN} - \dot{B}_{D,k}^{UN,EN}$	
Avoidable Endogenous ($\dot{B}_k^{PF,AV,EN}$, $\dot{B}_{D,k}^{AV,EN}$)	Avoidable impact within component *k* caused by the operation of the component itself	$\dot{B}_k^{PF,AV,EN} = \dot{B}_k^{PF,EN} - \dot{B}_k^{PF,UN,EN}$ $\dot{B}_{D,k}^{AV,EN} = \dot{B}_{D,k}^{EN} - \dot{B}_{D,k}^{UN,EN}$	
Avoidable Exogenous ($\dot{B}_k^{PF,AV,EX}$, $\dot{B}_{D,k}^{AV,EX}$)	Avoidable impact within component *k* caused by the remaining components	$\dot{B}_k^{PF,AV,EX} = \dot{B}_k^{PF,AV} - \dot{B}_k^{PF,AV,EN}$ $\dot{B}_{D,k}^{AV,EX} = \dot{B}_{D,k}^{EX} - \dot{B}_{D,k}^{UN,EX}$	

4. Application of the exergy-based analyses to the plants

This chapter includes details and particularities of the applied methods and the obtained results. Information about the application of the conventional exergy-based analyses can be found in Appendix B.2. Selected results for the considered plants of each method are presented in the respective sections and summarized in Table 4.5. Results for selected plant components are shown in Tables 4.6-4.13 (end of section 4.1), while analytical results are presented in Appendix A.

4.1 Conventional exergy-based analyses

4.1.1 Exergetic analysis

All of the plants are provided with the same amount of fuel. Thus, the derived rate of product exergy ($\dot{E}_{P,tot}$) depends on the operating characteristics of each plant and the requirements of each CO_2 capture technology. Selected results of the analysis are presented in Table 4.1.

Table 4.1: Selected results of the exergetic analysis

	Ref. Plant	AZEP 85	AZEP 100	CLC Plant	MEA-0.2	S-GRAZ	ATR Plant	MEA-0	MSR Plant	Simple oxy-fuel Plant
ε_{tot} (%)	56.5	53.4	51.7	51.5	48.4	48.0	46.5	45.8	45.8	42.7
$\dot{E}_{P,tot}$ (MW)	412.5	389.9	377.5	376.0	353.8	352.0	339.8	334.6	334.6	313.4
$\dot{E}_{F,tot}$ (MW)	300.4	313.4	320.7	307.4	349.1	349.3	358.1	368.3	338.7	388.7
$\dot{E}_{L,tot}$ (MW)	17.6	27.2	32.5	47.3	27.6	31.9	32.7	27.7	57.3	31.1
$y_{D,tot}$ (%)	41.1	42.9	43.9	42.1	47.8	47.6	49.0	50.4	46.4	53.0

The reference plant performs with an exergetic efficiency of 56.5%. Of the plants that include CO_2 capture, the AZEP 85 achieves the best performance (53.4%), followed by the AZEP 100 (51.7%) and the CLC plant (51.5%). MEA-0.2[1] is ranked fourth (48.4%), while the S-Graz cycle is ranked fifth (48.0%), followed by the ATR plant (46.5%). MEA-0 and the MSR plant operate with a similar efficiency (45.8%) and, therefore, occupy the same ranking place

[1] 0 and 0.2 stand for the assumed lean sorbent CO_2 loading (0 or 0.2 mol CO_2/mol MEA). See also section 2.3.2.

(the efficiency of the MSR plant is slightly lower than that of MEA-0). Lastly, the lowest efficiency is found for simple oxy-fuel plant (42.7%). The results of MEA-0.2 agree better with published work (Rubin and Rao, 2002). Therefore, although MEA-0 will some times be used for comparison purposes, MEA-0.2 is considered as the main representative plant for chemical absorption. If not otherwise stated, *MEA plant* refers to MEA-0.2.

The three most efficient plants (AZEP 85, AZEP 100 and CLC plant) are oxy-fuel concepts. This indicates that this general approach is relatively promising for CO_2 capture, as long as current implementation challenges, related to their operation and component feasibility, are met. When compared to the reference plant, these plants result in a relatively small reduction in the exergetic efficiency of about five percentage points. Although the total rate of exergy destruction ($\dot{E}_{D,tot}$) in the CLC plant is lower by 6-13 MW than that of the AZEPs, the rate of product exergy of both AZEPs is found to be higher. With the same $\dot{E}_{F,tot}$ and lower $\dot{E}_{D,tot}$, the lower $\dot{E}_{P,tot}$ of the CLC plant is explained by its larger rate of exergy loss ($\dot{E}_{L,tot}$). Indeed, the exergy loss of the AZEP 100 and AZEP 85 is 32.5 and 27.3 MW (4.5 and 3.7% of the $\dot{E}_{F,tot}$), respectively, while in the CLC plant it is 47.3 MW (6.5% of the $\dot{E}_{F,tot}$). The higher exergy loss in the latter is a result of the assumed 2% non-reacted methane (see also section 2.3.7). The lower exergy loss of the AZEP 85 is smaller than that of the AZEP 100, because of the reduced mass flow rates of (1) the captured CO_2, (2) the MCM working fluids and (3) the GT system, and the smaller mass flow rate and lower temperature of the exhaust gases. The combination of relatively low exergy destruction and loss in the AZEP 85 results in higher net power output, i.e. higher exergetic efficiency.

The large difference between the simple oxy-fuel concept and the S-Graz cycle results from a combination of factors. In the S-Graz, (1) additional power is produced in the low pressure GT (GT3), (2) the exergy destruction within the single-pressure level HRSG is lower when compared to that of the three-pressure level HRSG of the simple oxy-fuel plant, (3) the water separated through gas condensation is recycled and reused in the plant and (4) steam is added at different pressure levels of the GT system, increasing the expanding mass flow and allowing a low condenser working pressure. All of these points contribute to an increase in the net power output of the S-Graz cycle. The S-Graz cycle performs with lower efficiency when compared to the CLC plant and the AZEP concepts, mainly because of the large power demand of its recycle compressors.

The two pre-combustion plants perform with relatively low efficiencies. The justification of this result for the ATR plant is that it combines two costly CO_2 capture methods: chemical absorption and fuel de-carbonization. Chemical absorption requires large amounts of thermal energy, while the de-carbonization process includes a, strongly endothermic, reforming reaction that is fueled by a supplementary fuel burning. The low effectiveness of the MSR plant is explained by its high rate of exergy loss. The MSR plant presents the highest rate of exergy loss among all of the plants (7.8% of the $\dot{E}_{F,tot}$), due to the relatively high exergy rate of the stream exhausted to the environment.

The MEA plant results in an efficiency of 8 percentage points lower than that of the reference plant, with an exergy loss similar to that of the AZEP 85 because of the low exergy

rate of the exhaust gases. However, the MEA plant presents a lower overall efficiency of 3-5 percentage points when compared to the three most efficient oxy-fuel plants. The relatively low penalty of the three oxy-fuel plants stems from their more efficient combustion processes, the additional power produced in the additional expander (GT2 in Figures A.2.1, A.3.1 and A.5.1), and the additional HRSG (SH II, EV II, EC II) that increases heat-recovery.

As expected, the main exergy destruction in all of the plants occurs within their chemical reactors (CC, CLC reactors, DB), caused by the high irreversibilities incurred there. When the reactants are preheated, the thermodynamic irreversibilities within the reactors decrease significantly. The combustion process is realized more efficiently in the AZEPs and the CLC plant resulting in an exergy destruction ratio $\left(y_{D,CC}^{AZEP100} / y_{D,CC+DB}^{AZEP85} / y_{D,reactors}^{CLC} \right)$ 12-18% lower (the best case being the AZEP 100), when compared to the reference plant. Furthermore, in the AZEP 100 the exergy destruction ratio of the combustion process is lower than that of the AZEP 85, which includes both a CC and a DB. This is related to the lower exergetic efficiency of the DB. The exergy destruction within the CC of the MEA plant is exactly the same as that of the reference plant, because the GT systems of the two plants are identical.

Apart from the GT system, with a dominant influence due to its high values of $\dot{E}_{D,k}$, other components appear to be equally important. In the CAU of the MEA and ATR plants, 4-6%, and in the ASUs of the simple oxy-fuel plant and the S-Graz cycle, 5-6% of the plants' $\dot{E}_{F,tot}$ is destroyed. The CAU in the MEA plant, and the ASUs in the S-Graz and simple oxy-fuel plants have the second highest values of exergy destruction among the plant components. In the ATR plant, the second highest exergy destruction is found within the ATR, followed by the CAU. In the remaining plants, the CC is followed by the expander and the compressor of the GT system (GT1 and C1) in descending order of exergy destruction. The high-pressure level of the HRSG (HPHRSG) is the most important part of the HRSG in all of the plants, followed by its respective low-pressure level part (LPHRSG). Lastly, the LPST and the additional ST used to drive the CO_2 compressors (ST4) also present relatively significant values of exergy destruction. The CO_2 compression unit is responsible for approximately 3% of the $\dot{E}_{F,tot}$ in the AZEPs, the CLC and MSR plants, 2% in the MEA, simple oxy-fuel and S-Graz plants and 1% in the ATR plant.

In general, the AZEPs and the CLC plant perform comparably, resulting in similar component efficiencies. While on close inspection, the majority of the components in the AZEPs operate slightly more efficiently than those in the CLC plant, the total exergy destruction ratio in both of the AZEPs is higher because of the higher exergy destruction within the MCM reactors, HRSG II and ST4. ST4 presents a higher exergy destruction ratio in the AZEPs, because it covers both the CO_2 compression unit and the recycle compressor of the plants. HRSG II of the AZEPs has higher exergy destruction, because of the larger steam mass flows, which are a result of the larger amount of available thermal energy in the CO_2 stream. The CO_2 compression unit in the AZEP 100 operates with larger CO_2 mass flow, therefore requiring a higher mass flow of cooling water that results in higher exergy destruction compared to the AZEP 85. Between the AZEP 100 and the CLC plant, the CO_2 mass flow differences are significantly smaller and are caused by the lower amount of CH_4 reacting in the latter.

The subsequent analyses of sections 4.1.2 and 4.1.3 have been applied to the reference plant and four plants incorporating CO_2 capture: the MEA plants (MEA-0 and MEA-0.2), the CLC plant, the AZEP 100 and the AZEP 85. The chemical absorption technique has been chosen as representative of the most conventional CO_2 capture method, whereas the three oxy-fuel plants have been chosen due to their high efficiencies, when compared to the alternative technologies.

4.1.2 Exergy and economics

4.1.2.1 Results of the economic analysis

The investment cost of the reference plant is calculated to be 213 € million (Table 4.2). The largest cost increase is estimated for the AZEP 100 (414 € million), followed by the AZEP 85 (395 € million) and the CLC plant (362 € million). The MEA plants are found to be the least expensive alternatives, since an overall investment cost increase of 50% has been assumed.

Table 4.2: Selected results of the economic analysis

	Ref. Plant	**AZEP 85**	**AZEP 100**	**CLC**	**MEA 0.2**	**MEA 0.0**
FCI_{tot} (10^6€)	213	395	414	362	326	319
FCI MCM reactor (10^6€)*	-	130	153	-	-	
FCI CLC unit (10^6€)	-	-	-	123	-	
FCI CAU (10^6€)	-	-	-	-	52	55
$FCI_{CO2\ compr.\ unit}$ (10^6€)	-	40	45	43	40	39
FCI_{tot} (€/kW)	517	1012	1097	962	921	953
FCI_{tot} (10^6 €/kg CO_2 *captured*)	-	12.1	10.8	9.6	9.9	9.7

* it does not include the DB

Between the two MEA plants, the regeneration requirement in MEA-0.2 is reduced and the CAU is smaller and, therefore, cheaper. However, since a smaller steam mass flow is needed for the CAU, more steam will flow through the condenser of the plant (COND, Figure A.6.1). Thus, the cooling water requirement of the plant increases, resulting in a larger condenser and a larger *cooling tower* (CT). Moreover, the first CO_2 compressor (C3) is larger in MEA-0.2 than in MEA-0, because the outlet temperature of the CAU is calculated to be higher. Finally, the investment cost of MEA-0.2 (326 € million) is higher than that of the reference plant and slightly higher than that of MEA-0 (319 € million).

Taking into account the relative costs (€/kW), MEA-0.2 is the most economical alternative (921 €/kW), followed by MEA-0 (953 €/kW) and the CLC plant (962 €/kW). Although the relative cost based on the power output is more representative of the cost effectiveness of a plant, a relative cost based on the CO_2 captured should also be considered. Because the MEA plants only capture 85% of the produced CO_2, while the CLC plant captures essentially the complete amount of CO_2 produced, the relative cost per captured CO_2 is

calculated to be lower for the CLC plant (9.6 € million/kg CO_2 captured versus 9.7 and 9.9 € million/kg CO_2 captured for MEA-0 and MEA-0-2, respectively).

The most expensive parts of the plants are the components used for the production of the necessary oxygen or the combustion process. The CLC and MCM reactors are accountable for 34% and 33%/37% of the total investment cost of the CLC plant and the AZEP 85/AZEP 100, respectively. The lower cost associated with the reactor of the AZEP 85 is justified by its smaller size.

The CO_2 compression unit, i.e., the CO_2 compressors and coolers, is accountable for 10-11% of the investment cost in the AZEPs, and 12-13% in the CLC and MEA plants. The investment cost of both the main and the additional HRSG in the AZEP 100 is higher than that of the AZEP 85, due to the larger size of the equipment used. The cost of the main HRSG of the CLC plant is similar to that of the AZEP 100, while the cost of the secondary HRSG is estimated to be much lower, due to the decreased water/steam mass flow. Additionally, the main HRSG of all of the oxy-fuel plants is somewhat cheaper when compared to that of the reference plant, due to lower steam temperatures and mass flows. Lastly, the cost of the HRSG of the MEA plants is similar to that of the reference plant.

4.1.2.2 Results of the exergoeconomic analysis

Results for selected components of the exergoeconomic analysis are shown in Tables 4.6-4.13 at the end of section 4.1, while the complete results at the component and the stream level can be found in Appendix A.

An important outcome of the exergoeconomic analysis is the correlation of exergy destruction with costs. The cost rate of exergy destruction is calculated at the component level and it is then compared to the respective investment cost rates. The components are then ranked depending on their total cost rate, which consists of their investment and exergy destruction cost rates ($\dot{C}_{D,k} + \dot{Z}_k$). The higher this total cost, the higher the influence of the component on the overall plant and thus, the more significant the component is considered. This cost ranking exposes the components that should have improvement priority, in order to improve the cost effectiveness of the overall plant.

In the reference and the oxy-fuel plants, the three components with the highest cost rates are those constituting the GT system: reactors, GT1 and C1. In the reference plant, the components that follow the GT system in order of importance are the LPST and the HPHRSG. In the AZEPs, the components that follow are the group of the CO_2 compressors, the MCM LTHX and the MCM and in the CLC plant, the CO_2 compressors and the LPST, due to their relatively high exergy destruction. In the MEA plants, the CAU presents the second highest cost of exergy destruction and total cost, right after the CC of the plant. GT, C1 and the group of the CO_2 compressors, follow the CAU.

Although the cost of exergy destruction associated with the CLC reactors is lower than that of the CC of the reference plant, their total cost is higher, due to their approximately four times higher investment cost rate. The smaller reaction range in the MCM reactor of the AZEP 85, when compared to that of the AZEP 100, leads to lower exergy destruction and

investment cost rates of its constitutive components. The exergy destruction within the components of the GT system in the AZEP 85 is lower than in the AZEP 100, while the opposite is true for the investment costs of the compressor and the expander. As in the cost calculations GT1 and C1 are considered parts of the same GT system. The larger power output, related to the increased inlet temperature of the expander, in the AZEP 85 increases the cost of C1.

The LPST has a significantly large total cost in most of the plants. In the AZEP 85 this cost is higher than in the AZEP 100 because of the higher power output of the turbine, resulting from the higher inlet temperature of the expanded steam. Although the cost rate of exergy destruction of the LPST in the CLC plant is higher than in the AZEP 100 (and the same as in the AZEP 85), its investment cost rate is lower[2], resulting in a lower total cost. An important contribution to the overall cost is also made by ST4 in the AZEPs, because it drives the CO_2 compression unit and the recycle compressor of the MCM reactors (C6). In the CLC plant, the steam mass flow of this ST is reduced significantly, because it only drives the CO_2 compressors. The higher steam mass flow and inlet temperature, relative to the AZEP 100, increase the improvement priority of the HPHRSG in the AZEP 85 and the CLC plant above that of ST4. In the MEA plants, the HPHRSG performs similarly to that of the reference plant, exceeding the STs in cost.

Effective means to compare and evaluate different components are the exergoeconomic factor, f_k, and the relative cost difference, r_k (calculated with Equation 3.13). r_k is high for compressors and pumps, where electric power is used as fuel. r_k shows the theoretical improvement potential of the components. However, the exergoeconomic factor will be the main tool for evaluating the cost effectiveness of a considered component. High values of the exergoeconomic factor for components with high total cost suggest that a reduction of the investment cost should be considered. On the other hand, low values of the factor suggest that a reduction in the exergy destruction should be considered, even if this would increase the investment cost of the component.

The low exergoeconomic factors of the CC in the reference and MEA plants and the AZEPs, show that most of the component's total cost is related to exergy destruction. This, however, is common for reactors, due to the high level of irreversibilities present there. The exergoeconomic factor of the CLC reactors is substantially higher, due to the large size of the unit, which results in a relatively high investment cost.

In general, the values of the exergoeconomic factor are within the expected value ranges for the most influential components (see section 3.2.2). Exceptions could be the high exergoeconomic factors calculated for the MCM HTHX and LTHX, suggesting that a decrease in the investment cost of these components (if less expensive materials could be integrated) should be considered in an attempt to improve the cost effectiveness of the plant. The recycling compressor (C6) of the MCM reactor in the AZEPs and the CO_2 compressors (C2-C5 for the AZEPs, CLC; C3-C6 for MEA) also exhibit relatively high values of the

[2] The absolute investment cost of the LPST in the CLC plant is higher than that of the LPST in the AZEP 100, due to the slightly higher power output of the component. However, the investment cost rates for the CLC plant are found to be smaller due to its lower carrying charges, when compared to those of the AZEP 100.

exergoeconomic factor. It is thus likely that less expensive compressors (if possible) would be more cost effective for the overall plant. A low exergoeconomic factor is calculated for ST4 in all of the plants. This relates to the exergy destruction within this component, which is considered to be high both on its own and when it is compared to the other STs of the plants. Thus, to improve the overall operation of the plants, the efficiency of this ST should be increased. Lastly, relatively low exergoeconomic factors are found for the air preheaters (HX Air) and the natural gas preheaters (NGPHs). However, both of these results are associated with design requirements and calculation assumptions. The large value of exergy destruction in the HX Air results from the high temperature difference between the working fluids. This, however, is required to sustain the performance of the MCM reactor and to keep the inlet temperature of the GT2 within acceptable limits. The low factors for the NGPHs are associated with high pressure losses in the valve prior the heat exchangers, which are charged to them[3]. Additionally, for all of the plants, low factors are calculated in coolers and condensers, where relatively high exergy destruction is found.

Since all of the plants have the same c_F, the total cost rate of exergy destruction, $\dot{C}_{D,tot}$, depends on the $\dot{E}_{D,tot}$ of the plants (i.e., $\dot{C}_{D,tot} = c_F \dot{E}_{D,tot}$). Thus, the $\dot{C}_{D,tot}$ increases with increasing values of the $\dot{E}_{D,tot}$. The cost of exergy destruction of the oxy-fuel plants is comparable to that of the reference plant, while a larger difference is found for the MEA plants. Specifically, the $\dot{C}_{D,tot}$ of the AZEPs is higher by 4-7%, that of CLC plant by 2%, that of MEA-0 by 23% and that of MEA-0.2 by 16%. As expected, all cost differences are representative of the differences between the $\dot{E}_{D,tot}$ of the plants and that of the reference plant.

Values for the overall plants are shown in Table 4.5 and under *Total* in Tables 4.6-4.13. The overall exergoeconomic factor of the reference plant is calculated to be 40%. On the other hand, the two AZEPs present increased factors of 52 and 53%, slightly higher than that of the CLC plant (51%). These factors reveal roughly equal contributions between investment cost and cost of exergy destruction. The differences among the plants are essentially related to the high investment cost of the components used for oxygen production and/or CO_2 separation and compression. While the common components in all of the plants have comparable values, the MCM and CLC reactors increase the investment costs and, consequently, the exergoeconomic factors significantly. The total investment cost rates of the MEA plants are similar to that of the CLC plant, while their cost rates of exergy destruction are higher, resulting in lower overall exergoeconomic factors (43-45%).

The overall relative cost difference is higher for the plants with CO_2 capture than for the reference plant. This is justified with the additional charges of the supplementary equipment used. Among the oxy-fuel plants, the total relative cost difference remains essentially unchanged, while it becomes higher for the MEA plants.

[3] Approximately 40% of the total exergy destruction assigned to the NGPH is associated with the pressure losses of the valve.

To further compare the costs of the plants, the *cost of electricity* (COE) and the *cost of avoided CO_2* (COA-CO_2) are considered. The latter shows the added cost of electricity per ton of CO_2 avoided based on net plant capacity (Rubin and Rao, 2002):

$$\text{COA-}CO_2 = \frac{\left(€/kWh\right)_{capture} - \left(€/kWh\right)_{reference}}{\left(t_{CO_2}/kWh\right)^{emitted}_{ref.plant} - \left(t_{CO_2}/kWh\right)^{emitted}_{plant+capture}} \tag{4.1}$$

The COA-CO_2 cost relates only to the capture of the CO_2 and it does not include transportation or storage costs.

The resulting levelized COE and the COA-CO_2 for the plants are shown in Table 4.5. CO_2 capture causes a minimum increase in the cost of electricity of 22%, achieved by the AZEP 85. Increases of 23% and 28% are calculated for the CLC plant and the AZEP 100, respectively. Between the two MEA plants, a lower COE is achieved by MEA-0.2. The COE of this plant is 28% higher than that of the reference plant. Larger differences in the energy penalty of the plants are observed when the COA-CO_2 is considered. The cost differences between the MEA plants and the other plants are mainly associated with the high energy demand of the solvent regeneration in the CAU and the relatively low percentage of CO_2 capture (85%), in comparison to the close to 100% capture of the oxy-fuel concepts. While the AZEP 85 has the lowest COE, it is ranked second, after the CLC plant, when the COA-CO_2 is considered. The CLC plant has the same CO_2 emissions as the AZEP 100, but it results in a lower COA-CO_2, due to its lower COE.

The three oxy-fuel plants perform CO_2 capture in a relatively cost effective way. Some of the differences in the costs and the general results of the plants are based on calculation assumptions and design requirements. The choice of the best alternative can differ depending on the priorities of the decision-maker.

4.1.2.3 Sensitivity analyses

In order to examine the effect of the cost of the CAU, CLC and MCM reactors on the COE of the power plants, sensitivity analyses have been conducted (Figure 4.1). In these analyses the assumed costs have been varied from -50% to +100% of the base cost. The results show a lower influence of the CAU on the COE of the MEA plants, while a rapid increase in the COE of the AZEPs and the CLC plant is revealed with changes in the costs of the respective reactors. It should be noted that because the COE of the AZEP 100 increases rapidly with the cost of the MCM reactor and that the base COE of the AZEP 100 and the MEA plant are similar. The base COE of the MEA plant will eventually be surpassed by that of the AZEP 85 if an increase of approximately 50% in the cost of the MCM reactor takes place, while it will only be surpassed by that of the CLC plant if an increase of over 40% in the cost of the CLC reactors takes place. It can be concluded that the relationships among the COE of most plants is maintained for a wide range of cost values of the examined components.

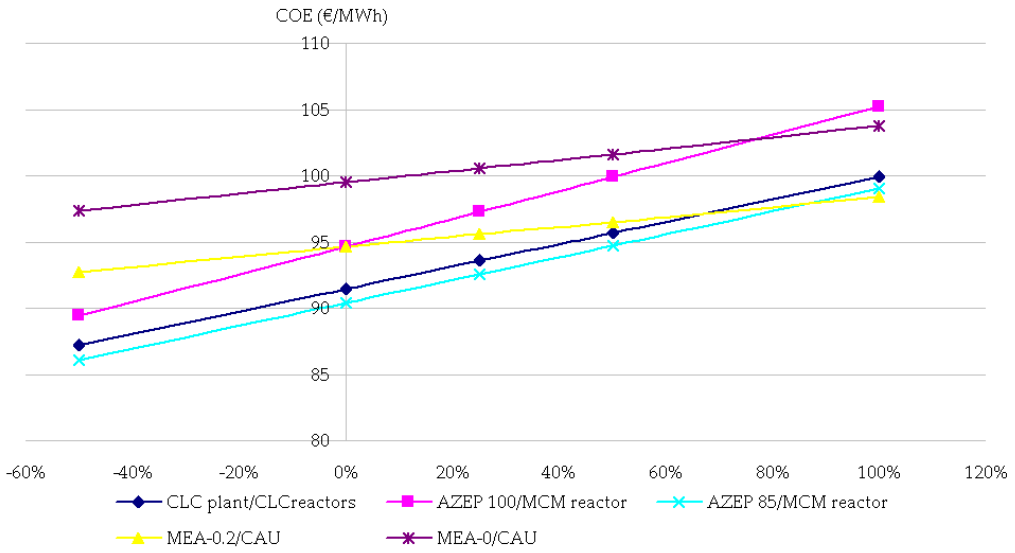

Figure 4.1: Influence of the investment cost of the MCM reactor, the CLC reactors and the CAU on the overall COE of the respective plants

A sensitivity analysis of the assumed cost of the fuel (7 €/GJ-LHV) has also been performed. It was found that while changes in the cost of the fuel affect the COE of the plants, the relative difference of the COE among the plants remains essentially unchanged.

4.1.3 Exergy and environmental impacts

4.1.3.1 Results of the life cycle assessment

The component-related environmental impacts determined by the LCA of the plants differ in relative magnitude from costs obtained in the economic analysis. While in the economic analysis, the cost rates (calculated in €/h), are relatively substantial, in the LCA, the component-related environmental impact rates, ($\dot{Y}_k$, in Pts/h) are much lower in scale. Relatively high values are calculated for components constructed with materials of higher environmental impact and for the CTs of the plants, due to their large size. As can be seen in Table 4.3, the MEA and CLC plants have the lowest increase in relative total environmental impact (Pts/kW), when compared to the reference plant, because of the similar equipment used in both plants. Comparing MEA-0 with MEA-0.2, the differences are also small. While the absorber of MEA-0.2 is smaller and results in a lower impact, its COND and CT are larger. This happens because of the larger mass of steam flowing through the COND, which is a direct result of the lower mass of steam extracted and used in the CAU of this plant. An impact ten times higher is found for the two AZEPs, mainly associated with the MCM reactors.

For the completion of the LCA, the environmental impact of pollutant formation $\dot{B}^{PF}$ (see section 3.2.3) of the reactors of each plant has been calculated separately. The specific environmental impact associated with each pollutant and the results of the calculations, including the impact that is avoided due to CO_2 capture, are shown in Table 4.4. As can be

seen, 60% of pollutant formation in the reference plant is related to the CO_2 emissions of the plant, while the remaining 40% is related to its NO_x emissions. The same NO_x emissions are considered for the MEA plants, while no NO_x emissions are considered for the oxy-fuel plants. In the DB of the AZEP 85, combustion takes place with air, but the NO_x emissions are low due to the lower amount of reacting methane. The environmental impact of pollutants, like CO_2, can affect the result of the overall analysis. A sensitivity analysis of the impact of CO_2 emissions for the reference and MEA-0.2 plant (with and without consideration of the environmental impact of CO_2 sequestration, Figures 4.2 and 4.3) has been performed in the exergoenvironmental analysis.

Table 4.3: Selected results of the LCA

	Ref. Plant	**AZEP 85**	**AZEP 100**	**CLC**	**MEA 0.2**	**MEA 0.0**
Total environmental impact (10^3 Pts)	2,592	26,066	26,061	3,414	3,223	2,871
Total environmental impact (Pts/kW)	6.3	66.9	69.0	9.1	9.1	8.6

Table 4.4: Environmental impact of overall and avoided pollutant formation due to CO_2 capture

	CO_2		**NO_x**		**CH_4**		$\dot{B}^{PF}$	$\dot{B}^{PF}_{CO_2-capt}$
	(kg/s)	**(Pts/t)**	**(kg/s)**	**(Pts/t)**	**(kg/s)**	**(Pts/t)**	**(Pts/h)**	**(Pts/h)**
Ref. Plant	38.41		0.05				1259	0
AZEP 85								
DB	5.76		0.03				459	0
CC	32.65	**5.4**		**2749.4**		**114.6**	641	-641
AZEP 100	38.42						754	-754
CLC plant	37.73				0.28		856	-741
MEA 0.2	38.42		0.05				1270	-646
MEA 0.0	38.42		0.05				1268	-646

4.1.3.2 Results of the exergoenvironmental analysis

As shown in Table 4.5, the component-related impact ($\dot{Y}_{tot}$) differs among the plants. However, this difference is almost negligible and differences among the total impact ($\dot{B}_{D,tot}+\dot{Y}_{tot}$) of the reference and oxy-fuel plants are determined by the impact of exergy destruction. This indicates that the construction phase is not the key area for reducing the environmental impact of these plants.

In the reference plant, the highest environmental impact ($\dot{B}_{D,k}+\dot{Y}_k$) corresponds to the CC, GT1, the LPST and C1. In the oxy-fuel plants, the highest impact is caused by the reactors, GT1, the FG COND and C1. In the AZEPs, the MCM LTHX also has a high impact. In the MEA plant, the CC is followed by the CAU, which presents a high environmental impact of exergy destruction. In the exergoenvironmental analysis, dissipative components become more important than in the exergoeconomic analysis: a high impact is calculated for

the condensers (COND and FG COND) of all of the plants. As already mentioned, in the exergoeconomic and exergoenvironmental analyses, the influence of the non-exergy related costs/impacts (investment cost rate and rate of the component-related impact) is different. Because in the exergoenvironmental analysis the component-related environmental impact is almost negligible, the exergy destruction and the specific environmental impact of fuel are the main deciding factors of the significance of a component. Differences between the results of the exergoenvironmental analysis and that of the exergetic analysis are found for the components constituting the MCM reactors. Here, the total environmental impact results in relatively high values, leading to conclusions that diverge from those obtained by the exergetic analysis.

The total exergoenvironmental factor is similar for plants with similar component-related environmental impact: approximately 4% for the AZEPs and around 0.5% for the reference, CLC and MEA plants. A reduction in the overall environmental impact could be achieved by increasing the exergetic efficiency of the GT system and the reactors. In general, a decrease in the irreversibilities present in reactors is difficult because they are mostly unavoidable. However, preheating of the reactants, as well as the use of different GT systems (e.g., steam-cooled expanders) would lead to better efficiencies, thus decreasing the incurred exergy destruction. In the case of the oxy-fuel plants, a further reduction of the overall environmental impact could be achieved by decreasing the component-related impact of the reactors (e.g., by replacing the construction materials assumed, with materials of lower impact), or by increasing the exergetic efficiency of the remaining components. In general, in order to reduce the overall impact of the plants, more attention should be given to the effectiveness of the component operation, thus the exergetic efficiencies of the components.

To compare the overall performance of the plants, the *environmental impact of electricity* (EIE) has been calculated, the results of which are presented in Table 4.5. The environmental impact of the electricity produced by the reference plant is found to be 25.1 Pts/MWh. This is comparable to the European average impact of low voltage electricity: 26 Pts/MWh (SimaPro 7.1 manual, 2000). When compared to the reference plant, the EIE of the oxy-fuel plants presents a relatively low reduction, while that of MEA-0.2 is increased by 2.3 Pts/MWh. Considering that no impact has been considered for pollutants generated by the processing of the solvent used in the plant, the case presented is considered the *best case scenario* of this plant.

4.1.3.3 Sensitivity analyses

The high environmental impact of the MEA plant can have two possible interpretations: (1) either the CO_2 capture technology has no environmental benefit, but a penalty due to the high decrease of the efficiency of the plant, or (2) the provided values of the environmental impact of pollutants/reactants are not trustworthy. To examine the latter, a sensitivity analysis of the environmental impacts of the CO_2 emissions has been investigated. MEA-0.2 has been further considered for the sensitivity analysis, because it represents the most realistic alternative between the two MEA plants and because it has the highest impact when compared to the oxy-fuel alternatives. The environmental impact of CO_2 emissions (used for the calculation of

pollutant formation) has been varied from -90% to +500% and the EIE has been calculated with and without the addition of impact associated with mineral storage of the CO_2 captured (Khoo and Tan, 2006). The influence of these variations on the EIE of the MEA and the reference plants is presented in Figures 4.2 and 4.3. As shown, CO_2 capture becomes meaningful when the environmental impact of CO_2 is higher than 20 Pts/t (when storage is also accounted for). This is a value approximately four times higher than that provided by Goedkoop and Spriensma (2000), shown by the grey, dotted line. As shown in Figure 4.3, when CO_2 transport and sequestration are not accounted for, the limit for a positive environmental impact of CO_2 capture decreases to 14 Pts/t.

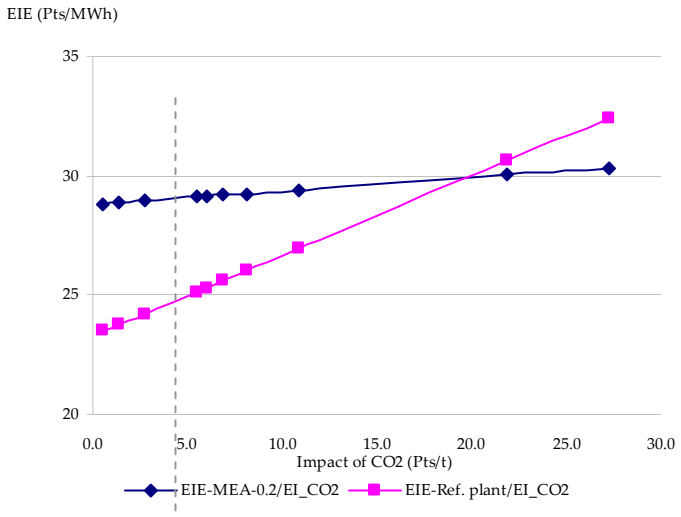

Figure 4.2: Influence of the specific environmental impact of CO_2 on the EIE of the reference and MEA-0.2 plants, with consideration of an environmental impact of 4.9 Pts/t of CO_2 associated with mineral storage (the grey, dotted line shows the chosen, base value of the impact of CO_2 emissions)

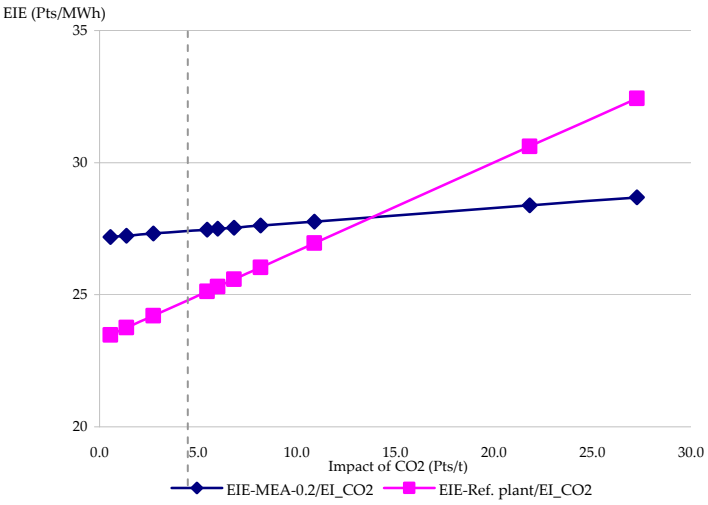

Figure 4.3: Influence of the specific environmental impact of CO_2 on the EIE of the reference and MEA-0.2 plants without consideration of the environmental impact associated with CO_2 mineral storage (the grey, dotted line shows the chosen, base value of the impact of CO_2 emissions)

Table 4.5: Results of the conventional exergy-based analyses for the overall plants

	Ref. Plant	AZEP 85	AZEP 100	CLC Plant	MEA 0.2	S-GRAZ	ATR Plant	MEA 0.0	MSR Plant	Simple oxy-fuel Plant
CO_2 emitted (kg/s)	38.72	6.06	0.35	0.35	5.81	0.00	9.62	5.81	0.26	0.13
CO_2 emitted (kg/MWh)	337.90	55.97	3.36	3.39	59.10	0.00	101.87	62.49	2.80	1.54
CO_2 captured (kg/s)	-	32.71	38.48	37.73	32.91	38.58	29.08	32.91	37.95	38.58
CO_2 captured (%)	-	84.4	99.1	99.1	85.0	100.0	75.2	85.0	99.3	99.7
Total FCI (10^6€)	213	395	414	362	326			319		
Total FCI (€/kW)	517	1012	1097	962	921			953		
Total FCI (10^6€/kg CO_2 capt.)	-	12.1	10.8	9.6	9.9			9.7		
Total environmental impact (Pts)	2,592	26,066	26,061	3,414	3,223			2,871		
Total environmental impact (Pts/kW)	6.3	66.9	69.0	9.1	9.1			8.6		
COE (€/MWh)	74.1	90.4	94.7	91.4	94.6			99.5		
COA-CO_2 (€/t)	N/A	57.8	61.6	52.0	73.5			92.2		
EIE (Pts/MWh)	25.1	24.9	24.5	24.5	27.4			29.0		

COA-CO_2: Cost of avoided CO_2, COE: Cost of electricity, EI: Environmental impact, EIE: Environmental impact of electricity, FCI: Fixed capital investment

Table 4.6: Selected results at the component level for the reference plant

Component, k	$\dot{E}_{F,k}$ (MW)	$\dot{E}_{P,k}$ (MW)	$\dot{E}_{D,k}$ (MW)	ε_k (%)	$y_{D,k}$ (%)	$c_{F,k}$ (€/GJ)	$c_{P,k}$ (€/GJ)	$\dot{C}_{D,k}$ (€/h)	$\dot{Z}_k$ (€/h)	$\dot{C}_{D,k}+\dot{Z}_k$ (€/h)	f_k (%)	r_k (%)	$b_{F,k}$ (Pts/GJ)	$b_{P,k}$ (Pts/GJ)	$\dot{B}_{D,k}$ (Pts/h)	$\dot{Y}_k$ (Pts/h)	$\dot{B}_{D,k}+\dot{Y}_k$ (Pts/h)	$f_{b,k}$ (%)	$r_{b,k}$ (%)
C1	242.68	231.30	11.38	95.3	1.56	16.9	19.5	693	1,423	2,116	67.3	15.0	6.1	6.4	249.71	0.24	249.94	0.09	4.9
CC	729.62	508.76	220.87	69.7	30.23	9.2	13.7	7,276	1,017	8,293	12.3	49.5	3.5	5.6	2746.20	0.38	2746.58	0.01	63.3
GT	551.15	530.67	20.47	96.3	2.80	15.5	16.9	1,140	1,627	2,766	58.8	9.4	5.9	6.1	432.58	1.12	433.71	0.26	3.9
HPSH	35.07	31.72	3.35	90.5		15.5	19.4					25.6	5.9	6.8					15.5
HPEV	43.64	39.91	3.73	91.5		15.5	19.0					23.1	5.9	6.7					13.6
HPEC	28.92	24.91	4.00	86.2	1.52	15.5	20.4	617	432	1,049	41.2	31.8	5.9	7.2	234.07	1.42	235.49	0.60	23.3
RH	26.47	23.89	2.58	90.3		15.5	19.4					25.4	5.9	6.8					15.8
IPSH	0.18	0.12	0.06	69.0		15.5	35.4					128.8	5.9	9.7					65.2
IPEV	6.10	5.67	0.43	92.9		15.5	20.5					32.8	5.9	6.5					11.1
IPEC	1.06	0.87	0.19	82.5	0.44	15.5	22.3	181	186	367	50.7	44.3	5.9	7.7	68.64	0.85	69.49	1.22	30.9
LPSH	1.43	1.04	0.38	73.3		15.5	29.5					90.9	5.9	9.0					53.0
LPEV	19.03	15.48	3.55	81.4		15.5	24.2					56.4	5.9	7.8					33.3
LPEC	11.49	7.71	3.78	67.1	1.06	15.5	30.8	429	287	716	40.1	99.3	5.9	10.1	162.97	0.23	163.20	0.14	71.3
LPST	70.99	61.35	9.64	86.4	1.32	21.4	29.7	743	764	1,508	50.7	38.5	7.2	8.8	251.49	0.49	251.98	0.20	21.5
Total	**730.58**	**412.54**	**300.41**	**56.5**	**41.12**	**9.2**	**20.6**	**9,897**	**6,519**	**16,416**	**39.7**	**124.8**	**3.5**	**7.0**	**3735.22**	**17.33**	**3752.54**	**0.46**	**101.7**
Exergy loss	**17.63**																		
$\dot{B}_k^{PF}$ **(Pts/h)**	**1259**																		

Table 4.7: Selected results at the component level for the AZEP 85

Component, k	$\dot{E}_{F,k}$ (MW)	$\dot{E}_{P,k}$ (MW)	$\dot{E}_{D,k}$ (MW)	ε_k (%)	$y_{D,k}$ (%)	$c_{F,k}$ (€/GJ)	$c_{P,k}$ (€/GJ)	$\dot{C}_{D,k}$ (€/h)	$\dot{Z}_k$ (€/h)	$\dot{C}_{D,k}+\dot{Z}_k$ (€/h)	f_k (%)	r_k (%)	$b_{F,k}$ (Pts/GJ)	$b_{P,k}$ (Pts/GJ)	$\dot{B}_{D,k}$ (Pts/h)	$\dot{Y}_k$ (Pts/h)	$\dot{B}_{D,k}+\dot{Y}_k$ (Pts/h)	$f_{b,k}$ (%)	$r_{b,k}$ (%)
C1	238.30	227.13	11.17	95.3	1.53	19.8	22.2	797	1,169	1,966	59.5	12.1	6.2	6.5	250.79	0.19	250.98	0.08	4.9
CC	620.26	466.61	153.65	75.2	21.03	9.3	12.7	5,120	746	5,866	12.7	37.7	3.5	5.0	1932.51	0.31	1932.82	0.02	43.9
MCM	82.65	77.03	5.62	93.2	0.77	13.6	18.9	275	1,192	1,468	81.2	38.9	5.1	8.9	103.16	53.34	156.50	34.08	75.2
MCM HTHX	120.72	119.49	1.24	99.0	0.17	13.6	15.4	61	696	757	92.0	12.9	5.1	5.2	22.79	32.67	55.46	58.90	2.5
MCM LTHX	221.06	211.51	9.55	95.7	1.31	13.6	15.7	467	1,113	1,580	70.4	15.3	5.1	5.4	175.99	67.57	243.56	27.74	6.2
DB	109.46	78.20	31.26	71.4	4.28	9.3	13.9	1,042	277	1,318	21.0	50.6	3.5	6.5	393.12	0.05	393.17	0.01	86.6
GT1	495.66	477.85	17.81	96.4	2.44	18.4	19.8	1,177	1,336	2,513	53.2	8.0	6.0	6.2	385.39	0.91	386.30	0.23	3.7
C6	7.31	7.07	0.24	96.8	0.03	36.4	61.5	31	607	638	95.1	68.9	10.0	10.4	8.54	0.60	9.14	6.53	3.6
AIR HX	6.91	5.15	1.76	74.5	0.24	13.1	18.0	83	8	91	8.8	37.5	5.1	6.8	32.09	0.00	32.09	0.01	34.2
NGPH	5.80	0.10	5.70	1.7	0.78	13.1	795.8	269	6	275	2.2	5974.4	5.1	301.0	103.97	0.00	103.97	0.00	5843.8
HPSH	31.65	28.65	3.00	90.5		18.4	22.6					23.1	6.0	6.9					14.9
HPEV	39.82	36.29	3.54	91.1		18.4	22.2					21.2	6.0	6.8					13.8
HPEC	26.17	22.65	3.52	86.6	1.38	18.4	23.6	664	383	1,047	36.6	28.6	6.0	7.3	217.49	1.29	218.78	0.59	21.9
LPSH	1.06	0.77	0.29	72.5		18.4	34.2					86.3	6.0	9.2					53.6
LPEV	15.25	12.50	2.75	81.9		18.4	27.6					50.4	6.0	7.9					31.1
LPEC	11.20	7.83	3.37	69.9	0.88	18.4	33.8	424	262	686	38.3	83.9	6.0	9.7	138.76	0.22	138.98	0.16	60.7
LPST	49.32	42.62	6.70	86.4	0.92	24.4	32.8	587	489	1,077	45.4	34.6	7.3	8.8	175.98	0.37	176.35	0.21	21.1
ST4	27.92	21.14	6.78	75.7	0.93	22.8	36.4	557	257	814	31.5	59.6	7.0	10.0	170.64	0.22	170.86	0.13	43.5
C2	3.38	2.81	0.57	83.3		36.4	169.1					364.3	10.0	39.8					297.3
C3	3.48	2.88	0.60	82.8		36.4	86.6					137.9	10.0	13.7					36.2
C4	3.47	2.85	0.62	82.2		36.4	91.2					150.5	10.0	14.3					42.9
C5	3.52	2.85	0.66	81.2	0.33	36.4	93.2	320	1,425	1,745	81.7	156.0	10.0	14.5	88.15	0.23	88.37	0.26	45.1
Total	**730.56**	**389.89**	**313.43**	**53.4**	**42.90**	**9.2**	**25.1**	**10,326**	**11,198**	**21,524**	**52.0**	**174.3**	**3.5**	**6.9**	**3897.09**	**174.95**	**4072.05**	**4.30**	**100.2**
Exergy loss	**27.25**																		
$\dot{B}^{PF}$ **(Pts/h)**	**641 (CC)** **459 (DB)**																		

Table 4.8: Selected results at the component level for the AZEP 100

Component, k	$\dot{E}_{F,k}$ (MW)	$\dot{E}_{P,k}$ (MW)	$\dot{E}_{D,k}$ (MW)	ε_k (%)	$y_{D,k}$ (%)	$c_{F,k}$ (€/GJ)	$c_{P,k}$ (€/GJ)	$\dot{C}_{D,k}$ (€/h)	$\dot{Z}_k$ (€/h)	$\dot{C}_{D,k}+\dot{Z}_k$ (€/h)	f_k (%)	r_k (%)	$b_{F,k}$ (Pts/GJ)	$b_{P,k}$ (Pts/GJ)	$\dot{B}_{D,k}$ (Pts/h)	$\dot{Y}_k$ (Pts/h)	$\dot{B}_{D,k}+\dot{Y}_k$ (Pts/h)	$f_{b,k}$ (%)	$r_{b,k}$ (%)
C1	280.47	267.32	13.15	95.3	1.80	20.6	22.8	975	1,133	2,108	53.8	10.6	6.1	6.4	288.47	0.18	288.65	0.06	4.9
CC	729.72	549.07	180.65	75.2	24.72	9.3	12.7	6,020	831	6,851	12.1	37.4	3.5	5.0	2272.15	0.30	2272.44	0.01	43.8
MCM	97.30	90.54	6.75	93.1	0.92	13.6	19.1	330	1,459	1,789	81.6	40.4	5.1	8.4	123.85	35.87	159.72	22.46	65.9
MCM HTHX	142.04	140.61	1.43	99.0	0.20	13.6	15.3	70	791	861	91.9	12.5	5.1	5.2	26.38	38.37	64.75	59.25	2.5
MCM LTHX	260.08	248.86	11.22	95.7	1.54	13.6	15.6	548	1,270	1,818	69.8	15.0	5.1	5.4	206.67	79.33	286.01	27.74	6.2
GT1	532.11	512.51	19.60	96.3	2.68	19.2	20.6	1,352	1,295	2,647	48.9	7.5	5.9	6.1	414.12	0.87	415.00	0.21	3.8
C6	8.59	8.31	0.28	96.8	0.04	37.7	61.5	38	675	713	94.7	63.1	9.9	10.2	9.85	0.60	10.44	5.71	3.5
AIR HX	8.20	6.12	2.09	74.6	0.29	13.1	18.0	98	9	107	8.6	37.3	5.1	6.8	38.02	0.00	38.02	0.01	34.1
NGPH	5.82	0.10	5.72	1.7	0.78	13.1	791.7	269	6	275	2.2	5955.1	5.1	300.1	104.32	0.00	104.32	0.00	5826.8
HPSH	18.82	17.15	1.68	91.1		19.2	23.8					24.2	5.9	6.7					14.1
HPEV	32.96	30.50	2.46	92.5		19.2	23.0					19.9	5.9	6.5					11.5
HPEC	22.53	19.04	3.49	84.5	1.04	19.2	25.3	526	340	866	39.3	32.2	5.9	7.4	161.13	1.03	162.16	0.63	26.1
LPSH	1.08	0.78	0.31	71.8		19.2	36.2					88.7	5.9	9.2					56.0
LPEV	16.73	13.76	2.97	82.2		19.2	28.6					49.5	5.9	7.7					30.8
LPEC	12.06	8.19	3.87	67.9	0.98	19.2	36.1	494	277	771	36.0	88.5	5.9	9.8	151.16	0.23	151.39	0.15	67.4
LPST	44.78	38.70	6.08	86.4	0.83	25.8	34.5	564	435	999	43.5	33.7	7.2	8.8	158.54	0.34	158.88	0.21	21.1
ST4	32.85	24.83	8.02	75.6	1.10	23.7	37.7	686	288	974	29.6	58.9	6.9	9.9	198.25	0.24	198.49	0.12	44.0
C2	3.96	3.31	0.66	83.4		37.7	167.7					344.5	9.9	39.4					298.4
C3	4.08	3.39	0.69	83.0		37.7	86.1					128.3	9.9	13.5					36.1
C4	4.07	3.35	0.72	82.2		37.7	90.7					140.4	9.9	14.1					42.9
C5	4.13	3.36	0.78	81.2	0.39	37.7	92.8	387	1,583	1,970	80.3	145.8	9.9	14.3	101.52	0.23	101.75	0.22	45.0
Total	**730.73**	**377.52**	**320.71**	**51.7**	**43.89**	**9.2**	**26.3**	**10,566**	**11,706**	**22,272**	**52.6**	**187.4**	**3.5**	**6.8**	**3987.65**	**174.91**	**4162.56**	**4.20**	**97.0**
Exergy loss	**32.50**																		
$\dot{B}_k^{PF}$ **(Pts/h)**	**754**																		

Table 4.9: Selected results at the component level for the CLC plant

Component, k	$\dot{E}_{F,k}$ (MW)	$\dot{E}_{P,k}$ (MW)	$\dot{E}_{D,k}$ (MW)	ε_k (%)	$y_{D,k}$ (%)	$c_{F,k}$ (€/GJ)	$c_{P,k}$ (€/GJ)	$\dot{C}_{D,k}$ (€/h)	$\dot{Z}_k$ (€/h)	$\dot{C}_{D,k}+\dot{Z}_k$ (€/h)	f_k (%)	r_k (%)	$b_{F,k}$ (Pts/GJ)	$b_{P,k}$ (Pts/GJ)	$\dot{B}_{D,k}$ (Pts/h)	$\dot{Y}_k$ (Pts/h)	$\dot{B}_{D,k}+\dot{Y}_k$ (Pts/h)	$f_{b,k}$ (%)	$r_{b,k}$ (%)
C1	281.78	268.57	13.21	95.3	1.81	19.3	21.3	919	964	1,884	51.2	10.1	6.0	6.3	286.48	0.19	286.67	0.07	4.9
CLC	694.73	500.67	194.06	72.1	26.56	9.1	15.5	6,391	4,974	11,365	43.8	68.9	3.5	5.3	2418.44	2.54	2420.97	0.10	52.5
GT1	540.99	521.34	19.65	96.4	2.69	18.1	19.3	1,278	1,102	2,380	46.3	7.0	5.8	6.0	410.68	0.91	411.59	0.22	3.8
NGPH	6.32	1.12	5.20	17.7	0.71	11.8	69.1	220	10	231	4.4	487.2	4.1	22.9	75.87	0.01	75.88	0.01	465.6
HPSH	22.43	20.43	1.99	91.1		18.1	22.2					22.7	5.8	7.1					14.3
HPEV	35.74	32.97	2.77	92.2		18.1	21.5					19.2	5.8	6.6					12.1
HPEC	24.25	20.58	3.67	84.9	1.15	18.1	23.7	548	301	850	35.5	31.2	5.8	6.5	176.20	1.16	177.36	0.65	25.6
RH	16.60	14.36	2.24	86.5		18.1	23.4					29.4	5.8	7.3					22.6
IPSH	0.63	0.49	0.14	78.1		18.1	30.2					67.0	5.8	8.2					40.5
IPEV	11.97	11.00	0.97	91.9		18.1	22.8					26.1	5.8	6.5					12.8
IPEC	2.03	1.70	0.33	83.6	0.50	18.1	24.8	240	161	400	40.1	37.4	5.8	7.4	77.03	0.53	77.56	0.69	28.2
LPSH	1.12	0.81	0.32	71.9		18.1	33.4					84.8	5.8	9.1					56.2
LPEV	17.03	13.99	3.03	82.2		18.1	26.7					47.7	5.8	7.6					31.2
LPEC	11.28	7.52	3.76	66.6	0.97	18.1	34.4	463	221	684	32.4	90.7	5.8	10.0	148.65	0.22	148.87	0.15	72.1
LPST	48.80	42.17	6.63	86.4	0.91	24.6	32.5	587	387	974	39.7	32.0	7.2	8.8	172.69	0.36	173.05	0.21	21.3
ST4	20.73	15.66	5.06	75.6	0.69	23.2	36.5	424	157	580	27.0	57.2	6.9	10.0	125.88	0.18	126.07	0.15	44.3
C1	3.85	3.24	0.61	84.1		36.5	165.8					353.6	10.0	40.4					305.3
C2	3.96	3.32	0.64	83.8		36.5	76.3					108.9	10.0	13.1					31.0
C3	3.91	3.27	0.64	83.5		36.5	78.8					115.8	10.0	13.5					35.5
C4	3.93	3.26	0.67	83.0	0.35	36.5	79.8	338	1,275	1,612	79.1	118.5	10.0	13.6	92.03	0.23	92.26	0.25	36.6
Total	**730.73**	**375.99**	**307.41**	**51.5**	**42.07**	**9.2**	**25.4**	**10,128**	**10,347**	**20,474**	**50.5**	**177.5**	**3.5**	**6.8**	**3822.32**	**22.84**	**3845.17**	**0.59**	**94.5**
Exergy loss	**47.33**																		
$\dot{B}_k^{PF}$ **(Pts/h)**	**856**																		

Table 4.10: Selected results at the component level for MEA-0.2

Component, k	$\dot{E}_{F,k}$ (MW)	$\dot{E}_{P,k}$ (MW)	$\dot{E}_{D,k}$ (MW)	ε_k (%)	$y_{D,k}$ (%)	$c_{F,k}$ (€/GJ)	$c_{P,k}$ (€/GJ)	$\dot{C}_{D,k}$ (€/h)	$\dot{Z}_k$ (€/h)	$\dot{C}_{D,k}+\dot{Z}_k$ (€/h)	f_k (%)	r_k (%)	$b_{F,k}$ (Pts/GJ)	$b_{P,k}$ (Pts/GJ)	$\dot{B}_{D,k}$ (Pts/h)	$\dot{Y}_k$ (Pts/h)	$\dot{B}_{D,k}+\dot{Y}_k$ (Pts/h)	$f_{b,k}$ (%)	$r_{b,k}$ (%)
C1	242.68	231.30	11.38	95.3	1.56	16.9	19.4	691	1,396	2,086	66.9	14.9	6.1	6.4	249.98	0.24	250.22	0.09	4.9
CC	729.62	508.76	220.87	69.7	30.23	9.2	13.7	7,276	997	8,273	12.0	49.4	3.5	5.6	2746.20	0.38	2746.59	0.01	63.5
GT	551.15	530.67	20.47	96.3	2.80	15.4	16.9	1,137	1,595	2,732	58.4	9.3	5.9	6.1	433.06	1.13	434.18	0.26	3.9
HPSH	35.06	31.72	3.34	90.5		15.4	18.9					22.6	5.9	6.7					13.5
HPEV	43.64	39.91	3.73	91.4		15.4	18.6					20.4	5.9	6.6					11.9
HPEC	28.92	24.91	4.01	86.1	1.52	15.4	19.6	615	424	1,040	40.8	27.3	5.9	7.1	234.36	1.46	235.82	0.62	20.4
RH	26.46	23.89	2.57	90.3		15.4	18.9					22.2	5.9	6.7					13.8
IPSH	0.18	0.12	0.06	69.0		15.4	33.3					115.7	5.9	9.2					57.1
IPEV	6.10	5.67	0.43	92.9		15.4	20.1					30.3	5.9	6.4					9.7
IPEC	1.06	0.87	0.19	82.5	0.44	15.4	21.3	180	182	362	50.3	38.2	5.9	7.5	68.58	0.83	69.41	1.19	27.0
LPSH	1.43	1.05	0.38	73.3		15.4	27.8					80.4	5.9	8.6					46.4
LPEV	19.02	15.47	3.54	81.4		15.4	23.1					49.8	5.9	7.6					29.1
LPEC	11.57	7.81	3.76	67.5	1.05	15.4	28.5	427	284	711	39.9	84.5	5.9	9.5	162.68	0.23	162.90	0.14	61.2
LPST	40.94	35.38	5.56	86.4	0.76	21.4	27.8	428	296	723	40.9	30.0	7.2	8.6	144.91	0.32	145.23	0.22	19.2
C2	18.53	16.93	1.59	91.4		22.5	43.6					94.0	7.2	8.0					10.3
C3	4.33	3.78	0.55	87.3		22.4	132.9					493.8	7.2	25.8					256.9
C4	3.45	2.86	0.59	82.9		22.4	100.1					347.2	7.2	16.3					125.2
C5	3.44	2.82	0.61	82.1	0.46	22.4	77.0	270	2,297	2,567	89.5	244.3	7.2	11.5	87.31	4.90	92.21	5.31	58.3
C6	3.49	2.83	0.66	81.1	0.09	22.4	77.4	53	354	406	87.0	245.7	7.2	11.4	17.13	0.20	17.34	1.18	57.5
CAU	59.28	-	40.59	-	5.56	23.7	-	3,463	1,023	4,486	22.8	-	6.9	-	1006.53	1.75	1008.28	0.17	-
Total	**730.58**	**353.82**	**349.14**	**48.4**	**47.79**	**9.2**	**26.3**	**11,502**	**9,440**	**20,942**	**45.1**	**187.0**	**3.5**	**7.6**	**4341.17**	**21.63**	**4362.80**	**0.50**	**120.7**
Exergy loss	**27.62**																		
$\dot{B}_k^{PF}$ **(Pts/h)**	**1270**																		

Table 4.11: Selected results at the component level for MEA-0

Component, k	$\dot{E}_{F,k}$ (MW)	$\dot{E}_{P,k}$ (MW)	$\dot{E}_{D,k}$ (MW)	ε_k (%)	$y_{D,k}$ (%)	$c_{F,k}$ (€/GJ)	$c_{P,k}$ (€/GJ)	$\dot{C}_{D,k}$ (€/h)	$\dot{Z}_k$ (€/h)	$\dot{C}_{D,k}+\dot{Z}_k$ (€/h)	f_k (%)	r_k (%)	$b_{F,k}$ (Pts/GJ)	$b_{P,k}$ (Pts/GJ)	$\dot{B}_{D,k}$ (Pts/h)	$\dot{Y}_k$ (Pts/h)	$\dot{B}_{D,k}+\dot{Y}_k$ (Pts/h)	$f_{b,k}$ (%)	$r_{b,k}$ (%)
C1	242.68	231.30	11.38	95.3	1.56	19.4	690	1,395	2,086	66.9	14.9	19.4	6.1	6.4	249.94	0.24	250.17	0.09	4.9
CC	729.62	508.76	220.87	69.7	30.23	13.7	7,276	997	8,273	12.0	49.4	13.7	3.5	5.6	2746.20	0.38	2746.59	0.01	63.5
GT	551.15	530.67	20.47	96.3	2.80	16.9	1,137	1,595	2,732	58.4	9.3	16.9	5.9	6.1	432.98	1.13	434.11	0.26	3.9
HPSH	35.06	31.72	3.34	90.5		18.7	615				20.9	18.7	5.9	6.6					12.1
HPEV	43.64	39.91	3.73	91.4		18.4	18.7				19.0	18.4	5.9	6.5					10.6
HPEC	28.92	24.91	4.01	86.1	1.52	19.3	19.6	423	1,039	40.8	24.9	19.3	5.9	6.9	234.32	1.45	235.77	0.62	18.2
RH	26.46	23.89	2.57	90.3		18.6	180				20.6	18.6	5.9	6.6					12.3
IPSH	0.18	0.12	0.06	69.0		32.2	33.3				108.7	32.2	5.9	8.9					51.0
IPEV	6.10	5.67	0.43	92.9		19.9	20.4				29.2	19.9	5.9	6.4					8.7
IPEC	1.06	0.87	0.19	82.5	0.44	20.8	21.2	182	362	50.3	35.0	20.8	5.9	7.3	68.57	0.83	69.40	1.19	24.1
LPSH	1.43	1.05	0.38	73.3		27.0	427				74.7	27.0	5.9	8.3					41.4
LPEV	19.02	15.47	3.54	81.4		22.6	23.1				46.3	22.6	5.9	7.4					26.0
LPEC	11.57	7.81	3.76	67.5	1.05	27.3	28.0	284	711	39.9	77.3	27.3	5.9	9.1	162.65	0.23	162.87	0.14	54.6
LPST	17.84	15.42	2.42	86.4	0.33	29.3	200	134	334	40.1	27.9	29.3	7.5	8.8	65.52	0.19	65.71	0.29	17.4
C2	18.53	16.93	1.59	91.4		43.2	191				95.4	43.2	7.1	7.8					10.3
C3	3.54	3.00	0.54	84.6		153.7	161.9				594.8	153.7	7.1	30.2					325.7
C4	3.45	2.86	0.59	82.9		78.6	83.6				255.3	78.6	7.1	11.8					66.4
C5	3.44	2.82	0.61	82.1	0.33	77.2	82.2	1,435	1,626	88.2	249.1	77.2	7.1	11.3	61.40	1.32	62.72	2.11	58.7
C6	3.49	2.83	0.66	81.1	0.09	77.6	52	360	412	87.3	250.8	77.6	7.1	11.2	16.79	0.20	16.99	1.20	57.8
CAU	86.54	-	67.95	-	9.30	-	5,417	1,086	6,503	16.7	-	-	6.8	-	1658.02	3.50	1661.52	0.21	-
Total	**730.58**	**334.63**	**368.27**	**45.8**	**50.41**	**9.2**	**27.6**	**12,133**	**9,257**	**21,390**	**43.3**	**201.9**	**67.8**	**73.0**	**4579.01**	**19.27**	**4598.28**	**0.42**	**7.6**
Exergy loss	**27.68**																		
$\dot{B}_k^{PF}$ **(Pts/h)**	**1268**																		

Table 4.12: Selected results at the component level for the S-Graz cycle and the simple oxy-fuel plant

S-Graz cycle						ATR plant					
	$\dot{E}_{F,k}$	$\dot{E}_{P,k}$	$\dot{E}_{D,k}$	ε_k	$y_{D,k}$		$\dot{E}_{F,k}$	$\dot{E}_{P,k}$	$\dot{E}_{D,k}$	ε_k	$y_{D,k}$
Component, k	(MW)	(MW)	(MW)	(%)	(%)	Component, k	(MW)	(MW)	(MW)	(%)	(%)
C1	53.76	50.84	2.92	94.6	0.40	*C1*	56.60	53.53	3.07	94.6	0.42
CC	736.37	551.82	184.55	74.9	25.17	*CC*	733.81	512.57	221.24	69.9	30.18
GT1	264.57	253.32	11.25	95.7	1.53	*GT*	437.91	420.80	17.11	96.1	2.33
GT2	362.41	345.23	17.18	95.3	2.34	*HPSH*	41.65	35.88	5.78	86.1	2.44
GT3	78.21	69.56	8.65	88.9	1.18	*HPEV*	51.98	45.21	6.78	87.0	
HPSH	52.48	46.00	6.48	87.7		*HPEC*	33.59	28.22	5.37	84.0	
HPEV	65.48	58.00	7.47	88.6	1.91	*RH*	22.83	18.78	4.05	82.3	0.61
HPEC	1.35	1.27	0.08	93.9		*IPSH*	0.10	0.06	0.04	61.4	
NGPH	7.05	3.61	3.44	51.2	0.47	*IPEV*	4.45	4.20	0.25	94.4	
WPH1	5.57	3.09	2.48	55.5		*IPEC*	0.77	0.65	0.13	83.7	
WPH2	31.83	25.56	6.27	80.3	1.40	*LPSH*	0.85	0.62	0.23	72.9	0.67
WPH3	16.19	14.67	1.52	90.6		*LPEV*	12.43	10.24	2.20	82.3	
ASU	51.24	11.46	39.78	22.4	5.43	*LPEC*	10.23	7.73	2.50	75.6	
C2	12.45	11.04	1.41	88.7		*LPST*	51.25	44.29	6.96	86.4	0.95
C3	4.69	3.95	0.74	84.1	0.51	*ST4*	21.91	19.22	2.69	87.7	0.37
C4	4.70	3.93	0.77	83.5		*ASU*	53.95	11.59	42.36	21.5	5.78
C5	4.75	3.94	0.81	83.0		*C2*	4.82	4.05	0.78	83.9	0.44
C7	92.86	86.56	6.30	93.2	1.90	*C3*	4.80	4.01	0.79	83.5	
C8	132.31	124.67	7.63	94.2		*C4*	4.76	3.95	0.81	83.0	
C9	16.43	13.73	2.70	83.5	0.75	*C5*	4.83	3.96	0.87	82.1	
C10	17.72	14.93	2.80	84.2		*C6*	62.77	57.08	5.70	90.9	1.03
Total	**733.16**	**352.01**	**349.26**	**48.0**	**47.64**	*C7*	56.67	54.82	1.85	96.7	
Exergy loss	**31.89**					*C8*	16.43	13.73	2.70	83.5	0.75
						C9	17.89	15.08	2.81	84.3	
						Total	**733.18**	**313.40**	**388.71**	**42.7**	**53.02**
						Exergy loss	**31.08**				

Table 4.13: Selected results at the component level for the MSR and ATR plants

MSR plant						ATR plant					
	$\dot{E}_{F,k}$	$\dot{E}_{P,k}$	$\dot{E}_{D,k}$	ε_k	$y_{D,k}$		$\dot{E}_{F,k}$	$\dot{E}_{P,k}$	$\dot{E}_{D,k}$	ε_k	$y_{D,k}$
Component, k	(MW)	(MW)	(MW)	(%)	(%)	Component, k	(MW)	(MW)	(MW)	(%)	(%)
C1	206.31	196.73	9.58	95.4	1.31	*C1*	221.95	211.43	10.53	95.3	1.44
CC	598.70	455.59	143.11	76.1	19.59	*CC*	659.64	502.80	156.84	76.2	21.47
DB	338.16	252.94	85.23	74.8	11.66	*GT1*	519.91	500.85	19.06	96.3	2.61
GT1	481.89	463.51	18.37	96.2	2.51	*HPSH1*	2.37	2.06	0.31	86.9	1.14
GT2	54.18	50.81	3.37	93.8	0.46	*HPSH2*	26.00	23.38	2.62	89.9	
HPSH	36.79	32.41	4.38	88.1		*HPEV*	36.90	32.76	4.14	88.8	
HPEV	47.13	40.95	6.17	86.9	2.38	*HPEC*	10.69	9.40	1.29	87.9	
HPEC	32.45	25.58	6.86	78.8		*RH1*	11.37	10.65	0.72	93.7	0.97
LPSH	3.17	2.40	0.77	75.7		*RH2*	8.76	7.95	0.81	90.8	
LPEV	27.16	21.11	6.05	77.7	1.56	*IPSH*	5.51	4.72	0.79	85.6	
LPEC	13.93	9.33	4.60	67.0		*IPEV*	30.37	26.75	3.62	88.1	
NGPH	32.62	28.56	4.06	87.6	0.56	*IPEC*	6.89	5.75	1.14	83.5	
LPST	22.33	19.29	3.03	86.4	0.42	*LPSH1*	1.54	1.14	0.40	74.1	1.25
MSR-H2	180.20	171.88	8.32	95.4	1.14	*LPSH2*	3.37	2.86	0.52	84.7	
C2	3.84	3.19	0.64	83.2		*LPEV*	19.39	15.73	3.66	81.1	
C3	4.06	3.37	0.69	83.0	0.38	*LPEC*	13.01	8.44	4.57	64.9	
C4	4.04	3.33	0.71	82.4		*NGPH*	34.36	30.19	4.17	87.9	0.57
C5	4.10	3.34	0.76	81.4		*H2 PH*	32.61	25.32	7.30	77.6	1.00
Total	**730.63**	**334.64**	**338.70**	**45.8**	**46.36**	*APH*	9.38	5.91	3.47	63.0	0.47
Exergy loss	**57.29**					*LPST*	23.85	20.61	3.24	86.4	0.44
						ATR	809.32	-	51.81	-	7.09
						SHIFTER1	690.54	-	3.43	-	0.47
						SHIFTER2	659.61	-	0.63	-	
						CAU	33.54	-	29.95	-	4.10
						Mix CH4/Air	428.31	419.98	8.33	98.1	1.14
						Mix CH4/H2O	507.54	500.94	6.60	98.7	0.90
						Total	**730.62**	**339.81**	**358.06**	**46.5**	**49.01**
						Exergy loss	**32.75**				

4.2 Advanced exergy-based analyses

The advanced exergetic, exergoeconomic and exergoenvironmental analyses have been applied to the reference plant and the two most economical plants performing CO_2 capture, the AZEP 85 and the CLC plant.

4.2.1 Advanced exergetic analysis

4.2.1.1 Application of the advanced exergetic analysis

To conduct the advanced exergetic analysis, the theoretical and unavoidable conditions for all the components must be defined (see section 3.3). For the calculation of the unavoidable exergy destruction, the best possible operating conditions are considered for each component. These calculations regard each component in isolation, thus simultaneous component interactions are not a concern here. On the other hand, the calculation of the endogenous exergy destruction involves theoretical operation of components, considers the overall plant and it, therefore, examines simultaneous component interactions (mexogenous exergy destruction, Equation 3.21) as well. For the calculation of the endogenous exergy destruction of component *k*, component *k* operates under real conditions, while all other components operate theoretically. For the calculation of component interactions, the examined components operate under real conditions in pairs, while all remaining components operate theoretically. The assumptions made for the theoretical and unavoidable operation of all of the components are shown in Table 4.14.

Assumptions related to the theoretical operation of components include zero pressure losses, high efficiencies, low temperature differences, etc. When a component operates without pressure losses, the pressure losses of any parallel components are also considered to be zero, even if the parallel components operate under real conditions. Additionally, changes in the minimum temperature differences of some components might affect the operation of parallel components by increasing or decreasing their exergy destruction. As already mentioned, in the description of the methodology (section 3.3.1), theoretical reactors are defined using the exergy balance, while the mass and energy balances of the components are not maintained. To achieve this, the plants are split into two parts after each reactor.

In the case of the reference plant, when either the CC or the neighboring components operate theoretically, streams 3 and 4 Figure 4.4[4] will differ to maintain the predefined (either real- or theoretical-related) exergy balance of the reactor. When theoretical operation is assumed for a component or a group of components, the mass flows of the required air and fuel are calculated through the net power output of the plant, $\dot{W}_{net}$, and the excess air fraction (λ) of the CC, which have the same values as in the real case. For the calculation of the endogenous exergy destruction, the CC must operate with its real exergetic efficiency

[4] For simplicity, the numbering of the streams in Figure 4.4 differs from that in Figure A.1.1. The correlation of the numbers in Figure 4.4 with Figure A.1.1 is the following: 1 is 1, 2 is 2, 3&4 are 4, 5 is 5 and 6 is 3.

Table 4.14: Assumptions related to the theoretical and unavoidable operation of the components

Component, k	$E_{D,k}^{real}$	*Theoretical operation*	$E_{D,k}^{UN}$	*Component, k*	$E_{D,k}^{real}$	*Theoretical operation*	$E_{D,k}^{UN}$
GT1	η_{is} =92-94% η_{mech} =99%	η_{is} =100% η_{mech} =100%	η_{is} =96% η_{mech} =100%	*C2-C5*	η_{is} =75-79% η_{mech} =99%	η_{is} =100% η_{mech} =100%	η_{is} =94% η_{mech} =100%
GT2	η_{is} =90-94% η_{mech} =99%	η_{is} =100% η_{mech} =100%	η_{is} =96% η_{mech} =100%	*C6*	η_{is} =96.8% η_{is} =85-88%	η_{is} =100% η_{mech} =100%	η_{is} =94% η_{mech} =100%
C1	η_{is} =91-94% η_{mech} =99%	η_{is} =100% η_{mech} =100%	η_{is} =94% η_{mech} =100%	*SH/RH*	ΔT_{min} =20°C ΔP_{HS}[a] ΔP_{CS} =5%[f]	ΔT_{min} =0 ΔP =0	ΔT_{min} =4 ΔP =0
CC	Q_{loss} =0.01 ΔP =3%[f] λ=2.05	Q_{loss} =0 ΔP =0 λ=2.05	Q_{loss} =0 ΔP =0 λ=1	*EV*	Pinch point =10°C Appr. T =6°C ΔP_{HS}[a] ΔP_{CS} =5%[b,f]	ΔT_{min} =0 Appr. T =0 ΔP =0	ΔT_{min} =1 Appr. T =0 ΔP =0
DB	Q_{loss} =0.01 ΔP =1%[f] λ=10	Q_{loss} =0 ΔP =0 λ=10 [d]	Q_{loss} =0 ΔP =0 λ=1	*EC*	ΔT_{min}=*dependant*[g] ΔP_{HS} [a] ΔP_{CS} =3%/100°C	ΔT_{min} =0 ΔP =0	ΔT_{min} =1 ΔP =0
STs	η =86-94% η_{mech} =99%	η_{is} =100% η_{mech} =100%	η_{is} =95% HP, IP 92% LP η_{mech} =100%				
CLC Reactors	Q_{loss} =0 ΔP =3%[f] λ=1.05	Q_{loss} =0 ΔP =0 λ=1.05	Q_{loss} =0 ΔP =0 λ=1	*NGPH*	ΔT_{min}=400[e] ΔP_{HP}=0.65% bar/100°C ΔP_{LP}=0.60% bar/100°C	ΔT_{min}=*dependant*[g] ΔP =0	ΔT_{min} =20 ΔP =0
MCM	Q_{loss} =0.0 Δp =0.3%[f] ΔT_{min} =60	Q_{loss} =0 Δp =0 ΔT_{min}=*dependant*[g]	Q_{loss} =0 Δp =0 ΔT_{min} =20	*Air HX*	ΔT_{min}=700[e] ΔP_{HP}=0.65% bar/100°C	ΔT_{min}=*dependant*[g] ΔP =0	ΔT_{min} =20 ΔP =0
CC MCM	Q_{loss} =0.01 ΔP =3%[f] λ=1.05	Q_{loss} =0 ΔP =0 λ=1.05	Q_{loss} =0 ΔP =0 λ=1	*COOL*	ΔT_{min} =20°C (10°C in FG COND) ΔP_{HS}[a] ΔP_{CS} =3%/100°C	ΔT_{min} =0 ΔP =0	ΔT_{min} =1 ΔP =0
MCM HTHX	ΔT_{min} =35°C ΔP_{HP}=0.65% bar/100°C	ΔT_{min}=*dependant*[g] ΔP =0	ΔT_{min} =20 ΔP =0	*Pumps*	η_{is} =67-90%[c] η_{mech} =98%	η_{is} =100% η_{mech} =100%	η_{is} =95% η_{mech} =100%
MCM LTHX	ΔT_{min} =60°C ΔP_{HP}=0.65% bar/100°C	ΔT_{min}=*dependant*[g] ΔP =0	ΔT_{min} =20 ΔP =0	*Motors*	η_{el} =80-95%	η_{el} =100%	η_{el} =98%
				Generators	η_{el}=98.5%	η_{el} =100%	η_{el} =99.5%

Here, HS: hot side and CS: cold side

[a] The ΔP_{HS} of a HX is calculated based on the pressure drop within the overall HRSG and the temperature variation within the HX (see Appendix B)

[b] Covered by an integrated pump

[c] See Appendix B for more details about the calculations

[d] Result of temperature limitation at the exit of the component

[e] Due to design requirements

[f] Percentage decrease based on the pressure of the incoming stream

[g] Depends on the operation of other components (see below)

($\dot{E}_2 + \varepsilon_{cc}\dot{E}_6 = \dot{E}_4$, with $\varepsilon_{cc} = \varepsilon_{CC}^{real}$), while in the theoretical case its exergy destruction must be set to zero ($\dot{E}_{D,CC} = 0 \Rightarrow \varepsilon_{CC} = 1 \Rightarrow \dot{E}_2 + \dot{E}_6 = \dot{E}_4$). The thermodynamic values of stream 4 agree with those of the real case throughout the analysis, while stream 2 differs depending on different combinations of operating states of the compressor (C1) and the CC. For example, when both of the components operate theoretically, no pressure losses are incurred within the CC. With lower pressure losses present, stream 1 must be compressed to a lower pressure, since the inlet pressure of the expander is kept constant, resulting in lower temperatures in streams 2 and 3. Moreover, the temperatures of streams 2 and 3 are also decreased by the high isentropic efficiency of the theoretical compressor. In total, there are two possible

thermodynamic states (real and theoretical) and two considered components (the CC and the compressor), thus 2^2=4 possible combinations to take into account when defining the exergy balance of the CC. The temperature and pressure of stream 2 is calculated for all 4 combinations and its exergy is provided as input to the respective simulation.

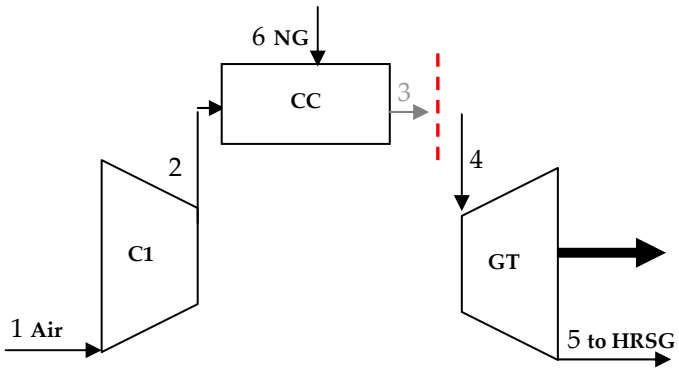

Figure 4.4: The GT system of the reference plant

In the CLC plant, there are two streams exiting the reactors (CLC unit in Figure 4.5[5]): the CO_2 stream (stream 8, led to GT2) and the oxygen-depleted air (stream 4, led to GT1). In order to control the exergy balance of the reactors, both exiting streams must be split.

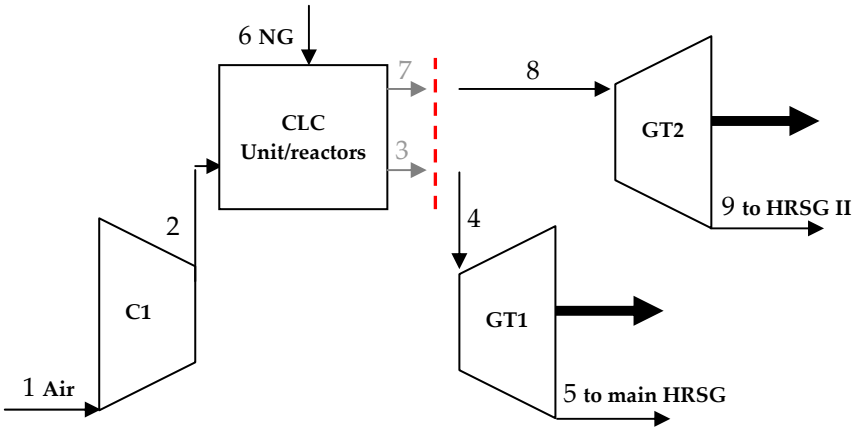

Figure 4.5: The CLC unit as part of the GT system of the CLC plant

Analogously to the reference plant, the $\dot{W}_{net}$ and the excess air fraction, controlled here through the mass flow ratio between the streams 1 and 6, are kept constant. When the reactors operate as in the real case, their exergetic efficiency agrees with that of the real case ($\dot{E}_2 + \varepsilon_{reactors}\dot{E}_6 = \dot{E}_4 + \dot{E}_8$ with $\varepsilon_{reactors} = \varepsilon_{reactors}^{real}$). When the CLC unit is assumed to operate theoretically its exergy destruction is set to zero ($\dot{E}_{D,reactors} = 0 \Rightarrow \varepsilon_{reactors} = 1 \Rightarrow \dot{E}_2 + \dot{E}_6 = \dot{E}_4 + \dot{E}_8$). To define all unknowns of the considered system, an auxiliary assumption is required for one of the two streams exiting the CLC unit. Due to material limitations, the temperatures of the streams exiting the CLC unit should not exceed 1200°C. Therefore, the temperature of stream

[5] For simplicity, the numbering of the streams in Figure 4.5 differs from that in Figure A.5.1. The correlation of the numbers in Figure 4.5 with Figure A.5.1 is the following: 1 is 1, 2 is 3, 3&4 are 4, 5 is 5, 6 is 60, 7&8 are 61 and 9 is 62.

4 has been kept constant at 1200°C and the temperature of stream 8 has been varied depending on simulation requirements. The exergy of stream 2 is also defined here based on the thermodynamic state of the components that affect it, i.e. C1 and the CLC unit. As in the reference plant, there are four possible component operating combinations that result in different values of exergy for stream 2.

In the case of the AZEP 85, things become more complex (Figure 4.6[6]). Here two reactors (CC and DB) are used and in order to maintain both of their exergy balances, the system must be separated in two places, once after each reactor. Analogously to the previous plants, the $\dot{W}_{net}$ and the excess air fractions of the CC and the DB are kept constant. When the CC operates as in the real case, its exergetic efficiency matches that of the real case ($\dot{E}_{21}+\varepsilon_{CC}\dot{E}_{22}=\dot{E}_{13}$ with $\varepsilon_{CC}=\varepsilon_{CC}^{real}$). When the CC operates theoretically, its exergy destruction is set to zero ($\dot{E}_{D,CC}=0\Rightarrow\varepsilon_{CC}=1\Rightarrow\dot{E}_{21}+\dot{E}_{22}=\dot{E}_{13}$). The same conditions apply for the DB of the plant: The real DB performs with the same efficiency as it does in the real case ($\dot{E}_{6}+\varepsilon_{DB}\dot{E}_{23}=\dot{E}_{8}$ with $\varepsilon_{DB}=\varepsilon_{DB}^{real}$), while the theoretical DB presents no exergy destruction ($\dot{E}_{D,DB}=0\Rightarrow\varepsilon_{DB}=1\Rightarrow\dot{E}_{6}+\dot{E}_{23}=\dot{E}_{8}$). The exergies of streams 21 and 6 at the inlet of the CC and the DB, depend on the operation of the components that can cause a change to their pressure and/or temperature. For example, the exergy of stream 21 depends on the MCM LTHX, the MCM, the MCM HTHX and the CC (16 possible combinations), while the exergy of stream 6 depends on the MCM LTHX, the MCM, the MCM HTHX and the C1 (16 possible combinations). When the pressures of streams 2 and 6 are defined, the pressures of streams 10 and 11 are adjusted accordingly. Because the predefinition of this many different exergy values is not recommended, a routine for the calculation of the physical exergy of streams has been added in the EbsScript of EbsilonProfessional (the chemical exergy of the streams agrees with the real case).

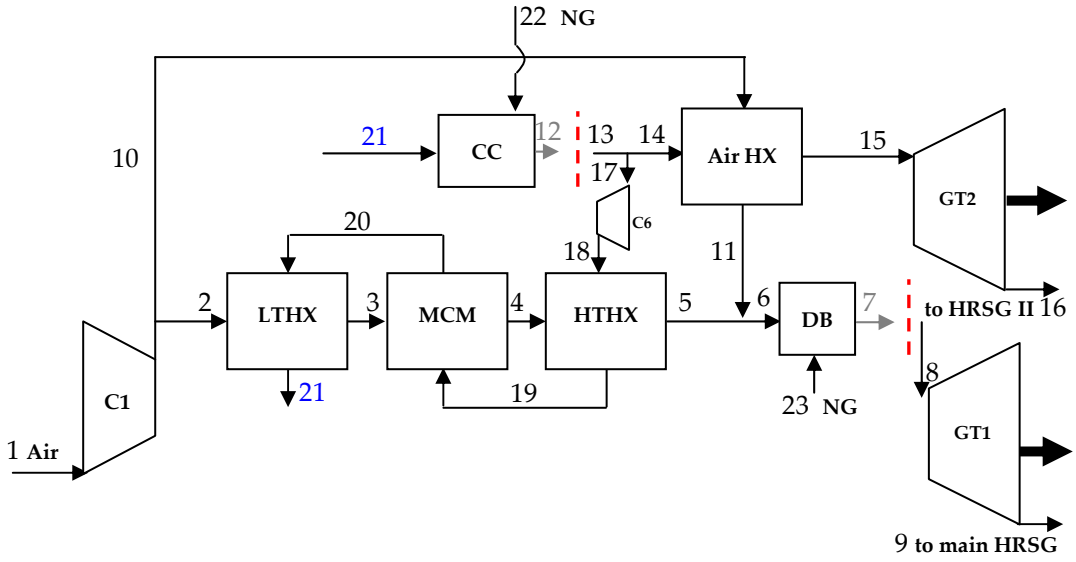

Figure 4.6: The MCM reactor as part of the GT system of the AZEP 85

[6] For simplicity, the numbering of the streams in Figure 4.6 differs from that in Figures A.2.1 and A.3.1. The correlation of the numbers in Figure 4.6 with Figure A.2.1/A.3.1 is the following: 1 is 1, 2 is 83, 3 is 84, 4 is 85, 5 is 88, 6 is 96, 7 and 8 are 4, 9 is 5, 10 is 82, 11 is 81, 12 and 13 are 90, 14 is 60, 15 is 61, 16 is 62, 17 is 91, 18 is 92, 19 is 86, 20 is 87, 21 is 89, 22 is 93 and 23 is 95.

Assumed restrictions related to the operation of the MCM inevitably lead to a strong interaction between the MCM and the MCM LTHX. When the LTHX is real, the inlet temperature of stream 20 must be high enough to achieve a ΔT_{min} (determined by streams 20 and 3) as close as possible to the real case. The minimum inlet temperature of the MCM is 900°C and the minimum temperature of stream 20 would, in this case, be 964°C. When the LTHX or the MCM operate theoretically, the temperatures of streams 4 and 20 are decreased to lower the ΔT_{min} of the components. Lastly, as in the previous cases, the inlet pressures of both of the GTs must agree with those of the real case and any pressure variations must be accounted for.

4.2.1.2 Splitting the exergy destruction

Results for selected components of the advanced exergetic analysis for the three analyzed plants are shown in Table 4.15 and were obtained using Equations (3.20)-(3.27). The complete results can be found in Appendix A and the supplemental data.

The main variable used to evaluate the potential for improvement of a plant is the avoidable exergy destruction, E_D^{AV}. Larger values of avoidable exergy destruction indicate significant improvement potential. A second quantity for consideration is the endogenous part of the exergy destruction, E_D^{EN}. Endogenous irreversibilities are usually easier to manipulate than exogenous (E_D^{EX}), because they depend on the operation of the component itself and not on component interactions that are more difficult to manage. Nonetheless, a change in the endogenous exergy destruction can alter component interactions as well. Thus, these two parts of the irreversibilities should be examined in parallel.

As already mentioned, in the conventional exergetic analysis, the larger the absolute value of the irreversibilities within a component, the higher its improvement priority must be. With the advanced exergetic analysis this value is scaled to refer only to its avoidable part. In general, the reactors in all of the three plants are the components with the highest absolute value of exergy destruction. However, the results related to the reactors of the AZEP 85 show some particularities. Although in the AZEP 85, the CC has a rate of exergy destruction almost five times higher than the DB of the plant, the DB results in a 23% higher E_D^{AV}. Thus, it has the highest improvement priority, followed by the CC, GT1, ST4 and C1. Moreover, while 68% and 67% of the exergy destruction in the reactors of the reference and CLC plants, respectively, is unavoidable, 91% of the exergy destruction in the CC of the AZEP 85 is unavoidable. The high unavoidable exergy destruction within the CC of the AZEP 85 is justified by its operation. Because preheated gases of high physical exergy are used, its exergy destruction decreases less with decreasing lambda than for the conventional CC of the reference plant. In the CLC plant, the reactors result in similar values to that of the CC of the reference plant. In the reference and CLC plants, GT1 and C1 follow the reactors in absolute values of avoidable exergy destruction. In the CLC, ST4 and the LPST follow C1.

In general, the majority of the exergy destruction within the components of the plants is unavoidable. Exceptions are the CO_2 compressors, the HXs that in the real case operate with high minimum temperature differences due to design requirements, ST4 of the oxy-fuel

plants, the DB of the AZEP 85 and GT1 in the reference plant and the AZEP 85. Moreover, most of the total exergy destruction of the plants is endogenous (83% in the reference plant, 77% in the AZEP 85 and 79% in the CLC plant). This shows that component interactions, represented by the exogenous exergy destruction, do not play a very significant role. Therefore, focus should be placed more on the improvement of internal component inefficiencies.

For the reactors, C1, the IPST, the LPST and the majority of the HXs, most of the endogenous exergy destruction is unavoidable ($E_{D,k}^{UN,EN}$). In contrast, more than half of the irreversibilities within the DB of the AZEP 85 are avoidable ($E_{D,k}^{AV,EN}$). Also, in all of the plants, GT1, the HPST and the CO_2 compressors (of the CLC plant and the AZEP 85), present higher avoidable endogenous exergy destruction. Similarly, the exogenous exergy destruction is found to be mostly unavoidable for the majority of the components.

Negative values calculated for the exogenous exergy destruction (Table 4.15) result from changes in the mass flow rates between the real and the endogenous cases. As already mentioned, for the calculation of each component's endogenous exergy destruction, the examined component operates under real conditions, while all other components operate theoretically. When the conditions of the theoretically operating components result in increased mass flows, the endogenous exergy destruction is higher than in the real case, E_D^{real}, and the E_D^{EX} is, therefore, found to be negative. For example, in the calculation of the E_D^{EN} of the generator of the GT system (GEN1) in the CLC and reference plants, the power output of the steam cycle is decreased, due to the lower temperature of the combustion products entering the HRSG – a result of the high isentropic efficiency of the theoretical expander. With this lower temperature, the power of the steam turbines is reduced. To keep the overall power output of the process constant, the power output of GT1 must increase. This is, however, determined by the mass flow, since the inlet temperature of GT1 remains constant. With increased mass flow, the E_D^{EN} of the generator is higher than its E_D^{real}, resulting in a negative E_D^{EX}. Similar explanations can be given for the negative values of the $E_D^{UN,EX}$, since their calculation depends on the calculation of the $E_D^{UN,EN}$, which is a function of the E_P^{EN} (see Equation 3.24). Generally, with the exception of the generators and motors that are influenced only by the components to which they are directly connected, the components with negative exergy destruction (e.g., some HXs of the IPHRSG, SH II and EV II and the CO_2 compressors and GT2 of the AZEP 85) should operate with reduced performance, in order to improve the overall system.

Table 4.15: Selected results at the component level of the advanced exergetic analysis (MW)

Ref. Plant	$E_{D,k}^{real}$	$E_{D,k}^{EN}$	$E_{D,k}^{EX}$	$E_{D,k}^{AV}$	$E_{D,k}^{UN}$	$E_{D,k}^{UN,EN}$	$E_{D,k}^{UN,EX}$	$E_{D,k}^{AV,EN}$	$E_{D,k}^{AV,EX}$	E_{P}^{real}	E_{P}^{EN}
C1	11.38	6.94	4.44	5.11	6.26	3.79	2.47	3.14	1.97	231.30	140.05
CC	220.87	193.06	27.80	71.03	149.84	130.81	19.03	62.25	8.77	508.76	444.15
GT	16.09	13.52	2.57	8.32	7.77	6.23	1.53	7.29	1.03	535.06	429.50
HPSH	3.35	1.78	1.57	0.87	2.48	1.30	1.18	0.48	0.38	31.72	16.59
HPEV	3.73	2.00	1.72	0.67	3.06	1.84	1.21	0.16	0.51	39.91	24.09
HPEC	4.00	2.24	1.76	1.28	2.72	1.75	0.97	0.49	0.79	24.91	16.00
LPEC	3.78	2.42	1.37	1.83	1.95	1.13	0.82	1.28	0.55	7.71	4.47
LPST	8.71	6.10	2.61	3.61	5.10	3.57	1.53	2.53	1.08	62.29	43.60
GEN1	4.39	4.76	**-0.38**	2.94	1.45	1.57	**-0.12**	3.19	**-0.25**	288.00	312.87
AZEP 85	$E_{D,k}^{real}$	$E_{D,k}^{EN}$	$E_{D,k}^{EX}$	$E_{D,k}^{AV}$	$E_{D,k}^{UN}$	$E_{D,k}^{UN,EN}$	$E_{D,k}^{UN,EX}$	$E_{D,k}^{AV,EN}$	$E_{D,k}^{AV,EX}$	E_{P}^{real}	E_{P}^{EN}
C1	11.17	7.39	3.78	5.02	6.15	4.06	2.09	3.33	1.69	227.13	149.88
CC	153.65	120.57	33.09	13.56	140.10	109.81	30.29	10.76	2.80	466.61	365.73
MCM	5.62	3.41	2.21	1.40	4.23	1.45	2.78	1.96	**-0.57**	77.03	26.35
MCM LTHX	9.55	4.58	4.97	4.90	4.65	3.54	1.11	1.05	3.86	211.51	160.99
DB	31.26	20.16	11.10	16.74	14.52	9.43	5.08	10.73	6.01	78.20	50.82
GT1	14.16	10.64	3.53	7.11	7.06	5.12	1.94	5.52	1.59	481.50	349.47
NGPH	5.70	3.72	1.98	5.66	0.05	0.01	0.04	3.71	1.95	0.10	0.02
HPEC	3.52	1.72	1.79	1.04	2.48	1.33	1.15	0.39	0.65	22.65	12.18
LPST	6.05	4.65	1.40	2.51	3.54	2.72	0.82	1.93	0.58	43.27	33.26
ST4	6.78	4.53	2.25	5.78	1.01	0.67	0.34	3.87	1.91	21.14	14
C5	0.66	0.91	**-0.25**	0.53	0.13	0.17	**-0.04**	0.74	**-0.20**	2.85	3.85
FG COND	13.52	18.21	**-4.69**	-	-	-	-	-	-	-	-
GEN1	3.65	3.39	0.26	**-1.24**	4.89	4.54	0.35	-1.15	**-0.09**	239.55	222.58
CLC	$E_{D,k}^{real}$	$E_{D,k}^{EN}$	$E_{D,k}^{EX}$	$E_{D,k}^{AV}$	$E_{D,k}^{UN}$	$E_{D,k}^{UN,EN}$	$E_{D,k}^{UN,EX}$	$E_{D,k}^{AV,EN}$	$E_{D,k}^{AV,EX}$	E_{P}^{real}	E_{P}^{EN}
C1	13.21	7.79	5.42	5.94	7.27	4.26	3.01	3.53	2.41	268.57	157.27
CLC	194.06	166.54	27.52	64.72	129.34	109.49	19.85	57.05	7.67	500.67	423.84
GT1	16.01	13.00	3.01	7.69	8.31	6.33	1.98	6.67	1.03	524.99	399.90
GT2	2.02	1.49	0.54	1.21	0.81	0.60	0.22	0.89	0.32	52.13	38.28
NGPH	5.20	2.98	2.22	0.04	5.17	2.84	2.33	0.14	**-0.10**	1.12	0.61
HPEV	2.77	1.26	1.51	0.79	1.98	1.03	0.95	0.23	0.56	32.97	17.16
HPEC	3.67	1.86	1.80	0.94	2.72	1.55	1.17	0.31	0.63	20.58	11.74
LPEV	3.03	1.52	1.52	0.83	2.20	1.24	0.97	0.28	0.55	13.99	7.85
LPEC	3.76	2.26	1.50	1.65	2.11	1.13	0.98	1.14	0.52	7.52	4.02
HPST	1.39	0.81	0.57	0.73	0.66	0.37	0.29	0.44	0.28	22.75	12.79
LPST	5.99	4.33	1.66	2.48	3.51	2.53	0.97	1.79	0.69	42.81	30.96
ST4	5.06	2.82	2.25	4.32	0.74	0.41	0.33	2.40	1.92	15.66	8.65
GEN1	3.65	3.99	**-0.34**	2.44	1.20	1.32	**-0.11**	2.67	**-0.23**	239.56	262.13

4.2.1.3 Splitting the exogenous exergy destruction

Table 4.16: Splitting the exogenous rate of exergy destruction (MW) [a]

Ref. plant	*Component, k*	$\dot{E}_{D,k}^{EX}$	*Component, r*	$\dot{E}_{D,k}^{EX,r}$	*Component, k*	$\dot{E}_{D,k}^{EX}$	*Component, r*	$\dot{E}_{D,k}^{EX,r}$
	CC	27.80	*C1*	5.59	*LPST*	2.61	*CC*	0.70
			GT1	8.84			*C1*	0.19
			LPST	3.39			*GT1*	1.07
			SUM	25.67 (7.96)			SUM	1.96 (4.57)
			MX	**2.14**			**MX**	**0.65**
	C1	4.44	*CC*	3.51	*GT1*	2.57	*CC*	1.12
			GT1	0.29			*C1*	0.29
			LPST	0.11			*LPST*	0.25
			SUM	4.18 (6.78)			SUM	2.22 (14.08)
			MX	**0.26**			**MX**	**0.35**
AZEP 85	*Component, k*	$\dot{E}_{D,k}^{EX}$	*Component, r*	$\dot{E}_{D,k}^{EX,r}$	*Component, k*	$\dot{E}_{D,k}^{EX}$	*Component, r*	$\dot{E}_{D,k}^{EX,r}$
	CC	33.09	*DB*	0.05	*GT1*	3.53	*CC*	2.21
			MCM LTHX	0.06			*DB*	0.01
			C1	3.44			*MCM LTHX*	0.01
			GT1	5.13			*C1*	0.15
			MCM	0.06			*MCM*	0.02
			ST4	0.81			*ST4*	0.10
			LPST	1.66			*LPST*	0.16
			SUM	24.68 (-5.86)			SUM	3.34 (11.78)
			MX	**8.41**			**MX**	**0.19**
	DB	11.10	*CC*	4.27	*MCM*	2.21	*CC*	0.66
			MCM LTHX	0.01			*DB*	0.03
			C1	0.46			*MCM LTHX*	-0.02
			GT1	0.71			*C1*	0.07
			MCM	0.01			*GT1*	0.19
			ST4	0.18			*ST4*	0.03
			LPST	0.35			*LPST*	0.07
			SUM	8.18 (0.26)			SUM	1.65 (0.57)
			MX	**2.92**			**MX**	**0.56**
	MCM LTHX	4.97	*CC*	0.76	*ST4*	2.25	*CC*	-1.17
			DB	0.04			*DB*	0.01
			C1	-0.27			*MCM LTHX*	0.07
			GT1	0.23			*C1*	0.31
			MCM	-0.20			*GT1*	0.14
			ST4	0.11			*MCM*	0.16
			LPST	-0.10			*LPST*	0.05
			SUM	2.84 (0.24)			SUM	1.85 (1.77)
			MX	**2.13**			**MX**	**0.40**
	C1	3.78	*CC*	1.59	*LPST*	1.40	*CC*	0.39
			DB	0.03			*DB*	0.04
			MCM LTHX	0.01			*MCM LTHX*	-0.10
			GT1	0.27			*C1*	0.14
			MCM	0.01			*GT1*	0.82
			ST4	0.07			*MCM*	0.00
			LPST	0.10			*ST4*	-0.25
			SUM	2.88 (6.98)			SUM	0.93 (0.54)
			MX	**0.91**			**MX**	**0.47**
CLC plant	*Component, k*	$\dot{E}_{D,k}^{EX}$	*Component, r*	$\dot{E}_{D,k}^{EX,r}$	*Component, k*	$\dot{E}_{D,k}^{EX}$	*Component, r*	$\dot{E}_{D,k}^{EX,r}$
	CLC	27.52	*C1*	3.13	*ST4*	2.25	*C1*	0.10
			GT1	8.27			*CLC*	0.39
			ST4	1.10			*GT1*	0.12
			SUM	23.46 (12.81)			SUM	1.63 (1.41)
			MX	**4.06**			**MX**	**0.62**
	C1	5.42	*CLC*	3.77	*GT1*	3.01	*C1*	0.34
			GT1	0.35			*CLC*	1.36
			ST4	0.05			*ST4*	0.08
			SUM	4.65 (5.17)			SUM	2.65 (14.23)
			MX	**0.78**			**MX**	**0.36**

[a] The sum of exergy destruction caused by component *k* to the remaining components *r* is shown in parentheses

Although the exogenous exergy destruction accounts for a relatively small amount of the exergy destruction in the plants, the determination of its specific sources can shed light onto improvement options. Splitting the exogenous irreversibilities (also used in the calculation of the mexogenous exergy destruction) requires additional simulations, because the components are considered to operate under real conditions in pairs, while the necessary quantities are calculated as defined in Chapter 3. The operating assumptions lead to a total of $\left(n^2+n\right)/2$ simulations, with n being the number of the components in the plant.

The results for the components with the highest exogenous exergy destruction of the plants and their mexogenous values (MX) are shown in Table 4.16. Four components have been chosen from the reference and CLC plants and eight from the AZEP 85 to be explained here. The complete results can be found in the supplemental data. As shown, the mexogenous values are relatively low for all of the plants. The highest difference between the starting results of the exogenous exergy destruction and the amount calculated through the splitting is found for the reactors, while for the remaining components, the mexogenous values are small. In the AZEP 85 the mexogenous exergy destruction of the CC is higher, revealing more intense component interactions. As shown in Table 4.16, 52%, 41% and 26% of the exogenous exergy destruction in the reactors of the reference plant, the CLC plant and the CC of the AZEP 85 stem from GT1 and C1, a small part of which is avoidable. Similarly, in GT1 and C1, the exogenous exergy destruction is mainly imposed by the reactors. Nonetheless, a large part of the exogenous exergy destruction stemming from the reactors is avoidable (32-33% for GT1 in the reference and CLC plants and 52% in the AZEP 85 and approximately 44% for C1 in all of the plants). It should be noted that the exogenous exergy destruction caused by GT1 is higher than that caused by the reactors by 77% in the reference plant and by 12% in the CLC plant (SUM, the value in parentheses in Table 4.16). In the AZEP 85, the exogenous exergy destruction caused by the CC is found to be negative. This is a result mainly determined by the components related to the CO_2 capture. Inefficiencies in the CC result in an improvement of GT2, and all of the components constituting the CO_2 compression unit. This contradicts the results of the reference and CLC plants, but it is justified with the more complex structure of the plant and the stronger interrelations of its components.

4.2.1.4 Calculating the total avoidable rate of exergy destruction

To better understand the improvement potential of the components, the variable $\dot{E}_{D,k}^{AV,\Sigma}$, as stated in Equation (3.28) has been calculated (Table 4.17). The total avoidable exergy destruction of component *k*, consists of both its avoidable endogenous and avoidable exogenous exergy destruction caused by it to the remaining components of the plant. When this value is high, the component is considered to have a large influence on the overall system.

In the reference plant, the avoidable exogenous exergy destruction of GT1 is 34% higher than that of the CC, in the CLC the two values are similar (with the exergy destruction of GT1 14% lower than that of the CLC reactors) and in the AZEP 85 both the CC and the DB have negative avoidable exogenous values. In the reference and CLC plants, due to the

significantly large endogenous exergy destruction of the reactors, their total avoidable exergy destruction ($\dot{E}_{D,k}^{AV,\Sigma}$) results in a value approximately five times higher, when compared to that of GT1. In the AZEP 85, the endogenous avoidable exergy destruction of the CC is relatively low and similar to that of the DB, while its exogenous exergy destruction is highly negative. Therefore, its total avoidable exergy destruction is low (1.61 MW). Because the $\dot{E}_{D,k}^{AV,EX}$ of the DB is slightly negative, the DB results in the largest total avoidable exergy destruction among the plant components of the AZEP 85, closely followed by GT1. When comparing GT1 with C1, GT1 causes higher avoidable exogenous exergy destruction in all of the plants. Additionally, due to the much higher avoidable endogenous exergy destruction of GT1, its total avoidable exergy destruction is found to be more than double that of C1 in the reference plant, approximately three times higher in the CLC plant and 54% higher in the AZEP 85.

Table 4.17: Splitting the rate of exergy destruction caused by each component (MW)

Ref. Plant *Component, k*	$\sum_{\substack{r=1 \\ r\neq k}}^{n} \dot{E}_{D,r}^{AV,EX,k}$	$\dot{E}_{D,k}^{AV,EN}$	$\dot{E}_{D,k}^{AV,\Sigma}$
CC	3.65 (6%)	62.25 (94%)	**65.90**
GT1	4.89 (40%)	7.29 (60%)	**12.18**
C1	2.52 (45%)	3.14 (55%)	**5.67**
LPST	1.81 (42%)	2.53 (58%)	**4.34**
AZEP 85 *Component, k*	$\sum_{\substack{r=1 \\ r\neq k}}^{n} \dot{E}_{D,r}^{AV,EX,k}$	$\dot{E}_{D,k}^{AV,EN}$	$\dot{E}_{D,k}^{AV,\Sigma}$
DB	-0.09	10.73	**10.64**
GT1	3.76 (41%)	5.52 (59%)	**9.28**
C1	2.68 (45%)	3.33 (55%)	**6.02**
MCM	0.63 (24%)	1.96 (76%)	**2.60**
LPST	0.63 (25%)	1.93 (75%)	**2.56**
CC	-9.15	10.76	**1.61**
MCM LTHX	0.10 (9%)	1.05 (91%)	**1.15**
CLC plant *Component, k*	$\sum_{\substack{r=1 \\ r\neq k}}^{n} \dot{E}_{D,r}^{AV,EX,k}$	$\dot{E}_{D,k}^{AV,EN}$	$\dot{E}_{D,k}^{AV,\Sigma}$
CLC	6.71 (11%)	57.05 (89%)	**63.76**
GT1	5.75 (46%)	6.67 (54%)	**12.42**
C1	0.74 (17%)	3.53 (83%)	**4.28**
ST4	0.66 (63%)	0.39 (37%)	**1.05**

4.2.2 Advanced exergoeconomic analysis

Selected results of the advanced exergoeconomic analysis at the component level are presented in Tables 4.19-4.20. More detailed tables can be found in Appendix A and in the supplemental data.

4.2.2.1 Splitting the investment cost rates

The assumptions made for the calculation of the unavoidable investment cost rates, $\dot{Z}_k^{UN}$, are shown in Table 4.18. Most of the cost of the GT system, the STs and the pumps was assumed here to be unavoidable, due to limited modification possibilities in their design. On the other hand, most of the investment cost of the HXs is found to be avoidable. The unavoidable cost associated with HXs is estimated through additional simulations, where each component is considered in isolation, operating with high irreversibilities, i.e. high minimum temperature differences and pressure drops. The lowest possible cost of production of the plant components is then estimated. The results from splitting the investment cost rates for selected components of the plants are shown in Table 4.19.

Table 4.18: Assumptions for the calculation of the unavoidable investment cost rates

Components[a]	$\dot{Z}_k^{UN}$ **(operating conditions or % of** $\dot{Z}_k^{real}$ **)**	**Components**	$\dot{Z}_k^{UN}$ **(operating conditions or % of** $\dot{Z}_k^{real}$ **)**
GT	90%	*SH/RH*	ΔT_{min} =100°C
GT2	90%		$\Delta P_{UN} = \Delta P_{real}$
C1	85%	*EV*	ΔT_{min} =50°C
C2-C5	90%		$\Delta P_{UN} = \Delta P_{real}$
C6	85%	*EC*	ΔT_{min} =75°C
CC	80%		$\Delta P_{UN} = \Delta P_{real}$
DB	80%	*NGPH*	ΔT_{min} =600°C
STs	90%		$\Delta P_{UN} = \Delta P_{real}$
CLC reactors	80%	*Air HX*	ΔT_{min} =800°C
MCM	80%		$\Delta P_{UN} = \Delta P_{real}$
CC MCM	80%	*Coolers*	ΔT_{min} =75°C
MCM HTHX	ΔT_{min} =100°C		$\Delta P_{UN} = \Delta P_{real}$
	$\Delta P_{UN} = \Delta P_{real}$	*Pumps*	60%
MCM LTHX	ΔT_{min} =100°C	*Motors*	Incl. with pumps
	$\Delta P_{UN} = \Delta P_{real}$	*Generators*	Incl. with turbines

[a] No distinction between avoidable and unavoidable investment cost rates has been made for mixers, de-aerators, or dissipative components.

The endogenous investment cost rate, $\dot{Z}_k^{EN}$, is found to be higher than the exogenous, $\dot{Z}_k^{EX}$, for all of the plant components, with the exception of the MCM and some HXs in the AZEP 85. This emphasizes again that internal design changes play a more significant role in the determination of each component's cost. In addition, the order of the spread between the absolute values of the endogenous and exogenous investment cost rates is significant in some cases: for the CC and GT1, for example, in all of the plants the endogenous investment cost rates are much higher than the exogenous rates (in the reference plant, seven and four times

Table 4.19: Splitting the investment cost rates (€/h)

Ref. Plant	$\dot{Z}_k^{real}$	$\dot{Z}_k^{UN}$	$\dot{Z}_k^{AV}$	$\dot{Z}_k^{EN}$	$\dot{Z}_k^{EX}$	$\dot{Z}_k^{AV}$		$\dot{Z}_k^{UN}$	
						$\dot{Z}_k^{AV,EN}$	$\dot{Z}_k^{AV,EX}$	$\dot{Z}_k^{UN,EN}$	$\dot{Z}_k^{UN,EX}$
C1	1423.3	1209.8	213.5	861.8	561.5	129.3	84.2	732.6	477.3
CC	1016.7	813.3	203.3	887.6	129.1	177.5	25.8	710.0	103.3
GT1	1626.7	1464.0	162.7	1305.7	320.9	130.6	32.1	1175.2	288.8
HPSH	111.2	50.8	60.4	73.5	37.7	39.9	20.5	33.6	17.2
HPEV	157.7	68.5	89.2	82.4	75.2	46.6	42.6	35.8	32.7
H ST	181.7	163.5	18.2	115.3	66.4	11.5	6.6	103.8	59.7
IPST	328.9	296.0	32.9	230.1	98.8	23.0	9.9	207.1	89.0
LPST	764.1	687.7	76.4	534.9	229.2	53.5	22.9	481.4	206.3
AZEP 85	$\dot{Z}_k^{real}$	$\dot{Z}_k^{UN}$	$\dot{Z}_k^{AV}$	$\dot{Z}_k^{EN}$	$\dot{Z}_k^{EX}$	$\dot{Z}_k^{AV}$		$\dot{Z}_k^{UN}$	
						$\dot{Z}_k^{AV,EN}$	$\dot{Z}_k^{AV,EX}$	$\dot{Z}_k^{UN,EN}$	$\dot{Z}_k^{UN,EX}$
C1	1169.3	993.9	175.4	771.7	397.7	115.7	59.7	655.9	338.0
MCM	1192.3	953.9	238.5	407.9	784.4	81.6	156.9	326.3	627.6
GT1	1336.4	1202.8	133.6	970.0	366.4	97.0	36.6	873.0	329.8
CC	745.9	596.7	149.2	584.6	161.3	116.9	32.3	467.7	129.0
DB	276.8	221.5	55.4	179.9	96.9	36.0	19.4	143.9	77.5
MCM LTHX	1113.0	320.2	764.5	847.1	265.8	558.5	206.0	288.7	31.6
MCM HTHX	696.3	108.9	548.8	434.4	261.9	309.8	239.0	124.7	**-15.8**
HP ST	182.6	164.3	18.3	124.4	58.2	12.4	5.8	112.0	52.3
IP ST	201.8	181.7	20.2	161.0	40.8	16.1	4.1	144.9	36.7
LP ST	489.2	440.3	48.9	376.1	113.2	37.6	11.3	338.5	101.8
LPEV	145.0	70.1	74.8	77.0	68.0	39.7	35.1	37.2	32.9
LPEC	102.5	44.1	58.4	59.0	43.5	33.6	24.8	25.4	18.7
ST4	256.7	231.1	25.7	170.0	86.8	17.0	8.7	153.0	78.1
GT2	247.3	222.5	24.7	341.1	**-93.9**	34.1	**-9.4**	307.0	**-84.5**
C2	347.9	295.7	52.2	448.8	**-100.9**	67.3	**-15.1**	381.5	**-85.8**
C3	358.4	304.6	53.8	479.9	**-121.5**	72.0	**-18.2**	407.9	**-103.3**
C4	356.9	303.3	53.5	480.3	**-123.5**	72.0	**-18.5**	408.3	**-104.9**
C5	362.1	307.8	54.3	488.2	**-126.1**	73.2	**-18.9**	415.0	**-107.2**
CLC plant	$\dot{Z}_k^{real}$	$\dot{Z}_k^{UN}$	$\dot{Z}_k^{AV}$	$\dot{Z}_k^{EN}$	$\dot{Z}_k^{EX}$	$\dot{Z}_k^{AV}$		$\dot{Z}_k^{UN}$	
						$\dot{Z}_k^{AV,EN}$	$\dot{Z}_k^{AV,EX}$	$\dot{Z}_k^{UN,EN}$	$\dot{Z}_k^{UN,EX}$
C1	964.4	819.7	144.7	564.7	399.7	84.7	59.9	480.0	339.7
CLC	4974.5	3979.6	994.9	4211.1	763.3	842.2	152.7	3368.9	610.7
GT1	1102.2	992.0	110.2	839.6	262.6	84.0	26.3	755.6	236.4
HPSH	105.2	40.6	64.6	46.0	59.2	28.2	36.4	17.8	22.9
HPEV	139.7	71.4	68.3	72.7	67.0	35.5	32.7	37.2	34.3
HPST	102.8	92.5	10.3	57.8	45.0	5.8	4.5	52.0	40.5
IPST	148.5	133.6	14.8	107.5	40.9	10.8	4.1	96.8	36.8
LPST	386.9	348.2	38.7	279.8	107.1	28.0	10.7	251.8	96.4
ST4	156.5	140.9	15.7	86.5	70.1	8.6	7.0	77.8	63.1
GT2	215.8	194.2	21.6	158.5	57.3	15.8	5.7	142.6	51.6
C2	313.8	266.7	47.1	216.8	97.0	32.5	14.6	184.3	82.5
C3	322.8	274.3	48.4	230.7	92.0	34.6	13.8	196.1	78.2
C4	318.4	270.7	47.8	228.8	89.6	34.3	13.4	194.5	76.2
C5	320.0	272.0	48.0	230.3	89.7	34.5	13.5	195.7	76.3

higher, in the CLC plant five and three times higher and in the AZEP 85 four and three times higher for the CC and GT1, respectively). For the compressor, this difference is smaller. Some HXs in all of the plants, as well as the CO_2 compressors in the AZEP 85 result in a $\dot{Z}_k^{EN}$ that is higher than the $\dot{Z}_k^{real}$. This is again related to increased mass flow rates in the endogenous case, when compared to the real process, which results in a higher rate of product exergy. The interpretation of these results is that the cost of a component with negative $\dot{Z}_k^{EX}$ increases when all other components operate under theoretical conditions. Thus, to decrease its cost, the irreversibilities within the other components must be increased.

The results from splitting the investment cost rates indicate that, priority should be given to the GT system, with the reactors first, C1 second and GT1 third for the CLC plant and C1 first, CC second and GT1 third for the reference plant. These components have the highest avoidable cost rates, while the components that follow priority-wise, in the reference and CLC plants, are the HXs of the high and low-pressure HRSG (ranking varies among the HPSH, HPEV and the LPEV). On the other hand, in the AZEP 85 priority should be given to the two HXs of the MCM reactor, the MCM, C1, the CC and then to GT1.

Since the components with the larger investment cost rates, $\dot{Z}_k$, are the main turbomachinery and the reactors and their investment cost is mainly unavoidable, the investment cost rate of the plant is largely unavoidable. Additionally, most of the exogenous values are relatively low, when compared to the endogenous values, showing that components interactions are not as important as the internal operation of the components. Specifically, 64-87% and 73-80% of the investment cost of the reactors and GT1, respectively, can be avoided through operating changes in the components themselves.

4.2.2.2 Splitting the cost rate of exergy destruction

The calculations used for splitting the cost of exergy destruction, $\dot{C}_{D,k}$, are based on the equations shown in Table 3.1. The results for selected components of the plants are shown in Table 4.20.

In all of the plants, the majority of the HXs, the LPST, the reactors (with the exception of the DB) and C1, present high rates of unavoidable exergy destruction. The opposite is true for GT1, the CO_2 compressors, the high- and intermediate-pressure ST. The highest values of both avoidable and unavoidable rate of exergy destruction are found for the reactors, GT1, C1 and the LPST. In the case of the reference plant, the LPST presents a 13% higher avoidable cost rate of exergy destruction when compared to that of C1.

In the reference and CLC plants, more than 67% of the total cost rate of exergy destruction of the reactors is considered unavoidable, while for the CC of the AZEP 85 this percentage reaches 91%. Yet, the absolute values of the avoidable cost rates of exergy destruction associated with these components are significantly larger than other plant components, with the exception of the CC in the AZEP 85 that results in a lower value than GT1 and the DB. Furthermore, 65-87% of the unavoidable cost of the reactors is endogenous.

Table 4.20: Selected results from splitting the exergy destruction cost rates (€/h)

Ref. Plant	$\dot{C}_{D,k}^{real}$	$\dot{C}_{D,k}^{UN}$	$\dot{C}_{D,k}^{AV}$	$\dot{C}_{D,k}^{EN}$	$\dot{C}_{D,k}^{EX}$	$\dot{C}_{D,k}^{AV}$		$\dot{C}_{D,k}^{UN}$	
						$\dot{C}_{D,k}^{AV,EN}$	$\dot{C}_{D,k}^{AV,EX}$	$\dot{C}_{D,k}^{UN,EN}$	$\dot{C}_{D,k}^{UN,EX}$
C1	692.7	381.3	311.4	422.3	270.4	191.5	119.9	230.9	150.4
CC	7276.3	4936.4	2339.9	6360.4	916.0	2050.8	289.1	4309.5	626.9
GT1	1139.7	432.3	707.4	752.7	387.0	405.6	301.7	347.0	85.3
HPEC	222.8	151.4	71.4	124.8	98.1	27.5	43.9	97.2	54.2
LPEV	197.5	166.0	31.5	93.4	104.1	1.4	30.1	91.9	74.0
LPEC	210.7	108.8	101.9	134.6	76.1	71.5	30.4	63.1	45.7
LPST	743.4	393.2	350.2	470.0	273.4	194.7	155.5	275.3	117.9
AZEP 85	$\dot{C}_{D,k}^{real}$	$\dot{C}_{D,k}^{UN}$	$\dot{C}_{D,k}^{AV}$	$\dot{C}_{D,k}^{EN}$	$\dot{C}_{D,k}^{EX}$	$\dot{C}_{D,k}^{AV}$		$\dot{C}_{D,k}^{UN}$	
						$\dot{C}_{D,k}^{AV,EN}$	$\dot{C}_{D,k}^{AV,EX}$	$\dot{C}_{D,k}^{UN,EN}$	$\dot{C}_{D,k}^{UN,EX}$
C1	797.1	438.8	358.3	527.2	269.8	237.7	120.6	289.6	149.2
MCM	275.3	206.8	68.5	166.9	108.4	96.2	**-27.7**	70.8	136.1
GT1	1176.9	466.3	710.6	702.9	474.0	364.5	346.2	338.4	127.9
CC	5120.2	4668.5	451.8	4017.7	1102.5	358.5	93.3	3659.2	1009.3
DB	1041.6	483.8	557.8	671.8	369.8	357.4	200.4	314.4	169.4
MCM LTHX	467.4	227.5	239.9	224.4	243.0	51.2	188.7	173.2	54.3
MCM HTHX	60.5	41.0	19.5	37.6	22.9	12.0	7.5	25.6	15.4
HPST	186.9	69.2	117.7	103.4	83.4	56.3	61.4	47.2	22.0
HPSH	198.0	142.6	55.4	67.0	131.0	6.8	48.6	60.2	82.4
HPEC	232.5	163.9	68.6	113.9	118.6	25.8	42.8	88.1	75.8
LPEV	182.0	152.3	29.7	85.4	96.5	4.6	25.1	80.8	71.4
LPEC	222.6	63.8	158.8	136.2	86.4	99.5	59.3	36.7	27.0
ST4	557.2	82.5	474.6	372.1	185.1	317.4	157.2	54.7	27.9
GT2	131.9	31.3	100.6	128.7	3.2	85.5	15.1	43.2	**-11.9**
C2	74.2	17.0	57.2	98.1	**-24.0**	76.2	**-19.0**	21.9	**-4.9**
C3	78.2	16.8	61.4	106.6	**-28.4**	84.2	**-22.7**	22.5	**-5.7**
C4	81.0	16.7	64.4	110.9	**-29.9**	88.5	**-24.1**	22.4	**-5.8**
C5	86.8	16.7	70.1	119.0	**-32.2**	96.5	**-26.4**	22.5	**-5.8**
NG PH	268.9	2.2	266.8	175.5	93.4	175.0	91.8	0.5	1.7
Air HX	83.0	15.9	67.1	104.2	**-21.2**	81.7	**-14.6**	22.4	**-6.5**
CLC plant	$\dot{C}_{D,k}^{real}$	$\dot{C}_{D,k}^{UN}$	$\dot{C}_{D,k}^{AV}$	$\dot{C}_{D,k}^{EN}$	$\dot{C}_{D,k}^{EX}$	$\dot{C}_{D,k}^{AV}$		$\dot{C}_{D,k}^{UN}$	
						$\dot{C}_{D,k}^{AV,EN}$	$\dot{C}_{D,k}^{AV,EX}$	$\dot{C}_{D,k}^{UN,EN}$	$\dot{C}_{D,k}^{UN,EX}$
C1	919.2	506.0	413.2	542.0	377.2	245.7	167.5	296.3	209.7
CLC	6390.8	4259.4	2131.4	5484.5	906.3	1878.7	252.7	3605.8	653.6
GT1	1277.8	540.4	737.4	845.2	432.6	433.5	303.9	411.7	128.8
HPEC	238.5	177.0	61.4	121.2	117.2	20.3	41.1	101.0	76.1
LPEV	197.3	143.3	54.0	98.7	98.6	18.3	35.7	80.4	62.9
LPEC	244.7	137.2	107.5	147.3	97.4	74.0	33.6	73.3	63.9
LPST	587.3	310.7	276.7	383.6	203.8	158.9	117.8	224.6	86.0
ST4	423.8	62.3	361.5	235.6	188.2	201.2	160.3	34.4	27.9
GT2	118.9	34.5	84.4	63.0	55.9	37.6	46.8	25.3	9.2
C4	84.6	19.2	65.4	61.8	22.8	48.0	17.4	13.8	5.4
C5	87.8	19.2	68.7	64.3	23.6	50.5	18.2	13.8	5.4
NGPH	220.5	5.7	214.8	126.3	94.2	5.9	208.9	120.4	**-114.7**

Similar to the investment cost rates, here the rates of exergy destruction are mostly endogenous for the majority of the components. Thus, most of the cost stems from the

operation of the components themselves and component interactions are of lower importance.

Evaluating the results of the sources of the cost of exergy destruction, the reference plant can potentially be improved through improvement of the CC, GT1, the LPST and C1. On the other hand, in the CLC plant, priority should be given to the CLC first, GT1 second, C1 third and last ST4. In the AZEP 85 the component with the highest avoidable cost of exergy destruction is GT1, followed by the DB, ST4 and then the CC.

4.2.2.3 Splitting the exogenous cost rates of investment and exergy destruction

Although the exogenous costs are of relatively low significance when compared to the endogenous costs, their sources can reveal additional improvement potential for the overall plant. The splitting of the exogenous costs for the components with the highest investment-related cost and exergy destruction-related costs is shown in Tables 4.21 and 4.22, respectively.

The main source of the exogenous investment cost rate for the reactors is GT1, with the exception of the DB in the AZEP 85 that is influenced more by the CC. The main source of the exogenous investment cost rate for C1 and GT1 of all plants is the reactors. The mexogenous cost, that is the cost difference between the calculated exogenous cost (shown in Tables 4.21 and 4.22) and the sum of the split parts caused to each of the remaining components (complete tables can be found in the supplemental data), is found to be very high for the MCM and the MCM LTHX because of their intense interaction.

The effect of the chemical reactors on the remaining components is critical, since they are responsible for large parts of the costs in other components. The reactors first and GT1 second, cause relatively high total exogenous costs in the CLC plant (SUM, values in parentheses in Tables 4.21 and 4.22), while the same is true for the investment cost rates of the reference plant. GT1 causes a higher exogenous cost rate of exergy destruction than the CC in the reference plant (SUM, values in parentheses in Table 4.22). In the AZEP 85, GT1 causes the highest rate of investment cost, followed by C1, the MCM HTHX (436.7 €/h) and the MCM (because of their large influence on the CO_2 compressors), while the exogenous investment cost of the CC is relatively low, due to its negative effect on other components (mainly those processing the CO_2 stream). Also, in the AZEP 85, GT1 causes the highest exogenous cost rate of exergy destruction, while the CC, has a negative exogenous value of exergy destruction, due to the inverse relationship between its efficiency and that of other equipment.

Table 4.21: Selected results from splitting the exogenous investment cost rate (€/h)[a]

Ref. plant	*Component, k*	$\dot{Z}_k^{EX}$	*Component, r*	$\dot{Z}_k^{EX,r}$	*Component, k*	$\dot{Z}_k^{EX}$	*Component, r*	$\dot{Z}_k^{EX,r}$
	CC	129.11	*C1*	24.62	*LPST*	229.19	*CC*	61.69
			GT1	40.65			*C1*	16.31
			LPST	15.58			*GT1*	93.66
			SUM	116.90 (741.68)			SUM	172.17 (68.57)
			MX	**12.22**			**MX**	**57.02**
	C1	561.51	*CC*	416.85	*GT1*	1305.74	*CC*	156.23
			GT1	36.39			*C1*	41.23
			LPST	13.98			*LPST*	24.15
			SUM	500.58 (110.47)			SUM	275.42 (352.64)
			MX	**60.93**			**MX**	**45.51**
AZEP 85	*Component, r*	$\dot{Z}_k^{EX}$	*Component, r*	$\dot{Z}_k^{EX,r}$	*Component, r*	$\dot{Z}_k^{EX}$	*Component, r*	$\dot{Z}_k^{EX,r}$
	CC	161.26	*DB*	0.22	*GT1*	366.45	*CC*	202.46
			MCM LTHX	0.28			*DB*	1.18
			C1	16.70			*MCM LTHX*	0.78
			GT1	24.87			*C1*	27.34
			MCM	0.48			*MCM*	1.47
			ST4	3.94			*ST4*	9.24
			LPST	8.05			*LPST*	14.51
			SUM	105.69 (138.96)			SUM	328.52 (757.44)
			MX	**55.57**			**MX**	**37.92**
	DB	96.93	*CC*	37.55	*MCM*	784.44	*CC*	114.35
			MCM LTHX	0.08			*DB*	17.88
			C1	4.29			*MCM LTHX*	13.17
			GT1	6.33			*C1*	-8.89
			MCM	0.13			*GT1*	3.47
			ST4	1.65			*ST4*	3.86
			LPST	3.11			*LPST*	25.36
			SUM	80.76 (403.28)			SUM	452.41 (430.00)
			MX	**16.17**			**MX**	**332.03**
	MCM LTHX	265.85	*CC*	28.82	*ST4*	86.76	*CC*	-43.98
			DB	44.11			*DB*	0.47
			C1	31.80			*MCM LTHX*	2.73
			GT1	77.08			*C1*	11.76
			MCM	-99.30			*GT1*	6.04
			ST4	53.97			*MCM*	5.88
			LPST	-82.20			*LPST*	2.05
			SUM	-34.14 (357.00)			SUM	70.49 (405.77)
			MX	**299.98**			**MX**	**16.28**
	C1	397.70	*CC*	166.14	*LPST*	113.16	*CC*	31.38
			DB	4.39			*DB*	3.02
			MCM LTHX	1.12			*MCM LTHX*	-7.79
			GT1	27.86			*C1*	11.08
			MCM	1.54			*GT1*	66.52
			ST4	7.54			*MCM*	0.00
			LPST	10.10			*ST4*	-0.25
			SUM	302.97 (611.92)			SUM	75.58 (329.87)
			MX	**94.73**			**MX**	**37.57**
CLC plant	*Component, k*	$\dot{Z}_k^{EX}$	*Component, r*	$\dot{Z}_k^{EX,r}$	*Component, k*	$\dot{Z}_k^{EX}$	*Component, r*	$\dot{Z}_k^{EX,r}$
	CLC	763.33	*C1*	141.71	*ST4*	70.06	*C1*	3.09
			GT1	209.03			*CLC*	12.02
			ST4	27.77			*GT1*	3.78
			SUM	655.70 (667.11)			SUM	50.53 (30.94)
			MX	**107.64**			**MX**	**19.52**
	C1	399.66	*CLC*	278.97	*GT1*	262.62	*C1*	31.50
			GT1	25.40			*CLC*	122.79
			ST4	3.39			*ST4*	5.11
			SUM	342.58 (246.67)			SUM	215.32 (478.35)
			MX	**57.09**			**MX**	**47.30**

[a] In parentheses the sum of exergy destruction caused by component *k* to the remaining components *r* is shown

Table 4.22: Selected results from splitting the exogenous cost rates of exergy destruction (€/h) [a]

Ref. plant	*Component, k*	$\dot{C}_{D,k}^{EX}$	*Component, r*	$\dot{C}_{D,k}^{EX,r}$	*Component, k*	$\dot{C}_{D,k}^{EX}$	*Component, r*	$\dot{C}_{D,k}^{EX,r}$
	CC	915.97	*C1*	184.26	*LPST*	273.40	*CC*	54.20
			GT1	291.31			*C1*	14.333
			LPST	111.65			*GT1*	82.276
			SUM	845.53 (488.33)			SUM	151.23 (175.24)
			MX	**70.44**			**MX**	**122.17**
	C1	270.36	*CC*	213.62	*GT1*	752.65	*CC*	62.20
			GT1	17.84			*C1*	16.414
			LPST	6.85			*LPST*	13.921
			SUM	254.65 (256.93)			SUM	123.55 (625.37)
			MX	**15.70**			**MX**	**263.49**
AZEP 85	*Component, k*	$\dot{C}_{D,k}^{EX}$	*Component, r*	$\dot{C}_{D,k}^{EX,r}$	*Component, k*	$\dot{C}_{D,k}^{EX}$	*Component, r*	$\dot{C}_{D,k}^{EX,r}$
	CC	1102.53	*DB*	1.51	*GT1*	474.05	*CC*	145.81
			MCM LTHX	1.90			*DB*	0.43
			C1	114.59			*MCM LTHX*	0.50
			GT1	170.92			*C1*	9.69
			MCM	2.15			*MCM*	1.02
			ST4	27.11			*ST4*	6.70
			LPST	55.32			*LPST*	10.51
			SUM	822.32(-560.5)			SUM	220.70 (605.62)
			MX	**280.21**			**MX**	**253.35**
	DB	369.78	*CC*	142.13	*MCM*	108.37	*CC*	32.14
			MCM LTHX	0.22			*DB*	1.67
			C1	15.45			*MCM LTHX*	-1.09
			GT1	23.63			*C1*	3.39
			MCM	0.36			*GT1*	9.11
			ST4	6.15			*ST4*	1.58
			LPST	11.74			*LPST*	3.37
			SUM	272.45 (16.80)			SUM	80.85 (33.25)
			MX	**97.33**			**MX**	**27.51**
	MCM LTHX	243.02	*CC*	37.21	*ST4*	185.09	*CC*	-95.71
			DB	2.05			*DB*	1.02
			C1	-13.05			*MCM LTHX*	5.98
			GT1	11.24			*C1*	25.70
			MCM	-9.92			*GT1*	11.88
			ST4	5.35			*MCM*	12.87
			LPST	-4.77			*LPST*	4.48
			SUM	138.75 (10.08)			SUM	151.85 (76.26)
			MX	**104.27**			**MX**	**33.24**
	C1	269.82	*CC*	113.52	*LPST*	179.60	*CC*	34.02
			DB	1.79			*DB*	3.27
			MCM LTHX	0.53			*MCM LTHX*	-8.46
			GT1	19.04			*C1*	12.01
			MCM	0.76			*GT1*	72.12
			ST4	5.15			*MCM*	0.00
			LPST	6.90			*ST4*	-0.25
			SUM	205.15 (350.05)			SUM	81.70 (109.45)
			MX	**64.67**			**MX**	**103.39**
CLC plant	*Component, k*	$\dot{C}_{D,k}^{EX}$	*Component, r*	$\dot{C}_{D,k}^{EX,r}$	*Component, k*	$\dot{C}_{D,k}^{EX}$	*Component, r*	$\dot{C}_{D,k}^{EX,r}$
	CLC	906.30	*C1*	103.23	*ST4*	188.20	*C1*	8.43
			GT1	272.24			*CLC*	32.72
			ST4	36.17			*GT1*	9.75
			SUM	772.62 (813.84)			SUM	136.13 (52.23)
			MX	**133.68**			**MX**	**52.07**
	C1	377.20	*CLC*	262.15	*GT1*	432.64	*C1*	22.37
			GT1	24.38			*CLC*	88.40
			ST4	3.25			*ST4*	5.14
			SUM	323.20 (236.06)			SUM	172.20 (689.31)
			MX	**54.00**			**MX**	**260.44**

[a] In parentheses the sum of exergy destruction caused by component *k* to the remaining components *r* is shown

4.2.2.4 Calculating the total avoidable cost rates associated with plant components

The total avoidable cost of component *k* is calculated through the addition of the avoidable cost of exergy destruction or investment cost caused by its operation on the remaining components and its endogenous cost of exergy destruction or investment cost. The results of the most influential components of the plants are shown in Tables 4.23 and 4.24. The total avoidable costs of component *k* are calculated using Equations (3.32)-(3.36).

Table 4.23: Avoidable investment cost rate (€/h)

Ref. Plant *Component, k*	$\sum_{\substack{r=1 \\ r\neq k}}^{n} \dot{Z}_r^{AV,EX,k}$	$\dot{Z}_k^{AV,EN}$	$\dot{Z}_k^{AV,\Sigma}$
CC	121.09 (40.6%)	177.51 (59.4%)	**298.60**
GT1	74.80 (36.4%)	130.57 (63.6%)	**205.38**
C1	20.41 (13.6%)	129.27 (86.4%)	**149.69**
LPST	12.71 (19.2%)	53.49 (80.8%)	**66.21**
AZEP 85 *Component, k*	$\sum_{\substack{r=1 \\ r\neq k}}^{n} \dot{Z}_r^{AV,EX,k}$	$\dot{Z}_k^{AV,EN}$	$\dot{Z}_k^{AV,\Sigma}$
MCM LTHX	346.02 (38.3%)	558.49 (61.7%)	**904.51**
CC	720.80 (86.0%)	116.93 (14.0%)	**837.73**
GT1	446.91 (82.2%)	97.00 (17.8%)	**543.91**
MCM	398.52 (77.5%)	115.75 (22.5%)	**514.27**
C1	391.29 (77.2%)	115.75 (22.8%)	**507.04**
DB	358.92 (90.9%)	35.98 (9.1%)	**394.90**
LPST	287.20 (88.4%)	37.61 (11.6%)	**324.81**
CLC Plant *Component, k*	$\sum_{\substack{r=1 \\ r\neq k}}^{n} \dot{Z}_r^{AV,EX,k}$	$\dot{Z}_k^{AV,EN}$	$\dot{Z}_k^{AV,\Sigma}$
CLC	109.79 (11.5%)	842.23 (88.5%)	**952.02**
GT1	102.51 (55.0%)	83.96 (45.0%)	**186.47**
C1	47.07 (35.7%)	84.71 (64.3%)	**131.78**
ST4	7.00 (44.7%)	8.65 (55.3%)	**15.65**

Table 4.24: Avoidable exergy destruction cost rate (€/h)

Ref. Plant *Component, k*	$\sum_{\substack{r=1 \\ r\neq k}}^{n} \dot{C}_{D,r}^{AV,EX,k}$	$\dot{C}_{D,k}^{AV,EN}$	$\dot{C}_{D,k}^{AV,\Sigma}$
CC	170.37 (7.7%)	2,050.85 (92.3%)	**2,221.22**
GT1	156.63 (27.9)	405.64 (72.1)	**562.27**
C1	84.82 (30.7)	191.45 (69.3)	**276.27**
LPST	51.15 (20.8)	194.71 (79.2)	**245.87**
AZEP 85 *Component, k*	$\sum_{\substack{r=1 \\ r\neq k}}^{n} \dot{C}_{D,r}^{AV,EX,k}$	$\dot{C}_{D,k}^{AV,EN}$	$\dot{C}_{D,k}^{AV,\Sigma}$
GT1	119.25 (24.7%)	364.45 (75.3%)	**483.70**
DB	-5.95	357.44	**351.49**
CC	-26.49	358.53	**332.04**
C1	67.37 (22.1%)	237.68 (77.9%)	**305.05**
LPST	44.69 (20.9%)	168.94 (79.1%)	**213.63**
MCM	34.02 (26.1%)	96.16 (73.9%)	**130.18**
MCM LTHX	3.95 (7.2%)	51.23 (92.8%)	**55.18**
CLC Plant *Component, k*	$\sum_{\substack{r=1 \\ r\neq k}}^{n} \dot{C}_{D,r}^{AV,EX,k}$	$\dot{C}_{D,k}^{AV,EN}$	$\dot{C}_{D,k}^{AV,\Sigma}$
CLC	241.83 (11.4%)	1,878.68 (88.6%)	**2,120.51**
GT1	179.12 (29.2%)	433.52 (70.8%)	**612.64**
C1	19.99 (7.5%)	245.71 (92.5%)	**265.70**
ST4	12.52 (5.9%)	201.17 (94.1%)	**213.69**

Among GT1, C1 and the reactors of the plants, the lowest avoidable exogenous investment cost rate is calculated for C1. The avoidable endogenous costs are similar for C1 and GT1 in the reference and CLC plants, while in the AZEP 85, C1 has a 19% higher cost rate. Nonetheless, C1 has lower total cost rates in all of the plants. It should be noted that GT1 and the reactors of the CLC plant cause similar total avoidable exogenous investment cost rates (first column in Table 4.23), but the reactors have a much higher total cost rate due to their significantly higher endogenous value.

Table 4.25: Ranking of the components with the highest total avoidable cost rate, $\dot{C}_{D,k}^{AV,\Sigma} + \dot{Z}_k^{AV,\Sigma}$ (€/h)

Component, *k*	**Ref. Plant**	Component, *k*	**AZEP 85**	Component, *k*	**CLC Plant**
CC	2,519.8	*CC*	1,169.8	*CLC*	3,072.5
GT1	767.7	*GT1*	1,027.6	*GT1*	799.1
C1	426.0	*MCM LTHX*	944.5	*C1*	397.5
LPST	312.1	*C1*	812.1	*ST4*	229.3
		DB	746.4		
		MCM	644.5		
		LPST	538.4		

While the differences in the investment cost rates are kept at relatively low levels, the differences in the exergy destruction-related costs show large spreads among the different components. The avoidable exogenous cost of exergy destruction of GT1 and the CC in the reference plant are relatively close. However, again, the significantly larger avoidable endogenous cost of exergy destruction for the CC, results in an overall cost rate that is approximately four times higher. C1 follows GT1 with an approximately two times lower overall cost of exergy destruction. In the CLC plant, the reactors result in a 35% higher avoidable exogenous cost rate of exergy destruction when compared to GT1 and since the difference between the endogenous values of the components is much larger, the total cost rate of the reactors is approximately three times higher. In the reference and CLC plants, the avoidable exogenous cost caused by GT1 is the second highest. C1 follows GT1 in cost. In the AZEP 85 the highest cost of avoidable exogenous exergy destruction is found for the MCM HTHX (200.2 €/h), followed by GT1 and C1. However, due to its low avoidable endogenous exergy destruction cost, the MCM HTHX has a low total avoidable cost and GT1 has the highest total cost. The total avoidable cost of exergy destruction of the CC is relatively reduced (ranked after GT1 and the DB) due to its negative avoidable exogenous cost rate.

The most important result of the component evaluation is the sum of the avoidable exergy destruction and investment costs. As shown in Table 4.25, the cost of exergy destruction is the main deciding parameter of the overall cost in the CLC and reference plants. On the other hand, in the AZEP, both costs affect the overall results. In all of the plants, the reactors are ranked first and GT1 second.

4.2.3 Advanced exergoenvironmental analysis

Selected results of the advanced exergoenvironmental analysis at the component level are presented in Tables 4.26-4.27. Detailed tables can be found in Appendix A and in the supplemental data. In contrast to the advanced exergoeconomic analysis, in the advanced exergoenvironmental analysis, the component-related environmental impact has not been split, due to its negligible influence on the total impact. Thus, here the environmental impacts associated with exergy destruction and pollutant formation are split.

4.2.3.1 Splitting the environmental impact of exergy destruction

Table 4.26: Selected results from splitting the environmental impact of exergy destruction (Pts/h)

Ref. Plant	$\dot{B}_{D,k}^{real}$	$\dot{B}_{D,k}^{UN}$	$\dot{B}_{D,k}^{AV}$	$\dot{B}_{D,k}^{EN}$	$\dot{B}_{D,k}^{EX}$	$\dot{B}_{D,k}^{AV}$		$\dot{B}_{D,k}^{UN}$	
						$\dot{B}_{D,k}^{AV,EN}$	$\dot{B}_{D,k}^{AV,EX}$	$\dot{B}_{D,k}^{UN,EN}$	$\dot{B}_{D,k}^{UN,EX}$
C1	69.36	38.18	31.18	42.29	27.07	19.17	12.01	23.12	15.06
CC	762.83	517.52	245.31	666.81	96.03	215.01	30.31	451.80	65.72
GT1	120.16	45.58	74.58	79.35	40.81	42.77	31.81	36.59	8.99
HPEC	23.49	15.96	7.53	13.15	10.34	2.90	4.63	10.25	5.71
LPEV	20.82	17.50	3.32	9.85	10.97	0.15	3.17	9.69	7.80
LPEC	22.21	11.47	10.74	14.19	8.02	7.54	3.21	6.66	4.82
LPST	69.86	36.95	32.91	44.17	25.69	18.30	14.61	25.87	11.08
AZEP 85	$\dot{B}_{D,k}^{real}$	$\dot{B}_{D,k}^{UN}$	$\dot{B}_{D,k}^{AV}$	$\dot{B}_{D,k}^{EN}$	$\dot{B}_{D,k}^{EX}$	$\dot{B}_{D,k}^{AV}$		$\dot{B}_{D,k}^{UN}$	
						$\dot{B}_{D,k}^{AV,EN}$	$\dot{B}_{D,k}^{AV,EX}$	$\dot{B}_{D,k}^{UN,EN}$	$\dot{B}_{D,k}^{UN,EX}$
C1	69.66	38.35	31.31	46.08	23.58	20.77	10.54	25.31	13.04
MCM	28.66	21.53	7.13	17.38	11.28	10.01	**-2.88**	7.37	14.17
GT1	107.05	42.41	64.64	63.93	43.12	33.15	31.49	30.78	11.63
CC	536.81	489.44	47.36	421.22	115.59	37.59	9.78	383.63	105.81
DB	109.20	50.72	58.48	70.43	38.77	37.47	21.01	32.96	17.76
MCM LTHX	48.89	23.79	25.09	23.47	25.42	5.36	19.73	18.11	5.68
MCM HTHX	6.33	4.29	2.04	3.93	2.40	1.26	0.78	2.68	1.61
HPST	16.06	5.95	10.11	8.89	7.17	4.83	5.28	4.05	1.89
HPSH	18.01	12.97	5.04	6.10	11.92	0.62	4.42	5.48	7.50
HPEC	21.15	14.91	6.24	10.36	10.79	2.34	3.90	8.02	6.89
LPEV	16.55	13.85	2.70	7.77	8.78	0.42	2.28	7.35	6.50
LPEC	20.25	5.80	14.44	12.39	7.86	9.05	5.40	3.34	2.46
ST4	47.40	7.02	40.38	31.65	15.75	27.00	13.37	4.65	2.37
GT2	14.16	3.36	10.80	13.82	0.34	9.18	1.62	4.64	**-1.28**
C2	5.67	1.30	4.37	7.50	**-1.83**	5.83	**-1.46**	1.67	**-0.38**
C3	5.98	1.28	4.70	8.16	**-2.17**	6.44	**-1.74**	1.72	**-0.44**
C4	6.20	1.27	4.92	8.48	**-2.29**	6.77	**-1.85**	1.71	**-0.44**
C5	6.64	1.28	5.36	9.10	**-2.47**	7.38	**-2.02**	1.72	**-0.44**
NG PH	28.88	0.23	28.65	18.84	10.04	18.79	9.85	0.05	0.18
Air HX	8.91	1.71	7.20	11.19	**-2.27**	8.78	**-1.57**	2.41	**-0.70**
CLC plant	$\dot{B}_{D,k}^{real}$	$\dot{B}_{D,k}^{UN}$	$\dot{B}_{D,k}^{AV}$	$\dot{B}_{D,k}^{EN}$	$\dot{B}_{D,k}^{EX}$	$\dot{B}_{D,k}^{AV}$		$\dot{B}_{D,k}^{UN}$	
						$\dot{B}_{D,k}^{AV,EN}$	$\dot{B}_{D,k}^{AV,EX}$	$\dot{B}_{D,k}^{UN,EN}$	$\dot{B}_{D,k}^{UN,EX}$
C1	79.58	43.81	35.77	46.92	32.65	21.27	14.50	25.65	18.15
CLC	671.79	447.74	224.05	576.52	95.27	197.48	26.56	379.04	68.71
GT1	114.08	48.25	65.83	75.45	38.62	38.70	27.13	36.75	11.50
HPEC	21.29	15.80	5.48	10.82	10.46	1.81	3.67	9.01	6.79
LPEV	17.62	12.80	4.82	8.81	8.81	1.63	3.19	7.18	5.62
LPEC	21.85	12.25	9.60	13.15	8.70	6.61	3.00	6.54	5.70
LPST	47.97	25.37	22.60	31.33	16.64	12.98	9.62	18.35	7.02
ST4	34.97	5.14	29.82	19.44	15.53	16.60	13.23	2.84	2.30
GT2	11.37	3.30	8.07	6.02	5.35	3.60	4.47	2.42	0.88
C4	6.41	1.45	4.96	4.68	1.73	3.64	1.32	1.04	0.41
C5	6.65	1.45	5.20	4.87	1.78	3.82	1.38	1.04	0.41
NGPH	21.08	0.55	20.53	12.07	9.00	0.56	19.97	11.51	**-10.96**

The splitting of the environmental impact of exergy destruction, $\dot{B}_{D,k}$, is based on the equations shown in Table 3.2. The results for selected components of the plants are shown in Table 4.26.

In the reference plant, the environmental impact is mostly unavoidable for the majority of the components, with the main exceptions of GT1, the HPST and IPST. The same is true for the AZEP 85 and the CLC plant. In the plants with CO_2 capture, most of the environmental impact is avoidable for the CO_2 compressors, ST4 and GT2. Moreover, more than half of the

impact associated with exergy destruction within the DB of the AZEP 85 is also avoidable (54%).

As in the previous analyses, most of the $\dot{B}_{D,k}$ is endogenous, again exhibiting lower significance of component interactions. Specifically, the endogenous environmental impact of the reactors of the reference and the CLC plants is 6-7 times higher than the exogenous impact. In the AZEP 85, the endogenous impact is approximately four and two times higher the exogenous impact for the CC and the DB, respectively. Similar results are obtained for the endogenous parts of the avoidable and unavoidable environmental impacts of the plants.

The conclusions drawn by the application of the advanced exergoenvironmental analysis are similar to those of the advanced exergoeconomic analysis. The reference plant can potentially be improved via better performance of the CC, GT1, the LPST and C1. In the CLC plant, priority should be given to the CLC first, GT1 second, C1 third and ST4 last. In the AZEP 85, the component with the highest avoidable cost of exergy destruction is GT1, followed by the DB, the CC and ST4.

4.2.3.2 Splitting the environmental impact of pollutant formation

The results from splitting the environmental impact of pollutant formation within the reactors of the plants are shown in Table 4.27.

Table 4.27: Splitting the environmental impact of pollutant formation (Pts/h)

	$\dot{B}_k^{PF,real}$	$\dot{B}_k^{PF,UN}$	$\dot{B}_k^{PF,AV}$	$\dot{B}_k^{PF,EN}$	$\dot{B}_k^{PF,EX}$	$\dot{B}_k^{PF,AV}$		$\dot{B}_k^{PF,UN}$	
						$\dot{B}_k^{PF,AV,EN}$	$\dot{B}_k^{PF,AV,EX}$	$\dot{B}_k^{PF,UN,EN}$	$\dot{B}_k^{PF,UN,EX}$
Ref. plant									
CC	349.69	209.5	140.19	332.56	17.12	149.67	-9.48	182.89	26.61
AZEP 85									
CC	178.11	178.11	0.00	125.93	52.18	0.00	0.00	139.60	38.51
DB	127.51	31.43	96.08	118.69	8.82	98.26	-2.18	20.42	11.01
CLC plant									
CC	237.89	205.89	32.09	206.46	31.44	32.24	-0.14	174.22	31.58

All CO_2 emissions are considered to be unavoidable because complete combustion is assumed. Avoidable emissions include remaining emissions (NO_X and CH_4). The endogenous environmental impact has been calculated using data from the simulations used in the calculation of the endogenous exergy destruction.

As shown, the majority of the environmental impact of pollutant formation is endogenous and unavoidable. Moreover, the avoidable impact of pollutant formation is endogenous and can, therefore, be decreased through changes to the respective reactors. Due to the obtained results, the impact of pollutant formation has not been split further.

4.2.3.3 Splitting the exogenous environmental impact of exergy destruction

Results from splitting the exogenous environmental impacts for selected components are shown in Table 4.28.

Table 4.28: Selected results from splitting the exogenous environmental impact of exergy destruction (Pts/h)[a]

Ref. plant	*Component, k*	$\dot{B}_{D,k}^{EX}$	*Component, r*	$\dot{B}_{D,k}^{EX,r}$	*Component, k*	$\dot{B}_{D,k}^{EX}$	*Component, r*	$\dot{B}_{D,k}^{EX,r}$
	CC	96.03	*C1*	19.32	*LPST*	25.69	*CC*	5.09
			GT1	30.54			*C1*	1.347
			LPST	11.71			*GT1*	7.732
			SUM	88.64 (48.92)			SUM	14.21 (18.04)
			MX	**7.39**			**MX**	**11.48**
	C1	27.07	*CC*	21.39	*GT1*	79.35	*CC*	6.56
			GT1	1.79			*C1*	1.73
			LPST	0.69			*LPST*	1.47
			SUM	25.50 (26.62)			SUM	13.03 (63.56)
			MX	**1.57**			**MX**	**27.78**
AZEP 85	*Component, k*	$\dot{B}_{D,k}^{EX}$	*Component, r*	$\dot{B}_{D,k}^{EX,r}$	*Component, k*	$\dot{B}_{D,k}^{EX}$	*Component, r*	$\dot{B}_{D,k}^{EX,r}$
	CC	115.59	*DB*	0.16	*GT1*	43.12	*CC*	13.26
			MCM LTHX	0.20			*DB*	0.04
			C1	12.01			*MCM LTHX*	0.05
			GT1	17.92			*C1*	0.88
			MCM	0.22			*MCM*	0.09
			ST4	2.84			*ST4*	0.61
			LPST	5.80			*LPST*	0.96
			SUM	86.21 (-47.92)			SUM	20.07 (56.03)
			MX	**29.38**			**MX**	**23.04**
	DB	38.77	*CC*	14.90	*MCM*	11.28	*CC*	3.35
			MCM LTHX	0.02			*DB*	0.17
			C1	1.62			*MCM LTHX*	-0.11
			GT1	2.48			*C1*	0.35
			MCM	0.04			*GT1*	0.95
			ST4	0.65			*ST4*	0.16
			LPST	1.23			*LPST*	0.35
			SUM	28.56 (1.50)			SUM	8.42 (3.13)
			MX	**10.20**			**MX**	**2.86**
	MCM LTHX	25.42	*CC*	3.89	*ST4*	15.75	*CC*	-8.14
			DB	0.21			*DB*	0.09
			C1	-1.36			*MCM LTHX*	0.51
			GT1	1.18			*C1*	2.19
			MCM	-1.04			*GT1*	1.01
			ST4	0.56			*MCM*	1.09
			LPST	-0.50			*LPST*	0.38
			SUM	14.51 (1.07)			SUM	12.92 (7.31)
			MX	**10.91**			**MX**	**2.83**
	C1	23.58	*CC*	9.92	*LPST*	14.95	*CC*	2.83
			DB	0.16			*DB*	0.27
			MCM LTHX	0.05			*MCM LTHX*	-0.70
			GT1	1.66			*C1*	1.00
			MCM	0.07			*GT1*	6.00
			ST4	0.45			*MCM*	0.00
			LPST	0.60			*ST4*	-0.25
			SUM	17.93 (32.80)			SUM	6.80 (10.39)
			MX	**5.65**			**MX**	**8.95**
CLC plant	*Component, k*	$\dot{B}_{D,k}^{EX}$	*Component, r*	$\dot{B}_{D,k}^{EX,r}$	*Component, k*	$\dot{B}_{D,k}^{EX}$	*Component, r*	$\dot{B}_{D,k}^{EX,r}$
	CLC	95.27	*C1*	10.85	*ST4*	16.06	*C1*	0.72
			GT1	28.62			*CLC*	2.79
			ST4	3.80			*GT1*	0.83
			SUM	81.22 (70.89)			SUM	11.23 (5.24)
			MX	**14.05**			**MX**	**4.30**
	C1	32.65	*CLC*	22.69	*GT1*	38.62	*C1*	2.00
			GT1	2.11			*CLC*	7.89
			ST4	0.28			*ST4*	0.46
			SUM	27.98 (22.92)			SUM	15.37 (64.16)
			MX	**4.67**			**MX**	**23.25**

[a] In parentheses the sum of exergy destruction caused by component *k* to the remaining components *r* is shown

High values of the exogenous environmental impact are found for the reactors and the components of the GT systems of the plants. A large part of the impact of the reactors is caused by C1 and GT1: 52%, 41% and 26% of the impact imposed to the reactors stems from GT1 and C1 in the reference plant, the CLC plant and the AZEP 85, respectively. This percentage decreases to 11% for the DB of the AZEP 85. Analogously, large amounts of the impact imposed on C1 and GT1 stem from the reactors.

Relatively high mexogenous values are found for GT1 in all of the plants, while the same is true for the reactors of the oxy-fuel plants with emphasis on the CC of the AZEP 85. In general, the mexogenous values of the AZEP 85 are higher than those of the other plants because of the more intense interactions of its constitutive components (e.g., a high mexogenous value of the FG COND due to the large influence of the CC).

In summary, in the CLC plant, the highest exogenous environmental impact is caused by the reactors, followed by GT1 and C1 (SUM, value in parentheses in Table 4.28). In the reference plant, GT1 causes the highest impact, followed by the CC and C1. In the AZEP 85, GT1 is followed by the MCM HTHX (35.2 Pts/h) and C1.

4.2.3.4 Calculating the total avoidable environmental impact of exergy destruction

The results of the most influential components of the plants are shown in Table 4.29. The total avoidable exogenous environmental impact is calculated using Equation (3.38).

Table 4.29: Avoidable environmental impact of exergy destruction (Pts/h)

Ref. Plant *Component, k*	$\sum_{\substack{r=1 \\ r\neq k}}^{n} \dot{B}_{D,r}^{AV,EX,k}$	$\dot{B}_{D,k}^{AV,EN}$	$\dot{B}_{D,k}^{AV,\Sigma}$
CC	17.15 (7.4%)	215.01 (92.6%)	**232.16**
GT1	15.95 (27.2%)	42.77 (72.8)	**58.72**
C1	8.82 (31.5%)	19.17 (68.5%)	**27.99**
LPST	5.35 (22.6%)	18.30 (77.4%)	**23.65**
AZEP 85 *Component, k*	$\sum_{\substack{r=1 \\ r\neq k}}^{n} \dot{B}_{D,r}^{AV,EX,k}$	$\dot{B}_{D,k}^{AV,EN}$	$\dot{B}_{D,k}^{AV,\Sigma}$
GT1	10.91 (24.8%)	33.15 (75.2%)	**44.06**
CC	1.24 (3.2%)	37.59 (96.8%)	**38.83**
DB	-0.71	37.47	**36.76**
C1	5.73 (21.6%)	20.77 (78.4%)	**26.50**
LPST	4.53 (24.4%)	14.06 (75.6%)	**18.59**
MCM	3.33 (25.0%)	10.01 (75.0%)	**13.34**
MCM LTHX	0.39 (6.8%)	5.36 (93.2%)	**5.75**
CLC Plant *Component, k*	$\sum_{\substack{r=1 \\ r\neq k}}^{n} \dot{B}_{D,r}^{AV,EX,k}$	$\dot{B}_{D,k}^{AV,EN}$	$\dot{B}_{D,k}^{AV,\Sigma}$
CLC	20.48 (9.4%)	197.48 (90.6%)	**217.96**
GT1	16.93 (30.4%)	38.70 (69.6%)	**55.63**
C1	1.31 (5.8%)	21.27 (94.2%)	**22.58**
ST4	1.34 (7.5%)	16.60 (92.5%)	**17.94**

In the reference plant, GT1 causes an avoidable exogenous environmental impact similar to that caused by the CC. However, the endogenous impact of the CC is approximately four

times higher than that of GT1, resulting in a two times higher overall impact ($\dot{B}_{D,k}^{AV,\Sigma}$). In the CLC plant, both the avoidable endogenous and exogenous values of the CLC reactor are higher when compared to those of GT1, resulting in a higher overall impact, as well. In the AZEP 85, the avoidable exogenous environmental impact of the DB is found to be negative, while that of the CC is rather small. For the CC, this is a result of its negative influence on the CO_2 compression unit, while for the DB it is a result of the negative influence of the component onto the MCM LTHX of the plant. Although the avoidable endogenous values of the CC and DB are similar, the CC has a slightly higher avoidable impact due to its higher avoidable exogenous part. The highest exogenous impact is caused by the MCM HTHX (19.9 Pts/h), followed by GT1 and C1. Again here, as in the case of the costs, the GT1 surpasses the MCM HTHX in total impact, due to its relatively high avoidable endogenous part and it is ranked first, followed by the CC and the DB.

5. Conclusions

In this thesis, eight power plants with CO_2 capture have been compared and evaluated based on a reference power plant of similar configuration without CO_2 capture. The plants have been analyzed using exergy-based analyses, i.e. conventional and advanced exergetic, exergoeconomic and exergoenvironmental analyses. Among the eight examined concepts, the conventional post-combustion approach with chemical absorption using monoethanolamine (MEA)[1] has also been considered. The remaining seven concepts include two pre-combustion concepts (MSR plant and ATR plant) and five post-combustion plants operating using oxy-fuel technology: the *chemical looping combustion* (CLC) plant, two variations of the *advanced zero emission plant* (AZEP) with 85% and 100% CO_2 capture (AZEP 85 and AZEP 100), the S-Graz cycle and a simple oxy-fuel plant. All of the plants have been examined using an exergetic analysis, while the reference, MEA, CLC plants and the two AZEP variations have been further evaluated with economic and environmental considerations. Advanced exergy-based analyses have been applied to the reference plant, the CLC plant and the AZEP 85.

Table 5.1: The four most influential components as ranked by each analysis

	A. Conventional analyses (based on: exergy destruction ratio, total costs and total environmental impacts)			**B. Advanced analyses (based on: total avoidable exergy destruction/costs/environmental impacts)**		
	A.1 Exergetic	**A.2 Exergoeconomic**	**A.3 Exergoenvironmental**	**B.1 Exergetic**	**B.2 Exergoeconomic**	**B.3 Exergoenvironmental**
Ref. Plant	CC	CC	CC	CC	CC	CC
	GT1	GT1	GT1	GT1	GT1	GT1
	C1	C1	C1	C1	C1	C1
	LPST	LPST	LPST	LPST	LPST	LPST
AZEP 85	CC	CC	CC	DB	CC	GT1
	DB	GT1	DB	GT1	GT1	CC
	GT1	C1	GT1	C1	MCM LTHX	DB
	C1	MCM LTHX	C1	MCM	C1	C1
CLC plant	CLC	CLC	CLC	CLC	CLC	CLC
	GT1	GT1	GT1	GT1	GT1	GT1
	C1	C1	C1	C1	C1	C1
	LPST	LPST	LPST	ST4	ST4	ST4
AZEP 100	CC	CC	CC	-	-	-
	GT1	GT1	GT1	-	-	-
	C1	C1	C1	-	-	-
	MCM LTHX	MCM LTHX	MCM LTHX	-	-	-

In general, CO_2 capture is a costly process, since it either involves expensive equipment that increases the overall investment cost of the facility or energy-demanding processes that decrease the efficiency, in turn increasing the fuel consumption (i.e. the fuel costs) of a plant. The CLC plant represents a promising process from the perspective of relatively low absolute values of investment cost and absolute component-related environmental impact. The resulting *cost of electricity* (COE) is found to be slightly lower for the AZEP 85, while the *cost of*

[1] Here, only MEA-0.2 is presented.

avoided CO_2 ($COA\text{-}CO_2$) is lower for the CLC plant due to its higher amount of CO_2 captured. The environmental analysis shows that the efficiency decrease of the plants causes a significant environmental burden. The oxy-fuel plants show only minor reductions in the overall impact compared to the reference plant. Furthermore, the conventional approach of chemical absorption results in a higher environmental impact compared to the reference plant, because of the high efficiency penalty associated with the technology used. Advanced exergy-based analyses have been used in order to pinpoint equipment and processes that must be altered to improve the economic and environmental effectiveness of the overall power plants.

As shown in Table 5.1, with the exception of the AZEP 85, the four most influential components are the same in all conventional analyses. Although the DB of the AZEP 85 is important from an exergetic perspective, it is relatively cheap and, therefore not so important from an exergoeconomic point of view. The results of the advanced analyses associated with the four most influential components of the reference and CLC plants, presented in Table 5.1, agree with those of the conventional analyses with the exception of the ST4 in the CLC plant. This is not the case when the AZEP 85 is considered, due to its more complicated configuration and interactions of its components.

A short summary of the main results from each analysis is presented below.

5.1. Exergetic analysis

When compared to the reference plant that has an exergetic efficiency of 56.5%, the best exergetic efficiency among all plants with CO_2 capture was achieved by the AZEP 85 (53.4%), followed by the AZEP 100 (51.7%) and the CLC plant (51.5%). The plant using chemical absorption resulted in an efficiency penalty of eight percentage points (48.4%).

The three most efficient plants revealed in the exergetic analysis (AZEP 85, AZEP 100 and CLC plant) are oxy-fuel concepts. Among the three plants, the CLC plant has the lowest exergy destruction and the highest exergy loss (a result of the assumed 2% non-reacted methane). The combination of relatively low exergy destruction and loss (related to lower mass flows of the exhausted gases) in the AZEP 85 results in higher net power output, i.e. a higher exergetic efficiency. The main advantage of the three oxy-fuel plants is that the added components associated with CO_2 capture do not consume high amounts of energy and the energy penalties are mainly related to the production of oxygen necessary for the oxy-combustion. Moreover, the irreversibilities of the combustion processes in these plants are lower compared with the reference and MEA plants, due to the nitrogen-free combustion and the preheating of the reactants used. The MEA plant results in a high efficiency penalty, due to the relatively high energy requirements of chemical absorption.

5.2. Economic analysis

The smallest cost increase, relative to the reference plant (total 213 € million), is estimated for the MEA plant (total 326 € million), followed by the CLC plant (total 362 € million), the AZEP 85 (total 395 € million) and the AZEP 100 (total 414 € million).

Relative costs based on the power output of the plants present the MEA plant as the most economical alternative (921 €/kW). However, if the cost is based on the amount of CO_2 captured, the CLC plant is found to be more economical than the MEA plant because of its approximately 100% CO_2 capture (9.6 € million/kg CO_2 captured versus 9.9 € million/kg CO_2 captured for the MEA).

5.3. Exergoeconomic analysis

The cost of exergy destruction of the oxy-fuel plants was found to be comparable to that of the reference plant, while a larger difference was found for the MEA plant. Since all of the plants have the same fuel cost rate (c_F), the total cost rate of exergy destruction ($\dot{C}_{D,tot}$) depends on the rate of exergy destruction ($\dot{E}_{D,tot}$; i.e., $\dot{C}_{D,tot} = c_F \dot{E}_{D,tot}$). Thus, all differences between exergy-related cost rates are representative of the differences between the rates of exergy destruction of the plants and that of the reference plant. Differences among the plants mainly result from the high investment cost of components used for oxygen production and/or facilitation of CO_2 separation and compression.

CO_2 capture causes a minimum increase in the cost of electricity of 22%, achieved by the AZEP 85. An increase of 23% is calculated for the CLC plant, while the higher investment cost of the AZEP 100 results in a more significant increase in the COE, similar to that of the MEA (28% higher than that of the reference plant).

Larger differences in the energy penalty of the plants are observed when the COA-CO_2 is considered. The cost differences between the MEA plant and the other plants are mainly associated with the high energy demand of the solvent regeneration and the relatively low percentage of CO_2 capture (85%), in comparison to the close to 100% capture of the oxy-fuel concepts. The CLC plant has the same CO_2 emissions as the AZEP 100, but it results in the lowest COA-CO_2, due to its lower COE.

5.4. Life cycle assessment

The construction phase of the two AZEP concepts is associated with a significantly higher environmental impact, with respect to the reference plant. The lowest relative component-related environmental impact (Pts/kW) among all plants with CO_2 capture is found for the CLC and MEA plants. However, the component-related environmental impact of the plants is negligible when compared to the impact associated with the exergy destruction that takes place during the operation phase of the plants.

5.5. Exergoenvironmental analysis

The calculation of the overall environmental impact is mainly influenced by the impacts of fuel processing (methane) and the impact of pollutant emission. With data provided by Goedkoop and Spriensma (2000), the impact of the produced electricity of the oxy-fuel plants is found to be slightly lower than that of the reference plant. Specifically, the CLC plant and the AZEP 85 present the lowest environmental impact (0.6 Pts/MWh lower than that of the reference plant). This marginal decrease in environmental impact raises questions concerning the real environmental and cost viability of CO_2 capture from power plants. Additionally, the impact of the electricity generated in the MEA plant is found to be significantly higher than that of the reference plant (2.4 Pts/MWh higher), due to the plant's high efficiency penalty. Considering that post-combustion is the most conventional way to capture CO_2 from power plants, the plant has been considered in a sensitivity analysis concerning the variation of the environmental impact of CO_2 emissions. This analysis showed that post-combustion technology will not decrease the environmental impact of power production, unless a specific environmental impact approximately four times higher than the present estimate is assigned to the CO_2 emissions.

5.6. Advanced exergetic analysis

Most of the exergy destruction of the plants is endogenous and, for the majority of the components, unavoidable. Thus, improvement potential lies with the internal operating conditions of the components (*endogenous exergy destruction*), while component interactions (*exogenous exergy destruction*) are less significant. To examine the overall significance of the different plant components, the total avoidable exergy destruction caused by each component has been calculated. The total avoidable exergy destruction includes the exergy destruction caused by each component both to itself and to the remaining components of the plant. The results are similar to those of the conventional analysis: the improvement priority of the reactors is ranked first, followed by GT1 and C1.

5.7. Advanced exergoeconomic analysis

In this analysis, the investment cost rate and the cost rate of exergy destruction are split into avoidable/unavoidable and endogenous/exogenous parts. The improvement potential is related to the avoidable part of the investment cost and the cost of exergy destruction. For the reference and CLC plants, the most important components in terms of the absolute values of the total avoidable costs are the reactors, GT1 and C1. In the AZEP 85, the ranking order differs slightly when the total avoidable cost is considered, due to the large avoidable investment cost of the MCM LTHX.

For the three most influential components of the plants, the largest part of their investment cost rates and their cost of exergy destruction is unavoidable. Moreover, for both

the investment cost and the cost of exergy destruction, the interactions of the components, represented by the exogenous part of the costs, are of lower importance, since for the majority of the components, the endogenous part of the costs is significantly larger.

5.8. Advanced exergoenvironmental analysis

The results of the advanced exergoenvironmental analysis generally agree with those obtained in the other analyses. In general, the most important components are those of the GT system, the LPST or ST4 and the MCM LTHX (in the case of the AZEP 85). A significantly different result stems from the influence of the CC in the AZEP 85: The CC has an inverse effect on the components processing the CO_2 stream. Therefore, a low avoidable environmental impact is caused by the CC, resulting in a small improvement priority of the component (following that of GT1). On the contrary, in the other two plants, the reactors have approximately four times higher total avoidable costs, when compared to GT1.

Similar to the results of the advanced exergoeconomic analysis, the majority of the environmental impact related to the exergy destruction is unavoidable and endogenous. Thus, the interactions of the components are of lower importance here as well.

5.9. Summary and future work

CO_2 capture from power plants is a costly process. However, for CCS to be deemed viable, the real economic and environmental benefits have to be considered. To do so, the environmental perspective must be examined in detail, and different databases must be compared and assessed. If it is decided that the obtained benefits represent realistic expectations, the most cost effective solutions should be further promoted for large-scale implementation.

In general, oxy-fuel concepts represent a relatively promising technology that keeps the energy penalty of CO_2 capture at relatively low levels, in contrast to the conventional approach: chemical absorption with MEA.

The exergoeconomic and exergoenvironmental analyses provide important information about how to improve both the structure and operating conditions of plants, in order to decrease their economic penalty and increase their environmental advantage. Advanced exergy-based analyses are valuable supplements to the conventional analyses, providing information about real improvement potential and component interactions. Nonetheless, the analyses need to be further developed for more reliable process-specific evaluation and easier data processing.

Additionally, for a fair comparison of different power plants, various decision parameters that may differ in importance from the point of view of technological availability, structure or operation must be considered. Further research is essential, in order to find and evaluate solutions which will avoid causing further environmental problems or creating additional needs.

Lastly, the information provided in this thesis should be used to realize improved designs of the plant structures provided. This will provide a helpful guide on how environmental and economic considerations interact and how optimized structures of the plants can be obtained.

Appendix A

Flow charts and simulation assumptions of the power plants

A.1: The reference plant

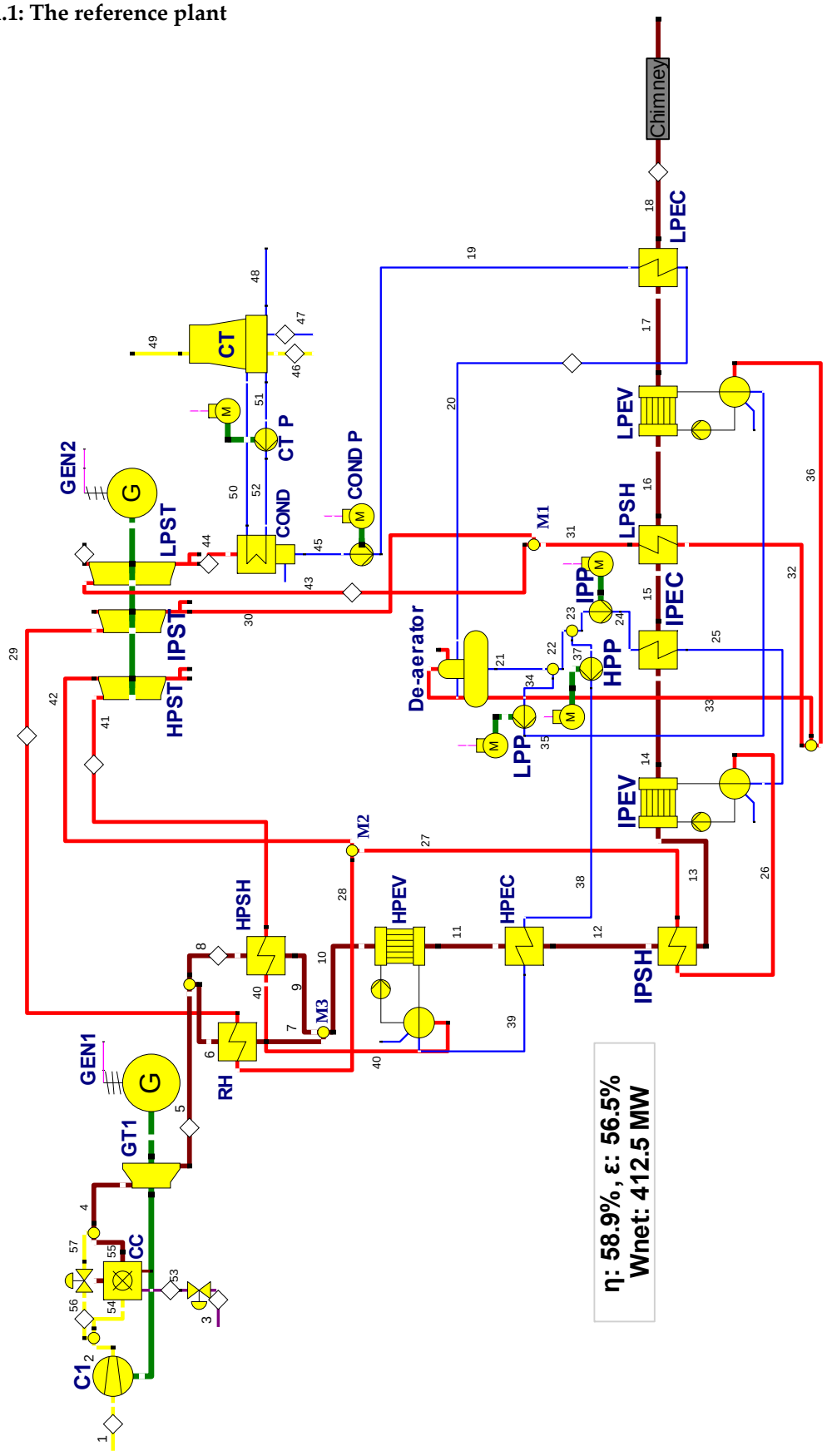

Figure A.1.1: Structure of the reference plant

Table A.1.1: Results of the year-by-year economic analysis for the reference plant

Ref. Plant								
Year	**Calendar year**	**Debt beg. of year**	**Book depreciation**	**Adjustment**	**Common Equity beg. of year**	**Book depreciation**	**Adjustment**	**TCR**
1	2013	145,843,425	7,292,171	461,985	145,843,425	5,027,429	1,102,609	13,884,195
2	2014	138,089,269	7,292,171	461,985	139,713,386	5,027,429	1,102,609	13,884,195
3	2015	130,335,112	7,292,171	461,985	133,583,348	5,027,429	1,102,609	13,884,195
4	2016	122,580,956	7,292,171	461,985	127,453,309	5,027,429	1,102,609	13,884,195
5	2017	114,826,800	7,292,171	461,985	121,323,271	5,027,429	1,102,609	13,884,195
6	2018	107,072,644	7,292,171	461,985	115,193,232	5,027,429	1,102,609	13,884,195
7	2019	99,318,487	7,292,171	461,985	109,063,194	5,027,429	1,102,609	13,884,195
8	2020	91,564,331	7,292,171	461,985	102,933,155	5,027,429	1,102,609	13,884,195
9	2021	83,810,175	7,292,171	461,985	96,803,117	5,027,429	1,102,609	13,884,195
10	2022	76,056,018	7,292,171	461,985	90,673,078	5,027,429	1,102,609	13,884,195
11	2023	68,301,862	7,292,171	461,985	84,543,040	5,027,429	1,102,609	13,884,195
12	2024	60,547,706	7,292,171	461,985	78,413,001	5,027,429	1,102,609	13,884,195
13	2025	52,793,550	7,292,171	461,985	72,282,963	5,027,429	1,102,609	13,884,195
14	2026	45,039,393	7,292,171	461,985	66,152,924	5,027,429	1,102,609	13,884,195
15	2027	37,285,237	7,292,171	461,985	60,022,886	5,027,429	1,102,609	13,884,195
16	2028	29,531,081	7,292,171	461,985	53,892,847	5,027,429	1,102,609	13,884,195
17	2029	21,776,925	7,292,171	-1,847,940	47,762,809	5,027,429	-1,207,316	9,264,345
18	2030	16,332,694	7,292,171	-1,847,940	43,942,695	5,027,429	-1,207,316	9,264,345
19	2031	10,888,462	7,292,171	-1,847,940	40,122,582	5,027,429	-1,207,316	9,264,345
20	2032	5,444,231	7,292,171	-1,847,940	36,302,469	5,027,429	-1,207,316	9,264,345
21	2033	0	0	0	32,482,355	0	0	0
Total		**1,457,438,358**	**145,843,425**	**0**	**1,798,503,086**	**100,548,585**	**12,812,485**	**259,204,494**

Table A.1.2: Results at the component level for the reference plant

Component, k	$\dot{E}_{F,k}$ **(MW)**	$\dot{E}_{P,k}$ **(MW)**	$\dot{E}_{D,k}$ **(MW)**	ε_k **(%)**	$y_{D,k}$ **(%)**	$c_{F,k}$ **(€/GJ)**	$c_{P,k}$ **(€/GJ)**	$\dot{C}_{D,k}$ **(€/h)**	$\dot{Z}_k$ **(€/h)**	$\dot{C}_{D,k}+\dot{Z}_k$ **(€/h)**	f_k **(%)**	r_k **(%)**	$b_{F,k}$ **(Pts/GJ)**	$b_{P,k}$ **(Pts/GJ)**	$\dot{B}_{D,k}$ **(Pts/h)**	$\dot{Y}_k$ **(Pts/h)**	$\dot{B}_{D,k}+\dot{Y}_k$ **(Pts/h)**	$f_{b,k}$ **(%)**	$r_{b,k}$ **(%)**
C1	242.68	231.30	11.38	95.3	1.56	16.9	19.5	693	1,423	2,116	67.3	15.0	6.1	6.4	249.71	0.24	249.94	0.09	4.9
CC	729.62	508.76	220.87	69.7	30.23	9.2	13.7	7,276	1,017	8,293	12.3	49.5	3.5	5.6	2746.20	0.38	2746.58	0.01	63.3
GT	551.15	530.67	20.47	96.3	2.80	15.5	16.9	1,140	1,627	2,766	58.8	9.4	5.9	6.1	432.58	1.12	433.71	0.26	3.9
HPSH	35.07	31.72	3.35	90.5	0.46	15.5	19.4	186	158	344	45.8	25.6	5.9	6.8	70.75	1.20	71.95	1.67	15.5
HPEV	43.64	39.91	3.73	91.5	0.51	15.5	19.0	207	185	392	47.1	23.1	5.9	6.7	78.75	0.13	78.88	0.16	13.6
HPEC	28.92	24.91	4.00	86.2	0.55	15.5	20.4	223	89	312	28.6	31.8	5.9	7.2	84.57	0.09	84.66	0.10	23.3
RH	26.47	23.89	2.58	90.3	0.35	15.5	19.4	143	111	255	43.7	25.4	5.9	6.8	54.42	0.80	55.22	1.46	15.8
IPSH	0.18	0.12	0.06	69.0	0.01	15.5	35.4	3	4	7	56.3	128.8	5.9	9.7	1.17	0.00	1.17	0.18	65.2
IPEV	6.10	5.67	0.43	92.9	0.06	15.5	20.5	24	65	90	73.1	32.8	5.9	6.5	9.13	0.04	9.16	0.42	11.1
IPEC	1.06	0.87	0.19	82.5	0.03	15.5	22.3	10	5	16	33.4	44.3	5.9	7.7	3.93	0.00	3.93	0.09	30.9
LPSH	1.43	1.04	0.38	73.3	0.05	15.5	29.5	21	19	41	47.7	90.9	5.9	9.0	8.05	0.01	8.06	0.16	53.0
LPEV	19.03	15.48	3.55	81.4	0.49	15.5	24.2	197	174	372	46.9	56.4	5.9	7.8	74.95	0.12	75.07	0.16	33.3
LPEC	11.49	7.71	3.78	67.1	0.52	15.5	30.8	211	93	304	30.7	99.3	5.9	10.1	79.97	0.09	80.07	0.12	71.3
HPST	31.29	29.18	2.11	93.2	0.29	20.3	24.2	155	182	336	54.0	18.9	7.0	7.7	53.51	0.28	53.79	0.51	10.0
IPST	37.39	35.21	2.18	94.2	0.30	20.3	24.7	159	329	488	67.4	21.7	7.0	7.6	54.88	0.32	55.20	0.57	8.6
LPST	70.99	61.35	9.64	86.4	1.32	21.4	29.7	743	764	1,508	50.7	38.5	7.2	8.8	251.49	0.49	251.98	0.20	21.5
COND P	0.04	0.04	0.01	78.8	0.00	20.0	84.2	1	7	8	91.3	321.6	6.7	9.3	0.23	0.00	0.23	0.13	37.5
HPP	1.12	0.96	0.17	85.3	0.02	20.0	36.7	12	40	52	77.3	83.8	6.7	8.4	4.00	0.00	4.00	0.01	24.0
IPP	0.03	0.02	0.01	65.3	0.00	20.0	147.4	1	8	8	91.4	637.6	6.7	11.7	0.25	0.00	0.25	0.01	73.8
LPP	0.00	0.00	0.00	67.2	0.00	20.0	406.5	0	3	3	97.4	1934.8	6.7	11.3	0.02	0.00	0.02	0.50	68.2
De-aerator	0.56	0.53	0.03	95.4	0.00	25.1	41.2	2	28	30	92.4	64.3	8.1	8.6	0.74	0.04	0.77	4.55	6.6
M1	1.81	1.63	0.18	90.1	0.02	20.3	22.8	13	0	13	0.0	12.2	7.0	7.8	4.52	0.00	4.52	0.00	12.1
M2	0.63	0.58	0.04	92.9	0.01	20.3	24.7	3	0	3	0.0	21.3	7.0	8.4	1.12	0.00	1.12	0.00	19.2
M3	0.18	0.18	0.00	99.9	0.00	15.5	15.5	0	0	0	0.0	0.1	5.9	5.9	0.00	0.00	0.00	0.00	0.1
COND	12.43	-	9.24	-	1.26	21.4	-	712	91	803	11.3	-	7.2	-	241.02	0.03	241.05	0.01	-
CT	3.19	-	2.04	-	0.28	-	-	-	96	-	-	-	-	-	-	11.95	-	-	-
Total	**730.58**	**412.54**	**300.41**	**56.5**	**41.12**	**9.2**	**20.6**	**9,897**	**6,519**	**16,416**	**39.7**	**124.8**	**3.5**	**7.0**	**3735.22**	**17.33**	**3752.54**	**0.46**	**101.7**
Exergy loss	**17.63**																		
$\dot{B}_k^{PF}$	**1258.87**																		

Table A.1.3: Results at the stream level for the reference plant

Stream, j	$\dot{m}_j$ (kg/s)	T_j (°C)	p_j (bar)	$\dot{E}_{PH,j}$ (MW)	$\dot{E}_{CH,j}$ (MW)	$\dot{E}_{tot,j}$ (MW)	c_j (€/GJ)	$\dot{C}_j$ (€/h)	b_j (Pts/GJ)	$\dot{B}_j$ (Pts/h)
1	614.5	15.00	1.01	0.00	0.96	0.96	0.0	0	0.0	0
2	614.5	392.90	17.00	231.30	0.96	232.25	19.4	16,198	6.4	5,326
3	14.0	15.00	50.00	8.15	721.47	729.62	9.2	24,037	3.5	9,072
4	628.5	1264.03	16.49	735.74	5.27	741.01	15.5	41,252	5.9	15,658
5	628.5	580.64	1.06	184.60	5.27	189.87	15.5	10,570	5.9	4,012
6	268.5	580.64	1.06	78.86	2.25	81.11	15.5	4,515	5.9	1,714
7	268.5	447.61	1.05	52.39	2.25	54.64	15.5	3,042	5.9	1,155
8	360.0	580.64	1.06	105.73	3.02	108.75	15.5	6,054	5.9	2,298
9	360.0	449.30	1.05	70.66	3.02	73.68	15.5	4,102	5.9	1,557
10	628.5	448.58	1.05	123.05	5.27	128.33	15.5	7,144	5.9	2,712
11	628.5	341.18	1.04	79.42	5.27	84.69	15.5	4,715	5.9	1,789
12	628.5	257.92	1.04	50.50	5.27	55.77	15.5	3,105	5.9	1,178
13	628.5	257.35	1.04	50.32	5.27	55.59	15.5	3,095	5.9	1,175
14	628.5	237.62	1.04	44.22	5.27	49.49	15.5	2,755	5.9	1,046
15	628.5	234.08	1.04	43.16	5.27	48.43	15.5	2,696	5.9	1,023
16	628.5	229.27	1.04	41.74	5.27	47.01	15.5	2,617	5.9	993
17	628.5	156.37	1.03	22.71	5.27	27.98	15.5	1,558	5.9	591
18	628.5	95.34	1.03	11.22	5.27	16.49	0.0	0	0.0	0
19	94.6	32.89	3.73	0.24	0.24	0.47	26.1	44	7.4	13
20	94.6	135.62	3.62	7.95	0.24	8.18	30.6	900	9.9	292
21	95.4	140.01	3.62	8.55	0.24	8.79	31.1	986	9.8	310
22	72.4	140.01	3.62	6.49	0.18	6.67	31.1	748	9.8	236
23	7.2	140.01	3.62	0.65	0.02	0.67	31.1	75	9.8	23
24	7.2	140.49	25.13	0.67	0.02	0.68	34.4	85	9.9	24
25	7.2	216.62	24.38	1.54	0.02	1.56	27.6	155	8.6	48
26	7.2	222.62	24.38	7.21	0.02	7.23	22.1	574	7.0	182
27	7.2	237.92	23.16	7.33	0.02	7.35	22.3	590	7.0	186
28	72.4	305.14	23.16	79.35	0.18	79.53	20.6	5,885	7.0	2,017
29	72.4	560.64	22.00	103.24	0.18	103.42	20.3	7,553	7.0	2,601
30	72.4	317.23	4.10	65.85	0.18	66.03	20.3	4,822	7.0	1,661
31	22.1	214.08	4.10	17.95	0.06	18.01	25.3	1,642	8.1	526
32	22.1	146.37	4.32	16.91	0.06	16.96	25.1	1,531	8.1	492
33	0.8	146.37	4.32	0.63	0.00	0.63	25.1	57	8.1	18
34	23.0	140.01	3.62	2.06	0.06	2.12	31.1	237	9.8	75
35	23.0	140.02	4.32	2.06	0.06	2.12	31.5	240	9.8	75
36	23.0	146.37	4.32	17.54	0.06	17.60	25.1	1,588	8.1	511
37	65.2	140.01	3.62	5.84	0.16	6.01	31.1	674	9.8	212
38	65.2	141.75	134.56	6.80	0.16	6.96	31.9	800	9.6	241
39	65.2	325.17	130.53	31.72	0.16	31.88	22.9	2,628	7.8	890
40	65.2	331.17	130.53	71.63	0.16	71.79	20.8	5,363	7.1	1,848
41	65.2	560.64	124.00	103.35	0.16	103.51	20.3	7,581	7.0	2,622
42	65.2	313.21	23.16	72.06	0.16	72.22	20.3	5,290	7.0	1,829
43	94.6	293.03	4.10	83.62	0.24	83.86	21.4	6,465	7.2	2,187
44	94.6	32.88	0.05	12.63	0.24	12.87	21.4	992	7.2	336
45	94.6	32.88	0.05	0.20	0.24	0.44	21.4	34	7.2	11
46	5177.4	15.00	1.01	0.00	8.06	8.06	0.0	0	0.0	0
47	135.6	15.00	1.01	0.00	0.34	0.34	0.0	0	0.0	0
48	74.0	16.00	1.01	0.00	0.18	0.19	0.0	0	0.0	0
49	5239.0	22.88	1.01	1.84	7.52	9.36	0.0	0	0.0	0
50	7396.2	22.88	1.33	3.51	18.47	21.98	-	-	-	-
51	7396.2	16.00	1.01	0.05	18.47	18.53	-	-	-	-
52	7396.2	16.00	1.37	0.32	18.47	18.80	-	-	-	-
53	14.0	15.00	17.00	5.90	721.47	727.37	-	-	-	-
54	498.5	392.90	17.00	187.64	0.78	188.41	-	-	-	-
55	512.5	1435.04	16.49	704.31	5.80	710.10	-	-	-	-
56	116.0	392.90	17.00	43.66	0.18	43.84	-	-	-	-
57	116.0	392.90	16.49	43.37	0.18	43.55	-	-	-	-
58	-	-	-	-	*C1*	242.68	16.9	14,775	6.1	5,326
59	-	-	-	-	*ST1*	29.18	24.2	2,542	7.7	813
60	-	-	-	-	*ST2*	35.21	24.7	3,130	7.6	962
61	-	-	-	-	*ST3*	61.35	29.7	6,549	8.8	1,944
62	-	-	-	-	*COND P*	0.04	20.0	3	6.7	1
63	-	-	-	-	*LPP*	0.00	20.0	0	6.7	0
64	-	-	-	-	*HPP*	1.12	20.0	81	6.7	27
65	-	-	-	-	*IPP*	0.03	20.0	2	6.7	1
66	-	-	-	-	*GT1*	288.00	16.9	17,534	6.1	6,321
67	-	-	-	-	*tot*	412.54	20.0	29,669	6.7	10,010

Table A.1.4: Splitting the exergy destruction in the reference plant (MW)

Component, k	$E_{D,k}^{real}$	$E_{D,k}^{EN}$	$E_{D,k}^{EX}$	$E_{D,k}^{AV}$	$E_{D,k}^{UN}$	$E_{D,k}^{UN,EN}$	$E_{D,k}^{UN,EX}$	$E_{D,k}^{AV,EN}$	$E_{D,k}^{AV,EX}$
C1	11.38	6.94	4.44	5.11	6.26	3.79	2.47	3.14	1.97
CC	220.87	193.06	27.80	71.03	149.84	130.81	19.03	62.25	8.77
GT	16.09	13.52	2.57	8.32	7.77	6.23	1.53	7.29	1.03
HPSH	3.35	1.78	1.57	0.87	2.48	1.30	1.18	0.48	0.38
HPEV	3.73	2.00	1.72	0.67	3.06	1.84	1.21	0.16	0.51
HPEC	4.00	2.24	1.76	1.28	2.72	1.75	0.97	0.49	0.79
RH	2.57	1.98	0.59	0.89	1.68	1.11	0.57	0.87	0.02
IPSH	0.06	0.09	**-0.03**	0.05	0.01	0.01	**-0.01**	0.07	**-0.03**
IPEV	0.43	0.41	0.02	0.15	0.28	0.25	0.03	0.16	**-0.01**
IPEC	0.19	0.16	0.03	0.07	0.12	0.18	**-0.06**	**-0.01**	0.08
LPSH	0.38	0.19	0.19	0.22	0.16	0.06	0.10	0.13	0.09
LPEV	3.74	1.68	2.06	0.76	2.98	1.65	1.33	0.03	0.73
LPEC	3.78	2.42	1.37	1.83	1.95	1.13	0.82	1.28	0.55
HPST	1.67	1.11	0.56	0.89	0.78	0.50	0.29	0.61	0.28
IPST	1.65	1.19	0.46	0.71	0.94	0.65	0.28	0.54	0.17
LPST	8.71	6.10	2.61	3.61	5.10	3.57	1.53	2.53	1.08
COND P	0.45	0.00	0.44	0.45	0.00	0.00	0.00	0.00	0.44
HPP	0.11	0.00	0.11	0.11	0.00	0.00	0.00	0.00	0.11
IPP	0.01	0.06	**-0.06**	**-0.03**	0.03	0.02	0.01	0.04	-0.07
LPP	0.03	0.01	0.02	0.02	0.00	0.00	0.00	0.01	0.02
COND	9.24	6.49	2.75	-	-	-	-	-	-
CT	2.04	1.30	0.74	-	-	-	-	-	-
GEN1	4.39	4.76	**-0.38**	2.94	1.45	1.57	**-0.12**	3.19	**-0.25**
GEN2	1.91	1.44	0.48	1.28	0.63	0.47	0.16	0.96	0.32
MOT1	0.01	0.00	0.01	0.00	0.00	0.00	0.00	0.00	0.01
MOT2	0.15	0.00	0.15	0.15	0.00	0.00	0.00	0.00	0.15
MOT3	0.06	0.00	0.06	0.04	0.02	0.01	0.01	**-0.01**	0.05
MOT4	0.00	0.00	0.00	0.00	0.00	0.00	0.00	0.00	0.00
Total	**300.97**	**248.94**	**52.03**						
Total (%)		**82.71**	**17.29**						

Table A.1.5: Splitting the investment cost rate in the reference plant (€/h)

						$\dot{Z}_k^{AV}$		$\dot{Z}_k^{UN}$	
Component, k	$\dot{Z}_k^{real}$	$\dot{Z}_k^{UN}$	$\dot{Z}_k^{AV}$	$\dot{Z}_k^{EN}$	$\dot{Z}_k^{EX}$	$\dot{Z}_k^{AV,EN}$	$\dot{Z}_k^{AV,EX}$	$\dot{Z}_k^{UN,EN}$	$\dot{Z}_k^{UN,EX}$
C1	1423.3	1209.8	213.5	861.8	561.5	129.3	84.2	732.6	477.3
CC	1016.7	813.3	203.3	887.6	129.1	177.5	25.8	710.0	103.3
GT	1626.7	1464.0	162.7	1305.7	320.9	130.6	32.1	1175.2	288.8
HPSH	111.2	50.8	60.4	73.5	37.7	39.9	20.5	33.6	17.2
HPEV	157.7	68.5	89.2	82.4	75.2	46.6	42.6	35.8	32.7
HPEC	185.0	102.6	82.4	111.7	73.4	49.7	32.7	61.9	40.7
RH	89.2	45.2	44.1	57.3	31.9	28.4	15.7	29.0	16.3
IPSH	4.0	1.2	2.8	7.1	**-3.1**	5.0	**-2.2**	2.1	**-0.9**
IPEV	65.5	31.5	33.9	58.2	7.2	30.2	3.7	28.1	3.5
IPEC	5.2	2.8	2.4	7.6	**-2.4**	3.5	**-1.1**	4.1	**-1.3**
LPSH	19.3	7.6	11.7	7.7	11.6	4.7	7.0	3.1	4.6
LPEV	174.2	89.2	85.0	96.5	77.7	47.1	37.9	49.4	39.8
LPEC	93.4	44.9	48.5	54.2	39.2	28.1	20.4	26.1	18.9
HPST	181.7	163.5	18.2	115.3	66.4	11.5	6.6	103.8	59.7
IPST	328.9	296.0	32.9	230.1	98.8	23.0	9.9	207.1	89.0
LPST	764.1	687.7	76.4	534.9	229.2	53.5	22.9	481.4	206.3
COND P	7.1	6.1	1.1	5.6	1.5	0.8	0.2	4.8	1.3
HPP	40.5	34.4	6.1	23.9	16.6	3.6	2.5	20.3	14.1
IPP	7.8	6.6	1.2	9.8	**-2.1**	1.5	-0.3	8.4	**-1.8**
LPP	2.5	2.1	0.4	0.0	2.5	0.0	0.4	0.0	2.1

Table A.1.6: Splitting the cost rate of exergy destruction in the reference plant (€/h)

	$\dot{C}_{D,k}^{real}$	$\dot{C}_{D,k}^{UN}$	$\dot{C}_{D,k}^{AV}$	$\dot{C}_{D,k}^{EN}$	$\dot{C}_{D,k}^{EX}$	$\dot{C}_{D,k}^{AV}$		$\dot{C}_{D,k}^{UN}$	
Component, k						$\dot{C}_{D,k}^{AV,EN}$	$\dot{C}_{D,k}^{AV,EX}$	$\dot{C}_{D,k}^{UN,EN}$	$\dot{C}_{D,k}^{UN,EX}$
C1	692.7	381.3	311.4	422.3	270.4	191.5	119.9	230.9	150.4
CC	7276.3	4936.4	2339.9	6360.4	916.0	2050.8	289.1	4309.5	626.9
GT	1139.7	432.3	707.4	752.7	387.0	405.6	301.7	347.0	85.3
HPSH	143.4	93.7	49.7	110.5	32.9	48.6	1.2	61.9	31.7
HPEV	186.4	138.2	48.2	99.2	87.2	27.0	21.2	72.3	65.9
HPEC	207.5	170.2	37.3	111.6	95.9	8.9	28.4	102.7	67.5
RH	222.8	151.4	71.4	124.8	98.1	27.5	43.9	97.2	54.2
IPSH	3.1	0.4	2.7	4.8	**-1.7**	4.1	**-1.4**	0.6	**-0.3**
IPEV	24.0	15.5	8.6	22.8	1.2	9.1	**-0.5**	13.7	1.7
IPEC	10.4	6.7	3.7	9.0	1.4	**-0.8**	4.5	9.8	**-3.1**
LPSH	21.2	8.9	12.3	10.8	10.4	7.2	5.1	3.6	5.3
LPEV	197.5	166.0	31.5	93.4	104.1	1.4	30.1	91.9	74.0
LPEC	210.7	108.8	101.9	134.6	76.1	71.5	30.4	63.1	45.7
HPST	154.7	57.3	97.4	81.0	73.7	44.6	52.8	36.4	20.9
IPST	159.3	68.3	91.0	86.9	72.5	39.1	51.9	47.8	20.5
LPST	743.4	393.2	350.2	470.0	273.4	194.7	155.5	275.3	117.9
COND P	0.7	0.1	0.6	0.2	0.5	0.1	0.4	0.1	0.0
HPP	11.9	2.5	9.4	4.5	7.4	3.0	6.4	1.5	1.0
IPP	0.7	0.0	0.7	0.6	0.2	0.5	0.2	0.1	0.0
LPP	0.1	0.0	0.1	0.0	0.1	0.0	0.1	0.0	0.0

Table A.1.7: Splitting the environmental impact of exergy destruction in the reference plant (Pts/h)

	$\dot{B}_{D,k}^{real}$	$\dot{B}_{D,k}^{UN}$	$\dot{B}_{D,k}^{AV}$	$\dot{B}_{D,k}^{EN}$	$\dot{B}_{D,k}^{EX}$	$\dot{B}_{D,k}^{AV}$		$\dot{B}_{D,k}^{UN}$	
Component, k						$\dot{B}_{D,k}^{AV,EN}$	$\dot{B}_{D,k}^{AV,EX}$	$\dot{B}_{D,k}^{UN,EN}$	$\dot{B}_{D,k}^{UN,EX}$
C1	69.4	38.2	31.2	42.3	27.1	19.2	12.0	23.1	15.1
CC	762.8	517.5	245.3	666.8	96.0	215.0	30.3	451.8	65.7
GT	120.2	45.6	74.6	79.4	40.8	42.8	31.8	36.6	9.0
HPSH	15.1	9.9	5.2	11.6	3.5	5.1	0.1	6.5	3.3
HPEV	19.7	14.6	5.1	10.5	9.2	2.8	2.2	7.6	7.0
HPEC	21.9	17.9	3.9	11.8	10.1	0.9	3.0	10.8	7.1
RH	23.5	16.0	7.5	13.2	10.3	2.9	4.6	10.3	5.7
IPSH	0.3	0.0	0.3	0.5	**-0.2**	0.4	**-0.1**	0.1	**0.0**
IPEV	2.5	1.6	0.9	2.4	0.1	1.0	**-0.1**	1.4	0.2
IPEC	1.1	0.7	0.4	0.9	0.1	**-0.1**	0.5	1.0	**-0.3**
LPSH	2.2	0.9	1.3	1.1	1.1	0.8	0.5	0.4	0.6
LPEV	20.8	17.5	3.3	9.8	11.0	0.2	3.2	9.7	7.8
LPEC	22.2	11.5	10.7	14.2	8.0	7.5	3.2	6.7	4.8
HPST	14.9	5.5	9.4	7.8	7.1	4.3	5.1	3.5	2.0
IPST	15.2	6.5	8.7	8.3	6.9	3.7	5.0	4.6	2.0
LPST	69.9	37.0	32.9	44.2	25.7	18.3	14.6	25.9	11.1
COND P	0.1	0.0	0.1	0.0	0.0	0.0	0.0	0.0	0.0
HPP	1.1	0.2	0.9	0.4	0.7	0.3	0.6	0.1	0.1
IPP	0.1	0.0	0.1	0.1	0.0	0.0	0.0	0.0	0.0
LPP	0.0	0.0	0.0	0.0	0.0	0.0	0.0	0.0	0.0

A.2: The AZEP 85

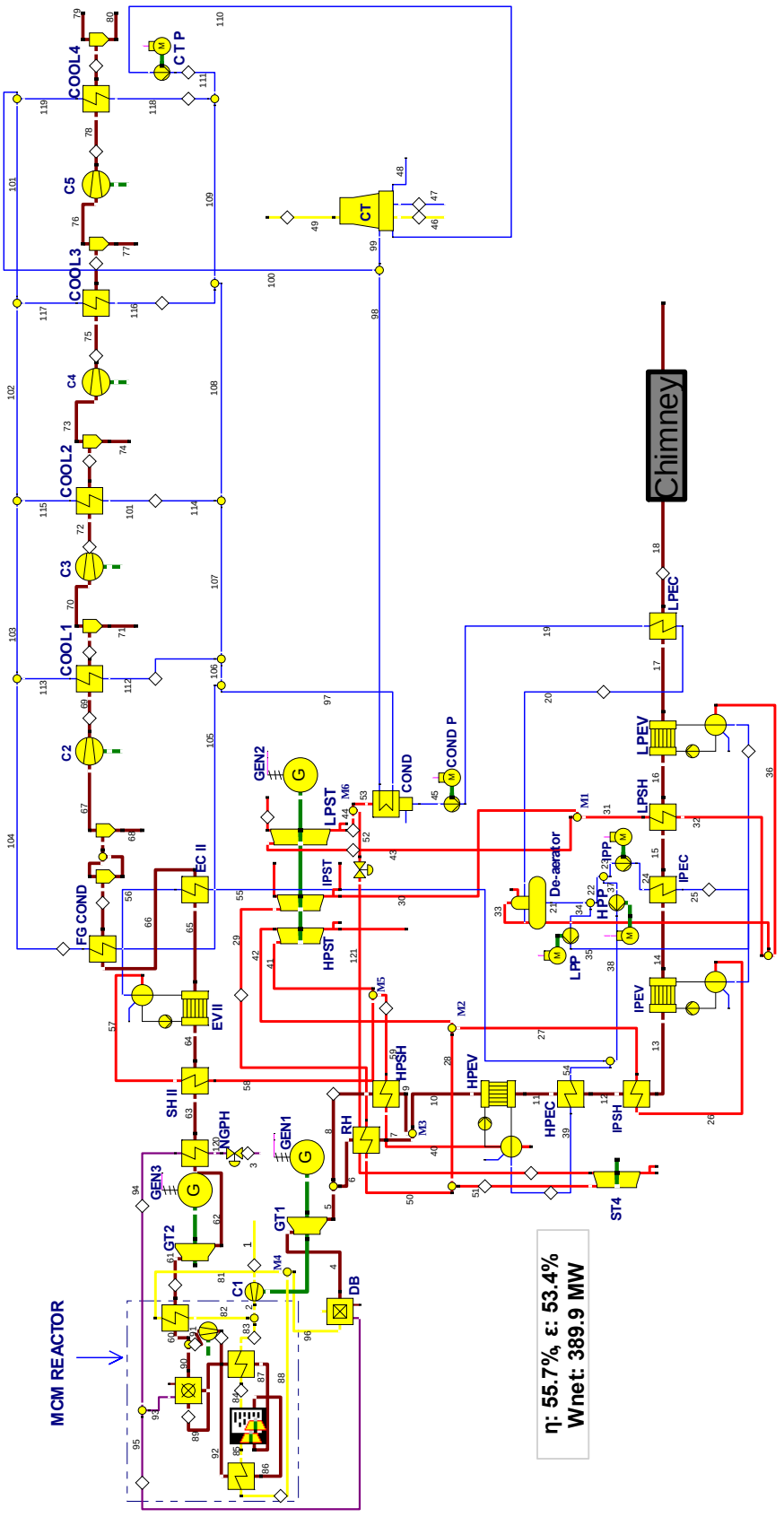

Figure A.2.1: Structure of the AZEP 85 (for the MCM reactor see Figure A.4.1)

Table A.2.1: Results of the economic analysis for the AZEP 85

Year	Calendar year	Debt beg. of year	Book depreciation	Adjustment	Common Equity beg. of year	Book depreciation	Adjustment	TCR
1	2013	254,669,410	12,733,471	849,998	254,669,410	9,933,140	2,026,210	25,542,819
2	2014	241,085,942	12,733,471	849,998	242,710,060	9,933,140	2,026,210	25,542,819
3	2015	227,502,474	12,733,471	849,998	230,750,709	9,933,140	2,026,210	25,542,819
4	2016	213,919,005	12,733,471	849,998	218,791,358	9,933,140	2,026,210	25,542,819
5	2017	200,335,537	12,733,471	849,998	206,832,008	9,933,140	2,026,210	25,542,819
6	2018	186,752,068	12,733,471	849,998	194,872,657	9,933,140	2,026,210	25,542,819
7	2019	173,168,600	12,733,471	849,998	182,913,306	9,933,140	2,026,210	25,542,819
8	2020	159,585,131	12,733,471	849,998	170,953,956	9,933,140	2,026,210	25,542,819
9	2021	146,001,663	12,733,471	849,998	158,994,605	9,933,140	2,026,210	25,542,819
10	2022	132,418,195	12,733,471	849,998	147,035,254	9,933,140	2,026,210	25,542,819
11	2023	118,834,726	12,733,471	849,998	135,075,904	9,933,140	2,026,210	25,542,819
12	2024	105,251,258	12,733,471	849,998	123,116,553	9,933,140	2,026,210	25,542,819
13	2025	91,667,789	12,733,471	849,998	111,157,202	9,933,140	2,026,210	25,542,819
14	2026	78,084,321	12,733,471	849,998	99,197,852	9,933,140	2,026,210	25,542,819
15	2027	64,500,852	12,733,471	849,998	87,238,501	9,933,140	2,026,210	25,542,819
16	2028	50,917,384	12,733,471	849,998	75,279,150	9,933,140	2,026,210	25,542,819
17	2029	37,333,916	12,733,471	-3,399,992	63,319,800	9,933,140	-2,223,779	17,042,840
18	2030	28,000,437	12,733,471	-3,399,992	55,610,439	9,933,140	-2,223,779	17,042,840
19	2031	18,666,958	12,733,471	-3,399,992	47,901,077	9,933,140	-2,223,779	17,042,840
20	2032	9,333,479	12,733,471	-3,399,992	40,191,716	9,933,140	-2,223,779	17,042,840
21	2033	0	0	0	32,482,355	0	0	0
Total		**2,538,029,145**	**254,669,410**	**0**	**2,879,093,873**	**198,662,808**	**23,524,248**	**476,856,466**

Table A.2.2: Results at the component level for the AZEP 85

Component, k	$\dot{E}_{F,k}$ (MW)	$\dot{E}_{P,k}$ (MW)	$\dot{E}_{D,k}$ (MW)	ε_k (%)	$y_{D,k}$ (%)	$c_{F,k}$ (€/GJ)	$c_{P,k}$ (€/GJ)	$\dot{C}_{D,k}$ (€/h)	$\dot{Z}_k$ (€/h)	$\dot{C}_{D,k}+\dot{Z}_k$ (€/h)	f_k (%)	r_k (%)	$b_{F,k}$ (Pts/GJ)	$b_{P,k}$ (Pts/GJ)	$\dot{B}_{D,k}$ (Pts/h)	$\dot{Y}_k$ (Pts/h)	$\dot{B}_{D,k}+\dot{Y}_k$ (Pts/h)	$f_{b,k}$ (%)	$r_{b,k}$ (%)
C1	238.30	227.13	11.17	95.3	1.53	19.8	22.2	797	1,169	1,966	59.5	12.1	6.2	6.5	250.79	0.19	250.98	0.08	238.30
CC	620.26	466.61	153.65	75.2	21.03	9.3	12.7	5,120	746	5,866	12.7	37.7	3.5	5.0	1932.51	0.31	1932.82	0.02	620.26
MCM	82.65	77.03	5.62	93.2	0.77	13.6	18.9	275	1,192	1,468	81.2	38.9	5.1	8.9	103.16	53.34	156.50	34.08	82.65
MCM HTHX	120.72	119.49	1.24	99.0	0.17	13.6	15.4	61	696	757	92.0	12.9	5.1	5.2	22.79	32.67	55.46	58.90	120.72
MCM LTHX	221.06	211.51	9.55	95.7	1.31	13.6	15.7	467	1,113	1,580	70.4	15.3	5.1	5.4	175.99	67.57	243.56	27.74	221.06
DB	109.46	78.20	31.26	71.4	4.28	9.3	13.9	1,042	277	1,318	21.0	50.6	3.5	6.5	393.12	0.05	393.17	0.01	109.46
GT1	495.66	477.85	17.81	96.4	2.44	18.4	19.8	1,177	1,336	2,513	53.2	8.0	6.0	6.2	385.39	0.91	386.30	0.23	495.66
GT2	56.53	53.73	2.80	95.1	0.38	13.1	15.1	132	247	379	65.2	15.0	5.1	5.3	50.98	0.19	51.18	0.38	56.53
C6	7.31	7.07	0.24	96.8	0.03	36.4	61.5	31	607	638	95.1	68.9	10.0	10.4	8.54	0.60	9.14	6.53	7.31
AIR HX	6.91	5.15	1.76	74.5	0.24	13.1	18.0	83	8	91	8.8	37.5	5.1	6.8	32.09	0.00	32.09	0.01	6.91
NGPH	5.80	0.10	5.70	1.7	0.78	13.1	795.8	269	6	275	2.2	5974.4	5.1	301.0	103.97	0.00	103.97	0.00	5.80
HPSH	31.65	28.65	3.00	90.5	0.41	18.4	22.6	198	141	339	41.6	23.1	6.0	6.9	64.85	1.10	65.94	1.66	31.65
HPEV	39.82	36.29	3.54	91.1	0.48	18.4	22.2	234	160	393	40.6	21.2	6.0	6.8	76.51	0.11	76.62	0.15	39.82
HPEC	26.17	22.65	3.52	86.6	0.48	18.4	23.6	233	82	314	26.1	28.6	6.0	7.3	76.14	0.08	76.22	0.11	26.17
RH	17.52	15.70	1.82	89.6	0.25	18.4	22.8	120	70	190	36.7	24.0	6.0	7.0	39.39	0.49	39.88	1.22	17.52
IPSH	0.11	0.07	0.05	57.5	0.01	18.4	50.2	3	3	6	46.2	173.5	6.0	12.3	1.05	0.00	1.05	0.14	0.11
IPEV	5.16	4.85	0.31	94.0	0.04	18.4	24.1	20	70	90	77.4	31.3	6.0	6.6	6.68	0.04	6.72	0.64	5.16
IPEC	0.90	0.75	0.15	83.5	0.02	18.4	25.6	10	5	15	33.7	39.5	6.0	7.7	3.20	0.00	3.20	0.10	0.90
LPSH	1.06	0.77	0.29	72.5	0.04	18.4	34.2	19	15	34	43.9	86.3	6.0	9.2	6.29	0.01	6.30	0.16	1.06
LPEV	15.25	12.50	2.75	81.9	0.38	18.4	27.6	182	145	327	44.3	50.4	6.0	7.9	59.58	0.10	59.68	0.17	15.25
LPEC	11.20	7.83	3.37	69.9	0.46	18.4	33.8	223	102	325	31.5	83.9	6.0	9.7	72.88	0.11	72.99	0.15	11.20
SH II	6.74	6.03	0.71	89.5	0.10	13.1	16.6	33	20	53	37.2	26.8	5.1	6.0	12.90	0.11	13.01	0.88	6.74
EV II	7.95	7.14	0.81	89.8	0.11	13.1	16.5	38	22	61	37.0	25.8	5.1	5.9	14.77	0.01	14.78	0.08	7.95
EC II	4.98	4.46	0.52	89.5	0.07	13.1	16.7	25	17	41	40.6	27.8	5.1	5.9	9.52	0.01	9.54	0.14	4.98
HPST	34.12	31.81	2.30	93.3	0.31	22.6	26.4	187	183	369	49.4	17.2	7.0	7.7	57.80	0.29	58.10	0.51	34.12
IPST	24.90	23.45	1.45	94.2	0.20	22.8	27.2	119	202	321	62.8	19.2	7.0	7.6	36.61	0.24	36.85	0.65	24.90
LPST	49.32	42.62	6.70	86.4	0.92	24.4	32.8	587	489	1,077	45.4	34.6	7.3	8.8	175.98	0.37	176.35	0.21	49.32
ST4	27.92	21.14	6.78	75.7	0.93	22.8	36.4	557	257	814	31.5	59.6	7.0	10.0	170.64	0.22	170.86	0.13	27.92
COND P	0.04	0.04	0.01	78.9	0.00	21.6	84.4	1	7	8	90.4	291.6	6.6	9.0	0.22	0.00	0.22	0.16	0.04
HPP	1.21	1.04	0.17	86.0	0.02	21.6	37.7	13	42	55	76.0	74.8	6.6	8.1	4.01	0.00	4.01	0.01	1.21
IPP	0.03	0.02	0.01	64.3	0.00	21.6	156.5	1	7	8	90.8	626.2	6.6	11.6	0.22	0.00	0.22	0.02	0.03
LPP	0.00	0.00	0.00	65.7	0.00	21.6	466.7	0	2	2	97.4	2065.1	6.6	11.3	0.02	0.00	0.02	0.63	0.00
C2	3.38	2.81	0.57	83.3	0.08	36.4	169.1	74	348	422	82.4	364.3	10.0	39.8	20.41	0.12	20.53	0.58	3.38
C3	3.48	2.88	0.60	82.8	0.08	36.4	86.6	78	358	437	82.1	137.9	10.0	13.7	21.53	0.05	21.58	0.23	3.48
C4	3.47	2.85	0.62	82.2	0.08	36.4	91.2	81	357	438	81.5	150.5	10.0	14.3	22.30	0.02	22.33	0.11	3.47
C5	3.52	2.85	0.66	81.2	0.09	36.4	93.2	87	362	449	80.7	156.0	10.0	14.5	23.90	0.03	23.93	0.15	3.52
De-aerator	0.46	0.44	0.02	95.6	0.00	28.4	47.1	2	27	29	92.9	65.4	8.1	8.6	0.59	0.04	0.62	5.66	0.46

M1	1.43	1.28	0.15	89.5	0.02	22.8	26.5	12	0	12	0.0	16.4	7.0	8.1	3.78	0.00	3.78	0.00	1.43
M2	0.60	0.55	0.05	92.3	0.01	22.6	25.2	4	0	4	0.0	11.7	7.0	7.8	1.16	0.00	1.16	0.00	0.60
M3	1.70	1.69	0.01	99.1	0.00	18.4	18.6	1	0	1	0.0	1.3	6.0	6.1	0.31	0.00	0.31	0.00	1.70
M4	37.46	34.20	3.26	91.3	0.45	18.7	20.5	220	0	220	0.0	9.5	5.9	6.4	68.92	0.00	68.92	0.00	37.46
FG COND	15.09	-	13.52	-	1.85	13.2	-	642	90	732	12.3	-	5.1	-	248.14	0.09	248.23	0.04	15.09
COOL1	0.68	-	0.61	-	0.08	46.3	-	101	9	110	8.2	-	12.5	-	27.28	0.01	27.28	0.02	0.68
COOL2	0.81	-	0.73	-	0.10	53.8	-	141	9	150	6.0	-	12.7	-	33.17	0.01	33.17	0.02	0.81
COOL3	0.76	-	0.69	-	0.09	59.9	-	149	8	157	5.2	-	12.9	-	32.15	0.01	32.15	0.02	0.76
COOL4	0.79	-	0.71	-	0.10	64.7	-	165	11	176	6.0	-	13.2	-	33.61	0.01	33.62	0.02	0.79
COND	12.29	-	9.14	-	1.25	23.9	-	786	87	874	10.0	-	7.2	-	237.06	0.03	237.09	0.01	12.29
CT	4.92	-	3.05	-	-	-	-	-	93	-	-	-	-	-	-	15.42	-	-	4.92
Total	**730.56**	**389.89**	**313.43**	**53.4**	**42.90**	**9.2**	**25.1**	**10,326**	**11,198**	**21,524**	**52.0**	**174.3**	**3.5**	**6.9**	**3897.09**	**174.95**	**4072.05**	**4.30**	**100.2**
Exergy loss	**27.25**																		
$\dot{B}_k^{PF}$	**CC**	**641.18**	**DB**	**459.05**															

Table A.2.3: Results at the stream level for the AZEP 85

Stream, j	$\dot{m}_j$ (kg/s)	T_j (°C)	p_j (bar)	$\dot{E}_{PH,j}$ (MW)	$\dot{E}_{CH,j}$ (MW)	$\dot{E}_{tot,j}$ (MW)	c_j (€/GJ)	$\dot{C}_j$ (€/h)	b_j (Pts/GJ)	$\dot{B}_j$ (Pts/h)
1	603.6	15.00	1.01	0.00	0.94	0.94	0.0	0	0.00	0
2	603.6	392.82	16.99	227.13	0.94	228.07	22.1	18,168	6.51	5,349
3	14.0	15.00	50.00	8.15	721.47	729.62	9.2	24,037	3.45	9,072
4	558.2	1301.93	16.81	649.44	1.43	650.87	18.4	43,005	6.01	14,082
5	558.2	578.70	1.06	153.78	1.43	155.21	18.4	10,255	6.01	3,358
6	218.2	578.70	1.06	60.11	0.56	60.67	18.4	4,009	6.01	1,313
7	218.2	466.96	1.05	42.59	0.56	43.15	18.4	2,851	6.01	934
8	340.0	578.70	1.06	93.67	0.87	94.54	18.4	6,246	6.01	2,045
9	340.0	447.82	1.05	62.02	0.87	62.89	18.4	4,155	6.01	1,361
10	558.2	455.31	1.05	104.60	1.43	106.03	18.4	7,007	6.01	2,294
11	558.2	341.18	1.04	64.78	1.43	66.21	18.4	4,375	6.01	1,433
12	558.2	252.75	1.04	38.61	1.43	40.03	18.4	2,646	6.01	866
13	558.2	252.34	1.04	38.49	1.43	39.92	18.4	2,638	6.01	864
14	558.2	232.62	1.04	33.33	1.43	34.76	18.4	2,297	6.01	752
15	558.2	229.08	1.04	32.43	1.43	33.86	18.4	2,238	6.01	733
16	558.2	224.88	1.04	31.38	1.43	32.80	18.4	2,168	6.01	710
17	558.2	156.37	1.03	16.13	1.43	17.55	18.4	1,160	6.01	380
18	558.2	84.65	1.03	4.92	1.43	6.35	0.0	0	0.00	0
19	95.0	32.89	3.73	0.24	0.24	0.48	28.4	49	7.34	13
20	95.0	136.37	3.62	8.07	0.24	8.31	33.5	1,001	9.53	285
21	95.7	140.01	3.62	8.58	0.24	8.82	34.1	1,082	9.47	300
22	77.1	140.01	3.62	6.91	0.19	7.11	34.1	873	9.47	242
23	6.2	140.01	3.62	0.55	0.02	0.57	34.1	70	9.47	19
24	6.2	140.50	25.13	0.57	0.02	0.59	37.6	79	9.53	20
25	6.2	216.62	24.38	1.32	0.02	1.34	30.9	148	8.49	41
26	6.2	222.62	24.38	6.18	0.02	6.19	25.6	570	6.97	155
27	6.2	232.75	23.16	6.24	0.02	6.26	25.8	581	7.03	158
28	77.1	307.14	23.16	84.69	0.19	84.88	22.8	6,971	6.99	2,135
29	48.4	558.70	22.00	68.78	0.12	68.91	22.8	5,656	6.99	1,734
30	48.4	315.74	4.10	43.88	0.12	44.00	22.8	3,612	6.99	1,107
31	17.9	209.08	4.10	14.40	0.04	14.45	28.7	1,495	8.13	423
32	17.9	146.37	4.32	13.64	0.04	13.68	28.4	1,401	8.07	398
33	0.7	146.37	4.32	0.52	0.00	0.53	28.4	54	8.07	15
34	18.5	140.01	3.62	1.66	0.05	1.71	34.1	210	9.47	58
35	18.5	140.02	4.32	1.66	0.05	1.71	34.5	212	9.47	58
36	18.5	146.37	4.32	14.16	0.05	14.21	28.4	1,455	8.07	413
37	71.0	140.01	3.62	6.36	0.18	6.54	34.1	803	9.47	223
38	71.0	141.72	134.56	7.40	0.18	7.57	34.6	943	9.28	253
39	59.3	325.17	130.53	28.83	0.15	28.98	26.0	2,714	7.75	809
40	59.3	331.17	130.53	65.12	0.15	65.27	23.9	5,620	7.24	1,702
41	71.0	561.95	124.00	112.61	0.18	112.79	22.6	9,158	6.98	2,833
42	71.0	314.23	23.16	78.50	0.18	78.67	22.6	6,388	6.98	1,976
43	66.2	286.89	4.10	58.13	0.17	58.30	24.4	5,112	7.30	1,532
44	66.2	32.88	0.05	8.81	0.17	8.98	24.4	787	7.30	236
45	95.0	32.88	0.05	0.20	0.24	0.44	23.9	38	7.21	11
46	6680.5	15.00	1.01	0.00	10.40	10.40	0.0	0	0.00	0
47	180.4	15.00	1.01	0.00	0.45	0.45	0.0	0	0.00	0
48	95.4	16.00	1.01	0.00	0.24	0.24	0.0	0	0.00	0
49	6765.5	23.60	1.01	2.88	9.72	12.60	0.0	0	0.00	0
50	48.4	307.14	23.16	53.09	0.12	53.21	22.8	4,370	6.99	1,338
51	28.8	307.14	23.16	31.60	0.07	31.68	22.8	2,601	6.99	797
52	28.8	32.88	0.05	3.68	0.07	3.75	22.8	308	6.99	94
53	95.0	32.88	0.05	12.49	0.24	12.73	23.9	1,095	7.21	330
54	59.3	141.72	134.56	6.18	0.15	6.33	34.6	788	9.28	211
55	11.7	141.72	134.56	1.22	0.03	1.25	34.6	155	9.28	42
56	11.7	325.17	130.53	5.67	0.03	5.70	20.6	424	6.67	137
57	11.7	331.17	130.53	12.82	0.03	12.85	18.3	848	6.25	289
58	11.7	578.56	124.00	18.85	0.03	18.87	17.8	1,208	6.16	418
59	59.3	558.70	124.00	93.77	0.15	93.92	23.5	7,950	7.14	2,415
60	59.4	1275.57	16.48	104.08	10.48	114.56	13.1	5,403	5.06	2,089
61	59.4	1200.00	16.47	97.17	10.48	107.65	13.1	5,077	5.06	1,963
62	59.4	684.07	1.04	40.64	10.48	51.12	13.1	2,411	5.06	932
63	59.4	598.56	1.04	34.84	10.48	45.32	13.1	2,137	5.06	826
64	59.4	490.15	1.04	28.10	10.48	38.58	13.1	1,820	5.06	703
65	59.4	341.18	1.03	20.15	10.48	30.63	13.1	1,445	5.06	558
66	59.4	222.27	1.02	15.17	10.48	25.65	13.1	1,210	5.06	468
67	33.6	30.00	1.01	0.04	10.42	10.45	13.1	493	5.06	191
68	25.7	30.00	1.01	0.04	0.06	0.10	0.0	0	0.00	0

69	33.6	138.23	3.22	2.85	10.42	13.26	46.2	2,204	12.43	594
70	33.4	40.00	3.21	2.16	10.41	12.58	46.2	2,091	12.43	563
71	0.3	40.00	3.21	0.00	0.00	0.00	0.0	0	0.00	0
72	33.4	152.09	10.22	5.05	10.41	15.46	53.7	2,990	12.66	705
73	33.2	40.00	10.21	4.23	10.42	14.65	53.7	2,833	12.66	668
74	0.2	40.00	10.21	0.00	0.00	0.00	0.0	0	0.00	0
75	33.2	153.10	32.46	7.08	10.42	17.50	59.8	3,768	12.93	815
76	33.1	40.00	32.45	6.31	10.43	16.74	59.8	3,603	12.93	779
77	0.1	40.00	32.45	0.00	0.00	0.00	0.0	0	0.00	0
78	33.1	155.13	103.09	9.16	10.43	19.59	64.7	4,561	13.17	929
79	33.1	30.00	103.09	8.36	10.44	18.80	0.0	0	0.00	0
80	0.0	30.00	103.09	0.00	0.00	0.00	0.0	0	0.00	0
81	60.4	522.50	16.98	27.86	0.09	27.96	21.4	2,151	6.57	661
82	60.4	392.82	16.99	22.71	0.09	22.81	22.1	1,817	6.51	535
83	543.2	392.82	16.99	204.41	0.85	205.26	22.1	16,351	6.51	4,814
84	543.2	900.00	16.96	415.92	0.85	416.77	18.9	28,284	5.97	8,955
85	495.7	1000.00	17.00	427.27	1.21	428.48	19.7	30,325	6.05	9,328
86	354.5	1060.23	17.09	507.81	62.58	570.39	13.6	27,918	5.12	10,512
87	402.0	964.22	17.02	492.04	61.01	553.05	13.6	27,069	5.12	10,192
88	495.7	1250.00	16.98	546.76	1.21	547.97	18.7	36,930	5.87	11,586
89	402.0	487.78	16.99	270.99	61.01	331.99	13.6	16,249	5.12	6,118
90	413.9	1275.57	16.48	725.55	73.06	798.60	13.1	37,664	5.06	14,561
91	354.5	1275.57	16.48	621.47	62.58	684.04	13.1	32,261	5.06	12,472
92	354.5	1286.22	17.10	628.54	62.58	691.11	13.6	33,826	5.12	12,736
93	11.9	250.00	16.99	7.01	613.25	620.26	9.3	20,669	3.49	7,801
94	14.0	250.00	16.98	8.25	721.47	729.72	9.3	24,317	3.49	9,178
95	2.1	250.00	16.98	1.24	108.22	109.46	9.3	3,647	3.49	1,377
96	556.1	1174.45	16.98	571.44	1.23	572.67	19.0	39,081	5.94	12,246
97	7314.8	16.00	1.37	0.32	18.27	18.59	-	-	-	-
98	7314.8	22.88	1.33	3.47	18.27	21.74	-	-	-	-
99	9543.6	23.60	1.33	5.34	23.84	29.18	-	-	-	-
100	2228.9	26.00	1.33	1.98	5.57	7.55	-	-	-	-
101	2137.4	26.00	1.33	1.90	5.34	7.24	-	-	-	-
102	2051.4	26.00	1.33	1.82	5.12	6.95	-	-	-	-
103	1956.4	26.00	1.33	1.74	4.89	6.62	-	-	-	-
104	1867.6	26.00	1.33	1.66	4.67	6.32	-	-	-	-
105	1867.6	16.00	1.37	0.08	4.67	4.75	-	-	-	-
106	9182.4	16.00	1.37	0.40	22.94	23.33	-	-	-	-
107	9271.1	16.00	1.37	0.40	23.16	23.56	-	-	-	-
108	9366.2	16.00	1.37	0.41	23.40	23.80	-	-	-	-
109	9452.1	16.00	1.37	0.41	23.61	24.02	-	-	-	-
110	9543.6	16.00	1.01	0.07	23.84	23.91	-	-	-	-
111	9543.6	16.00	1.37	0.41	23.84	24.25	-	-	-	-
112	88.8	16.00	1.37	0.00	0.22	0.23	-	-	-	-
113	88.8	26.00	1.33	0.08	0.22	0.30	-	-	-	-
114	95.1	16.00	1.37	0.00	0.24	0.24	-	-	-	-
115	95.1	26.00	1.33	0.08	0.24	0.32	-	-	-	-
116	85.9	16.00	1.37	0.00	0.21	0.22	-	-	-	-
117	85.9	26.00	1.33	0.08	0.21	0.29	-	-	-	-
118	91.5	16.00	1.37	0.00	0.23	0.23	-	-	-	-
119	91.5	26.00	1.33	0.08	0.23	0.31	-	-	-	-
120	14.0	15.00	17.00	5.90	721.47	727.37	-	-	-	-
121	28.8	45.81	0.10	6.02	0.07	6.09	-	-	-	-
122	-	-	-	-	*C1*	238.30	19.8	16,999	6.23	5,349
123	-	-	-	-	*ST1*	31.81	26.4	3,027	7.66	878
124	-	-	-	-	*ST2*	23.45	27.2	2,293	7.58	640
125	-	-	-	-	*ST3*	42.62	32.8	5,032	8.83	1,356
126	-	-	-	-	*COND P*	0.04	21.6	3	6.59	1
127	-	-	-	-	*LPP*	0.00	21.6	0	6.59	0
128	-	-	-	-	*HPP*	1.21	21.6	94	6.59	29
129	-	-	-	-	*IPP*	0.03	21.6	2	6.59	1
130	-	-	-	-	*GT1*	239.55	19.8	17,088	6.23	5,377
131	-	-	-	-	*GT2*	53.73	15.1	2,913	5.33	1,031
132	-	-	-	-	*C6*	7.31	36.4	958	10.02	264
133	-	-	-	-	*C2*	3.38	36.4	443	10.02	122
134	-	-	-	-	*C3*	3.48	36.4	456	10.02	126
135	-	-	-	-	*C4*	3.47	36.4	454	10.02	125
136	-	-	-	-	*C5*	3.52	36.4	461	10.02	127
137	-	-	-	-	*ST4*	21.14	36.4	2,771	10.02	763
138					*tot*	389.89	21.6	30.2	6.59	9,250

Table A.2.4: Splitting the exergy destruction in the AZEP 85 (MW)

Component, k	$E_{D,k}^{real}$	$E_{D,k}^{EN}$	$E_{D,k}^{EX}$	$E_{D,k}^{AV}$	$E_{D,k}^{UN}$	$E_{D,k}^{UN,EN}$	$E_{D,k}^{UN,EX}$	$E_{D,k}^{AV,EN}$	$E_{D,k}^{AV,EX}$
C1	11.17	7.39	3.78	5.02	6.15	4.06	2.09	3.33	1.69
CC	153.65	120.57	33.09	13.56	140.10	109.81	30.29	10.76	2.80
MCM	5.62	3.41	2.21	1.40	4.23	1.45	2.78	1.96	**-0.57**
MCM HTHX	1.24	0.77	0.47	0.40	0.84	0.52	0.32	0.25	0.15
MCM LTHX	9.55	4.58	4.97	4.90	4.65	3.54	1.11	1.05	3.86
DB	31.26	20.16	11.10	16.74	14.52	9.43	5.08	10.73	6.01
GT1	14.16	10.64	3.53	7.11	7.06	5.12	1.94	5.52	1.59
GT2	1.98	2.73	**-0.75**	1.31	0.66	0.92	**-0.25**	1.81	**-0.50**
C6	0.24	0.00	0.24	0.16	0.08	0.00	0.08	0.00	0.16
AIR HX	1.76	2.21	**-0.45**	1.42	0.34	0.48	**-0.14**	1.73	**-0.31**
NGPH	5.70	3.72	1.98	5.66	0.05	0.01	0.04	3.71	1.95
HPSH	3.00	1.01	1.98	0.84	2.16	0.91	1.25	0.10	0.74
HPEV	3.54	1.51	2.02	0.52	3.01	1.51	1.50	0.01	0.52
HPEC	3.52	1.72	1.79	1.04	2.48	1.33	1.15	0.39	0.65
RH	1.82	1.19	0.63	0.64	1.18	0.84	0.34	0.36	0.29
IPSH	0.05	0.07	**-0.02**	0.05	0.00	0.01	**-0.01**	0.07	**-0.02**
IPEV	0.31	0.38	**-0.07**	0.11	0.20	0.20	**-0.01**	0.17	**-0.06**
IPEC	0.15	0.13	0.02	0.05	0.09	0.13	**-0.03**	0.00	0.05
LPSH	0.29	0.15	0.14	0.18	0.11	0.05	0.06	0.10	0.08
LPEV	2.75	1.29	1.46	0.45	2.30	1.22	1.08	0.07	0.38
LPEC	3.37	2.06	1.31	2.40	0.96	0.56	0.41	1.51	0.90
SH II	0.71	0.89	**-0.18**	0.15	0.55	0.78	**-0.23**	0.11	0.05
EV II	0.81	1.13	**-0.32**	0.07	0.74	1.01	**-0.27**	0.12	**-0.05**
EC II	0.52	0.45	0.07	0.20	0.33	0.46	**-0.14**	**-0.01**	0.21
HPST	1.82	1.27	0.54	0.96	0.85	0.58	0.27	0.69	0.27
IPST	1.10	0.91	0.19	0.47	0.62	0.50	0.13	0.41	0.06
LPST	6.05	4.65	1.40	2.51	3.54	2.72	0.82	1.93	0.58
ST4	6.78	4.53	2.25	5.78	1.01	0.67	0.34	3.87	1.91
COND P	0.00	0.00	0.00	0.00	0.00	0.00	0.00	0.00	0.00
HPP	0.11	0.07	0.04	0.07	0.04	0.02	0.01	0.04	0.03
IPP	0.01	0.01	0.00	0.00	0.00	0.00	0.00	0.01	0.00
LPP	0.00	0.00	0.00	0.00	0.00	0.00	0.00	0.00	0.00
C2	0.57	0.75	**-0.18**	0.44	0.13	0.17	**-0.04**	0.58	**-0.15**
C3	0.60	0.81	**-0.22**	0.47	0.13	0.17	**-0.04**	0.64	**-0.17**
C4	0.62	0.85	**-0.23**	0.49	0.13	0.17	**-0.04**	0.68	**-0.18**
C5	0.66	0.91	**-0.25**	0.53	0.13	0.17	**-0.04**	0.74	**-0.20**
FG COND	13.52	18.21	**-4.69**	-	-	-	-	-	-
COOL1	0.61	0.47	0.14	-	-	-	-	-	-
COOL2	0.73	0.61	0.11	-	-	-	-	-	-
COOL3	0.69	0.57	0.12	-	-	-	-	-	-
COOL4	0.71	0.56	0.15	-	-	-	-	-	-
COND	9.14	6.40	5.89	-	-	-	-	-	-
CT	3.05	2.82	0.23	-	-	-	-	-	-
MOT1	0.01	0.00	0.00	0.00	0.00	0.00	0.00	0.00	0.00
MOT2	0.00	0.00	0.00	0.00	0.00	0.00	0.00	0.00	0.00
MOT3	0.06	0.03	0.03	0.05	0.01	0.00	0.00	0.03	0.03
MOT4	0.00	0.00	0.00	0.00	0.00	0.00	0.00	0.00	0.00
GEN1	3.65	3.39	0.26	**-1.24**	4.89	4.54	0.35	**-1.15**	**-0.09**
GEN2	1.49	1.24	0.25	**-0.51**	2.00	1.66	0.34	**-0.42**	**-0.09**
GEN3	0.82	1.22	**-0.40**	-0.28	1.10	1.64	**-0.54**	**-0.42**	0.14
Total	**309.94**	**238.45**	**74.63**						
Total (%)		**76.94**	**24.08**						

Table A.2.5: Splitting the investment cost rate in the AZEP 85 (€/h)

						$\dot{Z}_k^{AV}$		$\dot{Z}_k^{UN}$	
Component, k	$\dot{Z}_k^{real}$	$\dot{Z}_k^{UN}$	$\dot{Z}_k^{AV}$	$\dot{Z}_k^{EN}$	$\dot{Z}_k^{EX}$	$\dot{Z}_k^{AV,EN}$	$\dot{Z}_k^{AV,EX}$	$\dot{Z}_k^{UNEN}$	$\dot{Z}_k^{UN,EX}$
C1	1169.3	993.9	175.4	771.7	397.7	115.7	59.7	655.9	338.0
CC	745.9	596.7	149.2	584.6	161.3	116.9	32.3	467.7	129.0
MCM	1192.3	953.9	238.5	407.9	784.4	81.6	156.9	326.3	627.6
MCM HTHX	696.3	108.9	548.8	434.4	261.9	309.8	239.0	124.7	**-15.8**
MCM LTHX	1113.0	320.2	764.5	847.1	265.8	558.5	206.0	288.7	31.6
DB	276.8	221.5	55.4	179.9	96.9	36.0	19.4	143.9	77.5
GT1	1336.4	1202.8	133.6	970.0	366.4	97.0	36.6	873.0	329.8
GT2	247.3	222.5	24.7	341.1	**-93.9**	34.1	**-9.4**	307.0	**-84.5**
AIR HX	8.0	1.8	6.2	11.3	**-3.3**	8.7	**-2.5**	2.5	**-0.7**
NGPH	6.0	2.8	3.2	1.4	4.7	0.7	2.5	0.6	2.2
HPSH	141.3	58.6	82.6	59.7	81.6	34.9	47.7	24.8	33.9
HPEV	159.5	84.9	74.6	79.9	79.7	37.4	37.3	42.5	42.4
HPEC	81.9	39.3	42.6	44.0	37.9	22.9	19.7	21.1	18.2
RH	69.8	31.5	38.3	49.6	20.2	27.2	11.1	22.4	9.1
IPSH	2.7	0.7	2.0	8.0	**-5.3**	5.8	**-3.8**	2.2	**-1.4**
IPEV	69.9	25.6	44.3	72.5	**-2.6**	45.9	**-1.6**	26.6	**-0.9**
IPEC	5.0	2.3	2.7	6.8	**-1.8**	3.7	**-1.0**	3.1	**-0.8**
LPSH	15.1	5.6	9.4	6.3	8.8	3.9	5.5	2.3	3.3
LPEV	145.0	70.1	74.8	77.0	68.0	39.7	35.1	37.2	32.9
LPEC	102.5	44.1	58.4	59.0	43.5	33.6	24.8	25.4	18.7
SH II	19.7	8.8	11.0	27.9	**-8.1**	15.5	**-4.5**	12.4	**-3.6**
EV II	22.4	14.3	8.1	30.7	**-8.3**	11.1	**-3.0**	19.6	**-5.3**
EC II	16.8	7.3	9.6	23.8	**-7.0**	13.5	**-4.0**	10.3	**-3.0**
HPST	182.6	164.3	18.3	124.4	58.2	12.4	5.8	112.0	52.3
IPST	201.8	181.7	20.2	161.0	40.8	16.1	4.1	144.9	36.7
LPST	489.2	440.3	48.9	376.1	113.2	37.6	11.3	338.5	101.8
ST4	256.7	231.1	25.7	170.0	86.8	17.0	8.7	153.0	78.1
COND P	6.9	5.9	6.9	5.5	1.5	0.8	6.1	4.7	1.2
HPP	41.6	35.4	41.6	25.6	16.0	3.8	37.8	21.8	13.6
IPP	7.1	6.0	7.1	8.4	**-1.3**	1.3	**5.8**	7.1	**-1.1**
LPP	2.4	2.0	2.4	0.0	2.4	0.0	2.4	0.0	2.0
C2	347.9	295.7	52.2	448.8	**-100.9**	67.3	**-15.1**	381.5	**-85.8**
C3	358.4	304.6	53.8	479.9	**-121.5**	72.0	**-18.2**	407.9	**-103.3**
C4	356.9	303.3	53.5	480.3	**-123.5**	72.0	**-18.5**	408.3	**-104.9**
C5	362.1	307.8	54.3	488.2	**-126.1**	73.2	**-18.9**	415.0	**-107.2**
FG COND	90.4								
COOL1	9.1								
COOL2	9.0								
COOL3	8.2								
COOL4	10.6								
COND	6.0								

Table A.2.6: Splitting the cost rate of exergy destruction in the AZEP 85 (€/h)

	$\dot{C}_{D,k}^{real}$	$\dot{C}_{D,k}^{UN}$	$\dot{C}_{D,k}^{AV}$	$\dot{C}_{D,k}^{EN}$	$\dot{C}_{D,k}^{EX}$	$\dot{C}_{D,k}^{AV}$		$\dot{C}_{D,k}^{UN}$	
Component, k						$\dot{C}_{D,k}^{AV,EN}$	$\dot{C}_{D,k}^{AV,EX}$	$\dot{C}_{D,k}^{UN,EN}$	$\dot{C}_{D,k}^{UN,EX}$
C1	797.1	438.8	358.3	527.2	269.8	237.7	120.6	289.6	149.2
CC	5120.2	4668.5	451.8	4017.7	1102.5	358.5	93.3	3659.2	1009.3
MCM	275.3	206.8	68.5	166.9	108.4	96.2	**-27.7**	70.8	136.1
MCM HTHX	60.5	41.0	19.5	37.6	22.9	12.0	7.5	25.6	15.4
MCM LTHX	467.4	227.5	239.9	224.4	243.0	51.2	188.7	173.2	54.3
DB	1041.6	483.8	557.8	671.8	369.8	357.4	200.4	314.4	169.4
GT1	1176.9	466.3	710.6	702.9	474.0	364.5	346.2	338.4	127.9
GT2	131.9	31.3	100.6	128.7	3.2	85.5	15.1	43.2	**-11.9**
AIR HX	83.0	15.9	67.1	104.2	**-21.2**	81.7	**-14.6**	22.4	**-6.5**
NGPH	268.9	2.2	266.8	175.5	93.4	175.0	91.8	0.5	1.7
HPSH	198.0	142.6	55.4	67.0	131.0	6.8	48.6	60.2	82.4
HPEV	233.6	199.0	34.7	100.0	133.6	0.4	34.3	99.6	99.4
HPEC	232.5	163.9	68.6	113.9	118.6	25.8	42.8	88.1	75.8
RH	120.3	77.7	42.6	78.8	41.5	23.6	19.0	55.2	22.5
IPSH	3.2	0.2	3.0	4.8	**-1.6**	4.3	**-1.3**	0.5	-0.3
IPEV	20.4	13.0	7.4	25.0	-4.6	11.5	-4.1	13.4	-0.5
IPEC	9.8	6.2	3.6	8.5	1.3	0.1	3.5	8.4	**-2.3**
LPSH	19.2	7.3	11.9	9.9	9.3	6.8	5.1	3.1	4.3
LPEV	182.0	152.3	29.7	85.4	96.5	4.6	25.1	80.8	71.4
LPEC	222.6	63.8	158.8	136.2	86.4	99.5	59.3	36.7	27.0
SH II	33.4	26.1	7.3	41.8	**-8.5**	5.0	2.3	36.8	**-10.7**
EV II	38.2	34.8	3.4	53.4	**-15.2**	5.7	-2.3	47.7	**-12.9**
EC II	24.6	15.4	9.3	21.2	3.4	-0.6	9.8	**21.8**	**-6.4**
HPST	186.9	69.2	117.7	103.4	83.4	56.3	61.4	47.2	22.0
IPST	119.4	51.3	68.2	74.9	44.5	34.0	34.1	40.9	10.4
LPST	587.4	310.7	276.7	407.8	179.6	168.9	107.7	238.8	71.9
ST4	557.2	82.5	474.6	372.1	185.1	317.4	157.2	54.7	27.9
COND P	0.7	0.1	0.6	0.2	0.5	0.1	0.5	0.1	0.0
HPP	13.1	2.9	10.2	5.1	8.0	3.4	6.9	1.8	1.1
IPP	0.7	0.0	0.7	0.5	0.2	0.5	0.2	0.1	**0.0**
LPP	0.1	0.0	0.1	0.0	0.1	0.0	0.1	0.0	0.0
C2	74.2	17.0	57.2	98.1	**-24.0**	76.2	**-19.0**	21.9	**-4.9**
C3	78.2	16.8	61.4	106.6	**-28.4**	84.2	**-22.7**	22.5	**-5.7**
C4	81.0	16.7	64.4	110.9	**-29.9**	88.5	**-24.1**	22.4	**-5.8**
C5	86.8	16.7	70.1	119.0	**-32.2**	96.5	**-26.4**	22.5	**-5.8**
FG COND	716.8			864.6	**-147.8**				
COOL1	113.8			78.3	35.4				
COOL2	156.3			118.7	37.6				
COOL3	164.3			123.1	41.2				
COOL4	183.1			130.1	53.0				
COND	1057.6			550.4	507.1				

Table A.2.7: Splitting the environmental impact of exergy destruction in the AZEP 85 (Pts/h)

	$\dot{B}_{D,k}^{real}$	$\dot{B}_{D,k}^{UN}$	$\dot{B}_{D,k}^{AV}$	$\dot{B}_{D,k}^{EN}$	$\dot{B}_{D,k}^{EX}$	$\dot{B}_{D,k}^{AV}$		$\dot{B}_{D,k}^{UN}$	
Component, k						$\dot{B}_{D,k}^{AV,EN}$	$\dot{B}_{D,k}^{AV,EX}$	$\dot{B}_{D,k}^{UN,EN}$	$\dot{B}_{D,k}^{UN,EX}$
C1	69.7	38.3	31.3	46.1	23.6	20.8	10.5	25.3	13.0
CC	536.8	489.4	47.4	421.2	115.6	37.6	9.8	383.6	105.8
MCM	28.7	21.5	7.1	17.4	11.3	10.0	**-2.9**	7.4	14.2
MCM HTHX	6.3	4.3	2.0	3.9	2.4	1.3	0.8	2.7	1.6
MCM LTHX	48.9	23.8	25.1	23.5	25.4	5.4	19.7	18.1	5.7
DB	109.2	50.7	58.5	70.4	38.8	37.5	21.0	33.0	17.8
GT1	107.1	42.4	64.6	63.9	43.1	33.2	31.5	30.8	11.6
GT2	14.2	3.4	10.8	13.8	0.3	9.2	1.6	4.6	**-1.3**
AIR HX	8.9	1.7	7.2	11.2	**-2.3**	8.8	**-1.6**	2.4	**-0.7**
NGPH	28.9	0.2	28.6	18.8	10.0	18.8	9.9	0.1	0.2
HPSH	18.0	13.0	5.0	6.1	11.9	0.6	4.4	5.5	7.5
HPEV	21.3	18.1	3.2	9.1	12.2	0.0	3.1	9.1	9.0
HPEC	21.1	14.9	6.2	10.4	10.8	2.3	3.9	8.0	6.9
RH	10.9	7.1	3.9	7.2	3.8	2.1	1.7	5.0	2.0
IPSH	0.3	0.0	0.3	0.4	**-0.1**	0.4	**-0.1**	0.0	0.0
IPEV	1.9	1.2	0.7	2.3	**-0.4**	1.1	**-0.4**	1.2	0.0
IPEC	0.9	0.6	0.3	0.8	0.1	0.0	0.3	0.8	**-0.2**
LPSH	1.7	0.7	1.1	0.9	0.8	0.6	0.5	0.3	0.4
LPEV	16.6	13.9	2.7	7.8	8.8	0.4	2.3	7.4	6.5
LPEC	20.2	5.8	14.4	12.4	7.9	9.0	5.4	3.3	2.5
SH II	3.6	2.8	0.8	4.5	**-0.9**	0.5	0.2	4.0	**-1.2**
EV II	4.1	3.7	0.4	5.7	**-1.6**	0.6	**-0.2**	5.1	**-1.4**
EC II	2.6	1.7	1.0	2.3	0.4	**-0.1**	1.1	2.3	-0.7
HPST	16.1	5.9	10.1	8.9	7.2	4.8	5.3	4.1	1.9
IPST	10.2	4.4	5.8	6.4	3.8	2.9	2.9	3.5	0.9
LPST	48.9	25.9	23.0	33.9	14.9	14.1	9.0	19.9	6.0
ST4	47.4	7.0	40.4	31.7	15.7	27.0	13.4	4.6	2.4
COND P	0.1	0.0	0.1	0.0	0.0	0.0	0.0	0.0	0.0
HPP	1.1	0.2	0.9	0.4	0.7	0.3	0.6	0.2	0.1
IPP	0.1	0.0	0.1	0.0	0.0	0.0	0.0	0.0	0.0
LPP	0.0	0.0	0.0	0.0	0.0	0.0	0.0	0.0	0.0
C2	5.7	1.3	4.4	7.5	**-1.8**	5.8	**-1.5**	1.7	**-0.4**
C3	6.0	1.3	4.7	8.2	**-2.2**	6.4	**-1.7**	1.7	**-0.4**
C4	6.2	1.3	4.9	8.5	**-2.3**	6.8	**-1.8**	1.7	**-0.4**
C5	6.6	1.3	5.4	9.1	**-2.5**	7.4	**-2.0**	1.7	**-0.4**
FG COND	77.0			92.8	**-15.9**				
COOL1	8.5			5.9	2.7				
COOL2	10.2			7.8	2.5				
COOL3	9.9			7.4	2.5				
COOL4	10.4			7.4	3.0				
COND	88.6			39.4	49.2				

A.3: The AZEP 100

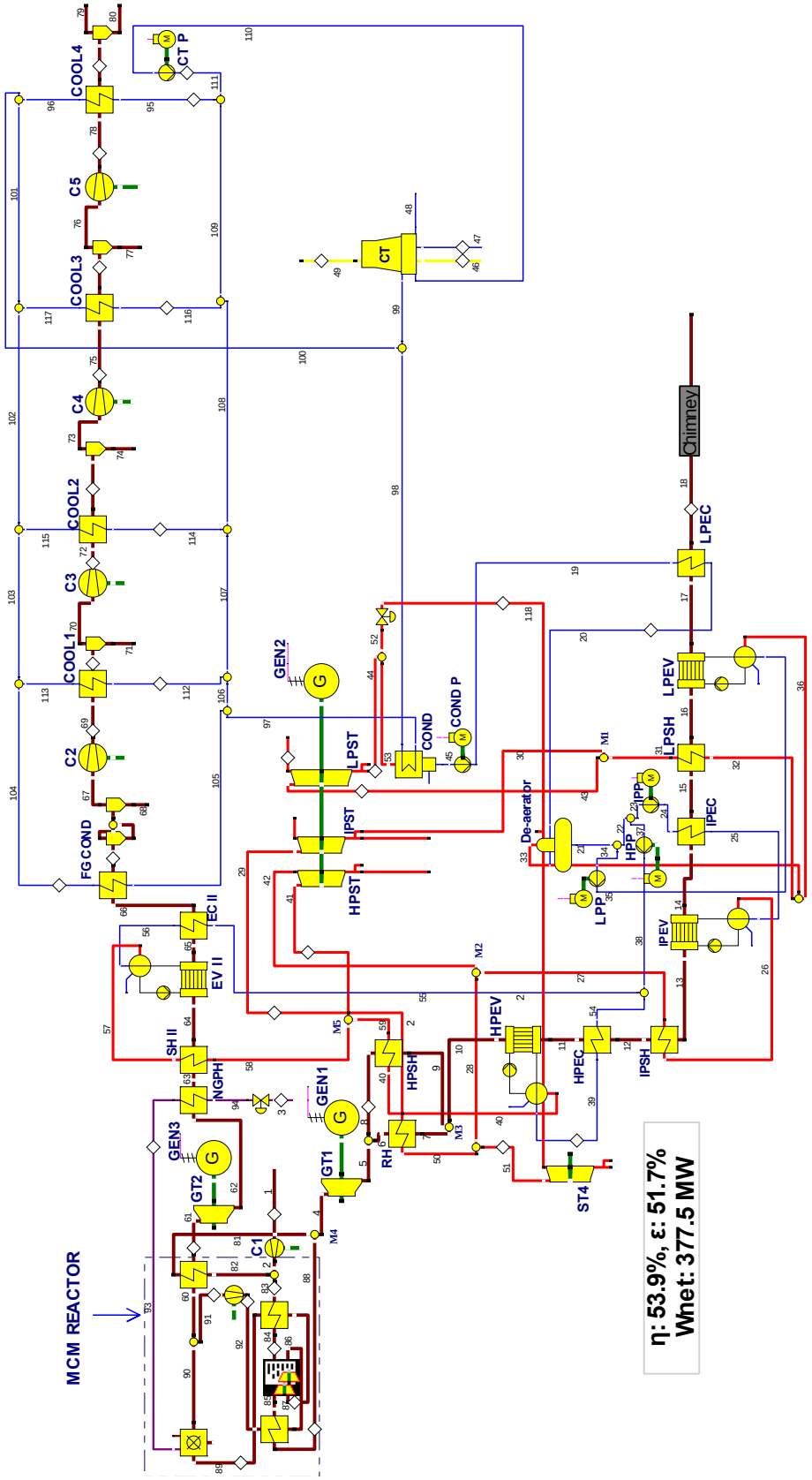

Figure A.3.1: Structure of the AZEP 100 (for the MCM reactor see Figure A.4.1)

Table A.3.1: Results of the economic analysis for the AZEP 100

AZEP 100								
Year	**Calendar year**	**Debt beg. of year**	**Book depreciation**	**Adjustment**	**Common Equity beg. of year**	**Book depreciation**	**Adjustment**	**TCR**
1	2013	266,444,264	13,322,213	891,981	266,444,264	10,463,934	2,126,142	26,804,270
2	2014	252,230,071	13,322,213	891,981	253,854,188	10,463,934	2,126,142	26,804,270
3	2015	238,015,877	13,322,213	891,981	241,264,112	10,463,934	2,126,142	26,804,270
4	2016	223,801,683	13,322,213	891,981	228,674,036	10,463,934	2,126,142	26,804,270
5	2017	209,587,489	13,322,213	891,981	216,083,960	10,463,934	2,126,142	26,804,270
6	2018	195,373,296	13,322,213	891,981	203,493,884	10,463,934	2,126,142	26,804,270
7	2019	181,159,102	13,322,213	891,981	190,903,808	10,463,934	2,126,142	26,804,270
8	2020	166,944,908	13,322,213	891,981	178,313,732	10,463,934	2,126,142	26,804,270
9	2021	152,730,714	13,322,213	891,981	165,723,656	10,463,934	2,126,142	26,804,270
10	2022	138,516,521	13,322,213	891,981	153,133,580	10,463,934	2,126,142	26,804,270
11	2023	124,302,327	13,322,213	891,981	140,543,504	10,463,934	2,126,142	26,804,270
12	2024	110,088,133	13,322,213	891,981	127,953,428	10,463,934	2,126,142	26,804,270
13	2025	95,873,939	13,322,213	891,981	115,363,352	10,463,934	2,126,142	26,804,270
14	2026	81,659,746	13,322,213	891,981	102,773,276	10,463,934	2,126,142	26,804,270
15	2027	67,445,552	13,322,213	891,981	90,183,200	10,463,934	2,126,142	26,804,270
16	2028	53,231,358	13,322,213	891,981	77,593,125	10,463,934	2,126,142	26,804,270
17	2029	39,017,164	13,322,213	-3,567,922	65,003,049	10,463,934	-2,333,761	17,884,464
18	2030	29,262,873	13,322,213	-3,567,922	56,872,875	10,463,934	-2,333,761	17,884,464
19	2031	19,508,582	13,322,213	-3,567,922	48,742,702	10,463,934	-2,333,761	17,884,464
20	2032	9,754,291	13,322,213	-3,567,922	40,612,528	10,463,934	-2,333,761	17,884,464
21	2033	0	0	0	32,482,355	0	0	0
Total		**2,654,947,891**	**266,444,264**	**0**	**2,996,012,620**	**209,278,684**	**24,683,225**	**500,406,174**

Table A.3.2: Results at the component level for the AZEP 100

Component, k	$\dot{E}_{F,k}$ (MW)	$\dot{E}_{P,k}$ (MW)	$\dot{E}_{D,k}$ (MW)	ε_k (%)	$y_{D,k}$ (%)	$c_{F,k}$ (€/GJ)	$c_{P,k}$ (€/GJ)	$\dot{C}_{D,k}$ (€/h)	$\dot{Z}_k$ (€/h)	$\dot{C}_{D,k}+\dot{Z}_k$ (€/h)	f_k (%)	r_k (%)	$b_{F,k}$ (Pts/GJ)	$b_{P,k}$ (Pts/GJ)	$\dot{B}_{D,k}$ (Pts/h)	$\dot{Y}_k$ (Pts/h)	$\dot{B}_{D,k}+\dot{Y}_k$ (Pts/h)	$f_{b,k}$ (%)	$r_{b,k}$ (%)
C1	280.47	267.32	13.15	95.3	1.80	20.6	22.8	975	1,133	2,108	53.8	10.6	6.1	6.4	288.47	0.18	288.65	0.06	4.9
CC	729.72	549.07	180.65	75.2	24.72	9.3	12.7	6,020	831	6,851	12.1	37.4	3.5	5.0	2272.15	0.30	2272.44	0.01	43.8
MCM	97.30	90.54	6.75	93.1	0.92	13.6	19.1	330	1,459	1,789	81.6	40.4	5.1	8.4	123.85	35.87	159.72	22.46	65.9
MCM HTHX	142.04	140.61	1.43	99.0	0.20	13.6	15.3	70	791	861	91.9	12.5	5.1	5.2	26.38	38.37	64.75	59.25	2.5
MCM LTHX	260.08	248.86	11.22	95.7	1.54	13.6	15.6	548	1,270	1,818	69.8	15.0	5.1	5.4	206.67	79.33	286.01	27.74	6.2
GT1	532.11	512.51	19.60	96.3	2.68	19.2	20.6	1,352	1,295	2,647	48.9	7.5	5.9	6.1	414.12	0.87	415.00	0.21	3.8
GT2	66.39	63.11	3.28	95.1	0.45	13.1	15.2	154	327	482	67.9	16.2	5.1	5.3	59.82	0.21	60.02	0.34	5.2
C6	8.59	8.31	0.28	96.8	0.04	37.7	61.5	38	675	713	94.7	63.1	9.9	10.2	9.85	0.60	10.44	5.71	3.5
AIR HX	8.20	6.12	2.09	74.6	0.29	13.1	18.0	98	9	107	8.6	37.3	5.1	6.8	38.02	0.00	38.02	0.01	34.1
NGPH	5.82	0.10	5.72	1.7	0.78	13.1	791.7	269	6	275	2.2	5955.1	5.1	300.1	104.32	0.00	104.32	0.00	5826.8
HPSH	18.82	17.15	1.68	91.1	0.23	19.2	23.8	116	113	229	49.5	24.2	5.9	6.7	35.40	0.85	36.25	2.35	14.1
HPEV	32.96	30.50	2.46	92.5	0.34	19.2	23.0	170	164	334	49.2	19.9	5.9	6.5	51.95	0.12	52.06	0.22	11.5
HPEC	22.53	19.04	3.49	84.5	0.48	19.2	25.3	241	62	303	20.5	32.2	5.9	7.4	73.79	0.06	73.85	0.08	26.1
RH	13.12	11.38	1.73	86.8	0.24	19.2	24.9	119	57	176	32.2	30.1	5.9	7.1	36.60	0.39	36.98	1.04	21.8
IPSH	0.80	0.63	0.17	79.0	0.02	19.2	31.6	12	11	23	48.7	65.0	5.9	8.1	3.54	0.01	3.55	0.20	37.8
IPEV	13.29	12.15	1.14	91.4	0.16	19.2	24.5	79	114	193	59.1	27.7	5.9	6.7	24.14	0.08	24.21	0.31	13.4
IPEC	2.24	1.88	0.37	83.6	0.05	19.2	26.5	25	11	37	30.9	38.1	5.9	7.5	7.76	0.01	7.77	0.11	27.9
LPSH	1.08	0.78	0.31	71.8	0.04	19.2	36.2	21	16	37	43.0	88.7	5.9	9.2	6.47	0.01	6.48	0.17	56.0
LPEV	16.73	13.76	2.97	82.2	0.41	19.2	28.6	205	162	367	44.1	49.5	5.9	7.7	62.81	0.11	62.93	0.18	30.8
LPEC	12.06	8.19	3.87	67.9	0.53	19.2	36.1	267	99	367	27.1	88.5	5.9	9.8	81.87	0.10	81.98	0.13	67.4
SH II	8.61	7.70	0.91	89.4	0.12	13.1	16.6	43	24	67	35.5	27.0	5.1	6.0	16.60	0.14	16.74	0.84	17.7
EV II	9.74	8.73	1.02	89.6	0.14	13.1	16.5	48	26	74	35.2	26.5	5.1	5.9	18.53	0.01	18.54	0.07	17.4
EC II	6.06	5.45	0.61	90.0	0.08	13.1	16.7	29	21	49	42.0	27.4	5.1	5.9	11.08	0.02	11.10	0.15	16.6
HPST	27.79	25.82	1.97	92.9	0.27	23.2	27.2	164	145	309	46.9	17.5	6.8	7.5	48.32	0.25	48.57	0.52	10.4
IPST	20.33	19.06	1.27	93.8	0.17	24.0	28.6	109	161	270	59.5	19.1	6.9	7.5	31.53	0.21	31.74	0.66	9.1
LPST	44.78	38.70	6.08	86.4	0.83	25.8	34.5	564	435	999	43.5	33.7	7.2	8.8	158.54	0.34	158.88	0.21	21.1
ST4	32.85	24.83	8.02	75.6	1.10	23.7	37.7	686	288	974	29.6	58.9	6.9	9.9	198.25	0.24	198.49	0.12	44.0
COND P	0.05	0.04	0.01	79.4	0.00	22.0	83.5	1	7	8	90.4	280.1	6.4	8.7	0.22	0.00	0.22	0.13	35.9
HPP	1.10	0.94	0.16	85.3	0.02	22.0	38.9	13	39	52	75.2	77.1	6.4	7.9	3.74	0.00	3.74	0.01	23.9
IPP	0.06	0.04	0.02	69.9	0.00	22.0	110.9	1	11	12	88.9	405.1	6.4	10.2	0.40	0.00	0.40	0.02	59.6
LPP	0.00	0.00	0.00	66.3	0.00	22.0	434.4	0	2	2	97.3	1877.8	6.4	10.9	0.02	0.00	0.02	0.47	70.6
C2	3.96	3.31	0.66	83.4	0.09	37.7	167.7	89	386	476	81.2	344.5	9.9	39.4	23.44	0.12	23.56	0.51	298.4
C3	4.08	3.39	0.69	83.0	0.10	37.7	86.1	94	398	492	80.8	128.3	9.9	13.5	24.73	0.05	24.78	0.20	36.1
C4	4.07	3.35	0.72	82.2	0.10	37.7	90.7	98	397	495	80.1	140.4	9.9	14.1	25.76	0.02	25.78	0.09	42.9
C5	4.13	3.36	0.78	81.2	0.11	37.7	92.8	105	402	508	79.3	145.8	9.9	14.3	27.60	0.03	27.63	0.13	45.0
De-aerator	0.48	0.46	0.02	95.6	0.00	29.6	48.3	2	28	30	92.6	63.0	7.9	8.4	0.60	0.04	0.63	5.54	6.2

M1	0.61	0.57	0.04	93.8	0.01	24.0	26.2	3	0	3	0.0	9.2	6.9	7.5	0.93	0.00	0.93	0.00	8.9
M2	0.16	0.15	0.00	98.9	0.00	23.2	23.5	0	0	0	0.0	1.6	6.8	6.9	0.04	0.00	0.04	0.00	1.6
M3	1.50	1.49	0.01	99.3	0.00	19.2	19.4	1	0	1	0.0	1.1	5.9	5.9	0.23	0.00	0.23	0.00	1.0
M4	43.99	40.18	3.82	91.3	0.52	18.9	20.7	260	0	260	0.0	9.5	5.8	6.4	79.79	0.00	79.79	0.00	9.5
M5	2.19	2.11	0.09	96.0	0.01	17.9	19.1	6	0	6	0.0	6.4	6.2	6.5	1.96	0.00	1.96	0.00	5.9
FG COND	17.60	-	15.75	-	2.16	13.2	0.0	747	105	852	12.4	-	5.1	-	289.12	0.11	289.23	0.04	-
COOL1	0.80	-	0.71	-	0.10	46.0	0.0	118	10	128	8.1	-	12.4	-	31.72	0.01	31.72	0.02	-
COOL2	0.95	-	0.85	-	0.12	53.5	0.0	164	10	174	6.0	-	12.6	-	38.52	0.01	38.53	0.02	-
COOL3	0.90	-	0.81	-	0.11	59.5	0.0	173	9	183	5.2	-	12.8	-	37.37	0.01	37.38	0.02	-
COOL4	0.92	-	0.83	-	0.11	64.3	0.0	193	12	205	6.0	-	13.0	-	39.04	0.01	39.05	0.02	-
COND	12.45	-	9.25	-	1.27	25.1	0.0	835	88	924	9.6	-	7.1	-	236.92	0.03	236.94	0.01	-
CT	0.00	-	3.24	-	0.44	-	-	-	94	-	-	-	-	-	-	15.80	-	-	-
Total	**730.73**	**377.52**	**320.71**	**51.7**	**43.89**	**9.2**	**26.3**	**10,566**	**11,706**	**22,272**	**52.6**	**187.4**	**3.5**	**6.8**	**3987.65**	**174.91**	**4162.56**	**4.20**	**97.0**
Exergy loss	**32.50**																		
$\dot{B}_k^{PF}$	**754.33**																		

Table A.3.3: Results at the stream level for the AZEP 100

Stream, j	$\dot{m}_j$ (kg/s)	T_j (°C)	p_j (bar)	$\dot{E}_{PH,j}$ (MW)	$\dot{E}_{CH,j}$ (MW)	$\dot{E}_{tot,j}$ (MW)	c_j (€/GJ)	$\dot{C}_j$ (€/h)	b_j (Pts/GJ)	$\dot{B}_j$ (Pts/h)
1	710.1	15.00	1.01	0.00	1.11	1.11	0.0	0	0.00	0
2	710.1	392.97	17.01	267.32	1.11	268.43	22.7	6,092	6.37	6,153
3	14.0	15.00	50.00	8.15	721.47	729.62	9.2	6,677	3.45	9,072
4	654.2	1174.58	17.00	672.40	1.45	673.85	19.2	12,914	5.87	14,238
5	654.2	496.96	1.06	140.29	1.45	141.74	19.2	2,716	5.87	2,995
6	299.2	496.96	1.06	64.17	0.66	64.83	19.2	1,242	5.87	1,370
7	299.2	431.87	1.05	51.05	0.66	51.71	19.2	991	5.87	1,093
8	355.0	496.96	1.06	76.13	0.79	76.91	19.2	1,474	5.87	1,625
9	355.0	417.44	1.05	57.30	0.79	58.09	19.2	1,113	5.87	1,227
10	654.2	424.04	1.05	108.35	1.45	109.80	19.2	2,104	5.87	2,320
11	654.2	341.17	1.05	75.39	1.45	76.84	19.2	1,473	5.87	1,624
12	654.2	277.38	1.04	52.86	1.45	54.31	19.2	1,041	5.87	1,148
13	654.2	274.97	1.04	52.06	1.45	53.51	19.2	1,026	5.87	1,131
14	654.2	232.62	1.04	38.77	1.45	40.22	19.2	771	5.87	850
15	654.2	225.00	1.04	36.52	1.45	37.97	19.2	728	5.87	802
16	654.2	221.25	1.04	35.44	1.45	36.89	19.2	707	5.87	780
17	654.2	156.37	1.03	18.71	1.45	20.16	19.2	386	5.87	426
18	654.2	91.97	1.03	6.65	1.45	8.10	0.0	0	0.00	0
19	99.3	32.89	3.73	0.25	0.25	0.50	29.4	15	7.23	13
20	99.3	136.37	3.62	8.44	0.25	8.68	35.8	310	9.68	302
21	100.0	140.01	3.62	8.96	0.25	9.21	36.3	335	9.60	318
22	79.6	140.01	3.62	7.13	0.20	7.33	36.3	266	9.60	253
23	15.5	140.01	3.62	1.39	0.04	1.43	36.3	52	9.60	49
24	15.5	140.43	25.13	1.43	0.04	1.47	38.4	56	9.62	51
25	15.5	216.62	24.38	3.30	0.04	3.34	31.7	106	8.43	101
26	15.5	222.62	24.38	15.45	0.04	15.49	26.0	403	7.04	393
27	15.5	257.38	23.16	16.08	0.04	16.12	26.3	423	7.08	411
28	79.6	265.73	23.16	83.45	0.20	83.65	23.7	1,987	6.87	2,068
29	44.0	476.96	22.00	57.58	0.11	57.69	24.0	1,383	6.92	1,438
30	44.0	253.39	4.10	37.25	0.11	37.36	24.0	896	6.92	931
31	19.7	205.00	4.10	15.82	0.05	15.87	29.9	475	7.97	455
32	19.7	146.37	4.32	15.04	0.05	15.09	29.6	447	7.91	430
33	0.7	146.37	4.32	0.55	0.00	0.55	29.6	16	7.91	16
34	20.4	140.01	3.62	1.83	0.05	1.88	36.3	68	9.60	65
35	20.4	140.02	4.32	1.83	0.05	1.88	36.7	69	9.60	65
36	20.4	146.37	4.32	15.59	0.05	15.64	29.6	463	7.91	445
37	64.1	140.01	3.62	5.74	0.16	5.90	36.3	215	9.60	204
38	64.1	141.74	134.56	6.68	0.16	6.84	36.7	251	9.37	231
39	49.8	325.17	130.53	24.24	0.12	24.36	27.8	678	7.83	687
40	49.8	331.17	130.53	54.74	0.12	54.86	25.1	1,379	7.12	1,405
41	64.1	501.53	124.00	95.16	0.16	95.32	23.2	2,207	6.82	2,339
42	64.1	267.78	23.16	67.37	0.16	67.53	23.2	1,563	6.82	1,657
43	63.7	238.34	4.10	53.03	0.16	53.19	25.8	1,371	7.24	1,387
44	63.7	32.88	0.05	8.25	0.16	8.41	25.8	217	7.24	219
45	99.3	32.88	0.05	0.21	0.25	0.46	25.1	12	7.11	12
46	7012.7	15.00	1.01	0.00	10.92	10.92	0.0	0	0.00	0
47	190.1	15.00	1.01	0.00	0.47	0.47	0.0	0	0.00	0
48	100.2	16.00	1.01	0.00	0.25	0.25	0.0	0	0.00	0
49	7102.6	23.69	1.01	3.09	10.20	13.30	0.0	0	0.00	0
50	44.0	265.73	23.16	46.19	0.11	46.30	23.7	1,100	6.87	1,145
51	35.5	265.73	23.16	37.26	0.09	37.35	23.7	887	6.87	923
52	35.5	32.88	0.05	4.41	0.09	4.49	23.7	107	6.87	111
53	99.3	32.88	0.05	12.66	0.25	12.91	25.1	324	7.11	330
54	49.8	141.74	134.56	5.20	0.12	5.32	36.7	195	9.37	180
55	14.3	141.74	134.56	1.49	0.04	1.52	36.7	56	9.37	51
56	14.3	325.17	130.53	6.93	0.04	6.97	21.0	147	6.66	167
57	14.3	331.17	130.53	15.66	0.04	15.70	18.5	291	6.26	354
58	14.3	592.48	124.00	23.36	0.04	23.40	17.9	419	6.16	519
59	49.8	476.96	124.00	71.88	0.12	72.01	24.8	1,787	7.02	1,819
60	69.9	1276.25	16.48	122.52	12.33	134.85	13.1	1,763	5.06	2,458
61	69.9	1200.00	16.47	114.31	12.33	126.64	13.1	1,656	5.06	2,308
62	69.9	685.00	1.05	47.92	12.33	60.25	13.1	788	5.06	1,098
63	69.9	612.48	1.05	42.10	12.33	54.43	13.1	712	5.06	992
64	69.9	495.75	1.04	33.49	12.33	45.82	13.1	599	5.06	835
65	69.9	341.18	1.04	23.75	12.33	36.08	13.1	472	5.06	657
66	69.9	217.57	1.03	17.69	12.33	30.02	13.1	393	5.06	547
67	39.6	30.00	1.01	0.04	12.25	12.30	13.1	161	5.06	224
68	30.3	30.00	1.01	0.05	0.08	0.12	0.0	0	0.00	0

69	39.6	137.96	3.22	3.35	12.25	15.60	45.8	715	12.34	693
70	39.3	40.00	3.21	2.55	12.25	14.80	45.8	678	12.34	657
71	0.3	40.00	3.21	0.00	0.00	0.00	0.0	0	0.00	0
72	39.3	151.81	10.22	5.93	12.25	18.19	53.3	970	12.54	821
73	39.0	40.00	10.21	4.98	12.26	17.24	53.3	920	12.54	779
74	0.3	40.00	10.21	0.00	0.00	0.00	0.0	0	0.00	0
75	39.0	152.95	32.46	8.33	12.26	20.59	59.4	1,223	12.80	949
76	38.9	40.00	32.45	7.42	12.27	19.69	59.4	1,170	12.80	908
77	0.1	40.00	32.45	0.00	0.00	0.00	0.0	0	0.00	0
78	38.9	154.99	103.09	10.77	12.27	23.05	64.3	1,481	13.03	1,081
79	38.9	30.00	103.09	9.84	12.28	22.12	0.0	0	0.00	0
80	0.0	30.00	103.09	0.00	0.00	0.00	0.0	0	0.00	0
81	71.0	523.80	17.00	32.85	0.11	32.96	21.8	719	6.45	765
82	71.0	392.97	17.01	26.73	0.11	26.84	22.7	609	6.37	615
83	639.1	392.97	17.01	240.59	0.99	241.58	22.7	5,483	6.37	5,538
84	639.1	900.00	17.00	489.45	0.99	490.44	19.1	9,365	5.89	10,407
85	583.2	1000.00	17.00	502.67	1.43	504.10	19.9	10,047	5.96	10,819
86	417.1	1060.92	17.09	597.85	73.62	671.47	13.6	9,112	5.12	12,366
87	473.0	964.88	17.02	579.28	71.77	651.06	13.6	8,835	5.12	11,990
88	583.2	1250.00	17.00	643.28	1.43	644.71	18.9	12,195	5.80	13,473
89	473.0	488.67	16.99	319.20	71.77	390.97	13.6	5,306	5.12	7,200
90	487.0	1276.25	16.48	854.10	85.95	940.04	13.1	12,291	5.06	17,133
91	417.1	1276.25	16.48	731.58	73.62	805.20	13.1	10,528	5.06	14,675
92	417.1	1286.89	17.10	739.89	73.62	813.51	13.6	11,040	5.12	14,982
93	14.0	250.00	16.99	8.25	721.47	729.72	9.3	6,755	3.49	9,178
94	14.0	15.00	17.00	5.90	721.47	727.37	-	-	-	-
95	107.5	16.00	1.37	0.00	0.27	0.27	-	-	-	-
96	107.5	26.00	1.33	0.10	0.27	0.36	-	-	-	-
97	7407.9	16.00	1.37	0.32	18.50	18.83	-	-	-	-
98	7407.9	22.88	1.33	3.51	18.50	22.02	-	-	-	-
99	10018.2	23.69	1.33	5.70	25.02	30.73	-	-	-	-
100	2610.2	26.00	1.33	2.32	6.52	8.84	-	-	-	-
101	2502.7	26.00	1.33	2.22	6.25	8.48	-	-	-	-
102	2401.8	26.00	1.33	2.13	6.00	8.13	-	-	-	-
103	2290.1	26.00	1.33	2.03	5.72	7.76	-	-	-	-
104	2186.0	26.00	1.33	1.94	5.46	7.40	-	-	-	-
105	2186.0	16.00	1.37	0.09	5.46	5.56	-	-	-	-
106	9593.9	16.00	1.37	0.42	23.96	24.38	-	-	-	-
107	9698.1	16.00	1.37	0.42	24.22	24.65	-	-	-	-
108	9809.7	16.00	1.37	0.43	24.50	24.93	-	-	-	-
109	9910.7	16.00	1.37	0.43	24.76	25.19	-	-	-	-
110	10018.2	16.00	1.01	0.07	25.02	25.10	-	-	-	-
111	10018.2	16.00	1.37	0.43	25.02	25.46	-	-	-	-
112	104.2	16.00	1.37	0.00	0.26	0.26	-	-	-	-
113	104.2	26.00	1.33	0.09	0.26	0.35	-	-	-	-
114	111.6	16.00	1.37	0.00	0.28	0.28	-	-	-	-
115	111.6	26.00	1.33	0.10	0.28	0.38	-	-	-	-
116	101.0	16.00	1.37	0.00	0.25	0.26	-	-	-	-
117	101.0	26.00	1.33	0.09	0.25	0.34	-	-	-	-
118	35.5	45.81	0.10	7.20	0.09	7.29	-	-	-	-
119	-	-	-	-	*C1*	280.47	20.6	5,777	6.09	6,153
120	-	-	-	-	*ST1*	25.82	27.2	703	7.53	700
121	-	-	-	-	*ST2*	19.06	28.6	544	7.55	518
122	-	-	-	-	*ST3*	38.70	34.5	1,334	8.77	1,222
123	-	-	-	-	*COND P*	0.05	22.0	1	6.41	1
124	-	-	-	-	*LPP*	0.00	22.0	0	6.41	0
125	-	-	-	-	*HPP*	1.10	22.0	24	6.41	25
126	-	-	-	-	*IPP*	0.06	22.0	1	6.41	1
127	-	-	-	-	*GT1*	232.04	20.6	4,780	6.09	5,091
128	-	-	-	-	*GT2*	63.11	15.2	959	5.33	1,210
129	-	-	-	-	*C6*	8.59	37.7	324	9.89	306
130	-	-	-	-	*C21*	3.96	37.7	150	9.89	141
131	-	-	-	-	*C3*	4.08	37.7	154	9.89	145
132	-	-	-	-	*C4*	4.07	37.7	154	9.89	145
133	-	-	-	-	*C5*	4.13	37.7	156	9.89	147
134	-	-	-	-	*ST4*	24.83	37.7	937	9.89	884
135	-	-	-	-	*tot*	377.52	22.0	8,292	6.41	8,713

A.4: The MCM reactor

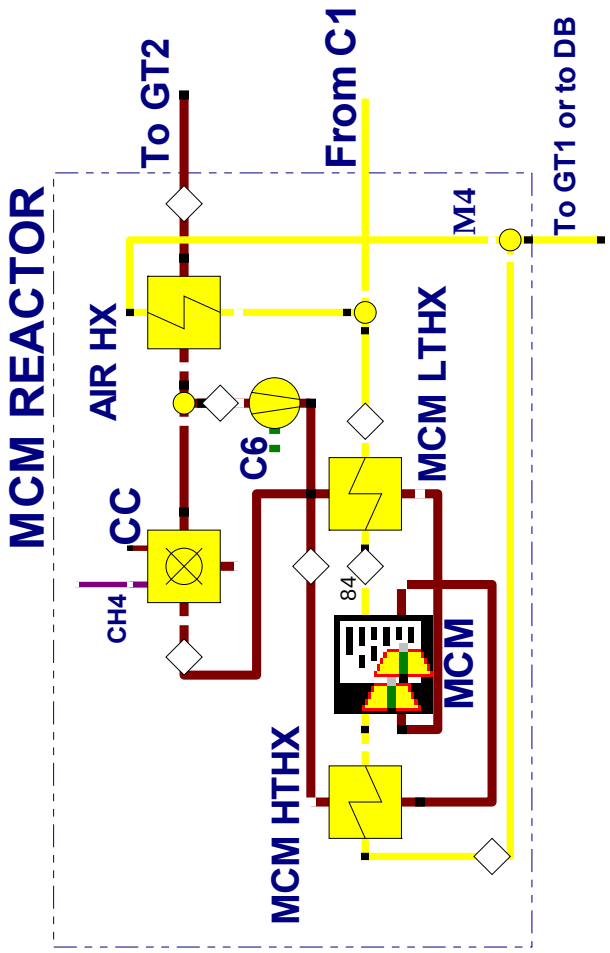

Figure A.4.1: The MCM reactor

A.5: The CLC plant

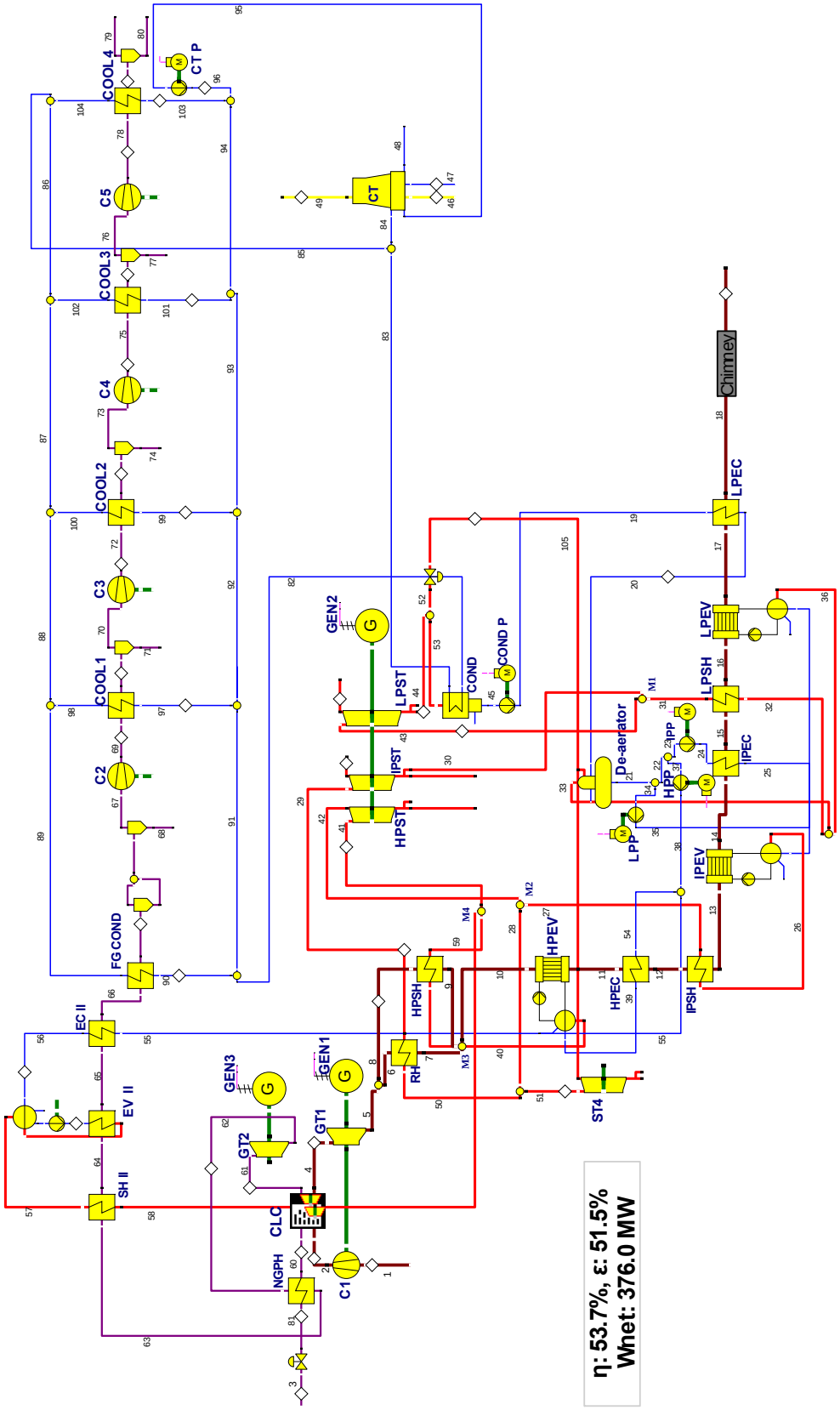

Figure A.5.1: Structure of the CLC plant

Table A.5.1: Results of the economic analysis for the CLC plant

CLC plant								
Year	**Calendar year**	**Debt beg. of year**	**Book depreciation**	**Adjustment**	**Common Equity beg. of year**	**Book depreciation**	**Adjustment**	**TCR**
1	2013	234,946,943	11,747,347	779,678	234,946,943	9,044,079	1,858,829	23,429,933
2	2014	222,419,917	11,747,347	779,678	224,044,035	9,044,079	1,858,829	23,429,933
3	2015	209,892,891	11,747,347	779,678	213,141,127	9,044,079	1,858,829	23,429,933
4	2016	197,365,866	11,747,347	779,678	202,238,219	9,044,079	1,858,829	23,429,933
5	2017	184,838,840	11,747,347	779,678	191,335,311	9,044,079	1,858,829	23,429,933
6	2018	172,311,814	11,747,347	779,678	180,432,403	9,044,079	1,858,829	23,429,933
7	2019	159,784,789	11,747,347	779,678	169,529,495	9,044,079	1,858,829	23,429,933
8	2020	147,257,763	11,747,347	779,678	158,626,587	9,044,079	1,858,829	23,429,933
9	2021	134,730,738	11,747,347	779,678	147,723,680	9,044,079	1,858,829	23,429,933
10	2022	122,203,712	11,747,347	779,678	136,820,772	9,044,079	1,858,829	23,429,933
11	2023	109,676,686	11,747,347	779,678	125,917,864	9,044,079	1,858,829	23,429,933
12	2024	97,149,661	11,747,347	779,678	115,014,956	9,044,079	1,858,829	23,429,933
13	2025	84,622,635	11,747,347	779,678	104,112,048	9,044,079	1,858,829	23,429,933
14	2026	72,095,609	11,747,347	779,678	93,209,140	9,044,079	1,858,829	23,429,933
15	2027	59,568,584	11,747,347	779,678	82,306,232	9,044,079	1,858,829	23,429,933
16	2028	47,041,558	11,747,347	779,678	71,403,325	9,044,079	1,858,829	23,429,933
17	2029	34,514,533	11,747,347	-3,118,714	60,500,417	9,044,079	-2,039,564	15,633,149
18	2030	25,885,899	11,747,347	-3,118,714	53,495,901	9,044,079	-2,039,564	15,633,149
19	2031	17,257,266	11,747,347	-3,118,714	46,491,386	9,044,079	-2,039,564	15,633,149
20	2032	8,628,633	11,747,347	-3,118,714	39,486,871	9,044,079	-2,039,564	15,633,149
21	2033	0	0	0	32,482,355	0	0	0
Total		**2,342,194,338**	**234,946,943**	**0**	**2,683,259,067**	**180,881,587**	**21,583,000**	**437,411,530**

Table A.5.2: Results at the component level for the CLC plant

	$\dot{E}_{F,k}$	$\dot{E}_{P,k}$	$\dot{E}_{D,k}$	ε_k	$y_{D,k}$	$c_{F,k}$	$c_{P,k}$	$\dot{C}_{D,k}$	$\dot{Z}_k$	$\dot{C}_{D,k}+\dot{Z}_k$	f_k	r_k	$b_{F,k}$	$b_{P,k}$	$\dot{B}_{D,k}$	$\dot{Y}_k$	$\dot{B}_{D,k}+\dot{Y}_k$	$f_{b,k}$	$r_{b,k}$
Component, k	**(MW)**	**(MW)**	**(MW)**	**(%)**	**(%)**	**(€/GJ)**	**(€/GJ)**	**(€/h)**	**(€/h)**	**(€/h)**	**(%)**	**(%)**	**(Pts/GJ)**	**(Pts/GJ)**	**(Pts/h)**	**(Pts/h)**	**(Pts/h)**	**(%)**	**(%)**
C1	281.78	268.57	13.21	95.3	1.81	19.3	21.3	919	964	1,884	51.2	10.1	6.0	6.3	286.48	0.19	286.67	0.07	4.9
CLC	694.73	500.67	194.06	72.1	26.56	9.1	15.5	6,391	4,974	11,365	43.8	68.9	3.5	5.3	2418.44	2.54	2420.97	0.10	52.5
GT1	540.99	521.34	19.65	96.4	2.69	18.1	19.3	1,278	1,102	2,380	46.3	7.0	5.8	6.0	410.68	0.91	411.59	0.22	3.8
GT2	54.16	51.35	2.81	94.8	0.38	11.8	13.6	119	216	335	64.5	15.4	4.1	4.3	40.91	0.19	41.11	0.47	5.5
NGPH	6.32	1.12	5.20	17.7	0.71	11.8	69.1	220	10	231	4.4	487.2	4.1	22.9	75.87	0.01	75.88	0.01	465.6
HPSH	22.43	20.43	1.99	91.1	0.27	18.1	22.2	130	105	235	44.8	22.7	5.8	6.6	41.68	0.97	42.66	2.28	14.3
HPEV	35.74	32.97	2.77	92.2	0.38	18.1	21.5	180	140	320	43.7	19.2	5.8	6.5	57.88	0.12	58.00	0.21	12.1
HPEC	24.25	20.58	3.67	84.9	0.50	18.1	23.7	238	56	295	19.1	31.2	5.8	7.3	76.64	0.07	76.70	0.09	25.6
RH	16.60	14.36	2.24	86.5	0.31	18.1	23.4	146	54	199	26.9	29.4	5.8	7.1	46.85	0.45	47.30	0.95	22.6
IPSH	0.63	0.49	0.14	78.1	0.02	18.1	30.2	9	8	17	46.5	67.0	5.8	8.2	2.89	0.01	2.89	0.21	40.5
IPEV	11.97	11.00	0.97	91.9	0.13	18.1	22.8	63	91	154	58.9	26.1	5.8	6.5	20.33	0.07	20.41	0.35	12.8
IPEC	2.03	1.70	0.33	83.6	0.05	18.1	24.8	22	9	30	28.3	37.4	5.8	7.4	6.95	0.01	6.96	0.11	28.2
LPSH	1.12	0.81	0.32	71.9	0.04	18.1	33.4	20	13	34	39.7	84.8	5.8	9.1	6.59	0.01	6.60	0.17	56.2
LPEV	17.03	13.99	3.03	82.2	0.42	18.1	26.7	197	135	332	40.7	47.7	5.8	7.6	63.42	0.11	63.54	0.18	31.2
LPEC	11.28	7.52	3.76	66.6	0.51	18.1	34.4	245	73	317	22.9	90.7	5.8	10.0	78.65	0.09	78.74	0.11	72.1
SH II	0.48	0.42	0.05	88.6	0.01	11.8	16.9	2	4	6	62.0	43.9	4.1	4.9	0.79	0.02	0.81	2.64	21.2
EV II	2.03	1.93	0.10	95.2	0.01	11.8	14.4	4	11	15	71.8	22.0	4.1	4.4	1.42	0.01	1.43	0.43	8.3
EC II	1.47	1.20	0.27	81.8	0.04	11.8	17.0	11	3	14	18.2	44.6	4.1	5.5	3.89	0.00	3.90	0.05	36.1
HPST	24.14	22.41	1.73	92.8	0.24	22.9	26.6	143	103	246	41.9	15.7	6.9	7.6	42.83	0.23	43.06	0.54	10.6
IPST	22.98	21.57	1.41	93.9	0.19	23.3	27.3	118	148	266	55.7	17.3	7.0	7.6	35.22	0.23	35.44	0.64	9.0
LPST	48.80	42.17	6.63	86.4	0.91	24.6	32.5	587	387	974	39.7	32.0	7.2	8.8	172.69	0.36	173.05	0.21	21.3
ST4	20.73	15.66	5.06	75.6	0.69	23.2	36.5	424	157	580	27.0	57.2	6.9	10.0	125.88	0.18	126.07	0.15	44.3
COND P	0.04	0.03	0.01	78.6	0.00	20.9	75.2	1	6	6	89.0	259.6	6.3	8.7	0.21	0.00	0.21	0.13	38.3
HPP	0.98	0.84	0.14	85.3	0.02	20.9	35.7	11	29	40	72.7	70.9	6.3	7.8	3.26	0.00	3.26	0.01	24.3
IPP	0.05	0.04	0.02	70.1	0.00	20.9	98.6	1	8	10	87.9	371.8	6.3	10.0	0.35	0.00	0.35	0.02	60.0
LPP	0.00	0.00	0.00	66.5	0.00	20.9	359.7	0	2	2	96.8	1620.6	6.3	10.7	0.02	0.00	0.02	0.48	71.1
C1	3.85	3.24	0.61	84.1	0.08	36.5	165.8	80	314	394	79.6	353.6	10.0	40.4	21.92	0.12	22.04	0.54	305.3
C2	3.96	3.32	0.64	83.8	0.09	36.5	76.3	85	323	407	79.2	108.9	10.0	13.1	23.09	0.05	23.13	0.21	31.0
C3	3.91	3.27	0.64	83.5	0.09	36.5	78.8	85	318	403	79.0	115.8	10.0	13.5	23.08	0.02	23.10	0.10	35.5
C4	3.93	3.26	0.67	83.0	0.09	36.5	79.8	88	320	408	78.5	118.5	10.0	13.6	23.95	0.03	23.98	0.15	36.6
De-aerator	0.44	0.42	0.02	95.6	0.00	27.7	43.3	2	21	23	91.7	56.6	7.9	8.4	0.55	0.03	0.58	5.31	6.3
M1	0.85	0.79	0.06	92.5	0.01	23.3	25.9	5	0	5	0.0	11.4	7.0	7.7	1.60	0.00	1.60	0.00	11.1

M2	0.08	0.08	0.00	99.3	0.00	22.9	23.2	0	0	0	0.0	0.9	6.9	6.9	0.01	0.00	0.01	0.00	0.9
M3	1.99	1.97	0.02	99.1	0.00	18.1	18.3	1	0	1	0.0	1.4	7.0	7.6	1.18	0.00	1.18	0.00	8.8
M4	0.77	0.73	0.05	93.9	0.01	23.2	25.3	4	0	4	0.0	9.1	7.2	7.2	0.00	0.00	0.00	0.00	0.0
FG COND	22.36	-	20.31	-	2.78	11.8	-	866	69	935	7.4	-	4.1	-	297.82	0.09	297.91	-	-
COOL1	0.77	-	0.69	-	0.09	28.7	-	71	9	79	10.8	-	8.1	-	19.88	0.01	19.89	-	-
COOL2	0.91	-	0.82	-	0.11	33.6	-	99	8	108	7.9	-	8.6	-	25.26	0.01	25.27	-	-
COOL3	0.85	-	0.77	-	0.10	37.9	-	104	8	112	6.9	-	9.0	-	24.85	0.01	24.86	-	-
COOL4	0.86	-	0.78	-	0.11	41.6	-	116	10	126	7.9	-	9.4	-	26.38	0.01	26.39	-	-
COND	11.52	-	8.57	-	1.17	24.3	-	749	68	818	8.3	-	7.2	-	220.83	0.02	220.86	-	-
CT	5.22	-	3.19	-	0.44	-	-	-	72	-	-	-	-	-	-	15.66	-	-	-
Total	**730.73**	**375.99**	**307.41**	**51.5**	**42.07**	**9.2**	**25.4**	**10,128**	**10,347**	**20,474**	**50.5**	**177.5**	**3.5**	**6.8**	**3822.32**	**22.84**	**3845.17**	**0.59**	**94.5**
Exergy loss	**47.33**																		
$\dot{B}_k^{PF}$	**856.41**																		

Table A.5.3: Results at the stream level for the CLC plant

Stream, j	$\dot{m}_j$ (kg/s)	T_j (°C)	p_j (bar)	$\dot{E}_{PH,j}$ (MW)	$\dot{E}_{CH,j}$ (MW)	$\dot{E}_{tot,j}$ (MW)	c_j (€/GJ)	$\dot{C}_j$ (€/h)	b_j (Pts/GJ)	$\dot{B}_j$ (Pts/h)
1	713.5	15.00	1.01	0.00	1.11	1.11	0.0	0	0.0	0
2	713.5	392.90	17.00	268.57	1.11	269.68	21.2	20,571	6.3	1,697
3	14.0	15.00	50.00	8.15	721.47	729.62	9.2	24,037	3.5	2,520
4	658.6	1200.00	16.49	691.60	1.43	693.03	18.1	45,058	5.8	4,023
5	658.6	517.40	1.06	150.61	1.43	152.04	18.1	9,885	5.8	882
6	313.6	517.40	1.06	71.72	0.68	72.40	18.1	4,707	5.8	420
7	313.6	439.94	1.05	55.12	0.68	55.80	18.1	3,628	5.8	324
8	345.0	517.40	1.06	78.89	0.75	79.64	18.1	5,178	5.8	462
9	345.0	421.11	1.05	56.46	0.75	57.21	18.1	3,720	5.8	332
10	658.6	430.09	1.05	111.56	1.43	113.00	18.1	7,348	5.8	656
11	658.6	341.18	1.05	75.83	1.43	77.26	18.1	5,024	5.8	449
12	658.6	272.65	1.04	51.58	1.43	53.02	18.1	3,448	5.8	308
13	658.6	270.73	1.04	50.95	1.43	52.39	18.1	3,407	5.8	304
14	658.6	232.62	1.04	38.98	1.43	40.41	18.1	2,628	5.8	235
15	658.6	225.76	1.04	36.95	1.43	38.38	18.1	2,496	5.8	223
16	658.6	221.92	1.04	35.83	1.43	37.26	18.1	2,423	5.8	216
17	658.6	156.37	1.03	18.80	1.43	20.23	18.1	1,316	5.8	117
18	658.6	97.65	1.03	7.52	1.43	8.95	0.0	0	0.0	0
19	91.1	32.89	3.73	0.23	0.23	0.46	28.1	46	7.3	3
20	91.1	136.37	3.62	7.74	0.23	7.97	34.1	978	9.8	78
21	91.8	140.01	3.62	8.23	0.23	8.46	34.5	1,050	9.7	82
22	71.0	140.01	3.62	6.37	0.18	6.54	34.5	813	9.7	64
23	14.0	140.01	3.62	1.26	0.04	1.29	34.5	160	9.7	13
24	14.0	140.42	25.13	1.29	0.04	1.33	36.2	173	9.8	13
25	14.0	216.62	24.38	2.99	0.04	3.03	29.8	325	8.5	26
26	14.0	222.62	24.38	13.99	0.04	14.03	24.3	1,227	7.0	98
27	14.0	252.65	23.16	14.48	0.04	14.52	24.5	1,280	7.0	102
28	71.0	257.27	23.16	73.78	0.18	73.95	23.2	6,189	6.9	511
29	48.4	497.40	22.00	64.62	0.12	64.74	23.3	5,424	7.0	450
30	48.4	268.87	4.10	41.63	0.12	41.76	23.3	3,499	7.0	290
31	20.1	205.76	4.10	16.16	0.05	16.21	27.9	1,630	7.9	129
32	20.1	146.37	4.32	15.35	0.05	15.40	27.7	1,533	7.9	121
33	0.7	146.37	4.32	0.50	0.00	0.50	27.7	50	7.9	4
34	20.8	140.01	3.62	1.86	0.05	1.91	34.5	238	9.7	19
35	20.8	140.02	4.32	1.86	0.05	1.91	34.8	240	9.7	19
36	20.8	146.37	4.32	15.85	0.05	15.91	27.7	1,584	7.9	125
37	57.0	140.01	3.62	5.11	0.14	5.25	34.5	652	9.7	51
38	57.0	141.73	134.56	5.95	0.14	6.09	34.7	760	9.5	58
39	53.9	325.17	130.53	26.20	0.13	26.33	26.1	2,473	7.8	205
40	53.9	331.17	130.53	59.16	0.13	59.30	23.6	5,030	7.1	419
41	57.0	489.03	124.00	83.43	0.14	83.57	22.9	6,903	6.9	575
42	57.0	258.42	23.16	59.29	0.14	59.43	22.9	4,909	6.9	409
43	68.5	250.24	4.10	57.73	0.17	57.90	24.6	5,131	7.2	419
44	68.5	32.88	0.05	8.93	0.17	9.10	24.6	807	7.2	66
45	91.1	32.88	0.05	0.19	0.23	0.42	24.3	37	7.2	3
46	6785.2	15.00	1.01	0.00	10.56	10.56	0.0	0	0.0	0
47	184.7	15.00	1.01	0.00	0.46	0.46	0.0	0	0.0	0
48	96.9	16.00	1.01	0.00	0.24	0.24	0.0	0	0.0	0
49	6873.0	23.79	1.01	3.07	9.88	12.94	0.0	0	0.0	0
50	48.4	257.27	23.16	50.26	0.12	50.38	23.2	4,216	6.9	348
51	22.6	257.27	23.16	23.51	0.06	23.57	23.2	1,973	6.9	163
52	22.6	32.88	0.05	2.79	0.06	2.85	23.2	238	6.9	20
53	91.1	32.88	0.05	11.72	0.23	11.95	24.3	1,045	7.2	86
54	53.9	141.73	134.56	5.62	0.13	5.75	34.7	718	9.5	55
55	3.2	141.73	134.56	0.33	0.01	0.34	34.7	42	9.5	3
56	3.2	325.17	130.53	1.53	0.01	1.54	20.9	116	6.4	10
57	3.2	331.17	130.53	3.46	0.01	3.47	17.3	215	5.3	18
58	3.2	368.91	124.00	3.89	0.01	3.89	17.2	241	5.2	20
59	53.9	497.40	124.00	79.59	0.13	79.73	23.2	6,660	7.0	555
60	14.0	300.00	17.00	9.27	721.47	730.74	9.2	24,315	3.5	2,546
61	68.9	932.20	16.49	86.91	26.42	113.32	11.8	4,802	4.1	459
62	68.9	486.70	1.04	32.75	26.42	59.17	11.8	2,507	4.1	240
63	68.9	388.91	1.04	26.43	26.42	52.85	11.8	2,239	4.1	214
64	68.9	381.19	1.03	25.95	26.42	52.37	11.8	2,219	4.1	212
65	68.9	346.18	1.03	23.92	26.42	50.34	11.8	2,133	4.1	204
66	68.9	319.31	1.03	22.45	26.42	48.87	11.8	2,071	4.1	198
67	38.7	30.00	1.01	0.04	26.34	26.39	11.8	1,118	4.1	107
68	30.2	30.00	1.01	0.05	0.08	0.12	0.0	0	0.0	0

69	38.7	136.22	3.22	3.28	26.34	29.63	28.6	3,053	8.0	238
70	38.4	40.00	3.21	2.51	26.34	28.85	28.6	2,973	8.0	232
71	0.3	40.00	3.21	0.00	0.00	0.00	0.0	0	0.0	0
72	38.4	149.82	10.22	5.83	26.34	32.17	33.5	3,886	8.5	275
73	38.1	40.00	10.21	4.91	26.35	31.26	33.5	3,775	8.5	267
74	0.3	40.00	10.21	0.00	0.00	0.00	0.0	0	0.0	0
75	38.1	149.84	32.46	8.18	26.35	34.53	37.8	4,703	9.0	311
76	38.0	40.00	32.45	7.32	26.36	33.68	37.8	4,587	9.0	304
77	0.1	40.00	32.45	0.00	0.00	0.00	0.0	0	0.0	0
78	38.0	150.79	103.09	10.58	26.36	36.94	41.5	5,525	9.4	348
79	38.0	30.00	103.09	9.70	26.37	36.08	0.0	0	0.0	0
80	0.0	30.00	103.09	0.00	0.00	0.00	0.0	0	0.0	0
81	14.0	15.00	17.02	5.90	721.47	727.37	-	-	-	-
82	6859.0	16.00	1.37	0.30	17.13	17.43	-	-	-	-
83	6859.0	22.88	1.33	3.25	17.13	20.39	-	-	-	-
84	9693.2	23.79	1.33	5.64	24.21	29.85	-	-	-	-
85	2834.2	26.00	1.33	2.52	7.08	9.60	-	-	-	-
86	2731.6	26.00	1.33	2.43	6.82	9.25	-	-	-	-
87	2634.5	26.00	1.33	2.34	6.58	8.92	-	-	-	-
88	2525.9	26.00	1.33	2.24	6.31	8.55	-	-	-	-
89	2424.5	26.00	1.33	2.15	6.06	8.21	-	-	-	-
90	2424.5	16.00	1.37	0.11	6.06	6.16	-	-	-	-
91	9283.5	16.00	1.37	0.40	23.19	23.59	-	-	-	-
92	9384.9	16.00	1.37	0.41	23.44	23.85	-	-	-	-
93	9493.5	16.00	1.37	0.41	23.71	24.13	-	-	-	-
94	9590.6	16.00	1.37	0.42	23.96	24.37	-	-	-	-
95	9693.2	16.00	1.01	0.07	24.21	24.28	-	-	-	-
96	9693.2	16.00	1.37	0.42	24.21	24.63	-	-	-	-
97	101.4	16.00	1.37	0.00	0.25	0.26	-	-	-	-
98	101.4	26.00	1.33	0.09	0.25	0.34	-	-	-	-
99	108.6	16.00	1.37	0.00	0.27	0.28	-	-	-	-
100	108.6	26.00	1.33	0.10	0.27	0.37	-	-	-	-
101	97.1	16.00	1.37	0.00	0.24	0.25	-	-	-	-
102	97.1	26.00	1.33	0.09	0.24	0.33	-	-	-	-
103	102.6	16.00	1.37	0.00	0.26	0.26	-	-	-	-
104	102.6	26.00	1.33	0.09	0.26	0.35	-	-	-	-
105	22.6	45.81	0.10	4.56	0.06	4.61	-	-	-	-
106					*C1*	281.78	19.3	19,606	6.0	1,697
107					*ST1*	22.41	26.6	2,142	7.6	171
108					*ST2*	21.57	27.3	2,121	7.6	163
109					*ST3*	42.17	32.5	4,933	8.8	370
110					*COND P*	0.04	20.9	3	6.3	0
111					*LPP*	0.00	20.9	0	6.3	0
112					*HPP*	0.98	20.9	74	6.3	6
113					*IPP*	0.05	20.9	4	6.3	0
114					*GT1*	239.56	19.3	16,669	6.0	1,443
115					*GT2*	51.35	13.6	2,511	4.3	219
116					*C2*	3.85	36.5	507	10.0	38
117					*C2*	3.96	36.5	521	10.0	39
118					*C3*	3.91	36.5	514	10.0	39
119					*C4*	3.93	36.5	517	10.0	39
120					*ST4*	15.66	36.5	2,061	10.0	156
					tot	375.99	20.9	28,295	6.3	2,360

Table A.5.4: Splitting the exergy destruction in the CLC plant (MW)

Component, k	$E_{D,k}^{real}$	$E_{D,k}^{EN}$	$E_{D,k}^{EX}$	$E_{D,k}^{AV}$	$E_{D,k}^{UN}$	$E_{D,k}^{UN,EN}$	$E_{D,k}^{UN,EX}$	$E_{D,k}^{AV,EN}$	$E_{D,k}^{AV,EX}$
C1	13.21	7.79	5.42	5.94	7.27	4.26	3.01	3.53	2.41
CLC	194.06	166.54	27.52	64.72	129.34	109.49	19.85	57.05	7.67
GT1	16.01	13.00	3.01	7.69	8.31	6.33	1.98	6.67	1.03
GT2	2.02	1.49	0.54	1.21	0.81	0.60	0.22	0.89	0.32
NGPH	5.20	2.98	2.22	0.04	5.17	2.84	2.33	0.14	**-0.10**
HPSH	1.99	0.66	1.33	0.68	1.31	0.57	0.74	0.09	0.59
HPEV	2.77	1.26	1.51	0.79	1.98	1.03	0.95	0.23	0.56
HPEC	3.67	1.86	1.80	0.94	2.72	1.55	1.17	0.31	0.63
RH	2.24	1.35	0.89	0.69	1.55	1.00	0.55	0.34	0.34
IPSH	0.14	0.15	**-0.01**	0.11	0.03	0.03	0.00	0.11	0.00
IPEV	0.97	0.85	0.12	0.40	0.57	0.46	0.11	0.39	0.01
IPEC	0.33	0.21	0.12	0.10	0.23	0.23	0.01	**-0.02**	0.12
LPSH	0.32	0.17	0.14	0.21	0.11	0.05	0.06	0.13	0.08
LPEV	3.03	1.52	1.52	0.83	2.20	1.24	0.97	0.28	0.55
LPEC	3.76	2.26	1.50	1.65	2.11	1.13	0.98	1.14	0.52
SH II	0.05	0.02	0.03	0.04	0.02	0.01	0.01	0.01	0.02
EV II	0.10	0.04	0.05	0.05	0.05	0.03	0.02	0.02	0.03
EC II	0.27	0.16	0.11	0.13	0.14	0.10	0.04	0.06	0.07
HPST	1.39	0.81	0.57	0.73	0.66	0.37	0.29	0.44	0.28
IPST	1.08	0.81	0.27	0.45	0.62	0.45	0.17	0.36	0.10
LPST	5.99	4.33	1.66	2.48	3.51	2.53	0.97	1.79	0.69
ST4	5.06	2.82	2.25	4.32	0.74	0.41	0.33	2.40	1.92
COND P	0.00	0.00	0.00	0.00	0.00	0.00	0.00	0.00	0.00
HPP	0.09	0.05	0.04	0.06	0.03	0.02	0.01	0.03	0.03
IPP	0.01	0.01	0.00	0.01	0.00	0.00	0.00	0.01	0.00
LPP	0.00	0.00	0.00	0.00	0.00	0.00	0.00	0.00	0.00
C1	0.61	0.43	0.18	0.46	0.15	0.10	0.05	0.33	0.13
C2	0.64	0.47	0.18	0.50	0.15	0.11	0.04	0.36	0.13
C3	0.64	0.47	0.17	0.50	0.15	0.10	0.04	0.37	0.13
C4	0.67	0.49	0.18	0.52	0.15	0.10	0.04	0.38	0.14
FG COND	20.31	14.84	5.47	-	-	-	-	-	-
COOL1	0.69	0.31	0.38	-	-	-	-	-	-
COOL2	0.82	0.40	0.42	-	-	-	-	-	-
COOL3	0.77	0.37	0.39	-	-	-	-	-	-
COOL4	0.78	0.36	0.41	-	-	-	-	-	-
COND	8.57	5.62	2.95	-	-	-	-	-	-
CT	3.06	2.23	0.83	-	-	-	-	-	-
MOT1	0.01	0.00	0.00	0.00	0.00	0.00	0.00	0.00	0.00
MOT2	0.00	0.00	0.00	0.00	0.00	0.00	0.00	0.00	0.00
MOT3	0.05	0.02	0.03	0.03	0.02	0.01	0.01	0.02	0.02
MOT4	0.01	0.00	0.00	0.01	0.00	0.00	0.00	0.00	0.00
GEN1	1.31	0.99	0.32	0.88	0.43	0.33	0.10	0.67	0.21
GEN2	3.65	3.99	**-0.34**	2.44	1.20	1.32	**-0.11**	2.67	**-0.23**
GEN3	0.78	0.62	0.16	0.52	0.26	0.21	0.05	0.42	0.11
Total	**307.13**	**242.77**	**64.36**						
Total (%)		**79.04**	**20.96**						

Table A.5.5: Splitting the investment cost rate in the CLC plant (€/h)

						$\dot{Z}_k^{AV}$		$\dot{Z}_k^{UN}$	
Component, k	$\dot{Z}_k^{real}$	$\dot{Z}_k^{UN}$	$\dot{Z}_k^{AV}$	$\dot{Z}_k^{EN}$	$\dot{Z}_k^{EX}$	$\dot{Z}_k^{AV,EN}$	$\dot{Z}_k^{AV,EX}$	$\dot{Z}_k^{UN,EN}$	$\dot{Z}_k^{UN,EX}$
C1	964.4	819.7	144.7	564.7	399.7	84.7	59.9	480.0	339.7
CLC	4974.5	3979.6	994.9	4211.1	763.3	842.2	152.7	3368.9	610.7
GT1	1102.2	992.0	110.2	839.6	262.6	84.0	26.3	755.6	236.4
GT2	215.8	194.2	21.6	158.5	57.3	15.8	5.7	142.6	51.6
NGPH	10.2	2.7	7.6	5.6	4.6	4.2	3.4	1.5	1.2
HPSH	105.2	40.6	64.6	46.0	59.2	28.2	36.4	17.8	22.9
HPEV	139.7	71.4	68.3	72.7	67.0	35.5	32.7	37.2	34.3
HPEC	56.3	30.3	26.0	32.1	24.2	14.9	11.2	17.3	13.0
RH	53.6	25.0	28.6	34.7	18.9	18.5	10.1	16.2	8.8
IPSH	7.8	2.5	5.3	8.9	**-1.1**	6.0	**-0.7**	2.8	**-0.3**
IPEV	90.7	38.5	52.2	73.2	17.5	42.1	10.0	31.1	7.4
IPEC	8.6	4.1	4.5	8.3	0.2	4.3	0.1	4.0	0.1
LPSH	13.5	5.0	8.5	6.0	7.5	3.8	4.7	2.2	2.8
LPEV	135.2	64.8	70.4	75.8	59.3	39.5	30.9	36.3	28.4
LPEC	72.5	35.0	37.5	38.8	33.8	20.1	17.5	18.7	16.3
SH II	3.8	1.2	2.6	1.9	1.8	1.3	1.3	0.6	0.6
EV II	10.5	5.4	5.2	5.4	5.2	2.6	2.6	2.7	2.6
EC II	2.5	1.6	0.9	1.8	0.7	0.6	0.2	1.2	0.4
HPST	102.8	92.5	10.3	57.8	45.0	5.8	4.5	52.0	40.5
IPST	148.5	133.6	14.8	107.5	40.9	10.8	4.1	96.8	36.8
LPST	386.9	348.2	38.7	279.8	107.1	28.0	10.7	251.8	96.4
ST4	156.5	140.9	15.7	86.5	70.1	8.6	7.0	77.8	63.1
COND P	5.6	4.8	0.8	4.1	1.5	0.6	0.2	3.5	1.3
HPP	28.9	24.6	4.3	15.3	13.6	2.3	2.0	13.0	11.6
IPP	8.4	7.2	1.3	7.1	1.3	1.1	0.2	6.1	1.1
LPP	2.0	1.7	0.3	0.0	2.0	0.0	0.3	0.0	1.7
C1	313.8	266.7	47.1	216.8	97.0	32.5	14.6	184.3	82.5
C2	322.8	274.3	48.4	230.7	92.0	34.6	13.8	196.1	78.2
C3	318.4	270.7	47.8	228.8	89.6	34.3	13.4	194.5	76.2
C4	320.0	272.0	48.0	230.3	89.7	34.5	13.5	195.7	76.3
FG COND	69.1								
COOL1	8.6								
COOL2	8.5								
COOL3	7.7								
COOL4	10.0								
COND	10.2								

Table A.5.6: Splitting the cost rate of exergy destruction in the CLC plant (€/h)

	$\dot{C}_{D,k}^{real}$	$\dot{C}_{D,k}^{UN}$	$\dot{C}_{D,k}^{AV}$	$\dot{C}_{D,k}^{EN}$	$\dot{C}_{D,k}^{EX}$	$\dot{C}_{D,k}^{AV}$		$\dot{C}_{D,k}^{UN}$	
Component, k						$\dot{C}_{D,k}^{AV,EN}$	$\dot{C}_{D,k}^{AV,EX}$	$\dot{C}_{D,k}^{UN,EN}$	$\dot{C}_{D,k}^{UN,EX}$
C1	919.2	506.0	413.2	542.0	377.2	245.7	167.5	296.3	209.7
CLC	6390.8	4259.4	2131.4	5484.5	906.3	1878.7	252.7	3605.8	653.6
GT1	1277.8	540.4	737.4	845.2	432.6	433.5	303.9	411.7	128.8
GT2	118.9	34.5	84.4	63.0	55.9	37.6	46.8	25.3	9.2
NGPH	220.5	5.7	214.8	126.3	94.2	5.9	208.9	120.4	**-114.7**
HPSH	129.7	85.3	44.4	43.0	86.7	5.8	38.7	37.3	48.0
HPEV	180.1	129.0	51.1	81.9	98.2	14.7	36.3	67.2	61.9
HPEC	238.5	177.0	61.4	121.2	117.2	20.3	41.1	101.0	76.1
RH	145.8	38.9	106.9	87.7	58.1	22.4	84.5	65.3	-26.4
IPSH	9.0	2.0	7.0	9.5	**-0.5**	7.3	**-0.2**	2.2	**-0.3**
IPEV	63.3	37.1	26.2	55.2	8.1	25.3	0.9	29.9	7.1
IPEC	21.6	15.1	6.5	13.7	7.9	**-1.0**	7.5	14.7	0.4
LPSH	20.5	7.1	13.4	11.3	9.2	8.2	5.2	3.1	3.9
LPEV	197.3	143.3	54.0	98.7	98.6	18.3	35.7	80.4	62.9
LPEC	244.7	137.2	107.5	147.3	97.4	74.0	33.6	73.3	63.9
SH II	2.3	0.7	1.6	0.9	1.4	0.6	1.0	0.3	0.3
EV II	4.1	2.1	2.0	1.9	2.2	0.8	1.2	1.1	1.0
EC II	11.3	5.8	5.5	6.7	4.6	2.5	3.0	4.3	1.6
HPST	142.8	54.6	88.2	67.2	75.6	36.5	51.7	30.7	23.9
IPST	117.9	52.3	65.6	67.7	50.2	29.8	35.8	37.9	14.4
LPST	587.3	310.7	276.7	383.6	203.8	158.9	117.8	224.6	86.0
ST4	423.8	62.3	361.5	235.6	188.2	201.2	160.3	34.4	27.9
COND P	0.7	0.1	0.6	0.2	0.5	0.1	0.5	0.1	0.0
HPP	10.9	2.3	8.6	3.6	7.3	2.4	6.2	1.2	1.1
IPP	1.2	0.1	1.1	0.6	0.6	0.5	0.6	0.1	0.0
LPP	0.1	0.0	0.1	0.0	0.1	0.0	0.1	0.0	0.0
C1	80.4	19.6	60.8	56.9	23.5	43.4	17.4	13.6	6.1
C2	84.7	19.5	65.2	61.6	23.1	47.6	17.6	13.9	5.6
C3	84.6	19.2	65.4	61.8	22.8	48.0	17.4	13.8	5.4
C4	87.8	19.2	68.7	64.3	23.6	50.5	18.2	13.8	5.4
FG COND	952.8			632.3	320.5				
COOL1	79.8			32.1	47.6				
COOL2	110.3			48.0	62.3				
COOL3	115.5			50.6	64.9				
COOL4	129.3			54.3	75.0				
COND	1007.8			491.2	516.7				

Table A.5.7: Splitting the environmental impact of exergy destruction in the CLC plant (Pts/h)

	$\dot{B}_{D,k}^{real}$	$\dot{B}_{D,k}^{UN}$	$\dot{B}_{D,k}^{AV}$	$\dot{B}_{D,k}^{EN}$	$\dot{B}_{D,k}^{EX}$	$\dot{B}_{D,k}^{AV}$		$\dot{B}_{D,k}^{UN}$	
Component, k						$\dot{B}_{D,k}^{AV,EN}$	$\dot{B}_{D,k}^{AV,EX}$	$\dot{B}_{D,k}^{UN,EN}$	$\dot{B}_{D,k}^{UN,EX}$
C1	79.6	43.8	35.8	46.9	32.7	21.3	14.5	25.7	18.2
CLC	671.8	447.7	224.0	576.5	95.3	197.5	26.6	379.0	68.7
GT1	114.1	48.2	65.8	75.5	38.6	38.7	27.1	36.8	11.5
GT2	11.4	3.3	8.1	6.0	5.3	3.6	4.5	2.4	0.9
NGPH	21.1	0.5	20.5	12.1	9.0	0.6	20.0	11.5	**-11.0**
HPSH	11.6	7.6	4.0	3.8	7.7	0.5	3.5	3.3	4.3
HPEV	16.1	11.5	4.6	7.3	8.8	1.3	3.2	6.0	5.5
HPEC	21.3	15.8	5.5	10.8	10.5	1.8	3.7	9.0	6.8
RH	13.0	3.5	9.5	7.8	5.2	2.0	7.5	5.8	**-2.4**
IPSH	0.8	0.2	0.6	0.8	0.0	0.6	0.0	0.2	0.0
IPEV	5.6	3.3	2.3	4.9	0.7	2.3	0.1	2.7	0.6
IPEC	1.9	1.3	0.6	1.2	0.7	**-0.1**	0.7	1.3	0.0
LPSH	1.8	0.6	1.2	1.0	0.8	0.7	0.5	0.3	0.4
LPEV	17.6	12.8	4.8	8.8	8.8	1.6	3.2	7.2	5.6
LPEC	21.8	12.2	9.6	13.1	8.7	6.6	3.0	6.5	5.7
SH II	0.2	0.1	0.2	0.1	0.1	0.1	0.1	0.0	0.0
EV II	0.4	0.2	0.2	0.2	0.2	0.1	0.1	0.1	0.1
EC II	1.1	0.6	0.5	0.6	0.4	0.2	0.3	0.4	0.1
HPST	11.9	4.6	7.3	5.6	6.3	3.0	4.3	2.6	2.0
IPST	9.8	4.3	5.4	5.6	4.2	2.5	3.0	3.1	1.2
LPST	48.0	25.4	22.6	31.3	16.6	13.0	9.6	18.3	7.0
ST4	35.0	5.1	29.8	19.4	15.5	16.6	13.2	2.8	2.3
COND P	0.1	0.0	0.0	0.0	0.0	0.0	0.0	0.0	0.0
HPP	0.9	0.2	0.7	0.3	0.6	0.2	0.5	0.1	0.1
IPP	0.1	0.0	0.1	0.0	0.0	0.0	0.0	0.0	0.0
LPP	0.0	0.0	0.0	0.0	0.0	0.0	0.0	0.0	0.0
C1	6.1	1.5	4.6	4.3	1.8	3.3	1.3	1.0	0.5
C2	6.4	1.5	4.9	4.7	1.8	3.6	1.3	1.1	0.4
C3	6.4	1.5	5.0	4.7	1.7	3.6	1.3	1.0	0.4
C4	6.7	1.5	5.2	4.9	1.8	3.8	1.4	1.0	0.4
FG COND	91.1			60.4	30.6				
COOL1	6.2			2.5	3.7				
COOL2	7.8			3.4	4.4				
COOL3	7.6			3.3	4.3				
COOL4	8.1			3.4	4.7				
COND	82.5			40.2	42.3				

A.6: The MEA plant

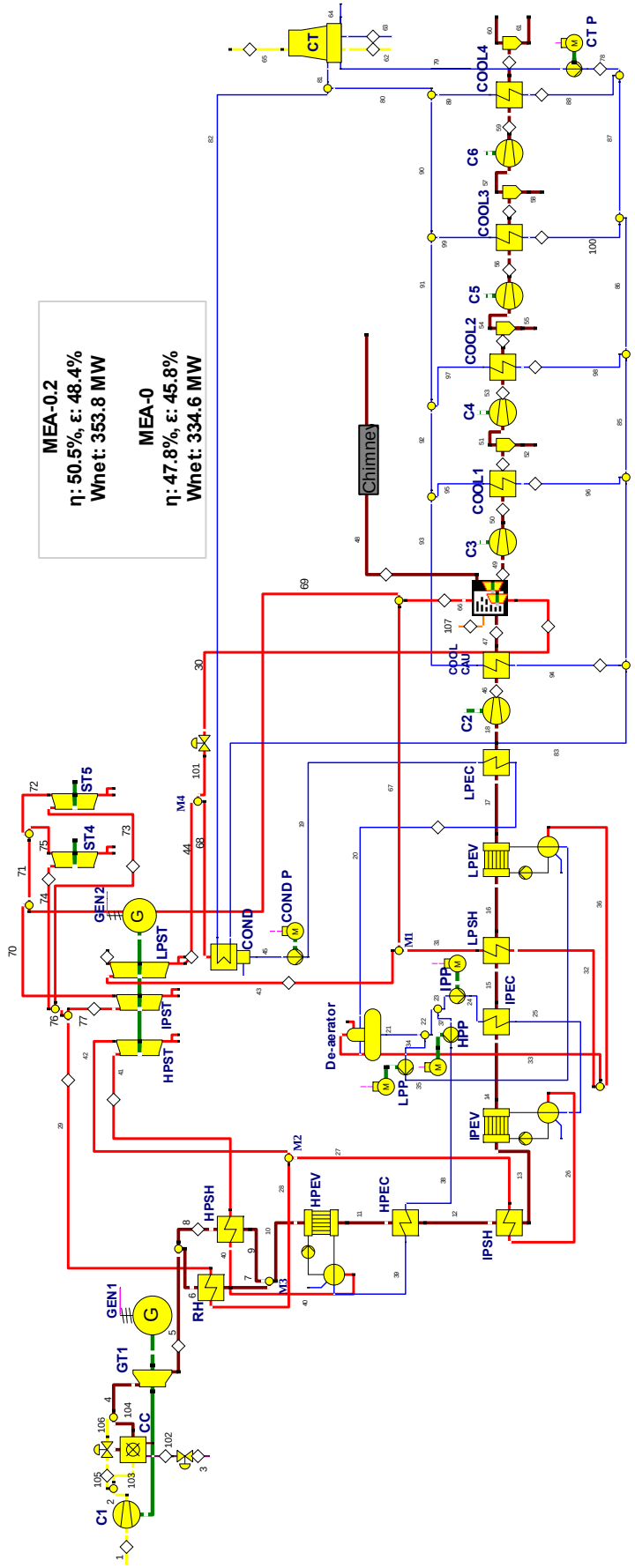

Figure A.6.1: Structure of the MEA plant

Table A.6.1: Results of the year-by-year economic analysis for MEA-0.2

Ref. Plant								
Year	**Calendar year**	**Debt beg. of year**	**Book depreciation**	**Adjustment**	**Common Equity beg. of year**	**Book depreciation**	**Adjustment**	**TCR**
1	2013	213,525,868	10,676,293	703,303	213,525,868	8,078,458	1,677,021	21,135,075
2	2014	202,146,272	10,676,293	703,303	203,770,389	8,078,458	1,677,021	21,135,075
3	2015	190,766,675	10,676,293	703,303	194,014,911	8,078,458	1,677,021	21,135,075
4	2016	179,387,078	10,676,293	703,303	184,259,432	8,078,458	1,677,021	21,135,075
5	2017	168,007,482	10,676,293	703,303	174,503,953	8,078,458	1,677,021	21,135,075
6	2018	156,627,885	10,676,293	703,303	164,748,474	8,078,458	1,677,021	21,135,075
7	2019	145,248,289	10,676,293	703,303	154,992,995	8,078,458	1,677,021	21,135,075
8	2020	133,868,692	10,676,293	703,303	145,237,516	8,078,458	1,677,021	21,135,075
9	2021	122,489,095	10,676,293	703,303	135,482,037	8,078,458	1,677,021	21,135,075
10	2022	111,109,499	10,676,293	703,303	125,726,559	8,078,458	1,677,021	21,135,075
11	2023	99,729,902	10,676,293	703,303	115,971,080	8,078,458	1,677,021	21,135,075
12	2024	88,350,306	10,676,293	703,303	106,215,601	8,078,458	1,677,021	21,135,075
13	2025	76,970,709	10,676,293	703,303	96,460,122	8,078,458	1,677,021	21,135,075
14	2026	65,591,112	10,676,293	703,303	86,704,643	8,078,458	1,677,021	21,135,075
15	2027	54,211,516	10,676,293	703,303	76,949,164	8,078,458	1,677,021	21,135,075
16	2028	42,831,919	10,676,293	703,303	67,193,686	8,078,458	1,677,021	21,135,075
17	2029	31,452,323	10,676,293	-2,813,213	57,438,207	8,078,458	-1,839,495	14,102,044
18	2030	23,589,242	10,676,293	-2,813,213	51,199,244	8,078,458	-1,839,495	14,102,044
19	2031	15,726,161	10,676,293	-2,813,213	44,960,281	8,078,458	-1,839,495	14,102,044
20	2032	7,863,081	10,676,293	-2,813,213	38,721,318	8,078,458	-1,839,495	14,102,044
21	2033	0	0	0	32,482,355	0	0	0
Total		**2,129,493,106**	**213,525,868**	**0**	**2,470,557,835**	**161,569,166**	**19,474,347**	**394,569,381**

Table A.6.2: Results of the year-by-year economic analysis for MEA-0

Ref. Plant								
Year	**Calendar year**	**Debt beg. of year**	**Book depreciation**	**Adjustment**	**Common Equity beg. of year**	**Book depreciation**	**Adjustment**	**TCR**
1	2013	209,287,081	10,464,354	688,190	209,287,081	7,887,380	1,641,047	20,680,970
2	2014	198,134,537	10,464,354	688,190	199,758,654	7,887,380	1,641,047	20,680,970
3	2015	186,981,993	10,464,354	688,190	190,230,228	7,887,380	1,641,047	20,680,970
4	2016	175,829,449	10,464,354	688,190	180,701,802	7,887,380	1,641,047	20,680,970
5	2017	164,676,905	10,464,354	688,190	171,173,376	7,887,380	1,641,047	20,680,970
6	2018	153,524,360	10,464,354	688,190	161,644,949	7,887,380	1,641,047	20,680,970
7	2019	142,371,816	10,464,354	688,190	152,116,523	7,887,380	1,641,047	20,680,970
8	2020	131,219,272	10,464,354	688,190	142,588,097	7,887,380	1,641,047	20,680,970
9	2021	120,066,728	10,464,354	688,190	133,059,670	7,887,380	1,641,047	20,680,970
10	2022	108,914,184	10,464,354	688,190	123,531,244	7,887,380	1,641,047	20,680,970
11	2023	97,761,640	10,464,354	688,190	114,002,818	7,887,380	1,641,047	20,680,970
12	2024	86,609,096	10,464,354	688,190	104,474,391	7,887,380	1,641,047	20,680,970
13	2025	75,456,552	10,464,354	688,190	94,945,965	7,887,380	1,641,047	20,680,970
14	2026	64,304,008	10,464,354	688,190	85,417,539	7,887,380	1,641,047	20,680,970
15	2027	53,151,464	10,464,354	688,190	75,889,113	7,887,380	1,641,047	20,680,970
16	2028	41,998,920	10,464,354	688,190	66,360,686	7,887,380	1,641,047	20,680,970
17	2029	30,846,376	10,464,354	-2,752,760	56,832,260	7,887,380	-1,799,904	13,799,070
18	2030	23,134,782	10,464,354	-2,752,760	50,744,784	7,887,380	-1,799,904	13,799,070
19	2031	15,423,188	10,464,354	-2,752,760	44,657,308	7,887,380	-1,799,904	13,799,070
20	2032	7,711,594	10,464,354	-2,752,760	38,569,831	7,887,380	-1,799,904	13,799,070
21	2033	0	0	0	32,482,355	0	0	0
Total		**2,087,403,945**	**209,287,081**	**0**	**2,428,468,674**	**157,747,595**	**19,057,131**	**386,091,806**

Table A.6.3: Results at the component level for MEA-0.2

Component, k	$\dot{E}_{F,k}$ (MW)	$\dot{E}_{P,k}$ (MW)	$\dot{E}_{D,k}$ (MW)	ε_k (%)	$y_{D,k}$ (%)	$c_{F,k}$ (€/GJ)	$c_{P,k}$ (€/GJ)	$\dot{C}_{D,k}$ (€/h)	$\dot{Z}_k$ (€/h)	$\dot{C}_{D,k}+\dot{Z}_k$ (€/h)	f_k (%)	r_k (%)	$b_{F,k}$ (Pts/GJ)	$b_{P,k}$ (Pts/GJ)	$\dot{B}_{D,k}$ (Pts/h)	$\dot{Y}_k$ (Pts/h)	$\dot{B}_{D,k}+\dot{Y}_k$ (Pts/h)	$f_{b,k}$ (%)	$r_{b,k}$ (%)
C1	242.68	231.30	11.38	95.3	1.56	16.9	19.4	691	1,396	2,086	66.9	14.9	6.1	6.4	249.98	0.24	250.22	0.09	4.9
CC	729.62	508.76	220.87	69.7	30.23	9.2	13.7	7,276	997	8,273	12.0	49.4	3.5	5.6	2746.20	0.38	2746.59	0.01	63.5
GT	551.15	530.67	20.47	96.3	2.80	15.4	16.9	1,137	1,595	2,732	58.4	9.3	5.9	6.1	433.06	1.13	434.18	0.26	3.9
HPSH	35.06	31.72	3.34	90.5	0.46	15.4	18.9	185	155	341	45.6	22.6	5.9	6.7	70.64	1.24	71.89	1.73	13.5
HPEV	43.64	39.91	3.73	91.4	0.51	15.4	18.6	207	181	389	46.7	20.4	5.9	6.6	78.95	0.13	79.07	0.16	11.9
HPEC	28.92	24.91	4.01	86.1	0.55	15.4	19.6	223	88	310	28.2	27.3	5.9	7.1	84.77	0.09	84.86	0.11	20.4
RH	26.46	23.89	2.57	90.3	0.35	15.4	18.9	143	109	252	43.3	22.2	5.9	6.7	54.34	0.79	55.13	1.42	13.8
IPSH	0.18	0.12	0.06	69.0	0.01	15.4	33.3	3	4	7	56.0	115.7	5.9	9.2	1.17	0.00	1.17	0.17	57.1
IPEV	6.10	5.67	0.43	92.9	0.06	15.4	20.1	24	64	88	72.8	30.3	5.9	6.4	9.13	0.04	9.17	0.41	9.7
IPEC	1.06	0.87	0.19	82.5	0.03	15.4	21.3	10	5	15	33.0	38.2	5.9	7.5	3.93	0.00	3.94	0.08	27.0
LPSH	1.43	1.05	0.38	73.3	0.05	15.4	27.8	21	19	40	47.4	80.4	5.9	8.6	8.10	0.01	8.12	0.16	46.4
LPEV	19.02	15.47	3.54	81.4	0.49	15.4	23.1	197	171	368	46.4	49.8	5.9	7.6	74.98	0.12	75.10	0.16	29.1
LPEC	11.57	7.81	3.76	67.5	0.51	15.4	28.5	209	94	303	31.0	84.5	5.9	9.5	79.59	0.10	79.68	0.12	61.2
HPST	31.29	29.18	2.11	93.2	0.29	19.7	22.6	150	122	272	44.9	14.9	6.9	7.5	52.44	0.28	52.72	0.53	8.9
IPST	2.62	2.46	0.15	94.2	0.02	19.6	23.5	11	21	31	65.7	19.5	6.8	7.4	3.76	0.10	3.86	2.53	7.8
LPST	40.94	35.38	5.56	86.4	0.76	21.4	27.8	428	296	723	40.9	30.0	7.2	8.6	144.91	0.32	145.23	0.22	19.2
ST4	19.39	18.54	0.85	95.6	0.12	19.6	22.5	60	114	174	65.4	14.4	6.8	7.2	21.04	0.20	21.25	0.95	5.7
ST5	15.39	14.71	0.68	95.6	0.09	19.6	22.4	48	86	134	64.2	14.0	6.8	7.2	16.70	0.18	16.87	1.05	5.7
COND P	0.04	0.04	0.01	78.8	0.00	18.5	80.0	1	7	8	91.7	333.3	6.5	8.7	0.22	0.00	0.22	0.13	33.6
HPP	1.12	0.96	0.16	85.4	0.02	18.5	34.2	11	40	51	78.8	85.2	6.5	7.9	3.83	0.00	3.83	0.01	21.4
IPP	0.03	0.02	0.01	61.0	0.00	18.5	140.4	1	8	8	90.3	660.4	0.5	10.7	0.02	0.00	0.02	0.11	1886.0
LPP	0.00	0.00	0.00	71.8	0.00	18.5	421.7	0	2	3	98.1	2183.8	78.1	19.4	0.21	0.00	0.21	0.05	-75.1
De-aerator	0.46	0.44	0.02	95.6	0.00	23.9	42.1	2	27	29	94.0	76.5	7.8	8.2	0.56	0.04	0.60	5.87	5.8
C2	18.53	16.93	1.59	91.4	0.22	22.5	43.6	129	1,159	1,288	90.0	94.0	7.2	8.0	41.57	3.78	45.35	8.33	10.3
C3	4.33	3.78	0.55	87.3	0.08	22.4	132.9	44	439	483	90.8	493.8	7.2	25.8	14.36	0.70	15.05	4.62	256.9
C4	3.45	2.86	0.59	82.9	0.08	22.4	100.1	48	350	398	88.0	347.2	7.2	16.3	15.40	0.28	15.68	1.81	125.2
C5	3.44	2.82	0.61	82.1	0.08	22.4	77.0	49	348	398	87.6	244.3	7.2	11.5	15.99	0.14	16.13	0.86	58.3
C6	3.49	2.83	0.66	81.1	0.09	22.4	77.4	53	354	406	87.0	245.7	7.2	11.4	17.13	0.20	17.34	1.18	57.5
M1	1.40	1.26	0.14	89.7	0.02	19.6	21.9	10	0	10	0.0	11.5	6.8	7.6	3.56	0.00	3.56	0.00	11.5
M2	0.63	0.58	0.04	92.9	0.01	19.7	21.2	3	0	3	0.0	7.6	6.9	7.4	1.10	0.00	1.10	0.00	7.6
M3	0.18	0.18	0.00	99.9	0.00	15.4	15.4	0	0	0	0.0	0.1	5.9	5.9	0.00	0.00	0.00	0.00	0.1
M4	3.11	2.96	0.15	95.0	0.02	21.4	22.5	12	0	12	0.0	5.2	7.2	7.6	4.02	0.00	4.02	0.00	5.2
CAU	59.28	-	40.59	-	5.56	23.7	-	3,463	1,023	4,486	22.8	-	6.9	-	1006.53	1.75	1008.28	0.17	-
COOL CAU	9.50	-	8.54	-	1.17	29.7	-	914	59	974	6.1	-	6.9	-	213.65	0.06	213.71	0.03	-
COOL1	2.30	-	2.15	-	0.29	55.7	-	432	10	441	2.2	-	11.7	-	90.74	0.01	90.74	0.01	-
COOL2	0.80	-	0.72	-	0.10	64.0	-	166	8	174	4.6	-	12.6	-	32.59	0.01	32.59	0.02	-
COOL3	0.75	-	0.68	-	0.09	66.0	-	162	7	170	4.3	-	12.4	-	30.43	0.01	30.44	0.02	-
COOL4	0.78	-	0.70	-	0.10	67.6	-	171	9	180	5.0	-	12.2	-	30.90	0.01	30.91	0.02	-
COND	7.03	-	5.23	-	0.72	21.8	-	410	54	464	11.7	-	7.4	-	138.99	0.01	139.00	0.01	-
CT	3.06	-	1.88	-	0.26	-	-	-	18	-	-	-	-	-	-	9.31	-	-	-
Total	**730.58**	**353.82**	**349.14**	**48.4**	**47.79**	**9.2**	**26.3**	**11,502**	**9,440**	**20,942**	**45.1**	**187.0**	**3.5**	**7.6**	**4341.17**	**21.63**	**4362.80**	**0.50**	**120.7**
Exergy loss	**27.62**																		
$\dot{B}_k^{PF}$	**1270.3**																		

Table A.6.4: Results at the component level for MEA-0

Component, k	$\dot{E}_{F,k}$ (MW)	$\dot{E}_{P,k}$ (MW)	$\dot{E}_{D,k}$ (MW)	ε_k (%)	$y_{D,k}$ (%)	$c_{F,k}$ (€/GJ)	$c_{P,k}$ (€/GJ)	$\dot{C}_{D,k}$ (€/h)	$\dot{Z}_k$ (€/h)	$\dot{C}_{D,k}+\dot{Z}_k$ (€/h)	f_k (%)	r_k (%)	$b_{F,k}$ (Pts/GJ)	$b_{P,k}$ (Pts/GJ)	$\dot{B}_{D,k}$ (Pts/h)	$\dot{Y}_k$ (Pts/h)	$\dot{B}_{D,k}+\dot{Y}_k$ (Pts/h)	$f_{b,k}$ (%)	$r_{b,k}$ (%)
C1	242.68	231.30	11.38	95.3	1.56	16.9	19.4	690	1,395	2,086	66.9	14.9	6.1	6.4	249.94	0.24	250.17	0.09	4.9
CC	729.62	508.76	220.87	69.7	30.23	9.2	13.7	7,276	997	8,273	12.0	49.4	3.5	5.6	2746.20	0.38	2746.59	0.01	63.5
GT	551.15	530.67	20.47	96.3	2.80	15.4	16.9	1,137	1,595	2,732	58.4	9.3	5.9	6.1	432.98	1.13	434.11	0.26	3.9
HPSH	35.06	31.72	3.34	90.5	0.46	15.4	18.7	185	155	340	45.5	20.9	5.9	6.6	70.63	1.24	71.87	1.72	12.1
HPEV	43.64	39.91	3.73	91.4	0.51	15.4	18.4	207	181	389	46.7	19.0	5.9	6.5	78.93	0.13	79.06	0.16	10.6
HPEC	28.92	24.91	4.01	86.1	0.55	15.4	19.3	223	87	310	28.2	24.9	5.9	6.9	84.76	0.09	84.85	0.11	18.2
RH	26.46	23.89	2.57	90.3	0.35	15.4	18.6	143	109	252	43.3	20.6	5.9	6.6	54.33	0.79	55.12	1.43	12.3
IPSH	0.18	0.12	0.06	69.0	0.01	15.4	32.2	3	4	7	55.9	108.7	5.9	8.9	1.17	0.00	1.17	0.17	51.0
IPEV	6.10	5.67	0.43	92.9	0.06	15.4	19.9	24	64	88	72.8	29.2	5.9	6.4	9.13	0.04	9.17	0.41	8.7
IPEC	1.06	0.87	0.19	82.5	0.03	15.4	20.8	10	5	15	33.0	35.0	5.9	7.3	3.93	0.00	3.94	0.08	24.1
LPSH	1.43	1.05	0.38	73.3	0.05	15.4	27.0	21	19	40	47.2	74.7	5.9	8.3	8.10	0.01	8.12	0.16	41.4
LPEV	19.02	15.47	3.54	81.4	0.49	15.4	22.6	197	171	368	46.4	46.3	5.9	7.4	74.97	0.12	75.09	0.16	26.0
LPEC	11.57	7.81	3.76	67.5	0.51	15.4	27.3	209	94	303	31.0	77.3	5.9	9.1	79.57	0.10	79.67	0.12	54.6
HPST	31.29	29.18	2.11	93.2	0.29	19.4	22.1	147	127	274	46.2	14.4	6.8	7.3	51.61	0.28	51.89	0.54	8.1
IPST	3.43	3.23	0.20	94.2	0.03	19.3	22.5	14	21	35	60.6	16.5	6.7	7.2	4.87	0.10	4.97	2.07	7.0
LPST	17.84	15.42	2.42	86.4	0.33	22.9	29.3	200	134	334	40.1	27.9	7.5	8.8	65.52	0.19	65.71	0.29	17.4
ST4	19.39	18.54	0.85	95.6	0.12	19.3	22.1	59	118	178	66.6	14.4	6.7	7.1	20.72	0.20	20.93	0.97	5.2
ST5	14.57	13.93	0.64	95.6	0.09	19.3	22.1	45	89	134	66.7	14.4	6.7	7.1	15.57	0.17	15.74	1.10	5.2
COND P	0.04	0.04	0.01	78.8	0.00	17.9	78.7	1	7	8	92.0	338.7	6.3	8.3	0.22	0.00	0.22	0.14	30.3
HPP	1.12	0.96	0.16	85.4	0.02	17.9	33.2	11	40	51	79.2	84.9	6.3	7.6	3.75	0.00	3.75	0.01	19.3
IPP	0.03	0.02	0.01	61.0	0.00	17.9	139.4	1	8	8	90.6	677.1	0.5	10.4	0.02	0.00	0.02	0.12	1880.4
LPP	0.00	0.00	0.00	71.8	0.00	17.9	405.7	0	2	3	98.1	2161.2	76.4	14.0	0.20	0.00	0.20	0.05	-81.7
De-aerator	0.46	0.44	0.02	95.6	0.00	23.3	41.4	2	27	29	94.1	77.9	7.6	8.0	0.55	0.04	0.58	6.02	5.3
C2	18.53	16.93	1.59	91.4	0.22	22.1	43.2	127	1,159	1,286	90.1	95.4	7.1	7.8	40.73	3.78	44.51	8.49	10.3
C3	3.54	3.00	0.54	84.6	0.07	22.1	153.7	43	365	408	89.4	594.8	7.1	30.2	13.88	0.70	14.57	4.78	325.7
C4	3.45	2.86	0.59	82.9	0.08	22.1	78.6	47	356	403	88.3	255.3	7.1	11.8	15.07	0.28	15.35	1.85	66.4
C5	3.44	2.82	0.61	82.1	0.08	22.1	77.2	49	354	403	87.9	249.1	7.1	11.3	15.67	0.14	15.81	0.87	58.7
C6	3.49	2.83	0.66	81.1	0.09	22.1	77.6	52	360	412	87.3	250.8	7.1	11.2	16.79	0.20	16.99	1.20	57.8
M1	0.30	0.26	0.03	88.5	0.00	19.3	21.8	2	0	2	0.0	12.9	6.7	7.6	0.83	0.00	0.83	0.00	12.9
M2	0.63	0.58	0.04	92.9	0.01	19.4	20.8	3	0	3	0.0	7.6	6.8	7.3	1.08	0.00	1.08	0.00	7.6
M3	0.18	0.18	0.00	99.9	0.00	15.4	15.4	0	0	0	0.0	0.1	5.9	5.9	0.00	0.00	0.00	0.00	0.1
M4	2.43	2.32	0.11	95.5	0.02	22.9	24.0	9	0	9	0.0	4.7	7.5	7.9	2.98	0.00	2.98	0.00	4.7
CAU	86.54	-	67.95	-	9.30	22.1	-	5,417	1,086	6,503	16.7	-	6.8	-	1658.02	3.50	1661.52	0.21	-
COOL CAU	9.50	-	8.54	-	1.17	29.5	-	908	60	968	6.2	-	6.9	-	211.13	0.06	211.20	0.03	-
COOL1	0.98	-	0.90	-	0.12	56.7	-	184	8	191	4.1	-	12.0	-	38.78	0.01	38.78	0.02	-
COOL2	0.80	-	0.72	-	0.10	60.8	-	157	8	165	4.9	-	12.0	-	30.92	0.01	30.93	0.02	-
COOL3	0.75	-	0.68	-	0.09	63.4	-	156	7	163	4.5	-	11.8	-	29.10	0.01	29.10	0.02	-
COOL4	0.78	-	0.70	-	0.10	65.4	-	165	9	174	5.2	-	11.7	-	29.65	0.01	29.66	0.02	-
COND	3.02	-	2.25	-	0.31	23.4	-	190	26	216	12.1	-	7.7	-	62.38	0.01	62.38	0.01	-
CT	1.99	-	1.17	-	0.16	-	-	-	11	-	-	-	-	-	-	5.34	-	-	-
Total	**730.58**	**334.63**	**368.27**	**45.8**	**50.41**	**9.2**	**27.6**	**12,133**	**9,257**	**21,390**	**43.3**	**201.9**	**67.8**	**73.0**	**4579.01**	**19.27**	**4598.28**	**0.42**	**7.6**
Exergy loss	**27.68**																		
$\dot{B}_k^{PF}$	**1268.4**																		

Table A.6.5: Results at the stream level for MEA-0.2

Stream, j	$\dot{m}_j$ (kg/s)	T_j (°C)	p_j (bar)	$\dot{E}_{PH,j}$ (MW)	$\dot{E}_{CH,j}$ (MW)	$\dot{E}_{tot,j}$ (MW)	c_j (€/GJ)	$\dot{C}_j$ (€/h)	b_j (Pts/GJ)	$\dot{B}_j$ (Pts/h)
1	614.50	15.00	1.01	0.00	0.96	0.96	0.00	0	0.0	0
2	614.50	392.90	17.00	231.30	0.96	232.25	19.28	16,124	6.4	5,332
3	14.00	15.00	50.00	8.15	721.47	729.62	9.15	24,037	3.5	9,072
4	628.50	1264.03	16.49	735.74	5.27	741.01	15.43	41,158	5.9	15,675
5	628.50	580.64	1.06	184.60	5.27	189.87	15.43	10,546	5.9	4,016
6	268.50	580.64	1.06	78.86	2.25	81.11	15.43	4,505	5.9	1,716
7	268.50	447.62	1.05	52.40	2.25	54.65	15.43	3,035	5.9	1,156
8	360.00	580.64	1.06	105.73	3.02	108.75	15.43	6,040	5.9	2,300
9	360.00	449.30	1.05	70.67	3.02	73.69	15.43	4,093	5.9	1,559
10	628.50	448.58	1.04	123.07	5.27	128.34	15.43	7,128	5.9	2,715
11	628.50	341.18	1.04	79.43	5.27	84.70	15.43	4,704	5.9	1,792
12	628.50	257.91	1.04	50.51	5.27	55.78	15.43	3,098	5.9	1,180
13	628.50	257.35	1.04	50.33	5.27	55.60	15.43	3,088	5.9	1,176
14	628.50	237.62	1.04	44.23	5.27	49.50	15.43	2,749	5.9	1,047
15	628.50	234.08	1.04	43.17	5.27	48.44	15.43	2,690	5.9	1,025
16	628.50	229.24	1.04	41.73	5.27	47.00	15.43	2,611	5.9	994
17	628.50	156.37	1.03	22.72	5.27	27.99	15.43	1,554	5.9	592
18	628.50	94.79	1.03	11.14	5.27	16.41	0.00	0	0.0	0
19	94.71	32.89	3.73	0.24	0.24	0.47	26.10	44	7.5	13
20	94.71	136.37	3.62	8.05	0.24	8.28	28.33	845	9.4	279
21	95.40	140.01	3.62	8.55	0.24	8.79	28.99	917	9.3	294
22	72.43	140.01	3.62	6.49	0.18	6.67	28.99	696	9.3	223
23	7.22	140.01	3.62	0.65	0.02	0.67	28.99	69	9.3	22
24	7.22	140.49	25.13	0.67	0.02	0.68	32.12	79	9.3	23
25	7.22	216.62	24.38	1.54	0.02	1.56	26.06	146	8.3	46
26	7.22	222.62	24.38	7.21	0.02	7.23	21.39	557	6.8	178
27	7.22	237.91	23.16	7.33	0.02	7.35	21.59	571	6.9	182
28	72.43	305.14	23.16	79.35	0.18	79.53	19.87	5,689	6.9	1,975
29	72.43	560.64	22.00	103.24	0.18	103.42	19.64	7,311	6.8	2,550
30	39.00	9.85	3.90	0.02	0.10	0.12	19.64	8	6.8	3
31	22.28	214.08	4.10	18.06	0.06	18.12	24.09	1,571	7.8	511
32	22.28	146.37	4.32	17.01	0.06	17.07	23.85	1,466	7.8	479
33	0.68	146.37	4.32	0.52	0.00	0.52	23.85	45	7.8	15
34	22.96	140.01	3.62	2.06	0.06	2.12	28.99	221	9.3	71
35	22.96	140.02	4.32	2.06	0.06	2.12	29.34	224	9.3	71
36	22.96	146.37	4.32	17.53	0.06	17.59	23.85	1,511	7.8	493
37	65.21	140.01	3.62	5.84	0.16	6.01	28.99	627	9.3	201
38	65.21	141.75	134.56	6.80	0.16	6.96	29.70	745	9.1	228
39	65.21	325.17	130.53	31.72	0.16	31.88	21.84	2,506	7.5	863
40	65.21	331.17	130.53	71.63	0.16	71.79	20.02	5,175	7.0	1,807
41	65.21	560.64	124.00	103.35	0.16	103.51	19.68	7,334	6.9	2,569
42	65.21	313.21	23.16	72.06	0.16	72.22	19.68	5,117	6.9	1,793
43	55.71	275.88	4.10	48.31	0.14	48.45	21.36	3,725	7.2	1,263
44	55.71	32.88	0.05	7.37	0.14	7.51	21.36	577	7.2	196
45	94.71	32.88	0.05	0.20	0.24	0.44	21.77	34	7.4	12
46	628.50	122.27	1.30	28.08	5.27	33.35	29.73	3,569	6.9	834
47	628.50	51.00	1.30	18.58	5.27	23.85	29.73	2,552	6.9	596
48	595.25	46.74	1.03	5.98	1.47	7.45	181.88	4,877	44.4	1,191
49	33.25	139.10	1.03	0.67	10.57	11.24	29.73	1,203	6.9	281
50	33.25	267.18	3.22	4.45	10.57	15.02	55.68	3,010	11.7	632
51	33.23	40.00	3.20	2.14	10.57	12.71	55.68	2,548	11.7	535
52	0.01	40.00	3.20	0.00	0.00	0.00	0.00	0	0.0	0
53	33.23	151.78	10.22	5.01	10.57	15.58	63.84	3,580	12.5	704
54	33.01	40.00	10.21	4.20	10.58	14.78	63.84	3,396	12.5	667
55	0.22	40.00	10.21	0.00	0.00	0.00	0.00	0	0.0	0
56	33.01	152.67	32.46	7.02	10.58	17.60	65.96	4,179	12.4	784
57	32.94	40.00	32.45	6.25	10.59	16.84	65.96	3,999	12.4	750

58	0.07	40.00	32.45	0.00	0.00	0.00	0.00	0	0.0	0
59	32.94	154.69	103.09	9.08	10.59	19.67	67.60	4,787	12.2	866
60	32.92	30.00	103.09	8.30	10.60	18.89	0.00	0	0.0	0
61	0.03	30.00	103.09	0.00	0.00	0.00	0.00	0	0.0	0
62	4036.07	15.00	1.01	0.00	6.28	6.28	0.00	0	0.0	0
63	109.58	15.00	1.01	0.00	0.27	0.27	0.00	0	0.0	0
64	57.66	16.00	1.01	0.00	0.14	0.14	0.00	0	0.0	0
65	4088.00	23.73	1.01	1.80	5.87	7.67	0.00	0	0.0	0
66	39.00	317.23	4.10	35.45	0.10	35.55	19.64	2,513	6.8	877
67	33.43	317.23	4.10	30.39	0.08	30.48	19.64	2,154	6.8	751
68	94.71	32.88	0.05	7.23	0.24	7.47	21.77	586	7.4	199
69	72.43	317.23	4.10	65.85	0.18	66.03	19.64	4,668	6.8	1,628
70	5.07	317.23	4.10	4.61	0.01	4.62	19.64	327	6.8	114
71	67.37	317.23	4.10	61.24	0.17	61.41	19.64	4,341	6.8	1,514
72	29.80	317.23	4.10	27.09	0.07	27.17	19.64	1,920	6.8	670
73	29.80	560.64	22.00	42.48	0.07	42.55	19.64	3,008	6.8	1,049
74	37.56	560.64	22.00	53.54	0.09	53.63	19.64	3,791	6.8	1,322
75	37.56	317.23	4.10	34.15	0.09	34.24	19.64	2,421	6.8	844
76	67.37	560.64	22.00	96.02	0.17	96.19	19.64	6,799	6.8	2,372
77	5.07	560.64	22.00	7.22	0.01	7.24	19.64	511	6.8	178
78	5765.82	16.00	1.37	0.25	14.40	14.65	_	_	-	-
79	5765.82	16.00	1.01	0.04	14.40	14.44	_	_	-	-
80	1580.32	26.00	1.33	1.40	3.95	5.35	_	_	-	-
81	5765.82	23.73	1.33	3.31	14.40	17.72	_	_	-	-
82	4185.50	22.88	1.33	1.99	10.45	12.44	_	_	-	-
83	4185.50	16.00	1.37	0.18	10.45	10.64	_	_	-	-
84	5320.01	16.00	1.37	0.23	13.29	13.52	_	_	-	-
85	5495.45	16.00	1.37	0.24	13.73	13.97	_	_	-	-
86	5589.87	16.00	1.37	0.24	13.96	14.21	_	_	-	-
87	5675.09	16.00	1.37	0.25	14.18	14.42	_	_	-	-
88	90.73	16.00	1.37	0.00	0.23	0.23	_	_	-	-
89	90.73	26.00	1.33	0.08	0.23	0.31	_	_	-	-
90	1489.59	26.00	1.33	1.32	3.72	5.04	_	_	-	-
91	1404.37	26.00	1.33	1.25	3.51	4.76	_	_	-	-
92	1309.95	26.00	1.33	1.16	3.27	4.44	_	_	-	-
93	1134.51	26.00	1.33	1.01	2.83	3.84	_	_	-	-
94	1134.51	16.00	1.37	0.05	2.83	2.88	_	_	-	-
95	175.44	26.00	1.33	0.16	0.44	0.59	_	_	-	-
96	175.44	16.00	1.37	0.01	0.44	0.45	_	_	-	-
97	94.42	26.00	1.33	0.08	0.24	0.32	_	_	-	-
98	94.42	16.00	1.37	0.00	0.24	0.24	_	_	-	-
99	85.22	26.00	1.33	0.08	0.21	0.29	_	_	-	-
100	85.22	16.00	1.37	0.00	0.21	0.22	_	_	-	-
101	39.00	9.94	0.05	0.00	0.10	0.10	_	_	-	-
102	14.00	15.00	17.00	5.90	721.47	727.37	_	_	-	-
103	498.50	392.90	17.00	187.64	0.78	188.41	_	_	-	-
104	512.50	1435.04	16.49	704.31	5.80	710.10	_	_	-	-
105	116.00	392.90	17.00	43.66	0.18	43.84	_	_	-	-
106	116.00	392.90	16.49	43.37	0.18	43.55	_	_	-	-
107	-	-	-	-	*C1*	242.68	16.86	14,728	6.1	5,332
108	-	-	-	-	*ST1*	29.18	22.61	2,375	7.5	789
109	-	-	-	-	*ST2*	2.46	23.47	208	7.4	65
110	-	-	-	-	*ST3*	35.38	27.78	3,538	8.6	1,099
111	-	-	-	-	*COND P*	0.04	18.46	3	6.5	1
112	-	-	-	-	*IPP*	0.03	18.46	2	6.5	1
113	-	-	-	-	*HPP*	1.12	18.46	74	6.5	26
114	-	-	-	-	*LPP*	0.00	18.46	0	6.5	0
115	-	-	-	-	*GT1*	288.00	16.86	17,479	6.1	6,328
116	-	-	-	-	*C2*	18.53	22.47	1,499	7.2	483
117	-	-	-	-	*C3*	4.33	22.38	349	7.2	113
118	-	-	-	-	*C4*	3.45	22.38	278	7.2	90

119	-	-	-	-	*C5*	3.44	22.38	277	7.2	90
120	-	-	-	-	*C6*	3.49	22.38	281	7.2	91
121	-	-	-	-	*ST4*	18.54	22.47	1,499	7.2	483
122	-	-	-	-	*ST5*	14.71	22.38	1,185	7.2	383
					tot	353.82	18.46	23,520	6.5	8,253

Table A.6.6: Results at the stream level for MEA-0

Stream, j	$\dot{m}_j$ (kg/s)	T_j (°C)	p_j (bar)	$\dot{E}_{PH,j}$ (MW)	$\dot{E}_{CH,j}$ (MW)	$\dot{E}_{tot,j}$ (MW)	c_j (€/GJ)	$\dot{C}_j$ (€/h)	b_j (Pts/GJ)	$\dot{B}_j$ (Pts/h)
1	614.50	15.00	1.01	0.00	0.96	0.96	0.0	0	0.0	0
2	614.50	392.90	17.00	231.30	0.96	232.25	19.3	4,479	6.4	5,331
3	14.00	15.00	50.00	8.15	721.47	729.62	9.2	6,677	3.5	9,072
4	628.50	1264.03	16.49	735.74	5.27	741.01	15.4	11,432	5.9	15,672
5	628.50	580.64	1.06	184.60	5.27	189.87	15.4	2,929	5.9	4,016
6	268.50	580.64	1.06	78.86	2.25	81.11	15.4	1,251	5.9	1,715
7	268.50	447.62	1.05	52.40	2.25	54.65	15.4	843	5.9	1,156
8	360.00	580.64	1.06	105.73	3.02	108.75	15.4	1,678	5.9	2,300
9	360.00	449.30	1.05	70.67	3.02	73.69	15.4	1,137	5.9	1,558
10	628.50	448.58	1.04	123.07	5.27	128.34	15.4	1,980	5.9	2,714
11	628.50	341.18	1.04	79.43	5.27	84.70	15.4	1,307	5.9	1,791
12	628.50	257.91	1.04	50.51	5.27	55.78	15.4	861	5.9	1,180
13	628.50	257.35	1.04	50.33	5.27	55.60	15.4	858	5.9	1,176
14	628.50	237.62	1.04	44.23	5.27	49.50	15.4	764	5.9	1,047
15	628.50	234.08	1.04	43.17	5.27	48.44	15.4	747	5.9	1,024
16	628.50	229.24	1.04	41.73	5.27	47.00	15.4	725	5.9	994
17	628.50	156.37	1.03	22.72	5.27	27.99	15.4	432	5.9	592
18	628.50	94.79	1.03	11.14	5.27	16.41	0.0	0	0.0	0
19	94.71	32.89	3.73	0.24	0.24	0.47	27.5	13	7.7	13
20	94.71	136.37	3.62	8.05	0.24	8.28	27.4	227	9.0	269
21	95.40	140.01	3.62	8.55	0.24	8.79	28.0	246	8.9	283
22	72.43	140.01	3.62	6.49	0.18	6.67	28.0	187	8.9	215
23	7.22	140.01	3.62	0.65	0.02	0.67	28.0	19	8.9	21
24	7.22	140.49	25.13	0.67	0.02	0.68	31.2	21	9.0	22
25	7.22	216.62	24.38	1.54	0.02	1.56	25.4	40	8.0	45
26	7.22	222.62	24.38	7.21	0.02	7.23	21.1	153	6.7	175
27	7.22	237.91	23.16	7.33	0.02	7.35	21.3	156	6.8	179
28	72.43	305.14	23.16	79.35	0.18	79.53	19.6	1,555	6.8	1,943
29	72.43	560.64	22.00	103.24	0.18	103.42	19.3	2,000	6.7	2,511
30	69.00	19.25	3.90	0.03	0.17	0.20	19.3	4	6.7	5
31	22.28	214.08	4.10	18.06	0.06	18.12	23.5	425	7.6	498
32	22.28	146.37	4.32	17.01	0.06	17.07	23.3	397	7.6	466
33	0.68	146.37	4.32	0.52	0.00	0.52	23.3	12	7.6	14
34	22.96	140.01	3.62	2.06	0.06	2.12	28.0	59	8.9	68
35	22.96	140.02	4.32	2.06	0.06	2.12	28.4	60	9.0	68
36	22.96	146.37	4.32	17.53	0.06	17.59	23.3	409	7.6	481
37	65.21	140.01	3.62	5.84	0.16	6.01	28.0	168	8.9	193
38	65.21	141.75	134.56	6.80	0.16	6.96	28.7	200	8.8	220
39	65.21	325.17	130.53	31.72	0.16	31.88	21.3	680	7.3	843
40	65.21	331.17	130.53	71.63	0.16	71.79	19.7	1,413	6.9	1,776
41	65.21	560.64	124.00	103.35	0.16	103.51	19.4	2,005	6.8	2,528
42	65.21	313.21	23.16	72.06	0.16	72.22	19.4	1,399	6.8	1,764
43	25.71	227.74	4.10	21.15	0.06	21.21	22.9	486	7.5	574
44	25.71	32.88	0.05	3.31	0.06	3.37	22.9	77	7.5	91
45	94.71	32.88	0.05	0.20	0.24	0.44	23.4	10	7.7	12
46	628.50	122.27	1.30	28.08	5.27	33.35	29.5	985	6.9	824
47	628.50	51.00	1.30	18.58	5.27	23.85	29.5	704	6.9	589
48	595.25	50.52	1.03	6.41	1.47	7.88	0.0	0	65.2	1,850
49	33.25	61.43	1.03	0.13	10.57	10.71	29.5	316	6.9	265
50	33.25	173.56	3.22	3.13	10.57	13.70	56.7	777	12.0	590
51	33.23	40.00	3.21	2.15	10.57	12.72	56.7	721	12.0	548
52	0.02	40.00	3.21	0.00	0.00	0.00	0.0	0	0.0	0
53	33.23	151.60	10.22	5.00	10.57	15.58	60.7	945	11.9	669
54	33.01	40.00	10.21	4.20	10.58	14.78	60.7	897	11.9	635
55	0.22	40.00	10.21	0.00	0.00	0.00	0.0	0	0.0	0
56	33.01	152.67	32.46	7.02	10.58	17.60	63.3	1,115	11.8	749
57	32.94	40.00	32.45	6.25	10.59	16.84	63.3	1,067	11.8	717
58	0.07	40.00	32.45	0.00	0.00	0.00	0.0	0	0.0	0
59	32.94	154.69	103.09	9.08	10.59	19.67	65.4	1,286	11.7	831
60	32.92	30.00	103.09	8.30	10.60	18.89	0.0	0	0.0	0
61	0.03	30.00	103.09	0.00	0.00	0.00	0.0	0	0.0	0
62	2312.94	15.00	1.01	0.00	3.60	3.60	0.0	0	0.0	0
63	64.32	15.00	1.01	0.00	0.16	0.16	0.0	0	0.0	0
64	33.04	16.00	1.01	0.00	0.08	0.08	0.0	0	0.0	0
65	2344.22	24.30	1.01	1.19	3.37	4.56	0.0	0	0.0	0
66	69.00	317.23	4.10	62.73	0.17	62.90	19.3	1,216	6.7	1,527
67	3.43	317.23	4.10	3.12	0.01	3.13	19.3	61	6.7	76
68	94.71	32.88	0.05	3.23	0.24	3.46	23.4	81	7.7	96

69	72.43	317.23	4.10	65.85	0.18	66.03	19.3	1,277	6.7	1,603
70	6.65	317.23	4.10	6.05	0.02	6.07	19.3	117	6.7	147
71	65.78	317.23	4.10	59.80	0.16	59.96	19.3	1,159	6.7	1,456
72	28.22	317.23	4.10	25.65	0.07	25.72	19.3	497	6.7	625
73	28.22	560.64	22.00	40.22	0.07	40.29	19.3	779	6.7	978
74	37.56	560.64	22.00	53.54	0.09	53.63	19.3	1,037	6.7	1,302
75	37.56	317.23	4.10	34.15	0.09	34.24	19.3	662	6.7	831
76	65.78	560.64	22.00	93.76	0.16	93.92	19.3	1,816	6.7	2,280
77	6.65	560.64	22.00	9.48	0.02	9.50	19.3	184	6.7	231
78	3304.20	16.00	1.37	0.14	8.25	8.40	-	-	-	-
79	3304.20	16.00	1.01	0.02	8.25	8.28	-	-	-	-
80	1504.35	26.00	1.33	1.34	3.76	5.09	-	-	-	-
81	3304.20	24.30	1.33	2.14	8.25	10.39	-	-	-	-
82	1799.85	22.88	1.33	0.85	4.50	5.35	-	-	-	-
83	1799.85	16.00	1.37	0.08	4.50	4.57	-	-	-	-
84	2934.36	16.00	1.37	0.13	7.33	7.46	-	-	-	-
85	3034.01	16.00	1.37	0.13	7.58	7.71	-	-	-	-
86	3128.25	16.00	1.37	0.14	7.81	7.95	-	-	-	-
87	3213.47	16.00	1.37	0.14	8.03	8.17	-	-	-	-
88	90.73	16.00	1.37	0.00	0.23	0.23	-	-	-	-
89	90.73	26.00	1.33	0.08	0.23	0.31	-	-	-	-
90	1413.62	26.00	1.33	1.26	3.53	4.79	-	-	-	-
91	1328.40	26.00	1.33	1.18	3.32	4.50	-	-	-	-
92	1234.16	26.00	1.33	1.10	3.08	4.18	-	-	-	-
93	1134.51	26.00	1.33	1.01	2.83	3.84	-	-	-	-
94	1134.51	16.00	1.37	0.05	2.83	2.88	-	-	-	-
95	99.65	26.00	1.33	0.09	0.25	0.34	-	-	-	-
96	99.65	16.00	1.37	0.00	0.25	0.25	-	-	-	-
97	94.24	26.00	1.33	0.08	0.24	0.32	-	-	-	-
98	94.24	16.00	1.37	0.00	0.24	0.24	-	-	-	-
99	85.22	26.00	1.33	0.08	0.21	0.29	-	-	-	-
100	85.22	16.00	1.37	0.00	0.21	0.22	-	-	-	-
101	69.00	19.34	0.05	0.00	0.17	0.18	-	-	-	-
102	14.00	15.00	17.00	5.90	721.47	727.37	-	-	-	-
103	498.50	392.90	17.00	187.64	0.78	188.41	-	-	-	-
104	512.50	1435.04	16.49	704.31	5.80	710.10	-	-	-	-
105	116.00	392.90	17.00	43.66	0.18	43.84	-	-	-	-
106	116.00	392.90	16.49	43.37	0.18	43.55	-	-	-	-
107	-	-	-	-	*C1*	242.68	16.9	4091.0	6.1	5,331
108	-	-	-	-	*ST1*	29.18	22.1	646.1	7.3	770
109	-	-	-	-	*ST2*	3.23	22.5	72.8	7.2	84
110	-	-	-	-	*ST3*	15.42	29.3	451.7	8.8	489
111	-	-	-	-	*COND P*	0.04	17.9	0.8	6.3	1
112	-	-	-	-	*IPP*	0.03	17.9	0.6	6.3	1
113	-	-	-	-	*HPP*	1.12	17.9	20.1	6.3	26
114	-	-	-	-	*LPP*	0.00	17.9	0.0	6.3	0
115	-	-	-	-	*GT1*	288.00	16.9	4855.0	6.1	6,327
116	-	-	-	-	*C2*	18.53	22.1	409.7	7.1	473
117	-	-	-	-	*C3*	3.54	22.1	78.3	7.1	90
118	-	-	-	-	*C4*	3.45	22.1	76.3	7.1	88
119	-	-	-	-	*C5*	3.44	22.1	76.0	7.1	88
120	-	-	-	-	*C6*	3.49	22.1	77.1	7.1	89
121	-	-	-	-	*ST4*	18.54	22.1	409.9	7.1	473
122	-	-	-	-	*ST5*	13.93	22.1	308.0	7.1	356
					tot	334.63	17.9	6004.1	6.3	7,643

A.7: The S-Graz cycle

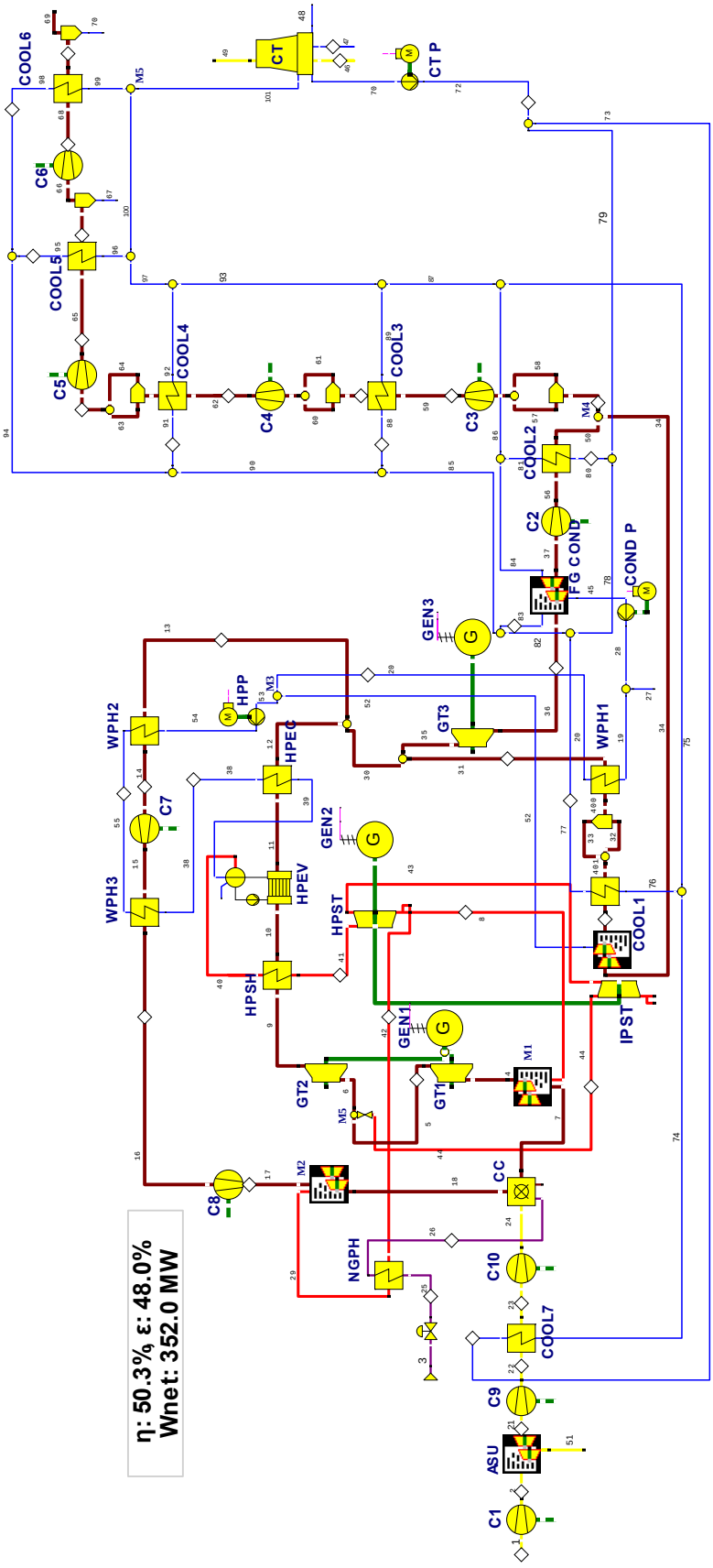

Figure A.7.1: Structure of the S-Graz cycle

Table A.7.1: Results at the component level for the S-Graz cycle

Component, k	$\dot{E}_{F,k}$ **(MW)**	$\dot{E}_{P,k}$ **(MW)**	$\dot{E}_{D,k}$ **(MW)**	ε_k **(%)**	$y_{D,k}$ **(%)**
C1	53.76	50.84	2.92	94.6	0.40
CC	736.37	551.82	184.55	74.9	25.17
GT1	264.57	253.32	11.25	95.7	1.53
GT2	362.41	345.23	17.18	95.3	2.34
GT3	78.21	69.56	8.65	88.9	1.18
HPSH	52.48	46.00	6.48	87.7	0.88
HPEV	65.48	58.00	7.47	88.6	1.02
HPEC	1.35	1.27	0.08	93.9	0.01
NGPH	7.05	3.61	3.44	51.2	0.47
WPH1	5.57	3.09	2.48	55.5	0.34
WPH2	31.83	25.56	6.27	80.3	0.85
WPH3	16.19	14.67	1.52	90.6	0.21
HPST	30.46	28.56	1.90	93.8	0.26
IPST	1.60	1.50	0.10	93.6	0.01
ASU	51.24	11.46	39.78	22.4	5.43
COND P	0.01	0.01	0.00	78.1	0.00
HPP	1.61	1.41	0.20	87.7	0.03
C2	12.45	11.04	1.41	88.7	0.19
C3	4.69	3.95	0.74	84.1	0.10
C4	4.70	3.93	0.77	83.5	0.11
C5	4.75	3.94	0.81	83.0	0.11
C6	4.84	3.97	0.87	81.9	0.12
C7	92.86	86.56	6.30	93.2	0.86
C8	132.31	124.67	7.63	94.2	1.04
C9	16.43	13.73	2.70	83.5	0.37
C10	17.72	14.93	2.80	84.2	0.38
M1	15.59	13.20	2.39	84.6	0.33
M2	13.73	11.40	2.33	83.0	0.32
M3	0.49	0.31	0.19	62.2	0.03
M4	0.04	0.02	0.02	40.8	0.00
M5	5.52	4.50	1.02	81.6	0.14
FG COND	13.67	-	7.36	-	1.00
COOL1	1.53	-	1.35	-	0.18
COOL2	4.55	-	4.30	-	0.59
COOL3	1.03	-	0.94	-	0.13
COOL4	1.03	-	0.94	-	0.13
COOL5	1.05	-	0.95	-	0.13
COOL6	19.22	-	1.00	-	0.14
COOL7	4.81	-	4.53	-	0.62
CT	7.42	-	3.63	-	0.50
Total	**733.16**	**352.01**	**349.26**	**48.0**	**47.64**
Exergy loss	**31.89**				

Table A.7.2: Results at the stream level for the S-Graz cycle

Stream, j	$\dot{m}_j$ (kg/s)	T_j (°C)	p_j (bar)	$\dot{E}_{PH,j}$ (MW)	$\dot{E}_{CH,j}$ (MW)	$\dot{E}_{tot,j}$ (MW)
1	256.1	15.00	1.01	0.00	0.40	0.40
2	256.1	218.93	6.00	50.84	0.40	51.24
3	14.1	15.00	50.00	8.19	724.58	732.76
4	379.1	1373.30	38.80	951.61	28.26	979.87
5	379.1	1069.85	10.71	687.04	28.26	715.30
6	383.8	1059.05	10.71	690.45	28.27	718.72
7	369.1	1401.51	38.80	941.38	28.24	969.62
8	10.0	393.86	42.96	12.62	0.02	12.65
9	383.8	614.29	1.04	328.04	28.27	356.31
10	383.8	504.92	1.03	275.56	28.27	303.83
11	383.8	346.17	1.02	210.08	28.27	238.36
12	383.8	342.48	1.02	208.74	28.27	237.01
13	213.0	342.48	1.02	115.83	15.69	131.52
14	213.0	144.00	1.01	84.00	15.69	99.69
15	213.0	394.07	6.33	170.57	15.69	186.26
16	213.0	315.00	6.33	154.38	15.69	170.07
17	213.0	646.91	40.00	279.05	15.69	294.74
18	293.0	547.48	40.00	370.66	15.89	386.55
19	85.1	36.16	1.03	0.26	0.21	0.48
20	85.1	95.00	1.00	3.35	0.21	3.57
21	62.0	15.00	1.01	0.00	7.40	7.40
22	62.0	297.19	6.80	13.73	7.40	21.13
23	62.0	60.00	6.79	8.92	7.40	16.31
24	62.0	359.60	40.00	23.84	7.40	31.24
25	14.1	15.00	40.02	7.72	724.58	732.30
26	14.1	330.00	40.00	11.80	724.58	736.37
27	31.5	36.16	1.03	0.10	0.08	0.18
28	116.7	36.16	1.03	0.36	0.29	0.65
29	80.0	331.66	40.81	93.94	0.20	94.14
30	170.8	342.48	1.02	92.90	12.58	105.49
31	13.1	342.48	1.02	7.12	0.96	8.09
32	6.4	89.12	1.01	1.32	0.95	2.27
33	6.7	89.11	1.01	0.23	0.02	0.25
34	3.5	30.00	1.00	0.00	0.94	0.94
35	157.7	342.48	1.02	85.78	11.62	97.40
36	157.7	75.09	0.06	7.57	11.62	19.19
37	41.1	36.16	0.06	-6.49	11.37	4.88
38	94.8	321.29	134.56	44.83	0.24	45.06
39	94.8	325.17	130.53	46.09	0.24	46.33
40	94.8	331.17	130.53	104.10	0.24	104.34
41	94.8	560.00	124.00	150.10	0.24	150.34
42	80.0	393.86	42.96	100.99	0.20	101.19
43	4.8	393.86	42.96	6.03	0.01	6.04
44	4.8	220.31	10.71	4.43	0.01	4.44
45	116.7	36.16	0.06	0.35	0.29	0.64
46	6143.5	15.00	1.01	0.00	9.56	9.56
47	177.2	15.00	1.01	0.00	0.44	0.44
48	87.8	16.00	1.01	0.00	0.22	0.22
49	6232.9	25.15	1.01	3.84	8.97	12.80
50	41.1	40.86	1.00	0.01	11.37	11.38
51	194.1	14.99	1.01	0.00	4.06	4.06
52	9.6	30.00	1.00	0.02	0.02	0.04
53	94.8	88.43	1.00	3.18	0.24	3.42
54	94.8	89.61	143.02	4.60	0.24	4.83
55	94.8	263.21	138.73	30.16	0.24	30.40
56	41.1	351.80	1.02	4.56	11.37	15.92
57	44.5	40.00	1.00	0.01	12.29	12.30
58	0.0	40.00	1.00	0.00	0.00	0.00
59	44.5	157.32	3.22	3.96	12.29	16.25
60	44.5	40.00	3.21	2.93	12.29	15.22
61	0.0	40.00	3.21	0.00	0.00	0.00
62	44.5	157.57	10.22	6.86	12.29	19.14
63	44.5	40.00	10.21	5.83	12.29	18.11
64	0.0	40.00	10.21	0.00	0.00	0.00
65	44.5	158.58	32.46	9.76	12.29	22.05
66	44.5	40.00	32.45	8.71	12.29	21.00
67	0.0	40.00	32.45	0.00	0.00	0.00
68	44.5	160.92	103.09	12.68	12.29	24.97

69	44.5	30.00	103.09	11.56	12.31	23.86
70	0.0	30.00	103.09	0.00	0.00	0.00
71	8776.5	16.00	1.01	0.06	21.92	21.99
72	8776.5	16.00	1.37	0.38	21.92	22.30
73	329.1	16.00	1.37	0.01	0.82	0.84
74	329.1	26.00	1.33	0.29	0.82	1.11
75	551.0	26.00	1.33	0.49	1.38	1.87
76	221.9	26.00	1.33	0.20	0.55	0.75
77	221.9	16.00	1.37	0.01	0.55	0.56
78	8156.4	16.00	1.37	0.35	20.37	20.73
79	8447.4	16.00	1.37	0.37	21.10	21.47
80	291.0	16.00	1.37	0.01	0.73	0.74
81	291.0	26.00	1.33	0.26	0.73	0.99
82	7934.5	16.00	1.37	0.34	19.82	20.16
83	7473.0	16.00	1.37	0.32	18.67	18.99
84	7473.0	25.00	1.33	5.54	18.67	24.21
85	461.5	16.00	1.37	0.02	1.15	1.17
86	7764.0	25.04	1.33	5.80	19.39	25.19
87	8315.0	25.10	1.33	6.29	20.77	27.06
88	111.1	16.00	1.37	0.00	0.28	0.28
89	111.1	26.00	1.33	0.10	0.28	0.38
90	350.4	16.00	1.37	0.02	0.88	0.89
91	111.3	16.00	1.37	0.00	0.28	0.28
92	111.3	26.00	1.33	0.10	0.28	0.38
93	8426.1	25.11	1.33	6.38	21.05	27.43
94	239.1	16.00	1.37	0.01	0.60	0.61
95	113.6	16.00	1.37	0.00	0.28	0.29
96	113.6	26.00	1.33	0.10	0.28	0.38
97	8537.4	25.12	1.33	6.48	21.33	27.81
98	125.5	16.00	1.37	0.01	0.31	0.32
99	125.5	26.00	1.33	0.11	0.31	0.43
100	8651.0	25.14	1.33	6.58	21.61	28.19
101	8776.5	25.15	1.33	6.69	21.92	28.62
102					*C7*	92.18
103					*C2*	12.52
104					*C3*	4.64
105					*C4*	4.70
106					*C5*	4.68
107					*C6*	4.76
108					*C1*	53.76
109					*C9*	16.43
110					*C10*	17.72
111					*P2*	1.52
112					*P1*	0.01
113					*C8*	132.38
114					*GT2*	344.16
115					*GT3*	69.50
116					*ST1*	28.71
117					*ST2*	1.65
118					*GT1*	253.37
119					*tot*	352.07

A.8: The ATR plant

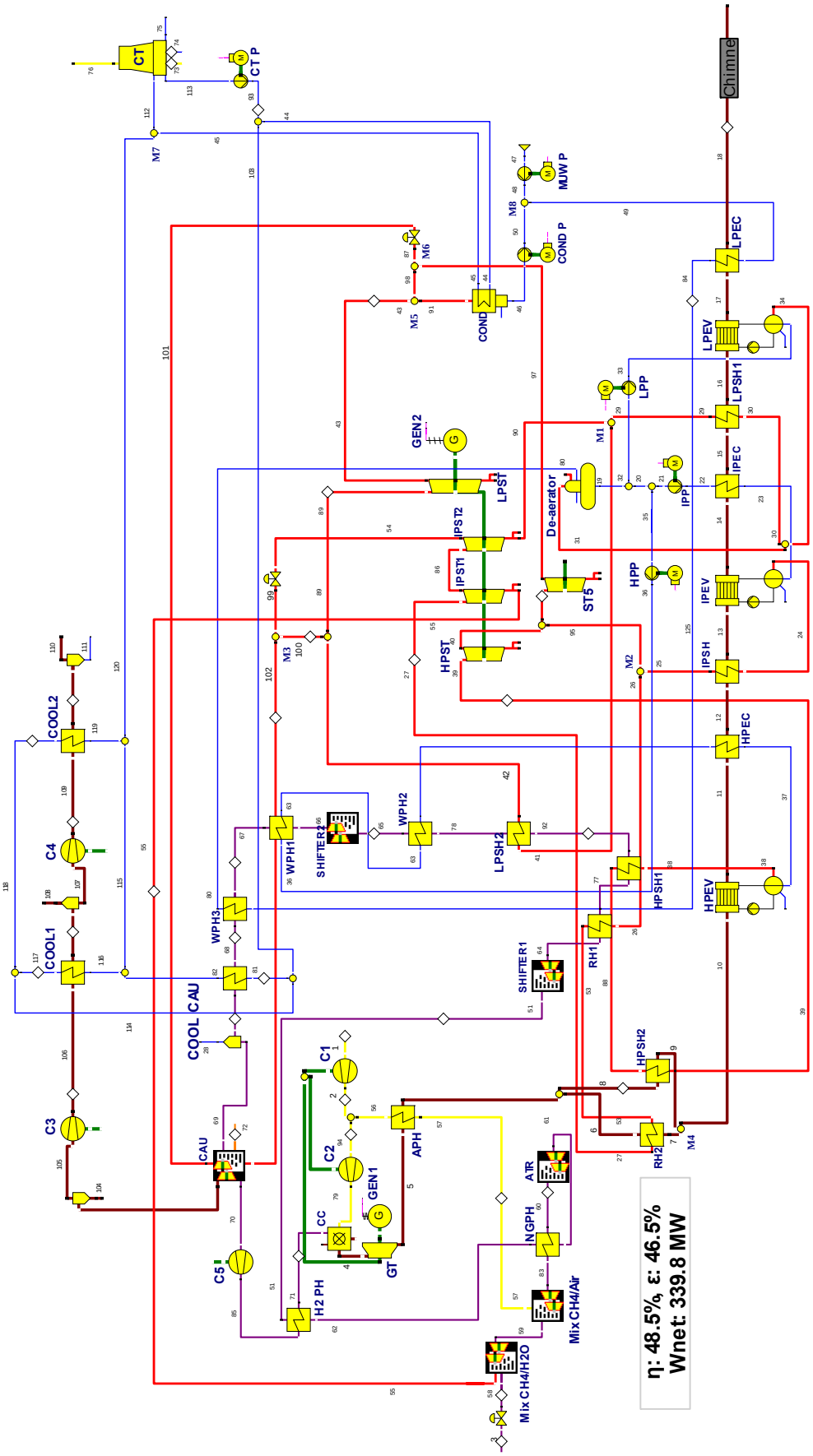

Figure A.8.1: Structure of the ATR plant

Table A.8.1: Results at the component level for the ATR plant

Component, k	$\dot{E}_{F,k}$ **(MW)**	$\dot{E}_{P,k}$ **(MW)**	$\dot{E}_{D,k}$ **(MW)**	ε_k **(%)**	$y_{D,k}$ **(%)**
C1	221.95	211.43	10.53	95.3	1.44
CC	659.64	502.80	156.84	76.2	21.47
GT1	519.91	500.85	19.06	96.3	2.61
HPSH1	2.37	2.06	0.31	86.9	0.04
HPSH2	26.00	23.38	2.62	89.9	0.36
HPEV	36.90	32.76	4.14	88.8	0.57
HPEC	10.69	9.40	1.29	87.9	0.18
RH1	11.37	10.65	0.72	93.7	0.10
RH2	8.76	7.95	0.81	90.8	0.11
IPSH	5.51	4.72	0.79	85.6	0.11
IPEV	30.37	26.75	3.62	88.1	0.50
IPEC	6.89	5.75	1.14	83.5	0.16
LPSH1	1.54	1.14	0.40	74.1	0.05
LPSH2	3.37	2.86	0.52	84.7	0.07
LPEV	19.39	15.73	3.66	81.1	0.50
LPEC	13.01	8.44	4.57	64.9	0.63
NGPH	34.36	30.19	4.17	87.9	0.57
H2 PH	32.61	25.32	7.30	77.6	1.00
APH	9.38	5.91	3.47	63.0	0.47
WPH1	3.05	2.69	0.36	88.1	0.05
WPH2	10.38	9.53	0.86	91.7	0.12
WPH3	1.26	1.10	0.16	87.2	0.02
HPST	19.56	18.30	1.26	93.6	0.17
IPST1	19.98	18.91	1.07	94.6	0.15
IPST2	15.88	14.64	1.24	92.2	0.17
LPST	23.85	20.61	3.24	86.4	0.44
ST5	11.30	9.91	1.39	87.7	0.19
ATR	809.32	-	51.81	-	7.09
SHIFTER1	690.54	-	3.43	-	0.47
SHIFTER2	659.61	-	0.63	-	0.09
CAU	33.54	-	29.95	-	4.10
COND P	0.04	0.03	0.01	77.5	0.00
HPP	1.05	0.89	0.17	84.3	0.02
IPP	0.18	0.14	0.04	77.8	0.01
LPP	0.05	0.01	0.03	28.9	0.00
MUW P	0.01	0.01	0.00	68.0	0.00
C2	10.21	9.84	0.37	96.4	0.05
C3	2.70	2.21	0.48	82.0	0.07
C4	2.87	2.33	0.54	81.2	0.07
C5	4.34	3.58	0.76	82.4	0.10
De-aerator	0.65	0.62	0.03	95.7	0.00
M1	0.17	0.16	0.01	95.9	0.00
M2	0.23	0.23	0.00	99.4	0.00
M4	1.79	1.78	0.01	99.2	0.00
M5	2.11	2.11	0.00	100.0	0.00
M6	1.01	0.95	0.06	94.1	0.01
M7	0.31	0.27	0.03	88.9	0.00
M8	0.08	0.04	0.05	43.0	0.01
Mix CH4/Air	428.31	419.98	8.33	98.1	1.14
Mix CH4/H2O	507.54	500.94	6.60	98.7	0.90
COOL CAU	13.71	-	12.63	-	1.73
COOL1	0.73	-	0.67	-	0.09
COOL2	0.62	-	0.56	-	0.08
COND	5.17	-	3.85	-	0.53
CT	2.50	-	1.48	-	0.20
Total	**730.62**	**339.81**	**358.06**	**46.5**	**49.01**
Exergy loss	**32.75**				

Table A.8.2: Results at the stream level for the ATR plant

Stream, j	$\dot{m}_j$ (kg/s)	T_j (°C)	p_j (bar)	$\dot{E}_{PH,j}$ (MW)	$\dot{E}_{CH,j}$ (MW)	$\dot{E}_{tot,j}$ (MW)
1	590.89	15.00	1.01	0.00	0.92	0.92
2	590.89	375.07	15.46	211.43	0.92	212.35
3	14.00	15.00	50.00	8.15	721.47	729.62
4	588.87	1250.87	16.49	701.33	1.78	703.11
5	588.87	577.02	1.11	181.42	1.78	183.19
6	178.87	562.53	1.06	52.24	0.54	52.78
7	178.87	498.89	1.05	43.48	0.54	44.02
8	410.00	562.53	1.06	119.78	1.24	121.02
9	410.00	479.33	1.05	93.78	1.24	95.02
10	588.87	485.28	1.05	137.25	1.78	139.03
11	588.87	395.77	1.05	100.35	1.78	102.13
12	588.87	367.81	1.05	89.66	1.78	91.43
13	588.87	352.91	1.05	84.14	1.78	85.92
14	588.87	263.09	1.04	53.77	1.78	55.55
15	588.87	240.05	1.04	46.88	1.78	48.66
16	588.87	234.70	1.04	45.34	1.78	47.11
17	588.87	158.26	1.03	25.95	1.78	27.72
18	588.87	83.81	1.03	12.94	1.78	14.72
19	112.53	142.17	3.84	10.41	0.28	10.69
20	89.32	142.17	3.84	8.26	0.22	8.48
21	34.11	142.17	3.84	3.15	0.09	3.24
22	34.11	142.74	39.68	3.30	0.09	3.38
23	34.11	242.09	38.49	9.05	0.09	9.13
24	34.11	248.09	38.49	35.80	0.09	35.89
25	34.11	347.81	36.57	40.52	0.09	40.61
26	78.85	352.99	36.57	94.21	0.20	94.41
27	78.85	532.53	33.00	112.81	0.20	113.01
28	17.69	60.00	13.20	0.26	0.04	0.30
29	22.26	220.05	4.32	18.30	0.06	18.35
30	22.26	148.26	4.54	17.16	0.06	17.21
31	0.95	148.26	4.54	0.74	0.00	0.74
32	23.21	142.17	3.84	2.15	0.06	2.20
33	23.21	142.56	4.54	2.16	0.06	2.22
34	23.21	148.26	4.54	17.89	0.06	17.95
35	55.21	142.17	3.84	5.11	0.14	5.24
36	55.21	144.16	146.05	5.99	0.14	6.13
37	55.21	329.19	137.40	27.61	0.14	27.74
38	55.21	335.19	137.40	60.37	0.14	60.51
39	55.21	542.53	124.00	85.81	0.14	85.94
40	55.21	356.97	36.57	66.25	0.14	66.39
41	30.28	228.43	4.32	25.12	0.08	25.19
42	30.28	331.00	4.10	27.97	0.08	28.05
43	30.28	32.88	0.05	4.12	0.08	4.20
44	3078.21	16.00	1.37	0.13	7.69	7.82
45	3078.21	22.88	1.33	1.46	7.69	9.15
46	80.52	32.88	0.05	0.17	0.20	0.37
47	31.05	15.00	1.01	0.00	0.08	0.08
48	31.05	15.02	4.08	0.01	0.08	0.09
49	111.57	27.92	4.08	0.17	0.28	0.44
50	80.52	32.90	4.08	0.20	0.20	0.41
51	105.94	350.00	14.06	66.40	624.13	690.54
52	55.21	268.18	141.65	18.21	0.14	18.34
53	78.85	457.45	34.74	104.86	0.20	105.06
54	39.77	251.79	4.32	33.83	0.10	33.93
55	31.05	411.52	15.00	36.56	0.08	36.64
56	60.89	375.07	15.46	21.79	0.09	21.88
57	60.89	530.00	14.69	27.70	0.09	27.79
58	14.00	15.00	15.00	5.63	721.47	727.11
59	45.05	297.03	15.00	38.14	721.51	759.66
60	105.94	640.00	14.67	92.02	717.30	809.32
61	105.94	850.00	14.09	133.33	624.18	757.51
62	105.94	619.43	14.07	99.01	624.13	723.15
63	55.21	178.15	141.67	8.68	0.14	8.82
64	105.94	470.24	13.63	76.00	611.10	687.10
65	105.94	200.00	13.62	48.51	611.10	659.61
66	105.94	212.43	13.21	48.67	610.31	658.98
67	105.94	170.00	13.20	45.62	610.31	655.93
68	105.94	150.00	13.20	44.36	610.31	654.67

69	88.25	60.00	13.20	30.39	610.27	640.65
70	58.87	63.12	12.94	26.00	604.75	630.75
71	58.87	510.46	17.00	54.89	604.75	659.64
72	1088.22	31.23	14.00	3.42	2.72	6.14
73	3363.76	15.00	1.01	0.00	5.24	5.24
74	90.98	15.00	1.01	0.00	0.23	0.23
75	48.05	16.00	1.01	0.00	0.12	0.12
76	3406.68	23.64	1.01	1.46	4.89	6.36
77	105.94	372.99	13.63	64.63	611.10	675.73
78	105.94	318.25	13.62	58.89	611.10	669.99
79	530.00	392.88	17.00	199.48	0.82	200.31
80	111.57	137.89	3.84	9.70	0.28	9.98
81	1552.28	16.00	1.37	0.07	3.88	3.94
82	1552.28	25.00	1.33	1.15	3.88	5.03
83	105.94	385.00	14.69	61.83	717.30	779.12
84	111.57	130.00	3.96	8.60	0.28	8.88
85	58.87	97.75	17.08	29.57	604.75	634.32
86	47.80	411.52	15.00	56.27	0.12	56.39
87	39.77	20.09	0.05	0.00	0.10	0.10
88	55.21	338.32	130.53	62.43	0.14	62.56
89	30.28	331.00	4.10	27.97	0.08	28.05
90	8.03	251.79	4.32	6.83	0.02	6.85
91	80.52	32.88	0.05	5.34	0.20	5.54
92	105.94	351.00	13.63	62.26	611.10	673.37
93	4805.37	16.00	1.37	0.21	12.00	12.21
94	530.00	375.07	15.46	189.64	0.82	190.47
95	44.74	356.97	36.57	53.69	0.11	53.80
96	10.46	356.97	36.57	12.56	0.03	12.58
97	10.46	32.88	0.05	1.26	0.03	1.29
98	50.24	32.88	0.05	1.22	0.13	1.35
99	39.77	251.43	4.10	33.56	0.10	33.66
100	0.00	331.00	4.10	0.00	0.00	0.00
101	39.77	20.00	4.10	0.02	0.10	0.12
102	39.77	251.43	4.10	33.56	0.10	33.66
103	1727.16	16.00	1.37	0.07	4.31	4.39
104	0.13	57.11	12.94	0.00	0.00	0.00
105	29.24	57.11	12.94	4.16	9.34	13.50
106	29.24	155.75	34.60	6.37	9.34	15.71
107	29.11	40.00	34.59	5.63	9.36	14.98
108	0.14	40.00	34.59	0.00	0.00	0.00
109	29.11	147.40	103.09	7.96	9.36	17.32
110	29.09	30.00	103.09	7.33	9.36	16.69
111	0.02	30.00	103.09	0.00	0.00	0.00
112	4805.37	23.64	1.33	2.71	12.00	14.71
113	4805.37	16.00	1.01	0.03	12.00	12.04
114	174.88	16.00	1.37	0.01	0.44	0.44
115	1643.63	25.00	1.33	1.22	4.11	5.32
116	91.35	25.00	1.33	0.07	0.23	0.30
117	91.35	16.00	1.37	0.00	0.23	0.23
118	83.53	16.00	1.37	0.00	0.21	0.21
119	83.53	25.00	1.33	0.06	0.21	0.27
120	1727.16	25.00	1.33	1.28	4.31	5.60
121					*C1*	221.95
122					*ST1*	18.30
123					*ST2*	18.91
124					*ST3*	14.64
125					*ST4*	20.61
126					*COND P*	0.04
127					*LPP*	0.05
128					*IPP*	0.18
129					*HPP*	1.05
130					*C2*	10.21
131					*MUW P*	0.01
132					*C5*	4.34
133					*C3*	2.70
134					*C4*	2.87
135					*GT1*	268.69
136					*ST5*	9.91
137					*tot*	339.81

A.9: The MSR plant

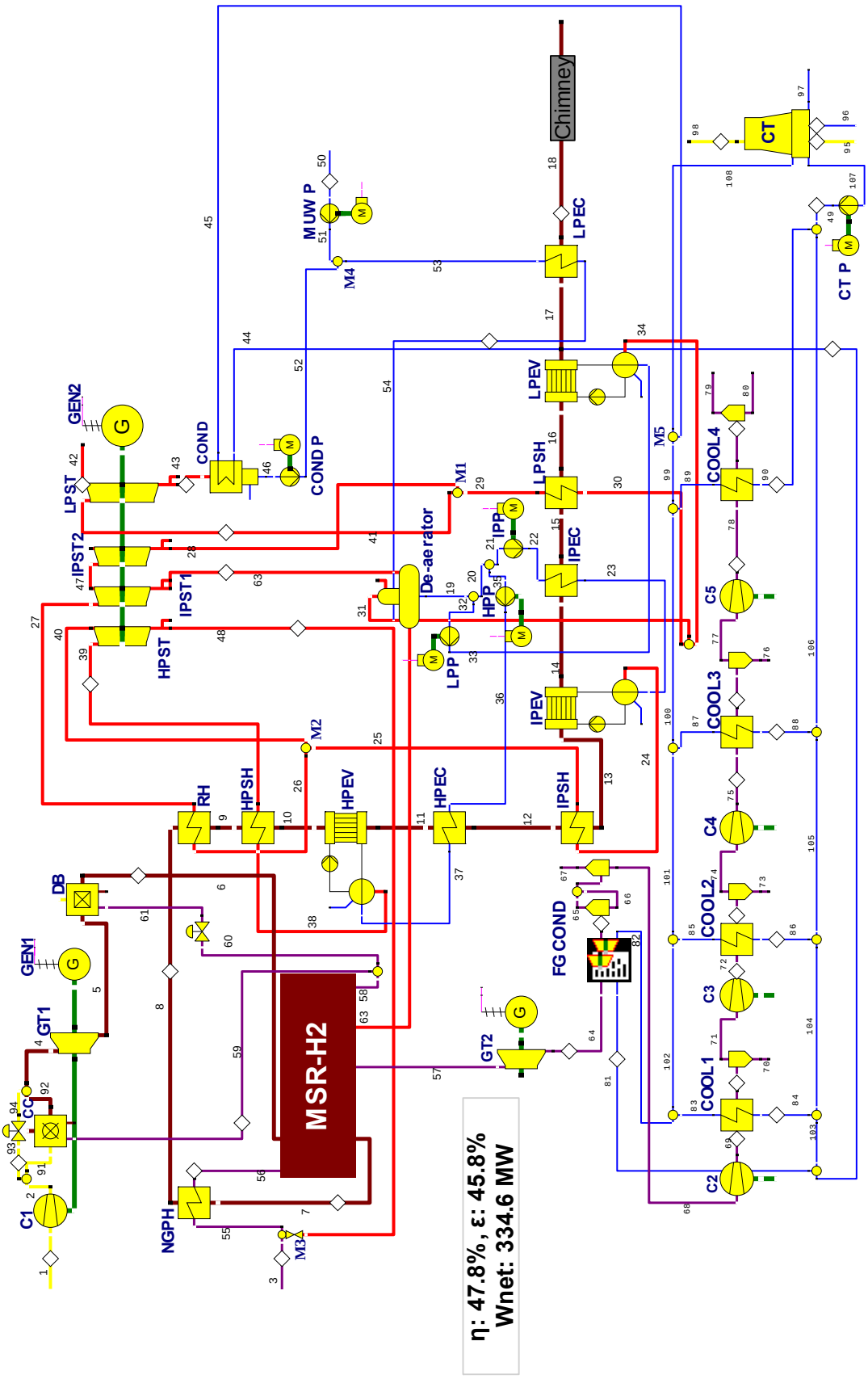

Figure A.9.1: Structure of the MSR plant

Table A.9.1: Results at the component level for the MSR plant

Component, k	$\dot{E}_{F,k}$ **(MW)**	$\dot{E}_{P,k}$ **(MW)**	$\dot{E}_{D,k}$ **(MW)**	ε_k **(%)**	$y_{D,k}$ **(%)**
C1	206.31	196.73	9.58	95.4	1.31
CC	598.70	455.59	143.11	76.1	19.59
DB	338.16	252.94	85.23	74.8	11.66
GT1	481.89	463.51	18.37	96.2	2.51
GT2	54.18	50.81	3.37	93.8	0.46
RH	8.28	7.21	1.07	87.1	0.15
HPSH	36.79	32.41	4.38	88.1	0.60
HPEV	47.13	40.95	6.17	86.9	0.84
HPEC	32.45	25.58	6.86	78.8	0.94
IPSH	0.70	0.59	0.11	83.7	0.02
IPEV	10.47	9.89	0.59	94.4	0.08
IPEC	3.45	2.84	0.62	82.2	0.08
LPSH	3.17	2.40	0.77	75.7	0.11
LPEV	27.16	21.11	6.05	77.7	0.83
LPEC	13.93	9.33	4.60	67.0	0.63
NGPH	32.62	28.56	4.06	87.6	0.56
HPST	17.71	16.64	1.08	93.9	0.15
IPST1	8.22	7.78	0.45	94.6	0.06
IPST2	0.29	0.27	0.02	93.6	0.00
LPST	22.33	19.29	3.03	86.4	0.42
MSR-H2	180.20	171.88	8.32	95.4	1.14
COND P	0.02	0.01	0.01	68.5	0.00
LPP	0.00	0.00	0.00	69.4	0.00
HPP	1.14	0.98	0.16	85.7	0.02
IPP	0.12	0.08	0.03	70.7	0.00
MUW P	0.03	0.02	0.01	77.0	0.00
C2	3.84	3.19	0.64	83.2	0.09
C3	4.06	3.37	0.69	83.0	0.09
C4	4.04	3.33	0.71	82.4	0.10
C5	4.10	3.34	0.76	81.4	0.10
De-aerator	0.51	0.49	0.02	95.6	0.00
M1	0.02	0.02	0.00	96.1	0.00
M2	1.17	1.07	0.10	91.5	0.01
M3	569.88	565.03	4.85	99.1	0.66
M4	0.06	0.01	0.05	22.9	0.01
M5	0.53	0.45	0.08	85.1	0.01
FG COND	16.69	-	15.06	-	2.06
COOL1	0.68	-	0.60	-	0.08
COOL2	0.94	-	0.85	-	0.12
COOL3	0.89	-	0.80	-	0.11
COOL4	0.92	-	0.83	-	0.11
COND	4.02	-	2.99	-	0.41
CT	2.93	-	1.62	-	0.22
Total	**730.63**	**334.64**	**338.70**	**45.8**	**46.36**
Exergy loss	**57.29**				

Table A.9.2: Results at the stream level for the MSR plant

Stream, j	$\dot{m}_j$ (kg/s)	T_j (°C)	p_j (bar)	$\dot{E}_{PH,j}$ (MW)	$\dot{E}_{CH,j}$ (MW)	$\dot{E}_{tot,j}$ (MW)
1	523.00	15.00	1.01	0.00	0.81	0.81
2	523.00	392.51	17.00	196.73	0.81	197.54
3	14.00	15.00	50.00	8.15	721.47	729.62
4	542.30	1230.15	16.49	652.06	1.07	653.13
5	542.30	567.08	1.11	170.17	1.07	171.25
6	553.20	994.77	1.10	422.50	1.69	424.18
7	553.20	674.76	1.06	242.30	1.69	243.98
8	553.20	609.47	1.06	209.68	1.69	211.37
9	553.20	592.38	1.06	201.40	1.69	203.09
10	553.20	513.25	1.05	164.61	1.69	166.30
11	553.20	401.68	1.05	117.48	1.69	119.17
12	553.20	314.01	1.04	85.04	1.69	86.72
13	553.20	311.97	1.04	84.34	1.69	86.02
14	553.20	280.43	1.04	73.86	1.69	75.55
15	553.20	269.55	1.04	70.41	1.69	72.09
16	553.20	259.32	1.04	67.23	1.69	68.92
17	553.20	156.38	1.03	40.07	1.69	41.76
18	553.20	72.68	1.03	26.14	1.69	27.82
19	111.13	139.81	3.60	9.93	0.28	10.21
20	79.81	139.81	3.60	7.13	0.20	7.33
21	12.89	139.81	3.60	1.15	0.03	1.18
22	12.89	140.86	57.12	1.24	0.03	1.27
23	12.89	264.43	55.40	4.07	0.03	4.11
24	12.89	270.43	55.40	13.96	0.03	13.99
25	12.89	294.01	52.63	14.55	0.03	14.58
26	23.81	347.74	52.63	28.84	0.06	28.90
27	23.81	559.47	50.00	36.05	0.06	36.10
28	0.83	217.70	4.10	0.67	0.00	0.68
29	30.57	249.55	4.10	25.74	0.08	25.82
30	30.57	146.37	4.32	23.34	0.08	23.42
31	0.75	146.37	4.32	0.58	0.00	0.58
32	31.32	139.81	3.60	2.80	0.08	2.88
33	31.32	139.82	4.32	2.80	0.08	2.88
34	31.32	146.37	4.32	23.92	0.08	24.00
35	66.92	139.81	3.60	5.98	0.17	6.15
36	66.92	141.54	134.56	6.96	0.17	7.13
37	66.92	325.17	130.53	32.54	0.17	32.71
38	66.92	331.17	130.53	73.50	0.17	73.67
39	66.92	559.38	124.00	105.91	0.17	106.08
40	10.92	422.41	52.63	14.39	0.03	14.41
41	31.40	248.71	4.10	26.42	0.08	26.50
42	0.00	32.88	0.05	0.00	0.00	0.00
43	31.40	32.88	0.05	4.09	0.08	4.17
44	2394.26	16.00	1.37	0.10	5.98	6.08
45	2394.26	22.88	1.33	1.14	5.98	7.12
46	31.40	32.88	0.05	0.07	0.08	0.15
47	0.83	392.96	17.00	0.97	0.00	0.97
48	56.00	422.41	52.63	73.81	0.14	73.95
49	4731.69	16.00	1.37	0.21	11.82	12.02
50	78.98	15.00	1.01	0.00	0.20	0.20
51	78.98	15.01	3.71	0.02	0.20	0.22
52	31.40	32.90	3.71	0.08	0.08	0.16
53	110.38	20.10	3.71	0.05	0.28	0.33
54	110.38	136.38	3.60	9.38	0.28	9.65
55	70.00	321.58	50.00	77.15	721.58	798.72
56	70.00	600.00	49.98	105.71	721.58	827.28
57	62.78	816.97	47.98	70.90	18.31	89.22
58	30.20	684.06	17.00	88.36	848.50	936.86
59	19.30	684.06	17.00	56.47	542.23	598.70
60	10.90	684.06	17.00	31.90	306.27	338.16
61	10.90	684.06	1.11	20.42	306.27	326.68
62	70.00	600.00	47.98	112.27	861.61	973.88
63	22.98	392.96	17.00	26.85	0.06	26.91
64	62.78	288.45	1.02	16.73	18.31	35.04
65	24.02	25.00	1.01	0.02	0.06	0.08
66	38.75	25.00	1.01	0.02	18.25	18.27
67	24.02	25.00	1.01	0.02	0.06	0.08
68	38.75	25.00	1.01	0.02	18.25	18.27

69	38.75	131.81	3.22	3.21	18.25	21.47
70	0.14	40.00	3.21	0.00	0.00	0.00
71	38.61	40.00	3.21	2.54	18.25	20.79
72	38.61	151.95	10.22	5.91	18.25	24.16
73	0.26	40.00	10.21	0.00	0.00	0.00
74	38.36	40.00	10.21	4.96	18.26	23.22
75	38.36	152.83	32.46	8.29	18.26	26.55
76	0.08	40.00	32.45	0.00	0.00	0.00
77	38.28	40.00	32.45	7.39	18.27	25.66
78	38.28	154.99	103.09	10.73	18.27	29.00
79	0.03	30.00	103.09	0.00	0.00	0.00
80	38.25	30.00	103.09	9.80	18.28	28.08
81	1932.57	16.00	1.37	0.08	4.83	4.91
82	1932.57	26.00	1.33	1.72	4.83	6.54
83	86.75	26.00	1.33	0.08	0.22	0.29
84	86.75	16.00	1.37	0.00	0.22	0.22
85	111.06	26.00	1.33	0.10	0.28	0.38
86	111.06	16.00	1.37	0.00	0.28	0.28
87	100.23	26.00	1.33	0.09	0.25	0.34
88	100.23	16.00	1.37	0.00	0.25	0.25
89	106.82	26.00	1.33	0.09	0.27	0.36
90	106.82	16.00	1.37	0.00	0.27	0.27
91	419.00	392.51	17.00	157.61	0.65	158.26
92	438.30	1392.45	16.49	624.23	1.04	625.27
93	104.00	392.51	17.00	39.12	0.16	39.28
94	104.00	392.51	16.49	38.86	0.16	39.02
95	3312.18	15.00	1.01	0.00	5.16	5.16
96	92.58	15.00	1.01	0.00	0.23	0.23
97	47.32	16.00	1.01	0.00	0.12	0.12
98	3357.45	24.42	1.01	1.75	4.83	6.57
99	2337.43	26.00	1.33	2.08	5.84	7.92
100	2230.61	26.00	1.33	1.98	5.57	7.55
101	2130.38	26.00	1.33	1.89	5.32	7.21
102	2019.32	26.00	1.33	1.79	5.04	6.84
103	4326.83	16.00	1.37	0.19	10.81	11.00
104	4413.58	16.00	1.37	0.19	11.02	11.22
105	4524.64	16.00	1.37	0.20	11.30	11.50
106	4624.87	16.00	1.37	0.20	11.55	11.75
107	4731.69	16.00	1.01	0.03	11.82	11.85
108	4731.69	24.42	1.33	3.13	11.82	14.95
109					*C1*	206.31
110					*ST1*	16.67
111					*ST2*	7.80
112					*ST3*	0.29
113					*ST4*	19.33
114					*COND P*	0.02
115					*LPP*	0.00
116					*HPP*	1.15
117					*IPP*	0.12
118					*GT1*	256.99
119					*GT2*	50.81
120					*MUW P*	0.03
121					*C2*	3.84
122					*C3*	4.06
123					*C4*	4.04
124					*C5*	4.10
125					*tot*	334.53

A.10: The simple oxy-fuel plant

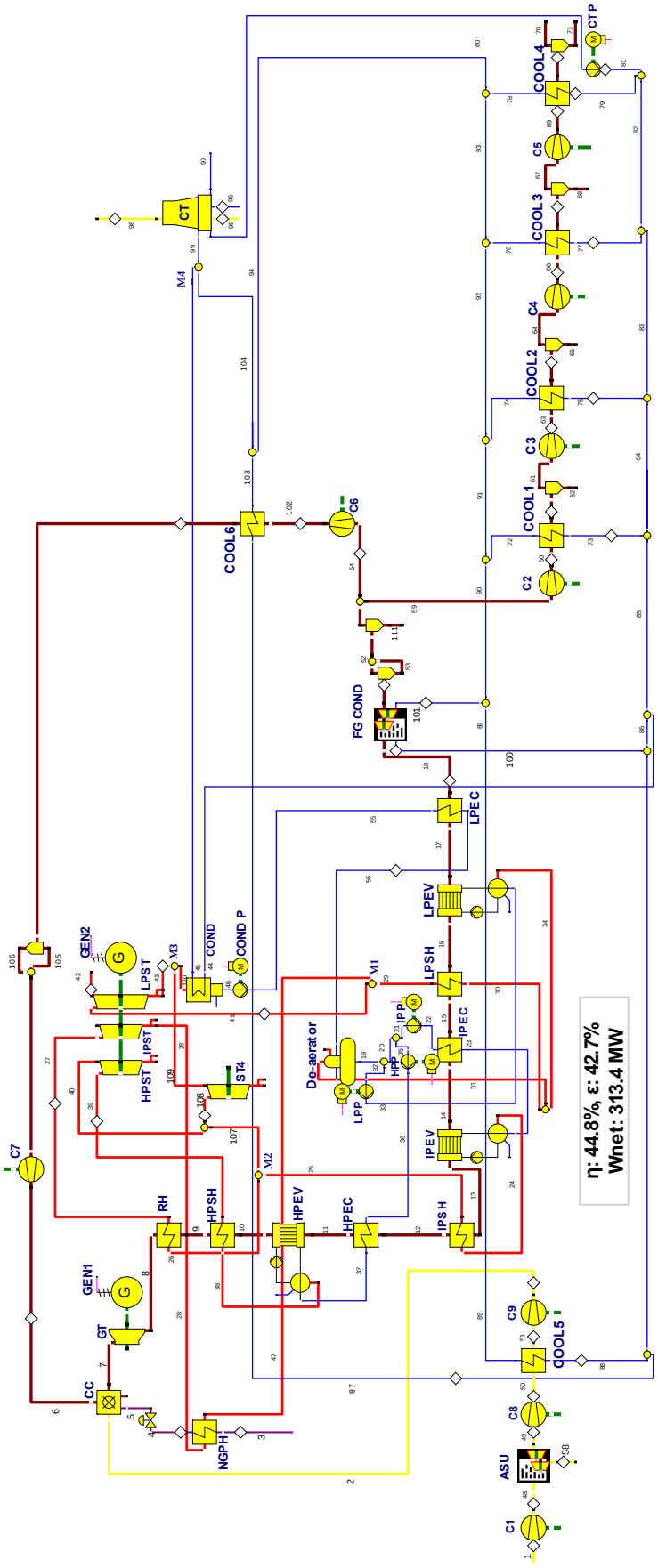

Figure A.10.1: Structure of the simple oxy-fuel plant

Table A.10.1: Results at the component level for the simple oxy-fuel plant

Component, k	$\dot{E}_{F,k}$ **(MW)**	$\dot{E}_{P,k}$ **(MW)**	$\dot{E}_{D,k}$ **(MW)**	ε_k **(%)**	$y_{D,k}$ **(%)**
C1	56.60	53.53	3.07	94.6	0.42
CC	733.81	512.57	221.24	69.9	30.18
GT	437.91	420.80	17.11	96.1	2.33
HPSH	41.65	35.88	5.78	86.1	0.79
HPEV	51.98	45.21	6.78	87.0	0.92
HPEC	33.59	28.22	5.37	84.0	0.73
RH	22.83	18.78	4.05	82.3	0.55
IPSH	0.10	0.06	0.04	61.4	0.01
IPEV	4.45	4.20	0.25	94.4	0.03
IPEC	0.77	0.65	0.13	83.7	0.02
LPSH	0.85	0.62	0.23	72.9	0.03
LPEV	12.43	10.24	2.20	82.3	0.30
LPEC	10.23	7.73	2.50	75.6	0.34
NGPH	3.56	1.04	2.52	29.3	0.34
HPST	35.41	33.02	2.39	93.2	0.33
IPST	28.63	26.97	1.66	94.2	0.23
LPST	51.25	44.29	6.96	86.4	0.95
ST4	21.91	19.22	2.69	87.7	0.37
ASU	53.95	11.59	42.36	21.5	5.78
COND P	0.04	0.03	0.01	78.5	0.00
LPP	0.00	0.00	0.00	64.3	0.00
HPP	1.25	1.08	0.17	86.1	0.02
IPP	0.02	0.01	0.01	63.9	0.00
C2	4.82	4.05	0.78	83.9	0.11
C3	4.80	4.01	0.79	83.5	0.11
C4	4.76	3.95	0.81	83.0	0.11
C5	4.83	3.96	0.87	82.1	0.12
C6	62.77	57.08	5.70	90.9	0.78
C7	56.67	54.82	1.85	96.7	0.25
C8	16.43	13.73	2.70	83.5	0.37
C9	17.89	15.08	2.81	84.3	0.38
De-aerator	0.46	0.44	0.02	95.6	0.00
M1	0.65	0.61	0.04	93.1	0.01
M2	0.50	0.46	0.04	92.4	0.01
M3	0.17	0.17	0.00	100.0	0.00
M4	1.20	1.02	0.18	84.9	0.02
FG COND	9.39	-	7.63	-	1.04
COOL1	1.16	-	1.03	-	0.14
COOL2	1.14	-	1.03	-	0.14
COOL3	1.07	-	0.97	-	0.13
COOL4	1.10	-	1.00	-	0.14
COOL5	4.87	-	4.59	-	0.63
COOL6	17.07	-	15.78	-	2.15
COND	11.84	-	8.81	-	1.20
CT	6.62	-	3.78	-	0.51
Total	**733.18**	**313.40**	**388.71**	**42.7**	**53.02**
Exergy loss	**31.08**				

Table A.10.2: Results at the stream level for the simple oxy-fuel plant

Stream, j	$\dot{m}_j$ (kg/s)	T_j (°C)	p_j (bar)	$\dot{E}_{PH,j}$ (MW)	$\dot{E}_{CH,j}$ (MW)	$\dot{E}_{tot,j}$ (MW)
1	269.63	15.00	1.01	0.00	0.42	0.42
2	62.00	362.30	40.00	23.94	7.40	31.33
3	14.06	15.00	50.00	8.19	724.58	732.76
4	14.06	200.00	49.99	9.70	724.58	734.27
5	14.06	200.00	40.00	9.23	724.58	733.81
6	382.00	190.05	40.00	95.67	102.82	198.49
7	458.06	1400.60	38.80	627.23	115.16	742.39
8	458.06	706.24	1.04	189.31	115.16	304.48
9	458.06	649.69	1.04	166.49	115.16	281.65
10	458.06	539.56	1.04	124.83	115.16	240.00
11	458.06	381.68	1.03	72.85	115.16	188.01
12	458.06	253.47	1.02	39.26	115.16	154.42
13	458.06	253.03	1.02	39.16	115.16	154.32
14	458.06	232.65	1.02	34.71	115.16	149.87
15	458.06	228.98	1.02	33.94	115.16	149.10
16	458.06	224.88	1.02	33.08	115.16	148.25
17	458.06	156.38	1.02	20.65	115.16	135.81
18	458.06	66.08	1.02	10.42	115.16	125.58
19	94.41	140.01	3.62	8.46	0.24	8.70
20	79.22	140.01	3.62	7.10	0.20	7.30
21	5.36	140.01	3.62	0.48	0.01	0.49
22	5.36	140.52	25.13	0.49	0.01	0.51
23	5.36	216.62	24.38	1.14	0.01	1.16
24	5.36	222.62	24.38	5.35	0.01	5.36
25	5.36	233.47	23.16	5.41	0.01	5.42
26	56.94	304.77	23.16	62.36	0.14	62.50
27	56.94	560.24	22.00	81.13	0.14	81.27
28	56.94	323.28	4.32	52.50	0.14	52.64
29	14.51	208.98	4.10	11.70	0.04	11.74
30	14.51	146.37	4.32	11.08	0.04	11.12
31	0.68	146.37	4.32	0.52	0.00	0.52
32	15.19	140.01	3.62	1.36	0.04	1.40
33	15.19	140.02	4.32	1.36	0.04	1.40
34	15.19	146.37	4.32	11.60	0.04	11.64
35	73.86	140.01	3.62	6.62	0.18	6.80
36	73.86	141.70	134.56	7.70	0.18	7.88
37	73.86	325.17	130.53	35.92	0.18	36.11
38	73.86	331.17	130.53	81.13	0.18	81.31
39	73.86	560.19	124.00	117.00	0.18	117.19
40	73.86	312.86	23.16	81.59	0.18	81.77
41	71.46	255.91	4.10	60.60	0.18	60.78
42	0.00	32.88	0.05	0.00	0.00	0.00
43	71.46	32.88	0.05	9.35	0.18	9.53
44	7048.82	16.00	1.37	0.31	17.61	17.91
45	7048.82	22.88	1.33	3.34	17.61	20.95
46	93.73	32.88	0.05	0.20	0.23	0.43
47	56.94	267.96	4.10	48.94	0.14	49.08
48	269.63	218.93	6.00	53.53	0.42	53.95
49	62.00	15.00	1.01	0.00	7.40	7.40
50	62.00	297.19	6.80	13.73	7.40	21.13
51	62.00	60.00	6.70	8.86	7.40	16.25
52	427.59	35.00	1.01	0.95	115.09	116.03
53	30.47	35.00	1.01	0.08	0.08	0.16
54	382.00	35.00	1.01	0.84	102.82	103.66
55	93.73	32.89	3.73	0.23	0.23	0.47
56	93.73	136.38	3.62	7.96	0.23	8.20
57	1851.17	16.00	1.37	0.08	4.62	4.70
58	207.63	15.00	1.01	0.00	4.19	4.19
59	45.59	35.00	1.01	0.10	12.27	12.37
60	45.59	150.46	3.22	4.15	12.27	16.42
61	44.93	40.00	3.21	2.99	12.27	15.26
62	0.66	40.00	3.21	0.00	0.00	0.00
63	44.93	157.80	10.22	7.00	12.27	19.27
64	44.62	40.00	10.21	5.85	12.28	18.12
65	0.31	40.00	10.21	0.00	0.00	0.00
66	44.62	158.62	32.46	9.80	12.28	22.08
67	44.53	40.00	32.45	8.71	12.29	21.00
68	0.09	40.00	32.45	0.00	0.00	0.00

69	44.53	160.61	103.09	12.67	12.29	24.97
70	44.49	30.00	103.09	11.56	12.31	23.86
71	0.04	30.00	103.09	0.00	0.00	0.00
72	147.63	26.00	1.33	0.13	0.37	0.50
73	147.63	16.00	1.37	0.01	0.37	0.38
74	131.16	26.00	1.33	0.12	0.33	0.44
75	131.16	16.00	1.37	0.01	0.33	0.33
76	118.20	26.00	1.33	0.11	0.30	0.40
77	118.20	16.00	1.37	0.01	0.30	0.30
78	125.21	26.00	1.33	0.11	0.31	0.42
79	125.21	16.00	1.37	0.01	0.31	0.32
80	11504.08	16.00	1.01	506.75	28.74	535.48
81	11504.08	16.00	1.37	0.50	28.74	29.24
82	11378.87	16.00	1.37	0.49	28.42	28.92
83	11260.66	16.00	1.37	0.49	28.13	28.62
84	11129.50	16.00	1.37	0.48	27.80	28.28
85	10981.87	16.00	1.37	0.48	27.43	27.91
86	3933.05	16.00	1.37	0.17	9.82	10.00
87	1522.06	16.00	1.37	0.07	3.80	3.87
88	329.12	16.00	1.37	0.01	0.82	0.84
89	329.12	26.00	1.33	0.29	0.82	1.11
90	2410.99	26.00	1.33	2.14	6.02	8.16
91	2558.62	26.00	1.33	2.27	6.39	8.66
92	2689.78	26.00	1.33	2.39	6.72	9.11
93	2807.99	26.00	1.33	2.49	7.01	9.51
94	2933.20	26.00	1.33	2.61	7.33	9.93
95	8052.86	15.00	1.01	0.00	12.53	12.53
96	221.94	15.00	1.01	0.00	0.55	0.55
97	115.04	16.00	1.01	0.00	0.29	0.29
98	8159.75	24.09	1.01	3.92	11.73	15.65
99	11504.08	24.09	1.33	7.12	28.74	35.86
100	2081.87	16.00	1.37	0.09	5.20	5.29
101	2081.87	26.00	1.33	1.85	5.20	7.05
102	382.00	210.13	6.37	57.92	102.82	160.74
103	1522.06	26.00	1.33	1.35	3.80	5.15
104	4455.26	26.00	1.33	3.96	11.13	15.09
105	377.84	60.00	6.36	40.80	102.81	143.61
106	4.16	60.00	6.36	0.06	0.01	0.07
107	51.59	312.86	23.16	56.99	0.13	57.12
108	22.27	312.86	23.16	24.60	0.06	24.66
109	22.27	32.88	0.05	2.70	0.06	2.75
110	93.73	32.88	0.05	12.04	0.23	12.28
111	30.47	35.00	1.01	0.08	0.08	0.16
112					*C1*	56.15
113					*C7*	56.23
114					*ST1*	32.70
115					*ST2*	27.64
116					*ST3*	44.23
117					*COND P*	0.04
118					*LPP*	0.00
119					*HPP*	1.17
120					*IPP*	0.03
121					*C6*	62.28
122					*C2*	4.78
123					*C3*	4.76
124					*C4*	4.73
125					*C5*	4.79
126					*GT1*	299.14
127					*C8*	16.30
128					*C9*	17.75
129					*ST4*	19.07
130					*tot*	312.27

Appendix B

Assumptions used in the simulations and the conventional analyses

B.1 Calculation of efficiencies and pressure drops for common components of the power plants

B.1.1 Compressors and expanders of GT systems (C1 and GT1) and CO_2/H_2O expanders (GT2)

The same polytropic efficiency has been assumed for C1, GT1 and GT2 (94% for the compressor and 91% for the expanders).

Table B.1: Efficiencies of C1 and GT1 GT2 (all components have a mechanical efficiency of 99%)

Compressors (C1) [a]			Expanders (GT1)[a]		
	η_{pol} (%)	η_{is} (%)		η_{pol} (%)	η_{is} (%)
Base	94.0	91.5	**Base**	91.0	93.4
MEA-0	94.0	91.5	**MEA-0**	91.0	93.4
MEA-0.2	94.0	91.5	**MEA-0.2**	91.0	93.4
Simple oxy-fuel	94.0	92.4	**Simple oxy-fuel**	91.0	93.1
S-Graz	94.0	92.4	**S-Graz**		
AZEP 85	94.0	91.5	**GT1**	91.0	92.0
AZEP 100	94.0	91.5	**GT2**	91.0	93.0
CLC	94.0	91.5	**AZEP 85**	91.0	93.5
MSR	94.0	91.6	**AZEP 100**	91.0	93.6
ATR			**CLC**	91.0	93.6
C1	94.0	91.6	**MSR**	91.0	93.3
C2	94.0	93.9	**ATR**	91.0	93.5

[a] If not otherwise stated

B.1.2 Remaining compressors

The polytropic efficiencies of other types of compressors have been determined based on their inlet volumetric flows and on whether or not they are centrifugal or axial. The CO_2 compressors in all of the plants with CO_2 capture, as well as fuel compressor (C5) in the ATR plant, operating with lower mass flows and higher pressure ratios, have been assumed to be

Table B.2: Efficiencies of the remaining compressors and expanders of the plants (the η_{mech} of all components is 99%)

Recycle compressors	η_{pol} (%)	η_{is} (%)	V_{in} (m³/s)
Simple oxy-fuel			
C6	88.9	86.6	291.40
C7	86.9	84.6	38.72
S-Graz			
C7	89.1	86.8	345.55
C8	87.6	85.0	77.61
AZEP 85 (C6)	87.9	87.9	103.36
AZEP 100 (C6)	88.1	88.0	121.65

Flue gas compressor	η_{pol} (%)	η_{is} (%)	V_{in} (m³/s)
MEA-0 (C2)	89.7	89.5	656.68
MEA-0.2 (C2)	89.7	89.5	656.68

O_2 compressors	η_{pol} (%)	η_{is} (%)	V_{in} (m³/s)
Simple oxy-fuel			
C8	77.1	71.2	45.00
C9	75.4	69.5	7.80
S-Graz			
C9	77.1	71.2	45.37
C10	75.4	69.5	7.83
Fuel compressor			
ATR (C5)	79.5	78.7	9.15

GT2	η_{pol} (%)	η_{is} (%)
S-Graz	91.0	90.0
AZEP 85	91.0	92.9
AZEP 100	91.0	92.9
CLC	91.0	93.0
MSR	91.0	93.8

CO_2 compressors	η_{pol} (%)	η_{is} (%)	V_{in} (m³/s)
MEA-0			
C3	80.3	78.1	20.66
C4	79.1	76.7	6.21
C5	78.0	75.6	1.92
C6	76.9	74.1	0.60
MEA-0.2			
C3	80.5	78.3	25.43
C4	79.2	76.7	6.22
C5	78.0	75.6	1.92
C6	76.9	74.1	0.60
Simple oxyfuel			
C2	80.8	78.2	34.99
C3	79.5	77.3	8.58
C4	78.3	76.5	2.65
C5	77.2	75.1	0.83
S-Graz			
C3	83.3	78.5	412.33
C4	80.6	78.2	27.19
C5	79.5	77.3	8.48
C6	78.3	76.5	2.67
C3	77.2	74.9	0.84

	η_{pol} (%)	η_{is} (%)	V_{in} (m³/s)
AZEP 85			
C2	80.3	77.9	19.58
C3	79.2	76.6	6.26
C4	78.0	75.6	1.94
C5	76.9	74.1	0.61
AZEP 100			
C2	80.4	78.1	23.03
C3	79.3	76.8	7.36
C4	78.2	75.7	2.28
C5	77.0	74.2	0.71
CLC			
C2	80.4	79.2	22.72
C3	79.3	78.0	7.26
C4	78.2	77.7	2.25
C5	77.0	76.9	0.70
MSR			
C2	80.4	78.2	22.32
C3	79.3	76.9	7.33
C4	78.2	76.0	2.27
C5	77.0	74.4	0.71
ATR			
C3	76.7	74.5	0.50
C4	77.7	75.2	1.37

centrifugal and their efficiencies have been calculated using Equation B.1 (Ludwig, 2001). The efficiencies of the remaining compressors have been calculated based on the calculation method used for axial compressors. However, depending on the size and operation of the compressors, their efficiencies have been adjusted analogously. Larger compressors, such as the recycle compressors in the S-Graz (C7 and C8) and the simple oxy-fuel processes (C6 and C7), as well as the flue gas compressor in the MEA plants (C2), have been assumed to be axial with polytropic efficiencies of about 6 percentage points higher than that calculated for the respective centrifugal compressors (Equation B.2). Oxygen compressors have also been considered as axial compressors. However, due to higher risk that requires stronger precaution measures, their efficiency has been estimated to be 10 percentage points lower than the efficiency of the respective axial compressor (Equation B.3). Through the polytropic

efficiencies, the isentropic efficiencies have been calculated as a function of mass flows, pressure ratios and compositions of the respective streams.

$0.0098\ln(\dot{V})+0.7736$, for centrifugal compressors (B.1)

$0.0098\ln(\dot{V})+0.8336$, for axial compressors (B.2)

$0.0098\ln(\dot{V})+0.7336$, for axial O_2 compressors (B.3)

Here, $\dot{V}$ is the volumetric flow rate of the gas entering the compressor. The resulting efficiencies for the remaining turbomachinery of the plants are shown in Table B.2 (Ludwig, 2001, Sinnott, 2005).

B.1.3 Steam turbines

The polytropic efficiencies of the high-, intermediate- and low-pressure steam turbines have been assumed to be 90%, 92% and 87%, respectively. Due to the similar STs used in all of the plants the isentropic efficiencies have been generalized for all processes: 91.6% for HPSTs, 93.3% for IPSTs and 88% for LPSTs and the additional ST4 of some plants.

B.1.4 Pumps

The isentropic efficiencies of the pumps have been calculated using Figure B.1, where the behaviour of the total efficiency of pumps versus the mass flow rate of the component is provided.

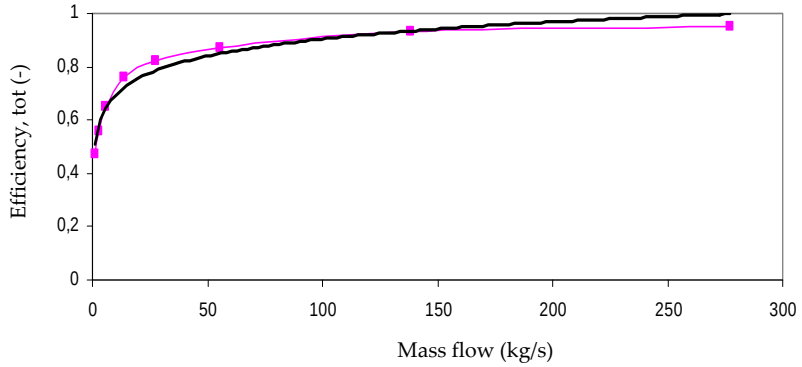

Figure B.1: Influence of mass flow on the pump efficiency (adopted from Peters, 2003)

The isentropic efficiency of the pumps has been calculated using Equation B.4 and assuming a mechanical efficiency of 98%. The results of the calculations are shown in Table B.3.

$\eta_{mech} \times \eta_{is} = \eta_{tot}$ (B.4)

Table B.3: Calculated efficiencies of pumps (the η_{mech} of all pumps is assumed to be 98%)

	Mass flow rate (kg/s)	η_{tot} (%)	η_{is} (%)	$W_{in,motor}$ (kW)	η_{motor} (%)
Reference plant					
COND P	94.6	89.9	91.7	45	87.2
HPP	65.2	86.5	88.2	1122	94.8
IPP	7.2	66.2	67.5	29	86.2
LPP	23.0	76.8	78.4	3	80.7
MEA-0					
COND P	94.5	89.9	91.7	45	87.2
HPP	65.4	86.5	88.3	1123	94.8
IPP	7.0	65.8	67.2	28	86.2
LPP	22.9	76.8	78.4	3	80.7
MEA-0.2					
COND P	94.5	90.0	91.7	45	87.2
HPP	65.4	86.5	88.3	1123	94.8
IPP	7.0	65.8	67.2	28	86.2
LPP	22.9	76.8	78.4	3	80.7
Simple oxy-fuel					
COND P	93.7	89.8	91.6	44	87.2
HPP	73.9	87.6	89.4	1255	95.1
IPP	5.3	63.3	64.6	22	85.6
LPP	15.2	73.0	74.5	2	79.9
S-Graz					
HPP	94.8	89.9	91.8	1648	95.7
LPP	116.7	91.8	93.7	15	84.7
AZEP 85					
COND P	95.6	90.0	91.8	45	87.2
HPP	71.0	87.3	89.0	1207	95.0
IPP	6.2	64.7	66.1	26	85.9
LPP	18.5	74.9	76.4	2	80.3
AZEP 100					
COND P	101.1	90.5	92.4	46	87.3
HPP	64.1	86.3	88.1	1100	94.7
IPP	15.5	73.2	74.7	58	87.8
LPP	20.4	75.8	77.3	3	80.5
CLC plant					
COND P	93.3	89.8	91.6	43	87.1
HPP	68.1	86.9	88.6	979	94.5
IPP	14.0	72.3	73.8	51	87.6
LPP	20.8	75.9	77.5	3	80.5
MSR plant					
COND P	31.3	79.7	81.3	16	84.8
HPP	67.4	86.8	88.5	1203	95.0
IPP	12.4	71.2	72.6	102	89.2
LPP	31.3	79.7	81.3	4	81.5
MUW P	79.0	88.2	90.0	32	86.4
ATR plant					
COND P	80.5	88.4	90.2	43	87.1
HPP	55.3	84.9	86.7	1073	94.7
IPP	34.1	80.5	82.1	185	90.6
LPP	23.2	76.9	78.5	50	87.5
MUW P	31.1	79.6	81.2	15	84.6

B.1.5 Generators and motors

The electrical efficiencies of the generators have been kept constant and equal to 98.5%, while the electrical efficiency of the motors follows the curve shown in Figure B.2.

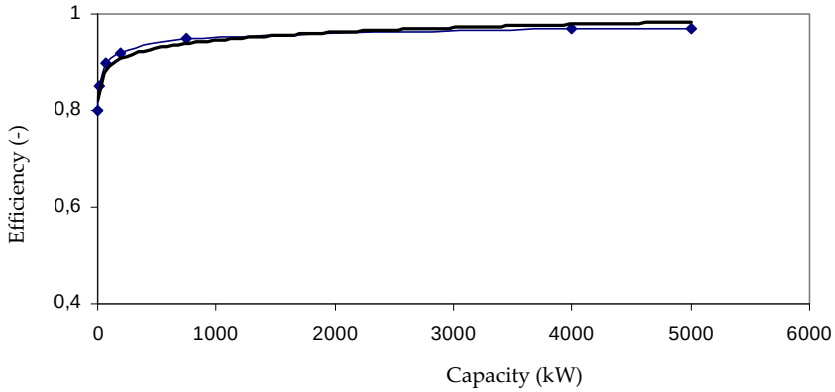

Figure B.2: Influence of the capacity on the pump efficiency (adopted from Sinnott, 2005)

B.1.6 Heat exchangers

B.1.6.1 Pressure drops

The pressure drops in the HXs have been determined depending on the working fluid and the temperature difference between the inlet and the outlet of this fluid. The pressure drop has been set to 3% and 5% of the inlet pressure for water and steam streams, respectively. In the evaporators, the pressure drops are handled by internal pumps. In gas/gas HXs, low-pressure and high-pressure gases have been assumed to suffer by 0.6% and 0.65% pressure drops per 100°C, respectively, always with respect to the inlet pressure.

For the HXs that constitute the HRSGs, the overall pressure drop of the hot side (HS, flue gas) has been considered to be 30 mbar in all of the plants, with the exception of the S-Graz cycle that includes a single-pressure level and has been assumed to have a pressure drop of 20 mbar (Ganapathy, 1991). These total pressure drops have been distributed among the HXs depending on their heat transfer. The outlet pressure of the HRSG has been set to 1.028 bar, assuming a 15 mbar pressure loss in the chimney.

The calculated pressure drop within each HX is provided in Table B.4.

Table B.4: Pressure drops within the HXs of the reference, MEA and simple oxy-fuel plants

	Reference plant		**MEA-0**		**MEA-0.2**		**Simple oxy-fuel plant**			
ΔP$_{HRSG}$ per 100°C	***0.58%***		***0.58%***		***0.58%***		***0.35%***			
	ΔT (°C)	**ΔP flue gas (10^{-2} bar)**	**ΔT (°C)**	**ΔP flue gas (10^{-2} bar)**	**ΔT (°C)**	**ΔP flue gas (10^{-2} bar)**	**ΔT (°C)**	**ΔP flue gas (10^{-2} bar)**	**ΔT (°C)**	**ΔP gas (10^{-2} bar)**
RH/RH1	132	0.82	129	0.79	129	0.79	57	0.25	---	---
RH2	---	---	---	---	---	---	---	---	---	---
HPSH/HPSH1	132	0.82	129	0.79	129	0.79	110	0.48	---	---
HPSH2	---	---	---	---	---	---	---	---	---	---
HPEV	107	0.66	108	0.67	108	0.67	158	0.69	---	---
HPEC	83	0.51	84	0.52	84	0.52	128	0.56	---	---
IPSH	1	0.00	1	0.00	1	0.00	0	0.00	---	---
IPEV	20	0.12	19	0.12	19	0.12	20	0.09	---	---
IPEC	4	0.02	3	0.02	3	0.02	4	0.02	---	---
LPSH/LPSH1	5	0.03	5	0.03	5	0.03	4	0.02	---	---
LPSH2	---	---	---	---	---	---	---	---	---	---
LPEV	73	0.45	73	0.45	73	0.45	68	0.30	---	---
LPEC	61	0.38	62	0.38	62	0.38	90	0.40	---	---
SH II	---	---	---	---	---	---	---	---	---	---
EV II	---	---	---	---	---	---	---	---	---	---
EC II	---	---	---	---	---	---	---	---	---	---
NGPH	---	---	---	---	---	---	185	1.11	57	0.05
Air HX	---	---	---	---	---	---	---	---	---	---
MCM LTHX	---	---	---	---	---	---	---	---	---	---
MCM HTHX	---	---	---	---	---	---	---	---	---	---
COOL1	---	---	133	0.80	227	1.36	110	0.66	---	---
COOL2	---	---	112	0.67	112	0.67	118	0.71	---	---
COOL3	---	---	113	0.68	113	0.68	119	0.71	---	---
COOL4	---	---	125	0.75	125	0.75	131	0.78	---	---
COOL5	---	---	---	---	---	---	237	1.54	---	---
COOL6	---	---	---	---	---	---	150	0.90	---	---
COOL7	---	---	---	---	---	---	---	---	---	---
COOL CAU	---	---	71	0.43	71	0.43	---	---	---	---
COND FG	---	---	---	---	---	---	34	0.20	---	---
WP1	---	---	---	---	---	---	---	---	---	---
WP2	---	---	---	---	---	---	---	---	---	---
WP3	---	---	---	---	---	---	---	---	---	---
H_2 PH	---	---	---	---	---	---	---	---	---	---

	S-Graz				**AZEP 85**				**AZEP 100**			
ΔP$_{HRSG}$ per 100°C	***0.73%***				***0.57%***				***0.70%***			
	ΔT (°C)	**ΔP flue gas (10^{-2} bar)**	**ΔT (°C)**	**ΔP flue gas (10^{-2} bar)**	**ΔT (°C)**	**ΔP flue gas (10^{-2} bar)**	**ΔT (°C)**	**ΔP flue gas (10^{-2} bar)**	**ΔT (°C)**	**ΔP gas (10^{-2} bar)**	**ΔT (°C)**	**ΔP flue gas (10^{-2} bar)**
RH/RH1	---	---	---	---	123	0.75	---	---	73	0.54	---	---
RH2	---	---	---	---	---	---	---	---	73	0.54	---	---
HPSH/HPSH1	109	0.81	---	---	123	0.75	---	---	---	---	---	---
HPSH2	---	---	---	---	---	---	---	---	---	---	---	---
HPEV	159	1.17	---	---	114	0.69	---	---	83	0.61	---	---
HPEC	4	0.03	---	---	88	0.54	---	---	64	0.47	---	---
IPSH	---	---	---	---	0	0	---	---	2	0.02	---	---
IPEV	---	---	---	---	20	0.12	---	---	42	0.31	---	---
IPEC	---	---	---	---	4	0.02	---	---	8	0.06	---	---
LPSH/LPSH1	---	---	---	---	4	0.03	---	---	---	---	---	---
LPSH2	---	---	---	---	---	---	---	---	4	0.03	---	---
LPEV	---	---	---	---	69	0.42	---	---	65	0.48	---	---
LPEC	---	---	---	---	72	0.44	---	---	64	0.48	---	---
SH II	---	---	---	---	108	0.43	---	---	117	0.47	---	---
EV II	---	---	---	---	149	0.6	---	---	155	0.62	---	---
EC II	---	---	---	---	119	0.48	---	---	124	0.5	---	---
NGPH	315	1.89	62	0.37	86	0.51	235	1.53	73	0.44	235	1.53
Air HX	---	---	---	---	76	0.49	130	0.84	76	0.5	131	0.85
MCM LTHX	---	---	---	---	476	3.1	507	3.3	476	3.1	507	3.3
MCM HTHX	---	---	---	---	226	1.47	250	1.63	226	1.47	250	1.63
COOL1	59	0.35	---	---	---	---	---	---	---	---	---	---
COOL2	311	1.87	---	---	98	0.59	---	---	98	0.59	---	---
COOL3	117	0.7	---	---	112	0.67	---	---	112	0.67	---	---
COOL4	118	0.71	---	---	113	0.68	---	---	113	0.68	---	---
COOL5	119	0.71	---	---	125	0.75	---	---	125	0.75	---	---
COOL6	131	0.79	---	---	---	---	---	---	---	---	---	---
COOL7	237	1.54	---	---	---	---	---	---	---	---	---	---

COOL CAU	---	---	---	---	---	---	---	---	---	---	---	---
COND FG	39	0.23	---	---	192	1.15	---	---	295	1.77	---	---
WP1	253	1.52	---	---	---	---	---	---	---	---	---	---
WP2	198	1.29	---	---	---	---	---	---	---	---	---	---
WP3	79	0.47	---	---	---	---			---	---	---	---
H2 PH	---	---	---	---					---	---	---	---

	CLC plant				**MSR plant**				**ATR plant**			
ΔP$_{HRSG}$ per 100°C	***0.68%***				***0.50%***				***0.56%***			
	ΔT (°C)	**ΔP flue gas (10^{-2} bar)**	**ΔT (°C)**	**ΔP flue gas (10^{-2} bar)**	**ΔT (°C)**	**ΔP flue gas (10^{-2} bar)**	**ΔT (°C)**	**ΔP flue gas (10^{-2} bar)**	**ΔT (°C)**	**ΔP gas (10^{-2} bar)**	**ΔT (°C)**	**ΔP flue gas (10^{-2} bar)**
RH/RH1	87	0.62	---	---	17	0.10	---	---	97	0.63	---	---
RH2	87	0.62	---	---	79	0.44	---	---	64	0.40	---	---
HPSH/HPSH1	---	---	---	---	---	---	---	---	22	0.14	---	---
HPSH2	---	---	---	---	---	---	---	---	83	0.52	---	---
HPEV	89	0.64	---	---	112	0.62	---	---	90	0.56	---	---
HPEC	69	0.49	---	---	88	0.49	---	---	28	0.18	---	---
IPSH	2	0.01	---	---	2	0.01	---	---	15	0.09	---	---
IPEV	38	0.27	---	---	31	0.18	---	---	90	0.56	---	---
IPEC	7	0.05	---	---	11	0.06	---	---	23	0.14	---	---
LPSH/LPSH1			---	---	---	---	---	---	33	0.21	---	---
LPSH2	4	0.03	---	---	10	0.06	---	---	5	0.03	---	---
LPEV	66	0.47	---	---	103	0.58	---	---	76	0.48	---	---
LPEC	59	0.42	---	---	84	0.47	---	---	74	0.47	---	---
SH II	8	0.03	---	---	---	---	---	---	---	---	---	---
EV II	35	0.14	---	---	---	---	---	---	---	---	---	---
EC II	27	0.11	---	---	---	---	---	---	---	---	---	---
NGPH	98	0.59	285	1.85	65	0.39	278	1.81	231	1.50	255	1.66
Air HX	---	---	---	---	---	---	---	---	---	---	---	---
MCM LTHX	---	---	---	---	---	---	---	---	---	---	---	---
MCM HTHX	---	---	---	---	---	---	---	---	---	---	---	---
COOL1	---	---	---	---	92	0.55	---	---	---	---	---	---
COOL2	96	0.58	---	---	112	0.67	---	---	102	0.61	---	---
COOL3	110	0.66	---	---	113	0.68	---	---	117	0.70	---	---
COOL4	110	0.66	---	---	125	0.75	---	---	---	---	---	---
COOL5	121	0.72	---	---	---	---	---	---	---	---	---	---
COOL6	---	---	---	---	---	---	---	---	---	---	---	---
COOL7	---	---	---	---	---	---	---	---	---	---	---	---
COOL CAU	---	---	---	---	---	---	---	---	90	0.54	---	---
COND FG	289	1.74	---	---	---	---	---	---	---	---	---	---
WP1	---	---	---	---	---	---	---	---	42	0.27	---	---
WP2	---	---	---	---	---	---	---	---	118	0.77	---	---
WP3	---	---	---	---	---	---	---	---	20	0.13	---	---
H2 PH	---	---	---	---	---	---	---	---	269	1.75	412	12.37

B.1.6.2 Minimum temperature differences (ΔT_{min})

In the evaporators of the HRSGs, the pinch point has been set to 10°C and the approach temperature to 6°C. The ΔT_{min} in the remaining HXs (superheaters and economizers) has been set to 20°C. The ΔT_{min} of the condenser, as well as the temperature increase of the cooling water, have been kept at 10°C. With some exceptions related to specific operating requirements, the ΔT_{min} of gas/gas HXs has been set to 60°C.

B.1.7 Reactors

In the CC of the GT systems and the CLC reactor the pressure losses have been set to 5 and 3% of the inlet pressure, respectively, while in the DBs it has been set to 1%.

B.2 Application of the conventional exergy-based methods

B.2.1 Application of the exergetic analysis

Matlab is the programming language used to perform the exergetic analysis. In Matlab, exergy balances are stated both at the component level and for the overall plant, i.e., balances regarding the rate of product exergy, the rate of fuel exergy and rate of exergy destruction for each component and for the overall system. The statements of the exergy rates are carried out based on the SPECO approach (Lazzaretto and Tsatsaronis, 2006). To calculate the (physical and chemical) exergies of streams, in order to use them in the exergy balances of the analysis, the software THESIS, originally developed at the RWTH Aachen, has been used. The main thermodynamic values of the streams (mass flows, temperatures and pressures) and their composition are exported from EbsilonProfessional using a *.dll* file and they are supplied as input to the exergy calculation software. The respective enthalpies, entropies and exergy values are then calculated. The number of the components and the streams included in each plant are shown in Table B.5.

Table B.5: Power plant characteristics

	Ref. plant	**Simple oxy-fuel plant**	**S-Graz cycle**	**MEA**	**CLC**	**AZEP 100**	**AZEP 85**	**ATR**	**MSR-H_2**
Number of streams	67 (10 shafts)	131 (19 shafts)	119 (18 shafts)	122 (17 shafts)	120 (16 shafts)	135 (17 shafts)	138 (17 shafts)	138 (17 shafts)	125 (17 shafts)
Number of components[a]	26	45	40	40	42	48	48	55	43
of which dissipative	2	9	9	8	7	7	7	9	7

[a] Not including valves, splitters, generators or motors

B.2.2 Application of the economic analysis

The main challenge in an analytical economic analysis is the estimation of the investment costs of plant components, since most of the available cost sources refer to relatively small-scale facilities. These values are difficult to adjust when large equipment is considered. In this thesis, various sources are combined and a large number of different data are used as reference. The reference data used for all components, their design characteristics and their sources are presented in Table B.6.

The size exponents have been used to extrapolate costs based on sizing parameters and have been calculated through cost comparisons with equipment found in the references. Temperatures, surface areas and heat transfer rates have also either been extracted from the reports used (Tsatsaronis and Winhold, 1984; Buchanan et al., 2000; Tsatsaronis and Cziesla, 2002; Turton et al., 2002; Framer, 2006) or they have been calculated after simulations in EbsilonProfessional. The modular factors shown in Table B.6 are used to convert PEC to FCI

and they have been derived from Buchanan et al. (2000) as a result of comparisons between equipment and total costs of components.

To calculate a HX's surface area, its overall heat transfer coefficient, U_o, must first be estimated. Typical value ranges of the overall heat transfer coefficients for variant component types can be found in literature (Naim Afgan et. al, 1996). Nonetheless, coefficient values are spread over wide ranges, and usually a mean value is chosen. In this thesis, the heat transfer coefficients have been calculated in detail, following the process described in Appendix C.

Construction materials are also important for cost calculations. However, at first, plant components in this thesis are assumed to be constructed with similar materials as the reference components. For high-temperature HXs, where no real economic data have been found, the materials have been assumed to be two to five times higher (depending on the operating temperature) than the base cost of the most economical HX (economizer). A detailed examination of different materials is performed in the LCA of the plants.

Because each part of the system (e.g., GT and ST systems) is simulated as a separate component, a strategy to split the system costs had to be defined. For example, in the GT system, 40% of the total cost is assumed to correspond to the expander, 35% to the compressor and 25% to the CC. In the ST system, the cost is shared among the different pressure-level STs, based on their contribution to the overall power output of the ST system. This is also in agreement with a general design assumption of the STs that lower pressure requires larger shuffles, thus it is associated with costlier construction.

To extrapolate the cost of the GT systems of the plants with CO_2 capture from the GT system of the reference plant, the respective system components have been compared, based on the power output (for the expander), the power input (for the compressor) and the mass flow of the combustion products (for the CC). The cost of the additional ST (ST4) is calculated based on the LPST of each plant, since the inlet and outlet pressures and temperatures of these components are comparable.

The MCM reactor was initially regarded as one component for the cost calculations. The costs of the included HXs and CC were calculated separately following the guidelines described above. Finally, the cost of the MCM is calculated by subtracting the cost of the CC and the HXs from the cost of the overall reactor.

In the CLC plant, the cost of the metal oxide has not been calculated because of high uncertainty (Lyngfelt and Thunman, 2005). However, even at the highest suggested prices and quantities it could be considered negligible in comparison to the total cost of the unit. The installation and the metal oxide costs of the CLC unit have been considered to be 20% of the equipment cost.

The cost of the CAU in MEA-0.2 was calculated based on a predefined 50% overall increase in the total FCI of the plant, when compared to the reference plant (IPCC report, 2005) and has then been split into its constitutive components: 55% absorber, 18% regenerator, 27% remaining components (Abu-Zahra et al., 2007). The extrapolation to MEA-0 has been performed based on comparison between the size of the equipment used here and that used in MEA-0.2. The absorber is designed as a packed vessel. The height and diameter of the absorption column have been estimated following calculations presented by Rubin and

Table B.6: Data for cost calculations[e]

	Ref. cost (10^6 €)	Design characteristic (varies)	Factor x (-)	Ref. year	Cost index	Type of cost	Modular factor (-)	Size exponent (-)	Reference	Comments
GT system, ref. plant (GT1, C1 and CC)	50.0	-		2006	15%	PEC	1.3	0.90 for expander/ compressor, 0.67 for CC	Framer, 2006; SGT4-4000F, 286 MW, $T_{out,fg}$= 1071°F	Splitting of the cost: 40% expander, 35% compressor and 25% CC
HRSG										
SH, SHII	1.3	4120 m²		2005	CEPCI	FCI	1.7	0.87	Javier Pisa, pers.com.	
EV, EVII	3.7	20474 m²		2005	CEPCI	FCI	1.7	0.87	Javier Pisa, pers.com.	
EC, ECII	2.0	16247 m²		2005	CEPCI	FCI	1.7	0.87	Javier Pisa, pers.com.	
COND	9.0	1 kW		1999	CEPCI	FCI	1.7	0.87	Buchanan et al., 2000, BEAMA, http://www.taftan.com/xl/condens.htm	U_o (Source: BEAMA, http://www.taftan.com/xl/condens.htm
STs	26.0	120 MW		1999	15%	FCI	1.5	-	Buchanan et al., 2000	Splitting of the cost to the different pressure levels, depending on the power output of each ST
HPP	1.4	3.37 MW		1990	CEPCI	FCI	1.3	0.80	Tsatsaronis et al., 1991	Differs from other pumps, due to its larger size (> 300 kW)
IPP	-	-		2001	CEPCI	FCI	1.3	-	Turton et al., 2002	
LPP	-	-		2001	CEPCI	FCI	1.3	-	Turton et al., 2002	
COND P	-	-		2001	CEPCI	FCI	1.3	-	Turton et al., 2002	
CT	18.3	217 MW		1999	CEPCI	FCI	1.5	1.00	Buchanan et al., 2000	Ebs. simulation for the calculation of the Q_{CT}
De-aerator	0.9	190 kg/sec		1990	CEPCI	FCI	1.5	1.00	Tsatsaronis et al., 1991	The mass flow refers to outgoing stream
GT2	-	-		2006	15%	PEC	1.5	-	Framer, 2006 ; different models	GT system with net power output half as that of the expander has been considered as reference. 40% of this cost is the cost of the GT2
ST4[a]	Cost of LPST			2008	15%	FCI	1.5	0.90	Tsatsaronis and Winhold, 1984 (used for comparison purposes)	Costs differ depending on the LPST in each plant
Recycle compr.[b]	3.8	1.42 MW		1990	15%	FCI	1.5	0.70	Tsatsaronis et al., 1991	
CO_2 compr.[c]	3.8	1.42 MW		1990	15%	FCI	1.5	0.70	Tsatsaronis et al., 1991	mean specific value (€/kW) has been used for all compressors, different in each plant
FG compr.[d]	3.8	1.42 MW		1990	15%	FCI	1.5	0.70	Tsatsaronis et al., 1991	
FG COND& COOLs	2.0	16247 m²		2005	CEPCI	FCI	1.7	0.87	Javier Pisa, pers.com.	New calculation of h_c and h_n for the overall heat transfer coefficient
DB	21.9	14 kg/sec fuel		2008	CEPCI	FCI	1.3	0.67		Ref. cost is the CC of the reference plant

MCM	0.2	1 MW_{th} fuel		2001	CEPCI	FCI	3.0	-	Möller et al., 2006	No exponent used, due to the already realized extrapolation of the given cost
MCM HTHX	2.0	16,247 m^2	5	2005	CEPCI	FCI	1.7	0.87	Javier Pisa, pers.com.	New calculation of h_c and h_n for the overall heat transfer coefficient
MCM LTHX	2.0	16,247 m^2	5	2005	CEPCI	FCI	1.7	0.87	Javier Pisa, pers.com.	New calculation of h_c and h_n for the overall heat transfer coefficient
NGPH	2.0	16,247 m^2	2	2005	CEPCI	FCI	1.7	0.87	Javier Pisa, pers.com.	New calculation of h_c and h_n for the overall heat transfer coefficient
Air PH	2.0	16,247 m^2	5	2005	CEPCI	FCI	1.7	0.87	Javier Pisa, pers.com.	New calculation of h_c and h_n for the overall heat transfer coefficient
CLC	16.2	180 m^3		2000	CEPCI	PEC	1.2	0.60	Klara (2007), Wolf et al. (2005), Lyngfeld and Thunman (2005)	
CAU	50%> FCI_{tot} of to ref. plant			-	-	FCI	3.0	sensitivity analysis 0.60	Abu-Zahra et al., 2007, IPCC 2005	Splitting of the cost: 55% absorber, 18% stripper and 27% remaining components

[a] ST4 and ST5 are considered part of the IPST in the MEA plant
[b] Recycle compr (C6, AZEPs)
[c] CO_2 compr.(C2-C5, AZEPs, CLC; C3-C6, MEA)
[d] FG compr (C2, MEA)
[e] 1€ = 1$

Table B.7: Assumptions involved in the economic analysis (reference year: 2009)

Parameter (units)	**Value**		
Average general inflation rate (%)			3
Average nominal escalation rate (%)			3
Average nominal escalation rate for NG (%)			4
Beginning of design and construction period			2011
Date of commercial operation			2013
Plant economic life (years)			20
Plant life for tax purposes (years)			15
Plant financing fractions and required returns on capital			
Type of financing	**Common equity**	**Debt**	
Financing fraction (%)	50	50	
Required annual return (%)	12	8	
Resulting average cost of money (%)		10	
Average combined income tax rate (%)			30
Average property tax rate (% of PFI)			
Average insurance rate (% of PFI)			
Average capacity factor (%)			85
Labor positions for opening and maintenance			30
Average labor rate (€/h)			50
Annual fixed operating and maintenance costs (10^6 €)			1.5
Annual fixed operating and maintenance costs at full capacity (10^3 €)			624
Unit cost of fuel (€/GJ-LHV:50,015 MJ/kg)			7
Allocation of plant facilities investment to the individual years of design and construction (%)			
Jan. 1-Dec. 31, 2011			40
Jan. 1-Dec. 31, 2012			60

Rao, 2002. The height of the regenerator agrees with that of the absorber, while its diameter is calculated based on its volume.

Generalized cost equations for common components of the plants, as an example for similar-sided equipment are provided in Appendix D.

After the estimation of the FCI of the plant, a detailed economic analysis following the TRR method (see Appendix A) was realized for each plant. The main assumptions made for this analysis are shown in Table B.7.

B.2.3 Application of the exergoeconomic analysis

The exergoeconomic analysis consists of a group of linear equations stated at the component level. The sum of all costs entering a component (cost of incoming streams plus investment cost of the component) must be equal to the cost of the streams exiting the component. The cost of air and water provided to the plants is considered to be zero.

Dissipative components (e.g., throttling valves, coolers, condensers, gas cleaning units) serve productive components in a system, facilitating an overall effective operation, cost reduction or achievement of required emission standards. Thus, costs associated with purchasing and operating a dissipative component are usually charged either to the

component(s) served by it or to the final product(s) of the system (Lazzaretto and Tsatsaronis, 2006). In this thesis, the costs related to dissipative equipment are charged to the components served by it (e.g., the cost of each cooler is charged to the subsequent compressor served). When more than one component is served by a dissipative component, the cost is apportioned to all of the components served, using weighting factors.

For example, the investment cost of a CT is charged to the condensers/coolers supplied with cooling water, using the respective heat transfer rates ($\dot{Q}$) as weighting factors. The condenser serves the components of the steam cycle, allowing the perpetuation of the water/steam cycle. The cost of the condenser is, therefore, shared by the components constituting the steam cycle, depending on the contribution of each component to their total exergy destruction. For the condenser and CT (Figure B.3), the exergy costing equation (with specific cost of water equal to zero) is written as:

$$\dot{C}_1 + \dot{Z}_{COND} + \dot{Z}_{CT} = \dot{C}_2 \overset{c_1=c_2}{\Rightarrow} c_1\dot{E}_1 + \dot{Z}_{COND} + \dot{Z}_{CT} = c_1\dot{E}_2 \Rightarrow c_1\left(\dot{E}_1 - \dot{E}_2\right) + \dot{Z}_{COND} + \dot{Z}_{CT} = \mathbf{0}$$ [1]

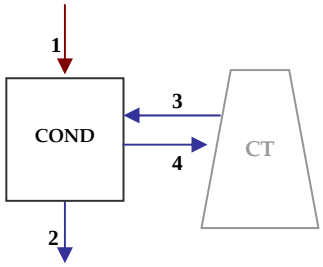

Figure B.3: Connection between condenser and cooling tower

However, because $c_1\left(\dot{E}_1 - \dot{E}_2\right) + \dot{Z}_{COND} + \dot{Z}_{CT} \neq \mathbf{0}$, an imaginary value, $\dot{C}_{diff}$, is introduced to maintain the cost balance:

$$c_1\left(\dot{E}_1 - \dot{E}_2\right) + \dot{Z}_{COND} + \dot{Z}_{CT} + \dot{C}_{diff} = \mathbf{0}$$

To calculate the $\dot{C}_{diff}$ and the exergy destruction used as weighting factor for the cost sharing, the exergoeconomic analysis must be realized. When all dissipative components have been accounted for, they are removed from the cycle and the analysis is repeated.

B.2.4 Application of the LCA

In an LCA, the component variables, the consumption and the release of materials are identified and quantified (Fiaschi and Lombardi, 2002). In order to identify the material inlet flows, the overall life cycle of each component of the plant must be considered and, hence, the

[1] The auxiliary equation of the condenser is c1=c2.

phases of construction, operation and dismantling must be taken into account. For the quantification of the materials needed, it is necessary to approximate the size of the plant and collect information about the main materials, their production processes and weights, as well as the scrap output of all equipment assembled for the plant. To shift from the manufactured materials to the raw substances and emissions inventory, the commercially available software Package *SimaPro 7.1* has been used (SimaPro, 2006).

The selection of construction materials, based on strength, corrosion resistance and cost of fabrication, is vital to process design estimates. Expertise about equipment can also assist in the final selection of materials. In general, carbon steel is used whenever possible because of its low cost and ease of fabrication (Seider, 2004). Details about component design and suitable construction materials are obtained from equipment design handbooks and manufacturing leaflets. Typical construction materials for conventional process equipment are listed in Table B.8.

Table B.8: Typical construction materials for process equipment

Component	**Materials**
GT expander[a]	Discs: High-strength steels, Vanes: Cobalt- Nickel-based alloys, Blades: Ni-based alloys
Compressor[a]	Discs: High-strength low steel, Blades: low-carbon steel
CC[a]	Cans: Ni-based sheet superalloys
ST	Valve chest, shafts, discs: Alloy steel, Steam rings, cylinders: Carbon steel, Blades: Stainless steel
HRSG	Carbon/Stainless steel
Storage/Process vessel	Steel/Reinforced steel
Condenser	Copper- Ni-alloys, Stainless steel, Titanium, Brass
De-aerator	Carbon/Stainless steel
Pump	Carbon/Stainless steel, Cast iron, Nickel, Titanium
CT[b]	Steel, Stainless steel, PVC, FRP, Concrete, Polyethylene

[a] The materials used in GT systems are in the range of metallurgical alloys from high-strength steel to lightweight aluminum or titanium and are mainly temperature-resistant.
[b] Materials to enhance corrosion resistance, reduce maintenance, and promote reliability and long service life are used

As mentioned in section 3.2.3, in order to quantitatively assess environmental impacts, the environmental impact indicator *Eco-indicator 99* is used. The Eco-indicator 99 impact assessment method ("Hierarchist-Average" database version) (SimaPro, 2006) is used in a similar way as costs in the exergoeconomic analysis. Standard Eco-indicator 99 points summarize the environmental impacts associated with the complete upstream chain (production and distribution) of 1 kg of each required raw material. Design estimates depend on the required construction materials. In order to accomplish this it is necessary to:

a) Estimate the equipment weight using product information sheets and mechanical design characteristics provided by manufacturers. In most cases, weight estimation is a function of the operating conditions and the mechanical design requirements of each unit. Thus, the equipment weight could be estimated based merely on mechanical design calculations and on "rules of thumb". Reference values are extrapolated taking the operating conditions of the considered processes into consideration.

b) Estimate the percentage of each construction material required to manufacture a component. This estimate is based on available manufacturing information data sheets and mechanical design standards.

For the estimation of environmental impacts, the environmental boundaries of the systems have been defined to incorporate all relevant processes (see section B.2.5). The construction stage includes the consumption of construction materials for the manufacture of system components, while the operating stage includes the consumption of fossil fuel as inflow stream and the gas emissions (mainly CO_2 and NO_x) as outflow streams.

The design characteristics, the construction materials, the references used and the environmental impact of the chosen materials, represented by the ECO-indicator, are presented for all types of components in Table B.9.

Table B.9: Design data for plant components

Component, *k*	Design Parameter	Design characteristics	Used construction materials	Eco-indicator 99 (Pts/t)	Material composition (%,w/w)	References
GT1/GT2	Power Exhaust volume flowrate	Conventional turbine for 200-300 MW power output	Steel Steel high alloy	86 910	25 75	Nuovo Pignone, 2009; Soares, 2002.
C1			Steel	86	33.33	
C2-C5 (C3-C6 for MEA plant)	Discharge pressure Volume flowrate	Centrifugal	Steel low alloy Cast iron	110 240	44.45 22.22	Cooper, 2009.
CC/ DB	Fuel/air mass flowrate	Sequential combustion with air	Steel Steel high alloy	86 910	33.34 66.66	Nuovo Pignone, 2009; Seider et al., 2004.
STs	Power Exhaust volume flowrate	30-60 MW power output	Steel Steel high alloy	86 910	25 75	Mitsubishi, 2009; Soares, 2002.
MCM reactor	Thermal power		Rhodium enriched (catalyzator)	12.000.000	1.24	
MCM/ HT&LTHX	Membrane density	Mixed conducting membrane with oxygen ion vacancies	Zinc coating (catalyst support) per m^2	49	11.16	Eriksson et al., 2007; Griffin et al., 2005; Sundkvist, 2005, 2007; Reinke, 2005; Kolbitsch, 2008; Seider et al., 2004.
	Thermal power	Monolit (membrane) volume = 47.18 m^3 Surface to volume ratio = >500 m^2/m^3	Steel high alloy Cast iron	910 240	56.94 30.66	
CLC reactors (AR & FR)	Oxygen carrier capacity	Energy density = 15 MW/m^3 Oxygen production rate = 37 mol $O_2/(m^3.s)$ Catalyzator active area = 0.26 m^2/g Two interconnected pressurised fluidised bed reactors with a cyclone system Solids inventory = 100- 200 kg/MW Solids residence time: AR = 4.8 s, FR = 60 s Gas velocity: AR = 10 m/s, FR = 15 m/s Oxygen carrier particles (NiO): mean diameter = 150 μm average density = 2400 kg/m^3	Steel high alloy Cast iron	910 240	65 35	www.hyundai.eu; Linderholm, 2008, Wolf, 2005; Kolbitsch, 2009; www.durofelguera.com; Naqvi, 2007; Naqvi, 2006.

HXs / HRSG	Heat transfer area Heat transfer coefficient	SH/RH, Air HX, NGPH OD=2 in, ID=1.738	Steel	86	26	Ganapathy, 1991, Perry and Green, 1997; committees.api.org/standards, 2009; Seider et al., 2004
		tube length=10 ft, thickn.=0.120 in	Steel high alloy	910	74	
		fin density=2 fin/in, height=0.500 in fin thickn.=0.075 in				
COND/ COOL/ EV/ EC		tube OD=2 in, ID=1.770 in	Steel	86	100	Soares, 2002; Seider et al., 2004.
		tube length=10 ft, thickn.=0.105 in fin density=4 fin/in, height=0.750 in fin thickn.=0.050 in				
CT	Water volume flowrate	Hyperbolic counterflow Natural-draft tower with PVC film fill	Concrete	3.8	91	www.gammonindia.com, June 2009;
	Heat transfer area		PVC (high impact)	280	9	www.evaptech.com, June 2009; Gould et al., 1999 ; http://process-equipment.globalspec.com; www.alpine-bau.de, June 2009.
Storage/Process Vessel						Perry and Green, 1997.
De-aerator	Volume flowrate capacity Pressure	Deaerating boiler feedwater	Steel	86	100	Gestra, 2009; committees.api.org/standards, 2009.
PUMP (P)	Fluid volume flowrate (GPM)	Centrifugal	Steel	86	35	www.pumpexpert.com, May 2009;
	Discharge pressure		Cast iron	240	65	Bloch et al., 1998; www.chempump.com, 2009.
CAU	Absorber: packed vessel. Height and diameter		Steel	86	1%	Rubin and Rao, 2002; Rennie, 2006; *www.sulzerchemtech.com*
	Stripper: regeneration heat requirement		Steel high alloy	910	99%	

B.2.5 Application of the exergoenvironmental analysis

The operating parameters of this analysis are the same as those considered in the economic analysis: 20 years of operation with 7446 h/yr. To determine the impact associated with the production of electricity, the same group of equations as in the exergoeconomic analysis is used. The difference here is that the cost rates are replaced with environmental impacts. The environmental impacts associated with the production of methane and with each component separately are correlated in the system of linear equations.

The environmental impact associated with the production of electricity in each energy conversion system is compared, taking the environmental impact of the outflow streams, such as CO_2 and NO_x emissions, into consideration (Table B.10). In the case of the three oxy-fuel technologies, AZEP 85, AZEP 100 and CLC, the environmental impact associated with the CO_2 sequestration of the separated CO_2 stream is also considered, using LCA data reported in recent publications (Khoo et al, 2006). The part of the pollutant formation related to the amount of CO_2 captured in each plant is subtracted from the overall environmental impact.

Exergoenvironmental variables are calculated in order to identify the relative importance of each component with respect to their environmental impact and, to identify the magnitude and location of the environmental impact caused by system inefficiencies. The results are used to evaluate and compare the environmental performance of the four considered power plants.

Table B.10: EI of incoming and exiting streams of the systems (Eco-indicator 99, HA)

Product	**System boundaries**	**Eco-indicator (Pts/t)**	**Reference**
Natural gas	Production and distribution	180.0	Goedkoop and Spriensma, 2000 SimaPro, 2006
CO_2	Emission	5.4	
CO_2	Sequestration	4.9	Khoo et al., 2006
CH_4	Emission	114.6	Goedkoop and Spriensma, 2000 SimaPro, 2006
NO_x	Emission	2749.4	

Appendix C

Design estimates for construction, operational costs and environmental impacts of heat exchangers

C.1 Calculation of the surface area, *A*

To calculate the area A of a HX in m², Equation C.1 is used:

$$A = \frac{\dot{Q}}{U_o \times \Delta T_{\log}} \tag{C.1}$$

Here, $\dot{Q}$ is the heat transfer rate (W), ΔT_{log} is the logarithmic mean temperature difference, $\Delta T_{\log} = \frac{\Delta T_A - \Delta T_B}{\ln\left(\frac{\Delta T_A}{\Delta T_B}\right)}$, with ΔT_A and ΔT_B the temperature differences on sides A and B (K), respectively, and U_o is the overall heat transfer coefficient (reciprocal of the overall thermal resistance) that differs depending on the design and operation, as well as the working fluid of the HX considered (W/m²K).

C.1.1 Calculation of the overall heat transfer coefficient

The overall heat transfer coefficient is a function of several variables such as tube size, spacing, and gas velocity (Ganapathy, 2003). For HRSGs in combined cycle power plants operating with natural gas, the overall heat transfer coefficient of a HX is calculated as (Ganapathy, 1991):

$$\frac{\mathbf{1}}{U_o} = \frac{\mathbf{1}}{h_o} + \frac{d_o}{h_i d_i} + \frac{d_o}{\mathbf{24} \times K_m} \times \ln\left(\frac{d_o}{d_i}\right) + ff_i \times \frac{d_o}{d_i} + ff_o \tag{C.2}$$

Here, h_i is the tube-side coefficient, h_o is the gas-side coefficient, d_o and d_i are the outside and inside diameters of a tube, respectively, ff_o and ff_i are the fouling factors on the outside

and the inside of the tubes, respectively, and K_m is the tube metal conductivity. The thermal resistance of gases affects the resistance distribution in a HX significantly, rendering the metal resistance and the fouling factors terms negligible. In other words, the main contributors to the overall heat transfer coefficient are the tube-side coefficient, h_i, and the gas-side coefficient, h_o. Thus, Equation C.2 becomes:

$$\frac{\mathbf{1}}{U_o} = \frac{\mathbf{1}}{h_o} + \frac{d_o}{h_i d_i} \tag{C.3}$$

In economizers and superheaters working with liquid or steam/water mixtures on the tube side and gas on the outside, the overall heat transfer coefficient is mainly determined by the gas-side coefficient (h_o), which presents the highest thermal resistance. This coefficient consists of the convective heat transfer, h_c, and the non-luminous heat transfer, h_N:

$$h_o = h_c + h_N \tag{C.4}$$

C.1.1.1 Calculation of the non-luminous heat transfer coefficient, h_N

h_N depends on (1) the partial pressures of triatomic gases (e.g., CO_2, H_2O and SO_2) formed during combustion of fossil fuels that contribute to radiation, (2) the beam length *L* of a tube, which depends on the pitch and arrangement of the tube bundle of the HX considered and (3) the temperatures of the gas stream and surface of the bundle. It can be calculated in a simplified way:

$$h_N = K\varepsilon_g \tag{C.5}$$

where ε_g is the emissivity of a gas (relative ability of a gas to emit energy by radiation). The factor *K* is calculated using Figure C.1, left panel. Assumed values of the beam length (Figure C.1, right panel), the longitudinal pitch, S_L, the transverse pitch, S_T and the outside tube diameter, d_o are shown in Table C.1.

The beam length and the flue gas temperature are the main deciding factors of ε_g, while the wall and flue gas temperatures determine *K*. An increase in the flue gas temperature, keeping the beam length and the wall temperature constant, decreases ε_g and increases *K*. Because h_N is influenced more by larger values of *K*, it increases as well. If the wall temperature is increased, while the flue gas temperature and the beam length are kept constant, ε_g remains unchanged, whereas *K* increases, resulting in an increase of h_N. Lastly, if the beam length is increased, while the wall and flue gas temperatures are kept constant, *K* remains unchanged, while ε_g increases, resulting in an increase of the h_N. Thus, if there is an

increase in the flue gas or wall temperature and/or in the beam length, h_N will increase as well.

Figures C.2-C.4 were obtained using data derived from Figure C1. Figure C.2 shows the variation of ε_g with the flue gas temperature and the beam length, while Figure C.3 shows the variation of *K* with the wall and flue gas temperatures. Figure C.4 combines the two previous figures, showing the overall influence of h_N by the wall and flue gas temperatures and the beam length. Next to each figure the polynomial trendlines of the different curves are shown. It can be seen that h_N is not strongly influenced by the wall temperature, especially for higher flue gas temperatures and smaller beam lengths. Thus, one general equation has been assumed for each different beam length (trendlines of Figure C.4).

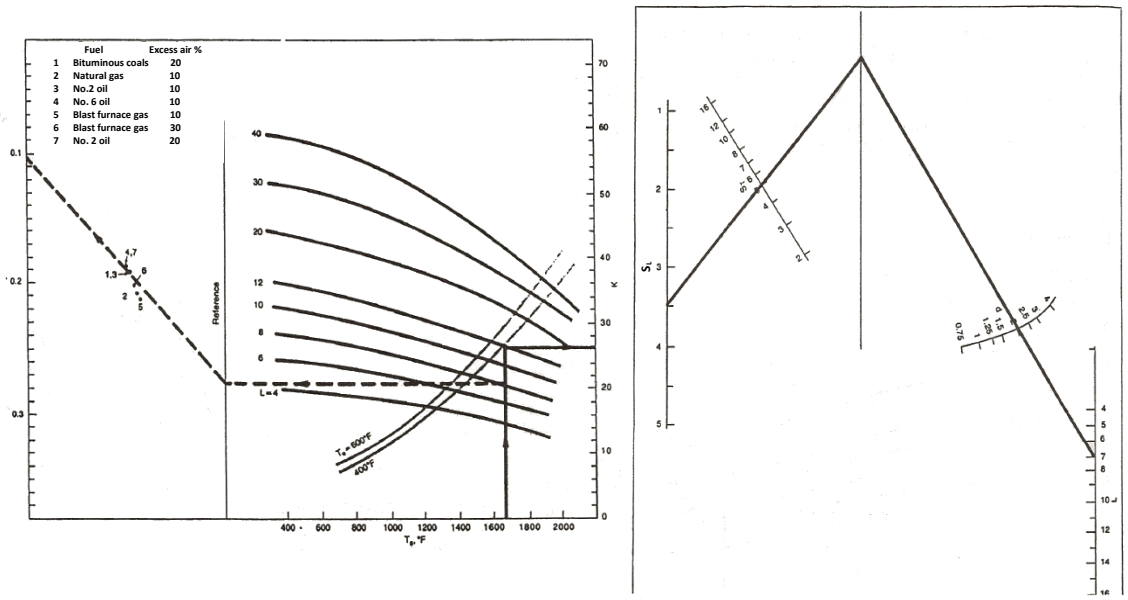

Figure C.1: Graphs used for the estimation of the h_N (left panel) and beam length evaluation (right panel). (Source: Ganapathy, 1991)

Table C.1: Beam length *L*

L (m)	d_o (in)	S_T * (in)	S_L * (in)
5	1.25	2.50	2.80
6	1.50	3.00	3.36
7	2.00	4.00	4.48
9	2.50	5.00	5.60

($S_T = \mathbf{2} \times d_o$ and $S_L = \mathbf{1.12} \times S_T$)

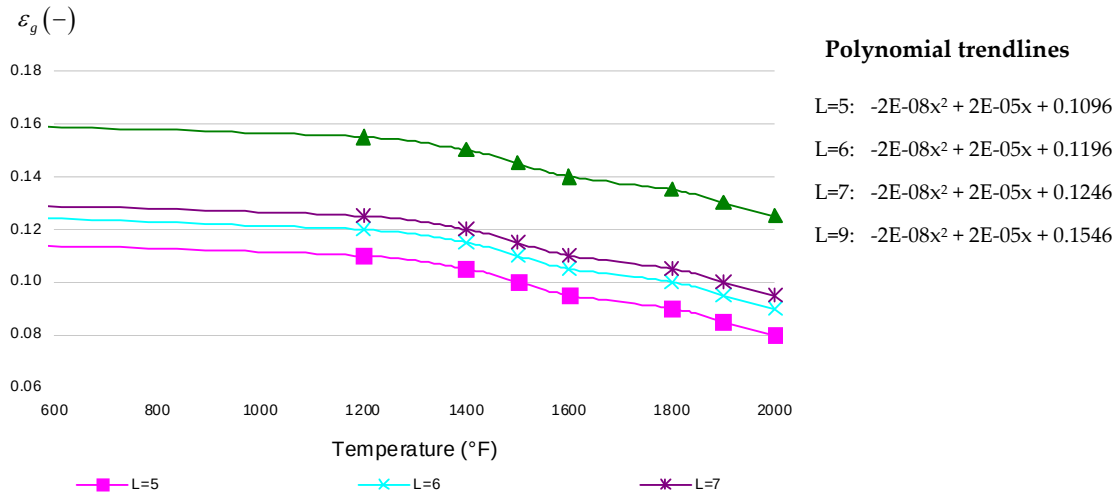

Figure C.2: Estimation of gas emissivity at different flue gas temperatures and beam lengths (L), $\in_g$

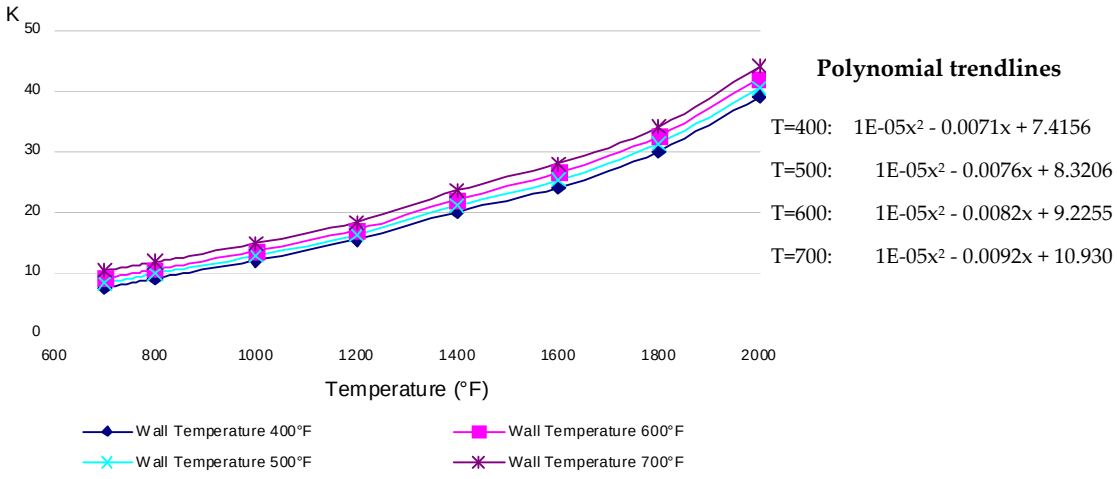

Figure C.3: Estimation of the factor K at different wall and flue gas temperatures

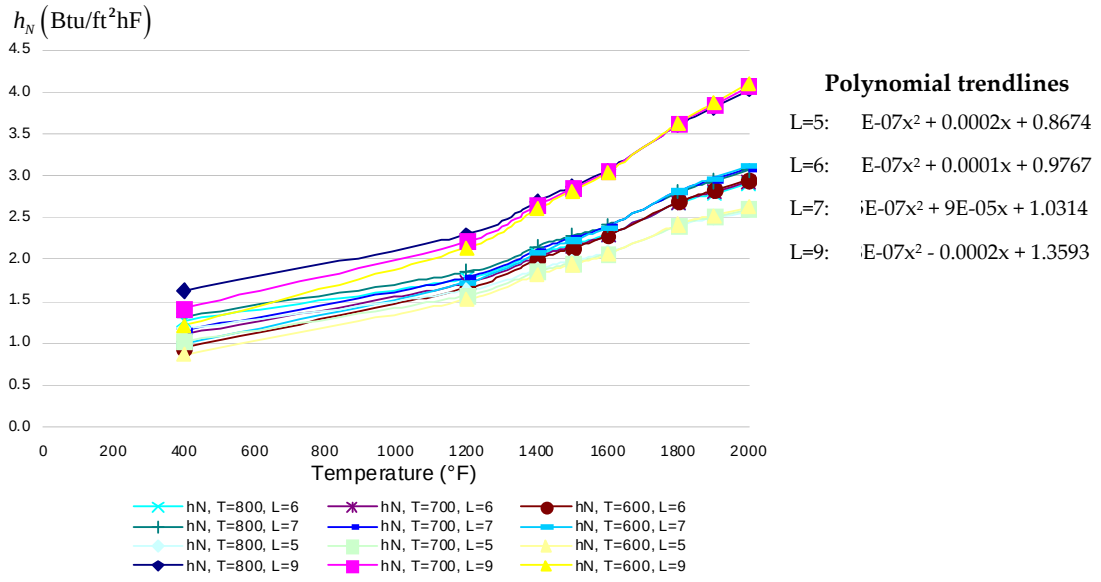

Figure C.4: Estimation of the h_N at different temperatures and beam lengths

$$K = \frac{(\mathbf{0.8} + \mathbf{1.6}\,p_w)(\mathbf{1} - \mathbf{0.38}T_g\,/\,\mathbf{1000})}{\sqrt{(p_c + p_w)L}} \times (p_c + p_w) \tag{C.6}$$

p_c and p_w are the partial pressures of CO_2 and water vapor included in the gas stream, and T_g is the average gas temperature (K). h_N is approximated anew using Equation C.5 and the new trendlines, obtained for streams with dominant concentrations of H_2O or CO_2 (shown in Table C.2).

Table C.2: Approximation of the h_N with mass ratios 8:1 H_2O and 25:1 CO_2 (based on the respective element content in the conventional flue gases)

Beam length (m)	**h_N**	
	8:1 H_2O	**25:1 CO_2**
L=5	1E-06x² + 0.0012x + 3.1418	6E-07x² + 0.0006x + 1.7772
L=6	1E-06x² + 0.0011x + 3.2511	7E-07x² + 0.0005x + 1.8865
L=7	1E-06x² + 0.001x + 3.3058	8E-07x² + 0.0005x + 1.9411
L=9	1E-06x² + 0.001x + 3.3604	8E-07x² + 0.0004x + 1.9958

C.1.1.2 Calculation of the convective heat transfer coefficient, h_c

The convective heat transfer coefficient is calculated using Equation C.7:

$$h_c = Nu\frac{\mathbf{12}k}{d_o} \tag{C.7}$$

Nu is the Nusselt number ($Nu = \mathbf{0.033}\,\mathrm{Re}^{\mathbf{0.6}}\,\mathrm{Pr}^{\mathbf{0.33}}$) and k the thermal conductivity in Btu/fthF. To calculate the Nusselt number, Re (Reynolds number) and Pr (Prandtl number) are estimated as:

$$\mathrm{Re} = \frac{Gd_o}{\mathbf{12}\mu} \tag{C.8}$$

$$\mathrm{Pr} = \frac{\mu C_p}{k} \tag{C.9}$$

G is the gas velocity in lb/ft²h, μ the viscosity in lb/fth and C_p the specific heat in Btu/lbF. The gas mass velocity G is defined as:

$$G = \frac{\mathbf{12}W_g}{\left(N_w\left(S_t - d_o\right)L\right)} \tag{C.10}$$

Here, N_w is the number of tubes wide and W_g the gas flow in lb/h.

Due to lack of input data, assumptions include steady flue gas and mass velocity of 35 ft/sec (10m/sec) and 5000 lb/ft²h, respectively, throughout the HRSG. With these values, the gas density, ρ_g, is found to be 0.04 lb/ft³ $\left(\rho_g = \frac{G}{\mathbf{3600}V_g}\right)$; an intermediate value of ρ_g is calculated with data derived from EbsilonProfessional. However, the viscosity, the specific heat and the conductivity vary with temperature (Table C.3) and result in different Re and Nu numbers. Also, the diameter of the tubes, d_o, depends on the HX. h_c has been estimated for different temperatures using a constant d_o of 2 in. (Figure C.5). When d_o is different than 2 in., the coefficient has been adjusted using the equation:

$$h_c = \frac{Nu\mathbf{12}k}{\left(d_o^{'}/d_o\right)} \tag{C.11}$$

Here, $d_o^{'}$ is a diameter different than 2 in.

Table C.3: Gas and steam properties (Source: Ganapathy, 1991)

Air (dry)				GT exhaust gas			
Temperature (°F)	**Cp (Btu/LbF)**	**μ (Lb/fth)**	**k (Btu/fthF)**	**Temperature (°F)**	**Cp (Btu/LbF)**	**μ (Lb/fth)**	**k (Btu/fthF)**
200	0.2439	0.0537	0.0188	**200**	0.2529	0.0517	0.0182
400	0.2485	0.0632	0.0221	**400**	0.2584	0.0612	0.0218
800	0.2587	0.0809	0.0287	**600**	0.2643	0.0702	0.0253
1200	0.2696	0.0968	0.0350	**800**	0.2705	0.0789	0.0287
1600	0.2800	0.1109	0.0412	**1000**	0.2767	0.0870	0.0321
2000	0.2887	0.1232	0.0473				
Water vapor				**CO_2**			
Temperature (°F)	**Cp (Btu/LbF)**	**μ (Lb/fth)**	**k (Btu/fthF)**	**Temperature (°F)**	**Cp (Btu/LbF)**	**μ (Lb/fth)**	**k (Btu/fthF)**
200	0.4532	0.0315	0.0134	**200**	0.2162	0.0438	0.0125
400	0.4663	0.0411	0.0197	**400**	0.2369	0.0544	0.0177
600	0.4812	0.0506	0.0261	**600**	0.2543	0.0645	0.0227
800	0.4975	0.0597	0.0326	**800**	0.2688	0.0749	0.0274
1000	0.5147	0.0687	0.0393	**1000**	0.2807	0.0829	0.0319
1200	0.5325	0.0773	0.0462	**1200**	0.2903	0.0913	0.0360
1400	0.5506	0.0858	0.0532	**1400**	0.2980	0.0991	0.0400
1600	0.5684	0.0939	0.0604	**1600**	0.3041	0.1064	0.0435
1800	0.5857	0.1019	0.0678	**1800**	0.3090	0.1130	0.0468
2000	0.6019	0.1095	0.0753	**2000**	0.3129	0.1191	0.0500

Air, GT exhaust gases and CO_2 streams present similar behavior, with respect to temperature changes. The h_c of steam streams, on the other hand, presents a much more intense change with temperature.

The composition of the gas passing through the secondary HRSGs differs from the conventional GT flue gases and, therefore, h_c must be adjusted properly. To reflect the percentage of CO_2 and H_2O included in a stream, the curves representing pure CO_2 and H_2O steams, shown in Figure C.5, are shifted depending on the relative concentrations of the two elements. In other words, the molecular fractions of carbon dioxide and water vapor in a stream are used as weighting factors for recalculating the multipliers of the CO_2 and H_2O curves (e.g., Table C.4).

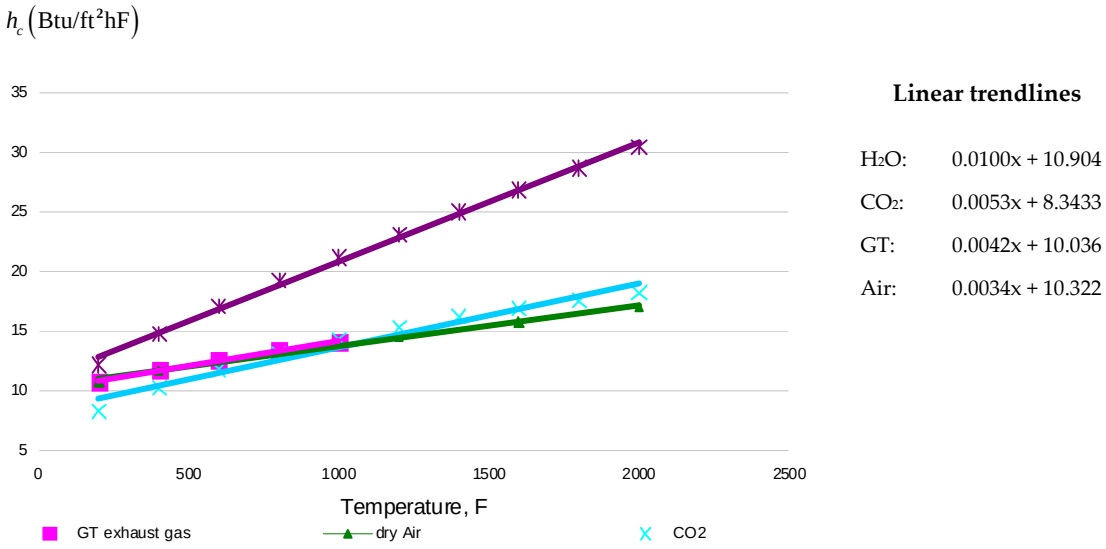

Figure C.5: Estimation of the h_c of different gases at different temperatures

Table C.4: Estimation of the h_c for high concentrations of CO_2 and H_2O

h_c	
2:1 CO_2:H_2O	**32:1 CO_2:H_2O**
0.0069x + 9.214	0.0054x + 8.420

C.1.1.3 Calculation of the tube-side coefficient, h_i

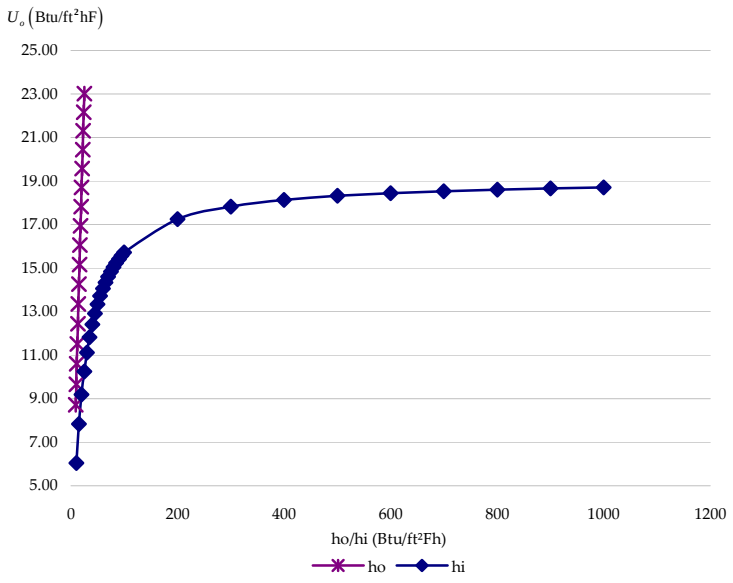

Figure C.6: Influence of the h_o and h_i variation on the U_o

h_i only influences the total heat transfer coefficient when it is small (Figure C.6). When gas flows on the outer side of tubes and high heat transfer coefficients are calculated for the tube side, the overall coefficient is governed by the gas-side resistance. Assuming the other

resistances contribute a specific percentage to the overall coefficient, the calculation of the U_o can be simplified to $\mathbf{0.8}-\mathbf{0.9}\times h_o$ (Ganapathy, 1991).

The following equations have been assumed depending on the component considered:

$U_o = \mathbf{0.9}\times h_o$ for economizers and evaporators,

$U_o = \mathbf{0.8}\times h_o$ for superheaters and

$U_o = \mathbf{0.6}\times h_o$ for gas-gas HXs, where h_i is significantly smaller and of a similar range as the h_o.

After the U_o and the surface area of a HX are calculated, its cost is estimated based on area comparison with reference costs and sizing factors. In Tables C.5-C.10 the calculated heat transfer coefficients and the resulting FCI of all HXs of the plants are presented.

Table C.5: Data for the reference plant

HX	Heat transfer (kW)	ΔT_{log} (K)	U_o (W/m²K)	Surface , A (m²)	FCI (2009)
RH	41,540	62.4	63.8	10,431	3,128,631
HPSH	55,003	55.2	63.9	15,585	4,436,778
HPEV	76,290	43.6	66.0	26,507	5,205,396
HPEC	57,804	50.5	62.1	18,425	2,510,897
IPSH	391	26.7	64.7	226	111,737
IPEV	13,535	23.5	71.7	8,031	1,842,071
IPEC	2,423	48.6	71.2	701	146,109
LPSH	3,287	44.2	53.3	1,395	543,582
LPEV	49,439	34.5	58.0	24,730	4,900,487
LPEC	40,883	37.9	55.6	19,424	2,628,905
COND	212,767	10.9	3,580.8	5,446	2,558,596

Table C.6: Data for the AZEP 85

HX	Heat transfer (kW)	ΔT_{log} (K)	U_o (W/m²K)	Surface , A (m²)	FCI (€, 2009)
RH	27,293	67.3	64.2	6,319	2,022,881
HPSH	49,710	54.8	63.8	14,215	4,095,394
HPEV	69,360	45.3	66.1	23,140	4,625,276
HPEC	52,562	49.1	62.0	17,285	2,375,214
IPSH	242	24.5	64.5	153	79,506
IPEV	11,594	18.1	71.5	8,959	2,025,853
IPEC	2,075	42.4	70.9	690	144,078
LPSH	2,465	42.8	53.1	1,085	436,722
LPEV	39,913	33.2	57.9	20,727	4,202,664
LPEC	41,374	33.4	55.4	22,351	2,970,409
COND	210,424	10.9	3,580.8	5,386	2,534,065
SH II	10,378	67.0	104.6	1,480	572,296
EV II	13,650	53.9	104.6	2,424	649,647
EC II	10,344	39.9	92.5	2,799	487,385
NGPH	8,433	505.1	43.1	388	174,490
AIR HX	8,526	779.8	58.4	187	231,586
FG COND	78,122	59.6	67.7	19,356	2,620,873
COOL1	3,713	51.0	52.8	1,379	263,311
COOL2	3,977	55.1	52.8	1,367	261,231
COOL3	3,595	55.4	52.8	1,229	238,128
COOL4	3,827	43.9	52.8	1,652	308,074
MCM LTHX	311,365	78.6	72.7	54,526	32,265,525
MCM HTHX	150,532	47.2	100.3	31,804	20,186,113

Table C.7: Data for the AZEP 100

HX	Heat transfer (kW)	ΔT_{log} (K)	U_o (W/m²K)	Surface , A (m²)	FCI (€, 2009)
RH	21,331	69.0	61.8	4,998	1,649,469
HPSH	30,867	45.3	61.5	11,063	3,292,736
HPEV	58,306	37.2	65.5	23,945	4,764,861
HPEC	44,177	56.0	62.5	12,633	1,808,108
IPSH	1,660	33.6	65.4	755	318,432
IPEV	29,009	25.6	72.0	15,747	3,309,015
IPEC	5,198	41.2	70.8	1,781	328,922
LPSH	2,551	41.6	53.0	1,158	462,291
LPEV	43,941	32.2	57.9	23,568	4,699,592
LPEC	43,235	36.1	55.5	21,573	2,880,176
COND	213,104	10.9	3,580.8	5,455	2,562,119
SH II	13,187	68.6	105.4	1,823	686,095
EV II	16,680	55.2	104.8	2,883	755,487
EC II	12,639	38.5	92.3	3,560	600,791
NGPH	8,433	511.9	43	382	172,468.5
AIR HX	10,121	779.4	58.5	222	268,813
FG COND	91,439	58.6	67.5	23,121	3,059,209
COOL1	4,358	50.9	52.8	1,622	303,140
COOL2	4,669	55.0	52.8	1,607	300,736
COOL3	4,224	55.4	52.8	1,445	274,204
COOL4	4,496	43.8	52.8	1,943	354,779
MCM LTHX	366,209	79.3	72.7	63,529	36,853,012
MCM HTHX	177,096	47.9	100.3	36,859	22,950,277

Table C.8: Data of the plant with CLC

HX	Heat transfer (kW)	ΔT_{log} (K)	U_o (W/m²K)	Surface , A (m²)	FCI (€, 2009)
RH	26,688	73.5	62.4	5,815	1,881,804
HPSH	36,418	46.5	62.0	12,621	3,692,758
HPEV	63,015	38.8	65.6	24,753	4,904,542
HPEC	47,749	54.7	62.4	14,000	1,977,257
IPSH	1,328	32.0	65.3	635	274,129
IPEV	26,268	24.3	71.9	15,057	3,182,549
IPEC	4,707	41.4	70.9	1,604	300,168
LPSH	2,635	41.8	53.0	1,190	473,220
LPEV	44,688	32.4	57.9	23,825	4,744,024
LPEC	39,692	38.1	55.6	18,724	2,546,260
COND	197,313	10.9	3,580.8	5,051	2,396,131
SH II	819	32.7	91.2	274	132,036
EV II	3,686	29.1	99.8	1,270	370,248
EC II	2,794	73.3	97.0	393	88,229
NGPH	10,582	269.6	44	889	359,222.7
FG COND	101,416	80.6	71.1	17,716	2,426,575
COOL1	4,242	50.4	52.4	1,607	300,747
COOL2	4,542	54.4	52.4	1,592	298,249
COOL3	4,062	54.5	52.4	1,424	270,650
COOL4	4,292	42.8	52.4	1,914	350,132

Table C.9: Data for MEA-0

HX	Heat transfer (kW)	ΔT_{log} (K)	U_o (W/m²K)	Surface , A (m²)	FCI (€, 2009)
RH	41,540	63.7	64.0	10,185	3,064,369
HPSH	55,519	54.2	63.8	16,049	4,551,454
HPEV	76,481	43.8	66.0	26,435	5,193,210
HPEC	57,949	50.3	62.1	18,545	2,525,057
IPSH	363	26.4	64.6	213	105,794
IPEV	13,036	23.3	71.7	7,817	1,799,282
IPEC	2,334	48.6	71.2	675	141,318
LPSH	3,299	44.3	53.3	1,400	545,022
LPEV	49,229	34.5	58.0	24,610	4,879,876
LPEC	41,165	37.0	55.6	20,003	2,696,976
COND	51,017	13.6	3,580.8	1,051	738,649
COOL CAU	47,121	61.6	65.0	11,778	1,701,151
COOL1	4,179	69.4	52.7	1,141	223,285
COOL2	3,941	62.6	52.7	1,193	232,104
COOL3	3,565	63.0	52.7	1,074	211,703
COOL4	3,796	53.2	52.7	1,354	259,001

Table C.10: Data for MEA-0.2

HX	Heat transfer (kW)	ΔT_{log} (K)	U_o (W/m²K)	Surface , A (m²)	FCI (€, 2009)
RH	41,540	63.8	64.0	10,185	3,170,644
HPSH	55,519	63.5	63.5	16,147	4,734,122
HPEV	76,481	66.0	66.0	26,435	5,373,316
HPEC	57,949	62.1	62.1	18,545	2,612,628
IPSH	363	64.3	64.3	214	110,040
IPEV	13,036	71.7	71.7	7,817	1,861,683
IPEC	2,334	71.2	71.2	675	146,219
LPSH	3,299	52.9	52.9	1,408	566,895
LPEV	49,229	58.0	58.0	24,610	5,049,115
LPEC	41,165	55.6	55.6	20,003	2,790,510
COND	120,636	3,580.8	3580.8	2,485	1,615,906
COOL CAU	47,121	765.1	65.0	11,778	1,760,149
COOL1	7,333	76.7	52.7	1,455	285,325
COOL2	3,941	62.9	52.7	1,193	240,154
COOL3	3,565	56.6	52.7	1,074	219,045
COOL4	3,796	71.4	52.7	1,354	267,984

C.1.2 Design of the tubes

The number and design of tubes in HXs are specified by setting their outside diameter and wall thickness. Smaller diameter tubes yield higher heat transfer coefficients, but larger diameter tubes are easier to clean and more rugged. Here, all outside diameters of the HXs are assumed to be 2.5 in, with the exception of the condenser, the IPHRSG and the secondary HRSG, where they are assumed to be 2 in, because of the smaller water/steam mass flows.

Fins can increase heat transfer and decrease the surface area of a HX. Four fins per in. of 0.75 in. height are assumed for economizers, condensers and coolers, and two fins per in. of 0.50 in. height are chosen for superheaters, reheaters and gas-gas HXs. To account for using fins in the HXs, Figure C.7 has been used. Assuming 16.5 MMBtuh are transferred without including fins and that 17.5 or 16.6 MMBtuh are transferred using four or two fins per in. of

0.75/0.50 in. height, respectively, the U_o values are increased by 6% or 0.6% (17.5/16.5=1.06 and 16.6/16.5=1.006). This increase has been considered here and it is included in the presented results.

The area of each finned tube is calculated as:

$$A = \frac{\pi n}{\mathbf{24}}\left[\mathbf{4}d_o h + \mathbf{4}h^2 + \mathbf{2}bd_o + \mathbf{4}bh\right] + \left\langle \frac{\pi d_o}{\mathbf{12}} \right\rangle (\mathbf{1} - nb) \tag{C.12}$$

Here, n is the fin density, h is the fin height and b is the fin thickness.

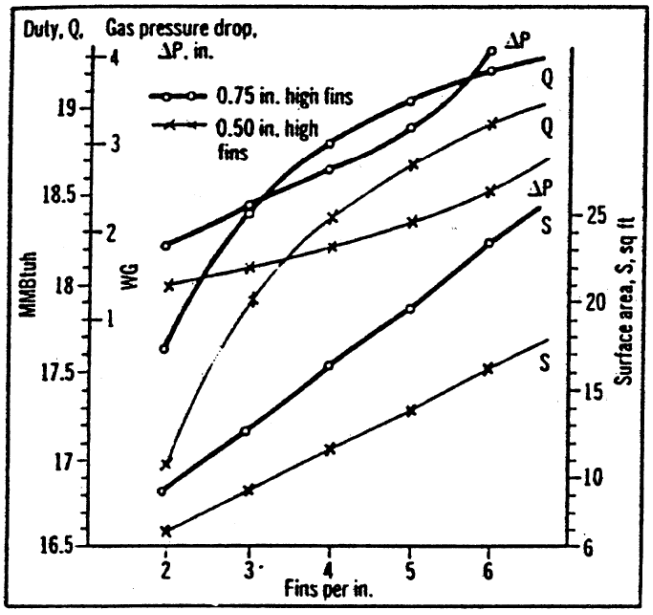

Figure C.7: Effect of fin geometry on performance. (Source: Ganapathy, 1991)

C.1.3 Materials

Materials widely used for the construction of tubes in HXs are those of group 178 of the grades A, C and D that stand for carbon steel, group 213 of the grades T11, T22, T5 and T91 that stand for intermediate alloys and group 213 of grades Tp-304, Tp-316, Tp-321 and Tp-347 that represent the use of stainless steel. The letters H and L indicate high and low carbon, respectively. Series 300 includes 0.15% carbon, a minimum of 16% chromium and sufficient nickel or manganese. The materials of the HXs comprising the HRSGs have been chosen depending on the outer wall temperature. For all of the plants, the materials have been kept the same for similar components, since the size and operating conditions are comparable. The maximum allowed temperatures for the most commonly used materials are shown in Table C.11:

Table C.11: Main construction materials of HRSGs (Ganapathy, 1991)

Material	**Maximum allowance temperature, °C**	**Component**
SA-178, grade A	482	HPEV, HPEC, IPEV, IPEC
SA-178, grade C	510	-
SA-213, grade T2	552	-
SA-213, grade T11	566	-
SA-213, grade T22	607	-
SA-213, grade T91	649	RH, HPSH
SA-213, grade Tp 304 H, 321 H	760	-

The names of the metals follow the American Society of Mechanical Engineers (ASME) specifications.

The appropriate materials for the rest of the HXs have been chosen in a similar way. In Table C.12 the design estimates related to the reference plant that lead to the calculation of the weight of the HXs are presented as an example of the calculations performed for all of the plants.

Table C.12: Design estimates for the HXs of the reference plant

	d_o	d_i	tube lenght	tube thickn.	fin density	fin height	fin thickn.	mat. density[a]	finned tube area	number of tubes	casing width	tubes/ row	weight/ tube	weight of fins	weight of tubes	weight of casing	total weight
Heat Exchanger	(in)	(in)	(ft)	(in)	(fin/in)	(in)	(in)	(lb/in)	(ft2)	(n)	(in)	(n)	(lb)	(lb)	(t)	(t)	(t)
HPSH	2.5	2.380	10	0.120	2	0.500	0.075	0.289	22.65	7,408	563.5	86	31.9	26.0	195	62.4	257
HPEV	2.5	2.395	10	0.105	4	0.750	0.050	0.283	58.38	4,887	458.4	70	27.4	54.1	181	40.5	221
HPEC	2.5	2.395	10	0.105	4	0.750	0.050	0.283	58.38	3,397	382.9	58	27.4	54.1	126	28.2	154
RH	2.5	2.380	10	0.120	2	0.500	0.075	0.289	22.65	4,958	461.7	70	31.9	26.0	130	41.9	172
IPSH	2.0	1.880	10	0.120	2	0.500	0.075	0.289	18.72	130	72.5	11	24.8	21.7	3	1.0	4
IPEV	2.0	1.895	10	0.105	4	0.750	0.050	0.283	49.22	1,756	255.5	42	21.8	45.8	54	12.6	66
IPEC	2.0	1.895	10	0.105	4	0.750	0.050	0.283	49.22	153	78.3	12	21.8	45.8	5	1.2	6
LPSH	2.5	2.380	10	0.120	2	0.500	0.075	0.289	22.65	663	171.4	26	31.2	26.0	17	5.8	23
LPEV	2.5	2.395	10	0.105	4	0.750	0.050	0.283	58.38	4,560	442.9	68	27.4	54.1	169	37.8	206
LPEC	2.5	2.395	10	0.105	4	0.750	0.050	0.283	58.38	3,581	393.0	60	27.4	54.1	132	29.7	162
COND	2.0	1.895	10	0.105	4	0.750	0.050	0.283	49.22	5,797	460.8	76	21.8	45.8	37	40.9	77

[a] Material densities of 0.289 and 0.283 lb/in are associated with stainless and carbon steel, respectively

Appendix D

Generalized costing equations

The following equations are based on cost calculations realized for this thesis and are shown here as a generalized guide for fixed capital cost calculations of similar-sized components. The sources used are shown in Table B.6 of Appendix B.

1. Gas turbine system[1,2] (reference year: 2009; *for other GT systems, see "Gas Turbine World"*; Framer, 2006).

$$Cost_{GT\_system} = \left(\frac{\dot{W}_{net}}{290}\right)^{0.9} \times 65.6 \times 10^{6}$$

Expander

$$Cost_{expander} = Cost_{GT\_system} \times 0.4$$

Compressor

$$Cost_{compressor} = Cost_{GT\_system} \times 0.35$$

Combustion chamber

$$Cost_{compressor} = Cost_{GT\_system} \times 0.25$$

Or

$$Cost_{CC} = \left(\frac{\dot{m}_{fg}}{628.5}\right)^{0.67} \times 21.9 \times 10^{6}$$

[1] Pressure ratio: 16.8

[2] The total cost has been shared among the three main components of the system as following: 40% to the expander, 35% to the compressor and 25% to the CC.

2. Heat recovery steam generator

Reheater, Superheater

$$Cost_{SH/RH} = \left(\frac{A_{SH/RH}}{4.1\times10^{3}}\right)^{0.87} \times 1.3\times10^{6} \times \frac{CI_{CEPSI}}{468.2}$$

Evaporator

$$Cost_{EV} = \left(\frac{A_{EV}}{20.5\times10^{3}}\right)^{0.87} \times 3.7\times10^{6} \times \frac{CI_{CEPSI}}{468.2}$$

Economizer

$$Cost_{EC} = \left(\frac{A_{EC}}{16.3\times10^{3}}\right)^{0.87} \times 2\times10^{6} \times \frac{CI_{CEPSI}}{468.2}$$

3. Condenser

$$Cost_{COND} = \left(\frac{\dot{Q}_{COND}}{213.0}\right)^{0.87} \times 1.9\times10^{6} \times \frac{CI_{CEPSI}}{390.6}$$

4. ST system (reference year 2009)[3]

$$Cost_{ST\_sys} = \left(\frac{\dot{W}}{120}\right)^{0.9} \times 26.4\times10^{6}$$

HPST

$$Cost_{HPST} = \left(\frac{\dot{W}}{\dot{W}_{tot}}\right) \times Cost_{ST\_system}$$

IPST

$$Cost_{IPST} = \left(\frac{\dot{W}\times1.5}{\dot{W}_{tot}}\right) \times Cost_{ST\_system}$$

LPST

$$Cost_{LPST} = \left(\frac{\dot{W}\times2}{\dot{W}_{tot}}\right) \times Cost_{ST\_system}$$

Where,

$$\dot{W}_{tot} = \dot{W}_{HPST} + 1.5\times\dot{W}_{IPST} + 2\times\dot{W}_{LPST}$$

[3] High pressure: 124 bar

5. Pumps[4]

a) For $\dot{W}_P \leq 0.3$ MW

- Oulet Pressure ~ 5 bar

$$Cost_{Pump} = -2.9 \times \dot{W}_P{}^2 + 2,328 \times \dot{W}_P + 61,233 \times \frac{CI_{CEPSI}}{357.6}$$

- Oulet Pressure ~ 25 bar

$$Cost_{Pump} = -4.05 \times \dot{W}_P{}^2 + 3,277 \times \dot{W}_P + 86,205 \times \frac{CI_{CEPSI}}{357.6}$$

- Oulet Pressure ~ 100 bar

$$Cost_{Pump} = -4.3 \times \dot{W}_P{}^2 + 3,795 \times \dot{W}_P + 102,268 \times \frac{CI_{CEPSI}}{357.6}$$

- Oulet Pressure ~ 130 bar

$$Cost_{Pump} = -4.8 \times \dot{W}_P{}^2 + 4,197 \times \dot{W}_P + 113,100 \times \frac{CI_{CEPSI}}{357.6}$$

For $\dot{W}_P > 0.3$ MW

$$Cost_{Pump} = \left(\frac{\dot{W}_P}{3.4} \right)^{0.8} \times 1.4 \times 10^6 \times \frac{CI_{CEPSI}}{357.6}$$

6. Cooling Tower

$$Cost_{CT} = \frac{\dot{Q}}{216.9} \times 1.8 \times 10^6 \times \frac{CI_{CEPSI}}{390.6}$$

7. De-aerator

$$Cost_{Deaerator} = 4.9 \times 10^3 \times \left(\dot{m}_s + \dot{m}_w \right) \times \frac{CI_{CEPSI}}{357.6}$$

II. Added components in plants with CO_2 capture

1. Steam Turbine (reference year 2009)

$$Cost_{ST} = \left(\frac{\dot{W}}{\dot{W}_{LPST}} \right)^{0.9} \times Cost_{LPST}$$

[4] Centrifugal; carbon steel pumps, including the cost of motors (Turton et al., 2002)

2. Recycle compressors and CO_2 compressors, (reference year 2009)

$\dot{W} \le 1.4$ MW

$$Cost_{comp} = \left(\frac{\dot{W}}{0.3}\right)^{0.5} \times 1.7 \times 10^6 \times 1.15$$

$\dot{W} > 1.4$ MW

$$Cost_{comp} = \left(\frac{\dot{W}}{1.4}\right)^{0.7} \times 4.2 \times 10^6 \times 1.15$$

3. CO_2 cooler and flue gas condenser

$$Cost_{Cooler} = \left(\frac{A_{Cooler}}{16.3 \times 10^3}\right)^{0.87} \times 2 \times 10^6 \times \frac{CI_{CEPSI}}{468.2}$$

4. Gas-gas heat exchanger

For $T_{\max} \ge 800°C$

$$Cost_{HX} = \left(\frac{A_{HX}}{16.3 \times 10^3}\right)^{0.87} \times 10^7 \times \frac{CI_{CEPSI}}{468.2}$$

For $T_{\max} < 800°C$

$$Cost_{HX} = \left(\frac{A_{HX}}{16.3 \times 10^3}\right)^{0.87} \times 4 \times 10^6 \times \frac{CI_{CEPSI}}{468.2}$$

5. Duct Burner (reference year 2009)

$$Cost_{DB} = \left(\frac{\dot{m}_{fuel}}{14}\right)^{0.67} \times 21.9 \times 10^6$$

A is the surface area in m², ($A_{SH\_RH}, A_{Evap}, A_{Econ}, A_{cond}, A_{HX}, A_{cooler} = \frac{\Delta\dot{Q} / \Delta T_{\log}}{U_o}$)

CI_{CEPSI} *is the CEPSI index of the calculation year,*

$\dot{m}_{fg}$ *is the mass flow rate of the combustion products in kg/sec,*

m_s and m_w *are the mass of steam and water entering the de-aerator in kg/sec,*

$\dot{Q}$ *is the heat rate in MW,*

$\dot{W}$ *is the total power produced by a component in MW and*

$\dot{W}_p$ *is the total power consumed in a pump in MW.*

References

Abad, A., Mattisson, T., Lyngfelt, A. and Rydén, M. (2006) Chemical-looping combustion in a 300 W continuously operating reactor system using a manganese-based oxygen carrier, Fuel, 85, 1174-1185.

Abad, A., Mattisson, T., Lyngfelt, A. and Johansson, M. (2007) The use of iron oxide as oxygen carrier in a chemical-looping reactor, Fuel, 86, 1021-1035.

Abu-Zahra, M.R.M., Niederer, J.P.M, Feron, P.H.M., Versteeg, G.F. (2007) CO_2 capture from power plants Part II. A parametric study of the economical performance based on mono-ethanolamine, International Journal of Greenhouse Gas Control, I, 135-142.

Afgan, N., et al. (1996) New Developments in Heat Exchangers, ISBN: 905699512X.

Anderson, R., MacAdam, S., Viteri, F., Davies, D., Downs, J. and Paliszewski, A. (2008) Adapting Gas Turbines to Zero Emission Oxy-fuel Power Plants, Proceedings of the ASME Turbo Expo, Berlin, G2008-51377.

Anderson, K. and Johnsson, F. (2006) Process evaluation of an 865 MWe lignite fired O_2/CO_2 power plant, Energy Conversion and Management, 47 (18-19), 3487-3498.

Anderson, K., Johnsson, F. and Strömberg, L. (2003) Large Scale CO_2 Capture-Applying the Concept of O_2/CO_2 Combustion to Commercial Process Data, VGB PowerTech 83, Heft 10, 29–33.

Aspen Plus, Aspentech, http://www.aspentech.com, accessed: December, 2009.

Bejan, A., Tsatsaronis, G. and Moran, M. (1996) Thermal Design and Optimization, J. Wiley, New York.

Benedict, M. and Gyftopoulos, E. P. (1980) Economic Selection of the Components of an Air Separation Process, in: Thermodynamics: Second Law Analysis (R.A. Gaggioli, Ed.) A.C. S. Symposium Series, 122, 195-203.

Benson, S. M. and Orr, Jr., F. M. (2008) Carbon Dioxide Capture and Storage, MRS Bulletin, 33, 303-305.

Bergmann, E. and Schmidt, K. R. (1965) Zur kostenwirtschaftlichen Optimierung der Warmeaustauscher für die regenerative Speisewasservorwarmung im Dampfkraftwerk - ein Storungsverfahren mit der Exergie, in: Energie und Exergie, VDI-Verlag, Düsseldorf, 63-89.

Beyer, J. (1979) Einige Probleme der praktischen Anwendung der exergetischen Methode in wärmewirtschaftlichen Untersuchungen industrieller Produktionsprozesse II, Energieanwendung 28 (2), 66-70.

Beyer, J. (1978) Einige Probleme der praktischen Anwendung der exergetischen Methode in wärmewirtschaftlichen Untersuchungen industrieller Produktionsprozesse I, Energieanwendung, 27 (6), 204-208.

Beyer, J. (1972) Zur Aufteilung der Primärenergiekosten in Koppelprozessen auf Grundlage der Strukturanalyse, Energieanwendung, 21 (6), 179-183.

Bloch, H. P. and Soares, C. (1998) Process Plant Machinery, Second Edition, Butterworth-Heinemann, USA, 249-276.

Bolhàr-Nordenkampf, J., Pröll, T., Kolbitsch, P., Hofbauer, H. (2008) Performance of a NiO-based oxygen carrier for Chemical Looping Combustion and reforming in a 120kW unit, 9th International Conference on Greenhouse Gas Technologies, Washington DC.

Bolland, O. and Mathieu, P. (1998) Comparison of two CO_2 removal options in combined cycle power plants, Energy Conversion and Management, 39, 1653-1663.

Bolland, O. (1991) Comparative evaluation of advanced combined cycle alternatives, Journal of Engineering for Gas Turbines and Power, 113, 190-197.

Bottino, A., Comite, A., Capannelli, G., di Felice, R. and Pinacci, P. (2006) Steam reforming of methane in equilibrium membrane reactors for integration in power cycles, Catalysis Today, 118, 214–222.

Boyano, A., Tsatsaronis, G., Morosuk, T. and Marigota, A. M. (2010) Advanced exergoenvironmental analysis of a steam methane reforming system for hydrogen production, ASME, IMECE2010-38551.

Boyano, A., Tsatsaronis, G., Morosuk, T. and Blanco-Marigorta, A. M. (2009) Advanced exergetic analyses of chemical processes, Proceedings of the ASME 2009 International Mechanical Engineering Congress and Exposition, Lake Buena Vista, IMECE2009-10463.

Brandvoll, Ø. and Bolland, O. (2004) Inherent CO_2 Capture Using Chemical Looping Combustion in a Natural Gas Fired Power Cycle, ASME Journal of Engineering for Gas Turbines and Power, 126, 316-321, GT-2002-30129.

Brandvoll, Ø., Kolbeinsen, L., Olsen, N. and Bolland, O. (2003) Chemical Looping Combustion – Reduction of nickel oxide/nickel aluminate with hydrogen, in: Proceedings of the Sixth Italian Conference on Chemical and Process Engineering, Pisa, Italy, Chemical Engineering Transactions, 3, 105-110.

Climate Change 2007: Synthesis Report (2007) (Pachauri, R. K. and Reisinger, A., Eds.), IPCC, Geneva, 104.

Chen, L., Hong, Q., Lin, J. and Dautzenberg, F. (2007) Hydrogen production by coupled catalytic partial oxidation and steam methane reforming at elevated pressure and temperature, Journal of Power Sources, 164, 803–808.

Cooper Turbocompressor Inc., Centrifugal Compressors, http://www.fluidenergy.com/pdf/cooper_ta_msg.pdf, accessed: May, 2009.

Cziesla, F., Tsatsaronis, G. and Gao, Z. (2006) Avoidable Thermodynamic Inefficiencies and Costs in an Externally-Fired Combined-Cycle Power Plant, Energy - The International Journal, 31, 1472-1489.

EES, Engineering Equation Solver, http://www.mhhe.com/engcs/mech/ees, accessed: July, 2009.

Eisermann, W., Hasberg, W. and Tsatsaronis, G. (1984) THESIS – Ein Rechnerprogramm zur Simulation und Entwicklung von Energieumwandlungsanlagen, Brennstoff Wärme Kraft, 36 (1/2), 45-51.

Eisermann, W. (1979) Analysis of Processes for Production of Synthetic Gaseous Fuels, Final Report, NATO Fellowship Contract No. 430-402-566-8, University of Kentucky.

El Sayed, Y. M. (2003) The Thermoeconomics of Energy Conversions, Pergamon, 1st edition.

El-Sayed, Y. M. and Tribus, M. (1983) Strategic use of thermoeconomics for system improvement, in: Efficiency and Costing Second Law Analysis of Processes, A. C. S. Symposium Series, 235, 215-238.

El-Sayed, Y. M. and Aplenc, A. J. (1970) Application of the thermoeconomic approach to the analysis and optimization of a vapor-compression desalting system, Trans. ASME, J. Eng. Power, 92, 17-26.

El-Sayed Y. M. and Evans, R. B. (1970) Thermoeconomics and the design of heat systems, Trans. ASME, J. Eng. Power, 92, 27-34.

Environmental management, Life cycle assessment, Principles and framework (2006), ISO 14040:2006.

Environmental Technology Best Practice Programme (ETBPP), Life Cycle Assessment - An Introduction for Industry, ET257 GUIDE, http://www.tangram.co.uk, accessed: March, 2000.

Buchanan, T., DeLallo, M., Schoff, R., White, J., Wolk, R. (2000) Evaluation of Innovative Fossil Fuel Power Plants with CO_2 Removal, Palo Alto, CA, U. S. Department of Energy — Office of Fossil Energy, Germantown, MD and U. S. Department of Energy/NETL, Pittsburgh, PA: 2000. 1000316.

Eriksson, O., Finnveden, G., Ekvall, T. and Björklund, A. (2007) Life cycle assessment of fuels for district heating: A comparison of waste incineration, biomass-and natural gas combustion, Energy policy, 35 (2), 1346-1362.

Evans, R. B., Kadaba, P. V. and Hendrix, W. A. (1983) Essergetic functional analysis for process design and synthesis, in: Efficiency and Costing Second Law Analysis of Processes, A. C. S. Symposium Series, 235, 239-261.

Evans, R. B. and Tribus, M. (1965) Thermo-Economics of Saline Water Conversion, Industrial and Engineering Chemistry, Process Design and Development, 4 (2), 195-206.

Evans, R.B. and Tribus, M. (1962) A Contribution to the Theory of Thermoeconomics, UCLA, Dept. of Engr.: Report No. 62/63, Los Angeles, CA.

Fehring, T. H. and Gaggioli, R. A. (1977) Economics of feedwater heater replacement, Trans. ASME, J. Eng. Power, 99, 482-489.

Fiaschi, D. and Lombardi, L. (2002) Integrated Gasifier Combined Cycle Power Plant with Integrated CO_2-H2S removal: Performance Analysis, Life Cycle Assessment and Exergetic Life Cycle Assessment, International Journal of Applied Thermodynamics, 5 (1), 13-24.

Framer, R. (2006) Gas Turbine World 2006 Handbook, Pequot Publishing, Fairfield, CT.

Frangopoulos, C. A. (1994) CGAM problem: Definition and conventional solution, Energy - The International Journal, 19 (3), 323-342.

Frangopoulos, C. A. (1992) Optimal synthesis and operation of thermal systems by the thermoeconomic functional approach, J Eng Gas Turbines Power, 114, 707-714.

Frangopoulos, C. A. (1988) Functional decomposition for optimal design of complex thermal systems, Energy - The International Journal, 13 (3), 239–244.

Frangopoulos, C. A. (1987) Thermo-economic functional analysis and optimization, Energy - The International Journal, 12 (7), 563–71.

Frangopoulos, C. A. (1983) Thermoeconomic functional analysis: a method for optimal design or improvement of complex thermal systems, Dissertation, Georgia Institute of Technology.

Gaggioli, R. A., El-Sayed, Y .M., El-Nashar, A. M. and Kamaluddin, B. (1986) Second Law Efficiency and Costing Analysis of a Combined Power and Desalination Plant, in: Computer-Aided Engineering of Energy Systems (Gaggioli, R. A., Ed.), 2-3, ASME, New York, 77-85.

Gaggioli, R. A. (1983) Second Law Analysis for Process and Energy Engineering, in: Efficiency and Costing Second Law Analysis of Processes (Gaggioli, R. A., Ed.), A. C. S. Symposium Series, 235, 3-50.

Gaggioli, R. A. (1977) Proper evaluation and pricing of energy, Proc. Int. Conf. Energy Use Management, 11 (24-28), 31-43.

Gaggioli, R. A., Rodriguez, L. and Wepfer, W. J. (1978) A Thermodynamic-Economic Analysis of the Synthane Process, Final Report prepared for the Pittsburgh Energy Technology Center, U.S. D.O.E., Contract No. EY-77-S-02-4589-1.

Ganapathy, V., (2003) Industrial Boilers and Heat Recovery Steam Generators, Marcel Dekker, New York.

Ganapathy, V., (1991) Waste Heat Boiler Desktop, The Fairmont Press, Lilburn, GA.

GE Enter Software LLC (2000), GateCycle, Menlo Park, CA.

Gestra, A. G., Deaerating Plant for Boiler Feedwater C4. FLOWSERVE - Flow Control Division,

http://www.flowserve.com/files/Files/Literature/ProductLiterature/FlowControl/Gestra/813938.pdf, accessed: May, 2009.

Goedkoop, M., Spriensma, R. (2000) The Eco-indicator 99: A Damage Oriented Method for Life Cycle Impact Assessment, Methodology Report, Amersfoort, Netherlands.

Griffin, T., Sundkvist, S. G., Asen, K. and Bruun, T. (2005) Advanced Zero Emissions Gas Turbine Power Plant, Journal of Engineering for Gas Turbines and Power, 127, 81-85.

Grubbström, J. (2008) Chemical Looping Combustion, Status of Development, ALSTOM, Chemical Looping Programme, Elforsk.

Guthrie, K. (1974) Process plant estimating, evaluation and control, ISBN: 0-910460-5-1.

Herzog, H. (2001) What Future for Carbon Capture and Sequestration?, Environmental Science and Technology, 35, 148.

Hesselmann, K. (1986) Heat exchanger networks – An exergoeconomical evaluation, in: Computer-Aided Engineering of Energy Systems, ASME, W.A.M., New York, 2-3, 23-34.

Horn, R., Williams, K., Degenstein, N., Bitsch-Larsen, A., Nogare, D. D., Tupy, S. and Schmidt, L. (2007) Methane catalytic partial oxidation on autothermal Rh and Pt foam catalysts: Oxidation and reforming zones, transport effects, and approach to thermodynamic equilibrium, Journal of Catalysis, 249, 380–393.

Hossain, M. M., de Lasa, H. I. (2008) Chemical-looping combustion (CLC) for inherent CO_2 separation – a review. Chemical Engineering Science, 63, 4433-4451.

INSPIRE, RTN supported by the European Community's Sixth Framework Programme, http://www.http.www.mc-inspire.net, accessed: July, 2009.

IPCC, Special Report on Carbon Dioxide Capture and Storage, Prepared by Working Group III of the Intergovernmental Panel on Climate Change (2005) (Metz, B., Davidson, O., de Coninck, H. C., Loos, M. and Meyer, L. A. Eds.), Cambridge University Press, Cambridge, United Kingdom and New York, NY, USA.

Ishida, M. and Jin, H. (1994) A novel combustor based on chemical-looping reactions and its reaction kinetics, Journal of Chemical Engineering of Japan, 27, 296-301.

Jericha, H., Lukasser, A. and Gatterbauer, W. (2000) Der Graz Cycle für Industriekraftwerke gefeuert mit Brenngasen aus Kohle- und Schwerölvergasung, VDI Berichte 1566, VDI Conference Essen, Germany.

Jericha, H. and Fesharaki, M. (1995) The Graz Cycle 1500 C Max Temperature-CO_2 Capture with CH_4-O_2 Firing, ASME paper 95-CTP-79, ASME Cogen-Turbo Power Conference, Vienna.

Jericha, H. (1985) Efficient Steam Cycles with Internal Combustion of Hydrogen and Stoichiometric Oxygen for Turbines and Piston Engines, CIMAC Conference Paper, Oslo, Norway.

Jin, H. and Ishida, M. (2004) A new type of coal gas fueled chemical-looping combustion, Fuel, 83, 2411-2417.

Johannessen, E. and Jordal, K. (2005) Study of a H2 separating membrane reactor for methane steam reforming at conditions relevant for power processes with CO_2 capture. Energy Conversion and Management, 46, 1059–1071.

Johansson, M., Mattisson, T., Lyngfelt, A. (2006) Comparison of oxygen carriers for Chemical-Looping Combustion, Thermal Science, 10, 93-107.

Jordal, K., Bredesen, R., Kvamsdal, H. and Bolland, O. (2004) Integration of H2-separating membrane technology in gas turbine processes for CO_2 capture, Energy, 29, 1269–1278.

Kakaras, E., Doukelis, A., Giannakopoulos, D. and Koumanakos, A. (2005) Emission reduction technologies for the fossil fuel fuelled electricity generation sector, Scientific conference HELECO.

Katalytisch, R. M. (2005) Stabilisierte Verbrennung von Ch4/Luft Gemischen und H_2O- und CO_2-Verdünnten Ch4/Luft Gemischen über Platin unter Hochdruckbedingungen. Dissertation. Eidgenössischen Technischen Hochschule Zürich, 26, 11-17.

Keenan, J. H. (1932) A steam chart for second law analysis, Trans. ASME, 54 (3), 195–204.

Kelly, S., Tsatsaronis G. and Morosuk, T. (2009) Advanced Exergetic Analysis: Approaches for Splitting the Exergy Destruction into Endogenous and Exogenous Parts, Energy – The International Journal, 34 (3), 384-391.

Kelly, S. (2008) Energy systems improvement based on endogenous and exogenous exergy destruction, Dissertation, Technische Universität Berlin, Berlin, Germany.

Kenney, W. F. (1984) Energy conservation in the process industries, Academic Press, Inc.

Khoo, H. H. and Tan, R. B. H. (2006) Life Cycle Evaluation of CO_2 Recovery and Mineral Sequestration Alternatives, Environmental Progress, 25 (3), 208-217.

Klara, J. M. (2007) Chemical-Looping Process in a Coal-to-Liquids, Independent Assessment of the potential of the OSU Chemical Looping Concept, U.S. Department of Energy, National Energy Technology Laboratory, DOE/NETL-2008/1307.

Knoche, K. F. and Funk, J. E. (1977) Entropie-Produktion, Wirkungsgrad und Wirtschaftlichkeit der thermodynamischen Erzeugung syntetischer Brennstoffe, Der Schwefelsäure-Hybrid-Prozess zur thermochemischen Wasserspaltung, BWK 29 (1), 23-27.

Knoche, K. F. and Hesselmann, K. (1986) Exergoeconomical Analysis of chemical processes – Evaluation of an Air separation plant, in: Computer-Aided Engineering of Energy Systems, ASME, W.A.M., New York, 2-3, 35-43.

Knoche, K. F. and Hesselmann, K. (1985) Exergoökonomische Bewertung einer Luftzerlegungs-Anlage, Chem.-Ing.-Techn., 57, 602-609.

Knoche, K. F., Richter, H. (1968) Verbesserung der Reversibilität von Verbrennungs-Prozessen, Brennstoff-Wärme- Kraft, 5, 205-210.

Kolbitsch, P., Pröll, T., Hofbauer H. (2008) Modeling of a 120kW chemical looping combustion reactor system using a NiO oxygen carrier, Chemical Engineering Science, 64, 99-108.

Kotas, T. J. (1985) The exergy method of thermal plant analysis, Butterworths, London.

Kothandaraman, A., Nord, L., Bolland, O., Herzog, H. J. and McRae, G. J. (2009) Comparison of solvents for post-combustion capture of CO_2 by chemical absorption, Energy Procedia, 1, 1373-1380.

Kvamsdal, H., Jordan, K. and Bolland, O. (2007) A quantitative comparison of gas turbine cycles with CO_2 capture, Energy, 32 (1), 10-24.

Lazzaretto, A. and Andreatta, R. (1995) Algebraic formulation of a process-based exergy-costing method, in: Symposium on thermodynamics and the design, analysis, and improvement of energy systems (Krane R. J., Ed.), 35. ASME, New York, 395–403.

Lazzaretto, A. and Tsatsaronis, G. (2006) SPECO: A Systematic and General Methodology for Calculating Efficiencies and Costs in Thermal Systems, Energy - The International Journal, 31, 1257-1289.

Lazzaretto, A. and Tsatsaronis, G. (1997) On the Quest for Objective Equations in Exergy Costing, Proceedings of the ASME, Advanced Energy Systems Division (Ramalingam, M. L., Lage, J. L., Mei, V. C., and Chapman, J. N., Eds.), 37, 197-210.

Lewis, W. K. and Gilliland, E.R. (1954) Production of pure carbon dioxide, US patent No. 2665972.

Lin, L. and Tsatsaronis, G. (1993) Cost Optimization of an Advanced IGCC Power Plant Concept Design, Thermodynamics and the Design, Analysis, and Improvement of Energy Systems – 1993 (Richter, H. J., Ed.), 30 (266), 157-166.

Linderholm C., Abad A., Mattisson T. and Lyngfelt A. (2008) 160 h of chemical-looping combustion in a 10 kW reactor system with a NiO-based oxygen carrier, The 4th Trondheim Conference on CO_2 Capture, Transport and Storage International Journal of Greenhouse Gas Control, 2 (4), 520-530.

Ludwig, E. (2001) Applied Process Design III, 3rd Edition, ISBN: 0-8841-5651-6.

Lyngfelt, A., Leckner, B. and Mattisson, T. (2001) A fluidized-bed combustion process with inherent CO_2 separation; application of chemical-looping combustion, Chemical Engineering Science, 56, 3101-3113.

Lyngfelt, A. and Thunman, H. (2005) Construction and 100 h of operational experience of a 10-kW chemical looping combustor, in: The CO_2 Capture and Storage Project (CCP) for Carbon Dioxide Storage in Deep Geologic Formations For Climate Change Mitigation, 1, 625-646.

Matlab 7, The MathWorks, Matlab online Documentation, http://www.mathworks.com/access/helpdesk/help/techdoc/math/f1-85462.html, accessed: December, 2009.

Mattison, T. and Lyngfelt, A. (2001) Applications of chemical-looping combustion with capture of CO_2, 2nd Nordic minisymposium on CO_2 capture and storage, Göteborg, Sweden.

Meyer, L., Tsatsaronis, G., Bushgeister, J. and Schebek, L. (2009) Exergoenvironmental analysis for evaluation of the environmental impact of energy conversion systems, Energy - The International Journal 34, 75-89.

MITSUBISHI Heavy Industries, LTD, Steam Turbine Generator, Standard Turbine Frames, http://www.mhi.co.jp/en/products/ pdf/at_turbine.pdf, accessed: April, 2009.

Moeller, B., Torisson, T., Assadi, M., Sundkvist, S. G. and Asen, K. I. (2006) AZEP Gas Turbine Combined Cycle Power Plants - Thermo-economic Analysis, International Journal of Thermodynamics, 9, 21-28.

Moran, M. J. (1982) Availability Analysis – A Guide to efficient energy use, Prentice-Hall, Inc..

Morosuk, T. and Tsatsaronis, G. (2009a) Advanced Exergy Analysis for Chemically Reacting Systems – Application to a Simple Open Gas-Turbine System, International Journal of Thermodynamics, 12 (3), 105-111.

Morosuk, T. and Tsatsaronis, G. (2009b) Advanced Exergetic Evaluation of Refrigeration Machines Using Different Working Fluids, Energy - The International Journal, 34 (12), 2248-2258.

Morosuk, T., and Tsatsaronis, G. (2008a) A New Approach to the Exergy Analysis of Absorption Refrigeration Machines Energy - The International Journal, 33 (6), 890-907.

Morosuk, T. and Tsatsaronis, G. (2008b) How to Calculate the Parts of Exergy Destruction in an Advanced Exergetic Analysis, in: Proceedings of the 21st International Conference on Efficiency, Costs, Optimization, Simulation and Environmental Impact of Energy Systems (Ziebik, A., Kolenda, Z. and Stanek, W. Eds.), Cracow-Gliwice, 185-194.

Morosuk, T. and Tsatsaronis, G. (2007) Exergoeconomic Evaluation of Refrigeration Machines Based on Avoidable Endogenous and Exogenous Costs, in: Proceedings of the 20th International Conference on Efficiency, Cost, Optimization, Simulation and Environmental Impact of Energy Systems (Mirandola, A., Arnas, O. and Lazzaretto, A., Eds.), Padova, 1, 1459-1467.

Morosuk, T. and Tsatsaronis, G. (2006a) Splitting the exergy destruction into endogenous and exogenous parts – application to refrigeration machines, in: Proceedings of the 19th International conference on efficiency, cost, optimization, simulation and environmental impact of energy systems (Frangopoulos, C., Rakopoulos, C. and Tsatsaronis, G., Eds.), Aghia Pelagia: Crete, 1, 165–172.

Morosuk, T. and Tsatsaronis, G. (2006b) The 'Cycle Method' used in the exergy analysis of refrigeration machines: from education to research, in: Proceedings of the 19th International conference on efficiency, cost, optimization, simulation and environmental impact of energy systems (Frangopoulos, C., Rakopoulos, C. and Tsatsaronis, G., Eds.), Aghia Pelagia: Crete, 1, 157-163.

Obert, E. F. and Gaggioli, R. A. (1963) Thermodynamics, McGraw-Hill, New York.

Naqvi, R. (2006) Analysis of Natural Gas-Fired Power Cycles with Chemical Looping Combustion for CO_2 Capture, Dissertation, Norwegian University of Science and Technology.

Naqvi, R. and Bolland, O. (2007) Multi-stage chemical looping combustion (CLC) for combined cycles with CO_2 capture. Int. J. of Greenhouse Gas Control, 1, 19-30.

Naqvi, R., Bolland, O. and Wolf, J. (2005) Off-Design Evaluation of a natural gas fired Chemical Looping Combustion combined cycle with CO_2 capture, Proceedings of The 18th International Conference on Efficiency, Cost, Optimization, Simulation and Environmental Impact of Energy Systems (ECOS), Trondheim, Norway, 827-834.

Nuovo Pignone S.p.A. GE Oil & Gas - Gas Turbines, http://www.geoilandgas.com/businesses/ge_oilandgas/en/downloads/gas_turb_cat.pdf, accessed: April, 2009.

Perry R. H. and Green, D. W. (1997) Perry´s Chemical Engineers´ Handbook, Seventh Edition, McGraw-Hill Companies, Inc., New York.

Peters, M. S. (2003) Plant design and economics for chemical engineers, 5th Edition, New York, ISBN: 0-07-239266-5.

Petrakopoulou F., Boyano A., Cabrera M. and Tsatsaronis G. (2010a) Exergoeconomic and exergoenvironmental analyses of a combined cycle power plant with chemical looping technology, International Journal of Greenhouse Gas Control, In press, DOI: 10.1016/j.ijggc.2010.06.008.

Petrakopoulou F., Tsatsaronis G., Boyano A. and Morosuk T. (2010b) Exergoeconomic and Exergoenvironmental Evaluation of power plants including CO_2 capture, Carbon Capture & Storage Special Issue of Chemical Engineering Research and Design, In press, DOI: 10.1016/j.cherd.2010.08.001.

Petrakopoulou F., Tsatsaronis G. and Morosuk T. (2010c) Conventional Exergetic and Exergoeconomic analyses of a power plant with chemical looping combustion for CO_2 capture, International Journal of Thermodynamics, Vol. 13 (3), pp. 77-86.

Petrakopoulou F., Boyano A., Cabrera M. and Tsatsaronis G. (2010d) Exergy-based analyses of an advanced zero emission plant, International Journal of Low-Carbon Technologies, Vol. 5 (4), pp. 231-238.

Petrakopoulou F., Tsatsaronis G., Morosuk T. and Carassai A. (2010e) Conventional and advanced Exergetic Analyses applied to a combined cycle power plant, ECOS 2010, Lausanne, Switzerland, pp. 1363-1371.

Petrakopoulou F., Tsatsaronis G., Morosuk T. and Carassai A. (2010f) Advanced Exergoeconomic Analysis applied to a complex energy conversion system, ASME IMECE 2010, Vancouver, Canada, CD-ROM, IMECE2010-38555.

Reistad, G. M. (1970) Availability: Concepts and Applications, Dissertation, The University of Wisconsin-Madison, USA.

Rennie, (2006) Corrosion and materials selection for amine service, Materials forum, 30, (Wuhrer, R. and Cortie, M., Eds.), Inst of Materials Engineering Austrialasia, Ltd.

Richter, H. J. and Knoche, K. F. (1983) Reversibility of combustion processes, ACS Symposium Series, 235, 9971-9985.

Rubin, E. S. and Rao, A. B. (2002) A Technical, Economic and Environmental Assessment of Amine-based CO_2 Capture Technology for Power Plant Greenhouse Gas Control, U.S. Department of Energy, National Energy Technology Laboratory, DOE/DE-FC26-00NT40935.

Sanz, W., Jericha, H., Moser, M. and Heitmeir, F. (2005) Thermodynamic and Economic Investigation of an Improved Graz Cycle Power Plant for CO_2 Capture, Engineering for Gas Turbines and Power, 127, 765-772.

Seider, W. D., Seader, J. D. and Lewin D. R. (2004) Product and Process Design Principles, Synthesis, Analysis and Evaluation, Second Edition, John Wiley and Sons, Inc., New York, 412-440, 785-786.

SimaPro LCA Software, Database Manual (2006), Eco-Indicator 99, PRé Consultants B.V., Amersfoort, Netherlands, http://www.pre.nl.

Sinnott, R. K. (2005) Chemical Engineering design, 4th Edition, Elsevier, Amsterdam, ISBN: 0-7506-6538-6.

Soares, C. (2002) Process Engineering Equipment Handbook, McGraw-Hill Handbooks, New York, C13-C16.

Sofbid, Ebsilon. http://www.sofbid.com, accessed: 2009.

Sundkvist, S. G., Julsrud, S., Vigeland, B., Naas, T., Budd, M., Leistner, H. and Winkler, D. (2007) Development and testing of AZEP reactor components. International journal of greenhouse gas control I 180-187.

Sundkvist, S. G., Klang, K., Sjödin, M., Wilhelmsen, K., Sen, K., Tintinelli, A., McCahey, S. and Huang, Y. (2005) Azep gas turbine combined cycle power plants - Thermal optimisation and LCA analysis. Greenhouse Gas Control Technologies 7, 263-271.

Sundkvist, S. G., Griffin, T. and Thorshaug, N. P. (2001) AZEP – Development of an Integrated Air Separation Membrane – Gas Turbine, 2nd Nordic minisymposium on CO_2 capture and storage, Göteborg, Sweden.

Szargut, J., Morris, D. R. and Steward, F.R. (1988) Exergy analysis of Thermal, Chemical, and Metallurgical Processes, Hemisphere Publishing Corporation, New York.

Szargut, J. (1974) Wärmeökonomische Probleme des Umweltschutzes/Energieanwendung, Energieanwendung, 23, 306-310.

Szargut, J. (1971) Anwendung der Exergie zur angenhärten wirtschaftlichen Optimierung, BWK, 23 (12), 516-519.

Szargut, J. (1967) Grenzen für die Anwendungsmöglichkeiten des Exergiebegriffs, BWK, 19 (6), 309-313.

Toffolo, A. and Lazzaretto, A. (2003) A new thermoeconomic method for the location of causes of malfunctions in energy systems, Proceedings of the ASME, Advanced Energy Systems Division, 43, 355-364.

Tribus, M. and El-Sayed, Y. M. (1981) A specific strategy for the improvement of process economics through thermoeconomic analysis, Proc. 2nd World Congress of chemical engineering II, Montreal, 278-281.

Tribus, M. and El-Sayed, Y. M. (1980) Thermoeconomic analysis of an industrial Process, Center for advanced Engineering Study, M.I.T., Cambridge, MA.

Tsatsaronis, G. and Morosuk, T. (2010) Advanced Exergetic Analysis of a Novel System for Generating Electricity and Vaporizing Liquefied Natural Gas, Energy - The International Journal, in press.

Tsatsaronis, G. (2009) Application of Thermoeconomics to the Design and Synthesis of Energy Plants, in: Exergy, Energy Systems Analysis and Optimization of the Encyclopedia of Life Support Systems II (Frangopoulos, C., Ed.), EOLSS Publishers, Oxford, 121-146.

Tsatsaronis, G. and Cziesla, F. (2009) Exergy, Energy Systems Analysis and Optimization, in: Encyclopedia of Life Support Systems, EOLSS Publishers, Oxford, UK, 1, 34-146.

Tsatsaronis, G., Morosuk, T. and Cziesla, F. (2009) LNG-based cogeneration systems. Part 2: Advanced exergy-based analyses of a concept, Proceedings of the ASME 2009 International Mechanical Engineering Congress and Exposition, Lake Buena Vista, IMECE2009-10460.

Tsatsaronis, G. (2008) Recent Developments in Exergy Analysis and Exergoeconomics, International Journal of Exergy, 5 (5/6), 489-499.

Tsatsaronis, G., Kapanke, K., and Blanco Marigorta, A. M. (2008) Exergoeconomic Estimates for a Novel Zero-Emission Process Generating Hydrogen and Electric Power, Energy - The International Journal, 33, 321-330.

Tsatsaronis, G. and Morosuk, T. (2008a) A general exergy-based method for combining a cost analysis with an environmental impact analysis. Part I – Theoretical Development, Proceedings of the ASME International Mechanical Engineering Congress and Exposition, Boston, IMECE2008-67218.

Tsatsaronis, G. and Morosuk, T. (2008b) A general exergy-based method for combining a cost analysis with an environmental impact analysis. Part II – Application to a cogeneration system, Proceedings of the ASME International Mechanical Engineering Congress and Exposition, Boston, IMECE2008-67219.

Tsatsaronis, G. and Morosuk, T. V. (2007a) Advanced Exergoeconomic Evaluation and its Application to Compression Refrigeration Machines, Proceedings of the ASME International Mechanical Engineering Congress and Exposition, Seattle, IMECE2007-412202.

Tsatsaronis, G. and Morosuk, T. (2007b) Design improvement of an energy conversion system based on advanced exergy analysis. Proceedings of the 4th European Congress 'Economics and management of energy in industry', Porto.

Tsatsaronis, G., Kelly, S. O., and Morosuk, T. V. (2006) Endogenous and Exogenous Exergy Destruction in Thermal Systems, Proceedings of the ASME International Mechanical Engineering Congress and Exposition, Chicago, IMECE2006-13675.

Tsatsaronis G. and Cziesla F. (2002) Thermoeconomics, in: Encyclopedia of Physical Science and Technology, 16, 3rd Edition, 659-680.

Tsatsaronis, G. and Park, M.-H. (2002) On Avoidable and Unavoidable Exergy Destructions and Investment Costs in Thermal Systems, Energy Conversion and Management, 43, 1259-1270.

Tsatsaronis, G. (1999a) Design optimization using exergoeconomics, in: Thermodynamic Optimization of Complex Energy Systems, (Bejan, A. and Mamut, E., Eds.), Kluwer Academic Publishers, Dordrecht, 101-115.

Tsatsaronis, G. (1999b) Strengths and limitations of exergy analysis, in: Thermodynamic Optimization of Complex Energy Systems, (Bejan, A. and Mamut, E., Eds.), Kluwer Academic Publishers, Dordrecht, 93-100.

Tsatsaronis, G. and Moran, M. J. (1997) Exergy-Aided Cost Minimization, Energy Conversion and Management, 38, 15-17, 1535-1542.

Tsatsaronis, G. (1995) Design Optimization of Thermal Systems Using Exergy-Based Techniques, Proceedings of the Workshop Second Law Analysis of Energy Systems: Towards the 21st Century (Sciubba, E. and Moran, M. J., Eds.), Rome, Italy, 5-7.

Tsatsaronis, G., Lin, L. and Tawfik, T. (1994a) Exergoeconomic Evaluation of a KRW-Based IGCC Power Plant, Journal of Engineering for Gas Turbines and Power, 116, 300-306.

Tsatsaronis, G., Tawfik, T. and Lin, L. (1994b) Exergetic Comparison of Two KRW-Based IGCC Power Plants, Journal of Engineering for Gas Turbines and Power, 116, 291-299.

Tsatsaronis, G. and Pisa, J. (1994c) Exergoeconomic Evaluation and Optimization of Energy Systems – The CGAM Problem, Energy – The International Journal, 19, 287-321.

Tsatsaronis, G., Krane, R. J. and Krause, A. (1994d) Thermoeconomic Evaluation of the Columbian Chemicals Standard Carbon Black Process, Final Report submitted to Columbian Chemicals Company, Swartz, Louisiana.

Tsatsaronis, G. (1993) Thermoeconomic Analysis and Optimization of Energy Systems, Progress in Energy and Combustion Systems, 19, 227-257.

Tsatsaronis, G., Lin, L., and Pisa, J. (1993) Exergy Costing in Exergoeconomics, Journal of Energy Resources Technology, 115, 9-16.

Tsatsaronis, G. (1987) A Review of Exergoeconomic Methodologies, Proceedings of the Fourth International Symposium, Second Law Analysis of Thermal Systems (Moran, M. J. and Sciubba, E., Eds.), 81-87.

Tsatsaronis, G. (1984) Combination of Exergetic and Economic Analysis in Energy Conversion Processes, in: Energy Economics and Management in Industry (Reis, A., Smith, I., Peube, J. L., Stephan, K., Eds.), Pergamon Press, Oxford, 151-157.

Tsatsaronis, G., Pisa, J., Lin, L. and Tawfik, T. (1992a) Optimization of an IGCC Power Plant – Part I: Optimized Cases, in: Thermodynamics and the Design, Analysis, and Improvement of Energy Systems – 1992 (Boehm, R. F., et al., Eds), 1992 Winter Annual Meeting of ASME, 27, 37-53.

Tsatsaronis, G. Lin, L. and Pisa, J. (1992b) Optimization of an IGCC Power Plant – Part II: Methodology and Parametric Studies, in: Thermodynamics and the Design, Analysis, and

Improvement of Energy Systems – 1992 (Boehm, R. F., et al., Eds), 1992 Winter Annual Meeting of ASME, 27, 55-67.

Tsatsaronis, G., Lin, L., Pisa, J. and Tawfik, T. (1991) Thermoeconomic Design Optimization of a KRW-Based IGCC Power Plant, Final Report submitted to Southern Company Services and the U.S. Department of Energy, DE-FC21-89MC26019, Center for Electric Power, Tennessee Technological University.

Tsatsaronis, G., Tawfik, T. and Lin, L. (1990) Assessment of Coal Gasification/Hot Gas Cleanup Based Advanced Gas Turbine Systems – Exergetic and Thermoeconomic Evaluation, Final Report submitted to Southern Company Services and the U.S. Department of Energy, DE_FC21_89MC26019, Center for Electric Power, Tennessee Technological University.

Tsatsaronis, G., Pisa, J. J. and Gallego, L. M. (1989) Chemical Exergy in Exergoeconomics, in: Thermodynamic Analysis and Improvement of Energy Systems, Proceedings of the International Symposium, Pergamon Press, 195-200.

Tsatsaronis, G., Winhold, M. and Stojanoff, C. G. (1986) Thermoeconomic Analysis of a Gasification-Combined-Cycle Power Plant, EPRI AP-4734, RP 2029-8, Final Report, Electric Power Research Institute, Palo Alto, CA.

Tsatsaronis, G. and Winhold, M. (1986) Exergoeconomic Analysis of an Integrated Coal Gasification-Combined-Cycle Power Plant, Winter Annual Meeting of the American Society of Mechanical Engineers, 2-3.

Tsatsaronis, G. and Winhold, M. (1985a) Exergoeconomic Analysis and Evaluation of Energy Conversion Plants. Part I-A New General Methodology, Energy - The International Journal, 10 (1), 69-80.

Tsatsaronis, G. and Winhold, M. (1985b) Exergoeconomic Analysis and Evaluation of Energy Conversion Plants. Part II - Analysis of a Coal-Fired Steam Power Plant, Energy -The International Journal, 10 (1), 81-94.

Tsatsaronis, G. and Winhold, M. (1984) Thermoeconomic Analysis of Power Plants, EPRI AP-3651, RP 2029-8, Final Report, Electric Power Research Institute, Palo Alto, CA.

Turton, R., Bailie, R.C., Whiting, W.B., Shaeiwitz, J.A. (2002) Analysis, Synthesis and Design of Chemical Processes, 2nd Edition, Part of the Prentice Hall International Series in the Physical and Chemical Engineering Sciences series, Prentice Hall, ISBN-13: 978-0-13-064792-4.

Valero, A., Lozano, M.A., Serra, L. and Torres, C. (1994) Application of the exergetic cost theory to the CGAM problem, Energy - The International Journal, 19 (3), 365-381.

Valero, A., Lozano, M. A. and Munoz, M. (1986) A General Theory of Exergy Saving, Part I: On the exergetic cost, Part II: On the thermoeconomic cost, Part III: Energy savings and thermoeconomics, in: Computer-Aided Engineering of Energy Systems (Gaggioli, R. A., Ed.), ASME, New York, 1-22.

Valero, A., Torres, C. and Lozano, M. A. (1989) On the Unification of Thermoeconomic Theories, in: Simulation of Thermal Energy Systems (Boehm, R. F., El-Sayed, Y. M., Eds.), ASME, New York, 63-74.

VGB PowerTech e.V. (2004), CO_2 capture and storage, VGB Report on the State of the Art, Essen.

Toffolo, A. and Lazzaretto, A., A new thermoeconomic method for the location of causes of malfunctions in energy systems, Proceedings of the ASME, Advanced Energy Systems Division, 43, 355-364, 2003.

Vilson, R. D., Air Separation Control Technology, YEAR.

von Spakovsky, M. R. (1994) Application of engineering functional analysis to the analysis and optimization of the CGAM problem, Energy - The International Journal, 19 (3), 343-364.

von Spakovsky, M. R. (1986) A practical generalized analysis approach to the optimal thermoeconomic design and improvement of real-world thermal systems, Dissertation, Georgia Institute of Technology.

von Spakovsky, M. R. and Evans, R. B. (1990) The Design and Performance Optimization of Thermal Systems, ASME Trans., Journal of Engineering for Gas Turbines and Power, 112 (1), 86-93.

von Spakovsky M. R. and Evans, R. B. (1990) The foundations of engineering functional analysis (Part I and II), in: A future for energy (Stecco, S. and Moran, M., Eds.), Flowers'90, Florence, Italy, May 28–June 1, 445–472.

Wepfer, W. J. (1980) Applications of Available-Energy Accounting, in: Thermodynamics: Second Law Analysis (R. A. Gaggioli, Ed.), A. C. S. Symposium Series, 122.

Wepfer, W. J. (1979) Application of the Second Law to the Analysis and Design of Energy Systems, Dissertation, The University of Wisconsin-Madison, USA.

Wilkinson, M., Simmonds, M., Allam, R. and White, V. (2003) Oxyfuel Conversion of Heaters and Boilers for CO_2 Capture, Second National Conference on Carbon Sequestration, Washington DC.

Wolf, J., Anheden, M., Yan, J. (2005) Comparison of nickel- and iron-based oxygen carriers in chemical looping combustion for CO_2 capture in power generation, Fuel, 84, 993-1006.

WorleyParsons (2009), Strategic Analysis of the Global Status of Carbon Capture and Storage Report 1: Status of Carbon Capture and Storage Projects Globally, Final Report, Commonwealth of Australia.